FOURIER TRANSFORM INFRARED SPECTROSCOPY

OF A SINGLE AEROSOL PARTICLE

Thesis by

Gideon Sageev Grader

In Partial Fulfillment of the Requirements

for the Degree of

Doctor of Philosophy

California Institute of Technology

Pasadena, California

1987

(Submitted December 10, 1986)

ACKNOWLEDGMENTS

The work described here evolved in the course of roughly three long years. During this period the progress of the project was very non-linear function of time. Were I to describe this progress as a mathematical function, perhaps an n-degree polynomial (where n is a LARGE integer), would be well suited. In retrospect I am also finding a very distinct correlation between the curvature of the polynomial above, and my interactions with the external world. In particular, whenever that curvature was positive, signifying a local minimum, my phone bill was unusually high for some odd reason. It is in this section that I come to grip with this oddity, and pay my tribute to all those who have assisted me during this project.

First I would like to thank my advisor, John H. Seinfeld, and my co-advisor, Richard C. Flagan, for their continued support and professional advice.

Then I would like to thank Stephen Arnold from the Brooklyn Polytechnic Institute for allowing me to spend the summer of 1984 in his laboratory. Spending that summer in Brooklyn catalyzed my later work at Caltech, as well as started a productive collaboration among us.

I would like to give special thanks to Tony Pluchino from the Aerospace Corporation for many conversations about this project as well as for lending me various pieces of expensive equipment (such as an MCT detector and photomultipliers), which helped me tremendously along the way.

When designing the electronic circuitry, I was assisted by John Lee and Tom Dunn of Caltech, and I would like to thank them for their help. For building a

part of the apparatus, teaching me how to use the lathe and milling machine, and lending me his personal tools to work with I would like to give many thanks to Floyd Litreal of the Chemical Engineering student shop.

I would like to acknowledge the fellow students in our research group: Carol Jones, Mark Cohen, Jennifer Stern, and Brian Wong, with whom my interaction was almost on a daily basis. In particular I would like to thank Jennifer Stern for proofreading this manuscript.

Finally, I would like to thank my wife, Orit, whose moral support and willingness to put up with my odd schedule was invaluable to the completion of this project.

To Kushilu

ABSTRACT

Throughout this thesis, the phenomenon of radiation-induced particle size change is studied both on a theoretical as well as experimental level. The thrust of this study is aimed at using the size changes due to heat absorption to develop a technique for obtaining the particle chemical composition.

The experiments here involve charged particles, generated with an impulse jet, and trapped by the electric field of an electrodynamic balance. The particles under study are all aqueous solutions of non-volatile salts, where upon heating a partial evaporation of water occurs. The evaporation and subsequent condensation processes are modeled in both the continuum and the transition regimes. The models developed are tested and the agreement between theory and experimental results is demonstrated. The models are also used to extract the values of the water, thermal, and mass accommodation coefficients from the data. The results for the thermal accommodation show that its value is near unity, however the corresponding results for the mass accommodation are not conclusive.

A method is developed for obtaining the molecular composition of a single suspended microparticle by Fourier transform infrared spectroscopy. The particle is irradiated simultaneously by the infrared output from a Michelson interferometer and the visible light from a dye laser. The laser is tuned to an edge of an optical resonance of the particle while the IR beam is chopped. Through evaporation and condensation the chopped IR beam causes a size modulation of the droplet, which in turn induces a fluctuation in the laser light scattered from the particle. The scattered light is detected at 90° with a photomultiplier, and the amplitude

of the light fluctuation is measured with a lock-in amplifier. The lock-in signal is then inverted by a discrete fast Fourier transform routine (FFT), to yield the particle absorption spectrum. Spectra of $(NH_4)_2SO_4$ droplets at different solute concentrations are presented.

TABLE OF CONTENTS

LIST OF TABLES

LIST OF FIGURES

IN CHAPTER 2

LIST OF FIGURES

IN CHAPTER 3

LIST OF FIGURES

IN CHAPTER 4

LIST OF FIGURES

IN CHAPTER 5

LIST OF FIGURES

IN CHAPTER 6

LIST OF FIGURES

IN CHAPTER 7

LIST OF FIGURES

CHAPTER 8

LIST OF FIGURES

IN APPENDIX A

LIST OF FIGURES

IN APPENDIX B

CHAPTER 1

INTRODUCTION

At the beginning of this work, roughly three years ago, the objective was to perform spectroscopy on a single aerosol particle, and apply it to the study of a chemically reactive system. The type of spectroscopy as well as the type of particle or reaction was not well defined, and thus to a large extent the definition of the project's specific objectives and directions emerged as the work progressed.

The initial work involved studying the interaction of an intense laser beam with aerosol particles consisting of aqueous solutions of nonvolatile salts. The laser beam energy absorbed by the particle increases the particle's temperature and causes the partial evaporation of water from the particle. The evaporation process is restrained by the increase in ionic strength inside the droplet. Of interest to us was the transient process occurring within the droplet. By solving the coupled heat and mass transfer equations numerically we plotted the transient evaporation and condensation processes occurring within the particle. This work is summarized in Chapter 2.

Following that initial work the first main decision made was to perform infrared spectroscopy on a particle. This early choice set the framework for the rest of this project. About that time Stephen Arnold lectured on campus about his technique for obtaining the spectrum of a single particle. After Arnold found out about our common interest in the topic, an agreement was reached to start a collaborative work in the area of single particle spectroscopy. As a part of this collaboration I went to New York for the summer of 1984 to work with Steve, assist him in his current work, and learn the technique he has developed. During that summer I learned the technique of single particle levitation and participated in the completion of an

experiment in which we developed and tested a model describing the evaporation and condensation from a single droplet. This work is summarized in Chapter 3.

Since one of the objectives was to study reaction kinetics where the time to obtain a spectrum must be short, we decided not to utilize Steve's original technique but instead to employ a Fourier transform method which potentially can have a larger resolution and take a shorter time than Steve's method. After returning to Caltech from Brooklyn I immediately proceeded to design and build the levitation system and vacuum enclosure. When planning the levitation electrodes I adapted the design used in Steve's apparatus. The electrodes are hyperbolic in shape and consist of two identical endcap electrodes and a ring electrode. The internal separation of the two endcaps is roughly 0.45 inch, while the internal diameter of the ring is 0.5 inch.

The building of the chamber and electrodes was completed within two months after my return to Caltech and by November the system was ready to trap particles. In order to study the performance of the levitation apparatus we decided to extend the continuum evaporation and condensation model, developed with Steve over the previous summer, into the transition regime. In this project John Seinfeld did the theoretical extension of the continuum model, while I carried out the experimental part of the work. In addition to testing the apparatus, one of the goals of the model extension was to get a value for the water thermal and mass accommodation coefficients. The theoretical developments as well as experimental results are summarized in Chapter 4.

Throughout this project it was always necessary to determine the size of the

particle under study. Usually we used the sedimentation method, where the aerodynamic particle size is found by measuring the terminal velocity of a falling particle. In this method one changes the DC voltage so that the particle is not balanced, then turns the AC field off and observe the particle fall under the combined gravitational and electric forces. By clocking the particle fall time through a known distance the terminal velocity is found. When working with particles at low pressures (where the drag is reduced), or with large particles (7 μm) the fall rate can become too fast for a manual measurement of the terminal velocity. In order to improve the precision with which the sizing is done, we developed an electronic technique for obtaining the particle size. This technique is described in Chapter 5.

Chapters 6 and 7 are devoted to the development of the Fourier transform infrared spectroscopy. The final method of performing the experiment was different than what we had originally planned. Before summarizing the course undertaken I would like to briefly describe the basis of the technique. In Fourier transform technique the basic element is the interferometer, which in our case consists of a broad band source, a beam splitter, and two mirrors. The light falls on the beam splitter and each of the splitted beams is redirected towards a mirror. The mirrors reflect the light back towards the beam splitter where upon meeting they undergo constructive and destructive interference. By moving the position of one of the mirrors, different wavelengths are destroyed and others are reconstructed. Thus the spectrum of the output (combined) beam of the interferometer is changing as the mirror position is changed.

In our experiment the particle is positioned at the focal point of the output

infrared beam. As described in earlier chapters, the particle absorbs some of the IR radiation and a partial evaporation of water occurs. The key problem in this experiment becomes the measurement of the particle size change as a function of the interferometer mirror position.

Originally we thought that the particle size change could be measured directly by a continuous monitoring of the particle balancing voltage. To monitor the balancing voltage automatically, we implemented a servo system which corrected for the change in the particle mass (due to evaporation) by an appropriate change in the DC voltage levitating the particle. The servo system was based on a proportional controller, however we found that the sensitivity of the servo was not sufficient for following the small mass changes induced by the changing IR intensity. In order to boost the sensitivity to small size changes in the particle, we decided to use the scattered light from the particle as the indicator of the particle size change. Here we rely on the resonance phenomenon (first predicted by Mie) in the scattered light from the particle. This non-linear phenomenon offers a large optical amplification for small size changes. Here again we first tried to obtain the spectrum by moving the mirror continuously. We have found that the signal-to-noise was too low.

In an effort to raise the signal-to-noise ratio of the measurement we finally decided to chop the IR radiation and phase-sensitively detect the scattered light fluctuation. The last approach was successful, however, it lengthened the time required to obtain the spectrum of a particle. The technique was applied to an ammonium sulfate particle, and the spectrum of the particle was obtained. The theory behind this method and the experimental results are summarized in Chap-

ter 6, while the instrument is described in Chapter 7. Finally, in Chapter 8 the conclusion of this work is presented.

CHAPTER 2

LASER HEATING OF AN AQUEOUS AEROSOL PARTICLE

by :

Gideon Sageev

John H. Seinfeld

Published in Applied Optics, **23**, 4368, (1984).

Reprinted from Applied Optics, Vol. 23, page 4368, December 1, 1984

Laser heating of an aqueous aerosol particle

Gideon Sageev and John H. Seinfeld

Approximate analytical and full numerical solutions are obtained for the transient response of both a pure water and solution droplets to both short- and long-time laser heating. The differences in the temperature and size histories between pure water and solution droplets are elucidated. The validity of of the approximate analytical solution, extended from that of Armstrong ["Aerosol Heating and Vaporization by Pulsed Light Beams," Appl. Opt. 23, 148 (1984)] in pure water droplets, is evaluated by comparison to solution of the full governing equations.

I. Introduction

Heating an aerosol particle on irradiation with a laser beam induces temperature gradients in the air surrounding the particle that change the air's index of refraction in the vicinity of the particle. These changes may cause the beam to diverge as it passes through the medium. To estimate the magnitude of this phenomenon, called thermal blooming, the particle's surface temperature must be known.

The amount of energy a particle absorbs from the incident light beam depends on the particle's complex index of refraction as well as on its optical size (where the optical size x is given by $x = 2\pi r_s/\lambda$, r_s and λ being the particle radius and laser wavelength, respectively). In this work, the beam wavelengths considered are much larger than the particle radius; thus the energy absorbed by the particle can be obtained from Rayleigh theory.[1] As the optical size of the particle increases, the absorption of energy by the particle may be enhanced by structure resonance;[2] however, in the present work, this effect is neglected.

The particles considered here are homogeneous liquid drops containing a solute. When the incident beam first strikes a volatile particle (which is assumed to be initially in equilibrium with its environment), all the absorbed energy goes into raising the particle's temperature. As the particle's temperature increases, the solvent in the particle begins to vaporize, and, at the same time, energy is lost from the particle by conduction into the gas phase. The processes of mass and heat transfer in the air surrounding the drop can be assumed to be at a pseudo-steady state as long as the characteristic times for changes in the temperature and concentration profiles in the gas are much shorter than that for the temperature of the drop. This is generally a good assumption for the drops of interest here. The relative amounts of energy dissipated by conduction and evaporation depend strongly on the presence of solutes in the drop. The effect of the solutes is to lower the vapor pressure of the solvent in the drop, thereby lowering the vaporization rate from that in the absence of solutes. As the vaporization continues, the solution droplet shrinks and approaches a new steady state size and temperature, at which point all the absorbed heat is released by conduction.

In a pure droplet, on the other hand, the evaporation rate is governed only by the effect of the droplet temperature on its vapor pressure. Since solutes are absent, the vaporization from the drop continues until the drop disappears. Thus, in a pure droplet, a fraction of the absorbed energy is always dissipated by vaporization.

The above description refers to situations in which either a solvent/solute droplet or a pure solvent droplet is continually heated with a laser. An alternative situation of practical interest is that in which a pulsed laser is used and the particle is heated by the laser for only a short period of time. When a pure solvent droplet is subject to a short pulse of laser light, its temperature increases initially before significant evaporation or conduction into the gas phase can take place. Consequently, in a short heating period, the particle can be assumed not to shrink due to loss of material by evaporation. When the laser is turned off, the droplet is no longer in equilibrium with its surroundings, and it begins to cool by the combined effects of conduction and vaporization. Eventually, the drop reaches a new equilibrium size at which point its temperature returns to that of its surroundings. The total amount of mass lost is related to the total energy input into the drop. When a solution drop is subject to a short-period laser

The authors are with California Institute of Technology, Department of Chemical Engineering, Pasadena, California 91125.

Received 27 June 1984.
0003-6935/84/234368-07$02.00/0.

heating, its temperature also rises quickly before appreciable conduction or evaporation can take place. After the laser is turned off, the droplet returns to its original temperature. However, eventually the droplet also returns to its initial equilibrium size due to replenishment of solvent from the vapor.

The aerosol temperature rise resulting from the long-time heating of a pure water drop by a laser beam was investigated numerically by Caledonia and Teare.[3] More recently, Armstrong[4] obtained an analytical solution to the heating of a pure water droplet by making a number of assumptions. First, Armstrong assumed that once the laser is turned on, even though conduction and vaporization are occurring during the heating process, the radius of the drop remains at its initial value. Eventually, a steady state is reached where the absorbed laser energy is balanced by energy losses due to conduction and vaporization, still assuming the particle retains its initial size. Once at steady state, the particle temperature is assumed to stay constant throughout the remaining heating period. The change in radius of the drop is then approximated from the solvent mass flux based on the steady state temperature of the drop. The assumption of constant particle size during the short heating times enables an analytical solution to be obtained.

Both works cited above apply to the heating of a pure water droplet. However, since atmospheric aerosols must contain solutes to exist in equilibrium in an environment where the relative humidity is <100%, it is important to investigate the effect of the presence of solutes on the aerosol heating process.

The main object of the present work is to obtain both approximate analytical and full numerical solutions to the transient response of both pure solvent and solution droplets to both short- and long-time laser heating. We will examine the differences between the temperature rise in a solution and that in a pure droplet. Also, by calculating the temperature rise by solving the full governing equations numerically, we can evaluate the validity of the approximate analytical solution.

In Sec. II, we develop the theory of heat and mass transfer from a droplet subject to internal heating. Section III is devoted to the thermodynamic data used in calculation of the droplet temperature rise. In Sec. IV, the analytical and numerical results based on a short heating period are shown and discussed. Finally, in Sec. V we present numerical results based on a long heating period.

II. Theory

The equations governing the concentration and temperature profiles surrounding a volatile particle that contains an internal heating source are well known.[5] In such a situation, when the Biot number in the drop–air system is much smaller than unity, the drop temperature can be assumed to be constant. In doing so, the overall energy balance over the drop is given by

$$\rho_d C_d \frac{dT}{dt} = I_0 \alpha \tau - \frac{3}{r_s}\left[-LD_a\left(\frac{\partial Y}{\partial r}\right)_{r=r_s} - k_a\left(\frac{\partial T}{\partial r}\right)_{r=r_s}\right], \quad (1)$$

where T and t are temperature and time; Y and D_a are the water mass fraction and diffusivity in the air; I_0 and α are the incident beam intensity and bulk absorption coefficient; C_d, k_a, and L are the heat capacity, thermal conductivity, and heat of vaporization; and ρ_d and r_s are the drop density and radius. The subscripts s, a, and d refer to conditions of the surface, air, and drop, respectively.

On the right-hand side of Eq. (1), $I_0\alpha$ is the heat source. The first term inside the brackets is due to mass transfer across the interface, while the second term is due to heat conduction from the surface. Both of the gradients $(\partial Y/\partial r)_{r=r_s}$ and $(\partial T/\partial r)_{r=r_s}$ appearing in Eq. (1) depend on the boundary conditions at the drop surface and far away from the drop. When the unsteady terms are neglected in the equations of mass and heat transfer outside the drop, the mass and heat fluxes from the drop surface are given by[6]

$$-D_a\left(\frac{\partial Y}{\partial r}\right)_{r=r_s} = J = \frac{D_a}{r_s}\ln\left(\frac{1-Y_\infty}{1-Y_s}\right), \quad (2)$$

$$-k_a\left(\frac{\partial T}{\partial r}\right)_{r=r_s} = \frac{JC_a(T_s - T_\infty)}{L\left[\exp\left(\frac{r_s JC_a}{k_a}\right) - 1\right]}, \quad (3)$$

where J is the mass flux, Y_∞ and T_∞ are the water mass fraction and temperature far away from the drop, and Y_s and T_s are the analogous properties at the surface.

When Eqs. (2) and (3) are substituted into Eq. (1) one obtains[4]

$$\frac{dT}{dt} = \frac{I_0\alpha}{\rho_d C_d} - \frac{3JL}{r_s\rho_d C_d}\left\{1 + \frac{C_a(T - T_\infty)}{L\left[\exp\left(\frac{r_s JC_a}{k_a}\right) - 1\right]}\right\}. \quad (4)$$

For a solution droplet,

$$Y_s(T) \approx a_w(T)Y^0(T), \quad (5)$$

where a_w is the water activity and Y^0 is the water mass fraction resulting from the vapor pressure of pure water at temperature T. Assuming that the vapor at the surface is at equilibrium with the drop, $Y^0(T)$ can be related to $Y^0(T_\infty)$ by using the Clausius-Clapeyron and the Kelvin equations. The resulting expression is

$$Y^0(T) = Y^0(T_\infty)\exp\left[-\frac{LM_w}{R}\left(\frac{1}{T} - \frac{1}{T_\infty}\right)\right]\exp\left(\frac{2\bar{v}\sigma}{RTr_s}\right), \quad (6)$$

where M_w is the water molecular weight and R, $\bar{v}$, and σ are the gas constant, the solution molar volume, and the surface tension, respectively.

The water activity can be expressed in terms of the solute molality m, the total number of ions the solute molecule dissociates into ν, and the molal osmotic coefficient φ (Refs. 7 and 8):

$$a_w(T) = \exp\left[-\frac{\nu m M_w}{1000}\varphi(T)\right]. \quad (7)$$

The osmotic coefficients is related to the solute activity coefficient γ by

$$\varphi(T) = 1 + \frac{1}{m}\int_0^m m\,d\ln|\gamma(T)|. \quad (8)$$

Finally, the temperature dependence of γ is obtained from the Van't Hoff equation:[7]

$$\frac{\partial}{\partial T}(\ln\gamma^2)_P = \frac{\bar{H}_i^0 - \bar{H}_i}{RT^2}, \tag{9}$$

where $\bar{H}_i^0$ and $\bar{H}_i$ are the partial molal enthalpies of the solute at infinite dilution and molality m, respectively. By integration of Eq. (9) with respect to T, followed by differentiation with respect to m and substitution into Eq. (8), we obtain the following equation for the temperature dependence of the osmotic coefficient:

$$\varphi(T) = \varphi(T_\infty) + \left(\frac{1}{T} - \frac{1}{T_\infty}\right)\frac{1}{m}\int_0^m m'\frac{\partial}{\partial m'}\left[\frac{(\bar{H}_i - \bar{H}_i^0)}{2R}\right]dm' - \left(\ln\frac{T}{T_\infty} + \frac{T_\infty}{T} - 1\right)\frac{1}{m}\int_0^m m'\frac{\partial}{\partial m'}\left[\frac{(\bar{C}_i - \bar{C}_i^0)}{2R}\right]dm', \tag{10}$$

where $\bar{C}_i$ and $\bar{C}_i^0$ are the the partial molal heat capacities of the solute at molality m and at infinite dilution, respectively. In Eq. (10), we assume that the partial molal heat capacities remain constant with temperature. The solution of Eq. (10) requires osmotic coefficient data as well as thermodynamic data concerning the partial molal enthalpy and heat capacity. Data on $\varphi(T_\infty)$ at $T_\infty = 25°C$ for many salts can be found in a comprehensive report by Hamer and Wu.[9] By expressing the partial molal quantities in power series,[7] the integrals in Eq. (10) reduces to the following series:

$$\delta = \frac{1}{m}\int_0^m m'\frac{\partial}{\partial m'}\left[\frac{(\bar{H}_i - \bar{H}_i^0)}{2R}\right]dm' = \sum_{n=1} A_n\left(\frac{n}{n+2}\right)m^{n/2}, \tag{11}$$

$$\beta = \frac{1}{m}\int_0^m m'\frac{\partial}{\partial m'}\left[\frac{(\bar{C}_i - \bar{C}_i^0)}{2R}\right]dm' = \sum_{n=1} B_n\left(\frac{n}{n+2}\right)m^{n/2}, \tag{12}$$

where A_n and B_n are fitting parameters to experimental data. Once Eq. (10) is solved, the water activity is found by substitution into Eq. (7). Equation (2) can now be rewritten as

$$J = \frac{D_a}{r_s}\ln\left[\frac{1 - Y_\infty}{f(T)}\right], \tag{13}$$

where $f(T)$ is given by

$$f(T) = 1 - Y^0(T_\infty)\exp\left\{\frac{A}{T} - B\left[\varphi T_\infty) + \delta\left(\frac{1}{T} - \frac{1}{T_\infty}\right) - \beta\left(\ln\frac{T}{T_\infty} + \frac{T_\infty}{T} - 1\right)\right] - C\left(\frac{1}{T} - \frac{1}{T_\infty}\right)\right\}, \tag{14}$$

and where

$$A = \frac{2\bar{v}\sigma}{Rr_s}, \quad B = \frac{\nu m M_w}{1000}, \quad C = \frac{LM_w}{R}.$$

Since a numerical solution to Eq. (4) can be obtained readily, an analytical solution is not an absolute necessity. The advantages of an analytical solution are that it allows one to obtain an expression for the characteristic time of the heating process and that it reveals the major physical contributions leading to the predicted behavior. To solve Eq. (4) analytically, one must first linearize Eq. (2) with respect to temperature; the linearized result is then substituted into Eq. (4), and the resulting expression is integrated. [Clearly Eqs. (2) and (4) are also functions of the radius; however, as shown earlier,[4] for small values of the product $(I_0\alpha r_s^2)$, the effect of small variations in r_s on the steady state temperature is negligible.] Analogous to the development of Armstrong,[4] an expansion of Eq. (2) in a second-order Taylor series of the dimensionless temperature X [where $X = (T - T_\infty)/T_\infty$] yields for the mass flux

$$J = \frac{D_a}{r_s}(\epsilon X + \psi X^2), \tag{15}$$

where

$$\epsilon = \left(\frac{Y_\infty}{1 - Y_\infty}\right)\left(\frac{-A + B\delta + C}{T_\infty}\right),$$

$$\psi = \epsilon\left[\frac{(-A + B\delta + C)}{2(1 - Y_\infty)T_\infty} - 1 + \frac{B\beta T_\infty}{2(-A + B\delta + C)}\right].$$

Equation (15) is identical in form to Eq. (9) of Armstrong,[4] except that in the latter equation the constants A, B, δ, and β do not appear, and the Y_∞ term does not include the effect of the water activity on the vapor pressure. Additionally, the droplet density and heat capacity in Eq. (15) are those of a solution, whereas the corresponding properties in Ref. 4 apply to a pure water droplet. In the limit of zero molality and negligible Kelvin effect, the water activity coefficient approaches unity, and Eq. (15) reduces to that given by Armstrong.

When the radius does not change appreciably during the heating period, Eq. (15) can be substituted into Eq. (4) (after nondimensionalizing the temperature). The resulting expression is then integrated to yield the droplet temperature as a function of time:[4]

$$X(t) = \begin{cases} \dfrac{2l_0\tau_h[1 - \exp(-t/\tau_h)]}{1 + l_1\tau_h + (1 - l_1\tau_h)[\exp(-t/\tau_h)]} & \text{if } t \le t_p \\ \dfrac{l_1 X(t_p)\exp(-l_1 t)}{l_1 + l_2 X(t_p)[1 - \exp(-l_1 t)]} & \text{if } t > t_p \end{cases}, \tag{16}$$

where t_p is the heating period, $X(t_p)$ is the dimensionless temperature at the end of the heating period, and τ_h is the characteristic time for the heating process. The constants in Eq. (16) are given by

$$l_0 = \frac{I_0\alpha}{\rho_d C_d T_\infty}$$

$$l_1 = \frac{3}{\rho_d C_d r_s^2}\left(\frac{D_a L}{T_\infty}\epsilon + k_a\right)$$

$$l_2 = \frac{3}{\rho_d C_d r_s^2}\left(\frac{D_a L}{T_\infty}\psi - \frac{C_a D_a}{2}\epsilon\right),$$

$$\tau_h = (l_1^2 + 4l_0 l_2)^{-1/2}.$$

III. Thermodynamic Data

In the evaluation of Eq. (16) we used activity coefficient data reported by Hamer and Wu[9] for NaCl at 298 K. The computation of the temperature dependence of the activity coefficient requires data on the partial molal enthalpy and heat capacity. This information [used in Eqs. (11) and (12)] was obtained by fitting tabulated data[10] to a power series in terms of molality. The following expressions were calculated for the relative apparent partial molal enthalpy and heat capacity (valid in the range of $0.1 < m < 6.0$):

Table I. Summary of the Values of Various Physical Constants used in the Calculation (at 298 K)

Symbol	Value	Units
T_∞	298.15	K
Y^0	2.0×10^{-2}	Dimensionless
L	584.0	cal g^{-1}
$I_0\alpha$	10^5, 10^8	W cm^{-3}
C_a	0.25	cal g^{-1} K^{-1}
D_a	3.0×10^{-4}	g cm^{-1} sec^{-1}
k_a	6.2×10^{-5}	cal cm^{-1} sec^{-1} K^{-1}
M_a	28.39	g $mole^{-1}$
M_2	58.45	g $mole^{-1}$
M_u	18.0	g $mole^{-1}$
ρ_u	0.997	g cm^{-3}
$\overline{C}_u^0$	1.0	cal g^{-1} K^{-1}
$\overline{C}_2^0$	−23.8	cal $mole^{-1}$ K^{-1}
σ	72.0	dyn cm^{-1}

[a] Subscripts u and 2 refer to the solvent (water) and solute, respectively.

$$\Phi_L = \Phi_H - \Phi_H^0 = 458.95m^{1/2} - 688.09m + 241.47m^{3/2} - 39.339m^2 + 4.3245m^{5/2} - 0.0449m^3, \quad (17)$$

$$\Phi_{C_P} - \Phi_{C_p}^0 = 10.291m^{1/2} - 3.6538m + 13.121m^{3/2} - 10.638m^2 + 3.5304m^{5/2} - 0.4282m^3, \quad (18)$$

where Φ_H and Φ_H^0 are the apparent partial molal enthalpy at molality m and at infinite dilution, respectively. [The terms in Eq. (18) have analogous meaning.] The units of Eqs. (17) and (18) are (cal $mole^{-1}$) and (cal $mole^{-1}$ K^{-1}), respectively.

The relative partial molal enthalpy and heat capacity are then calculated from[8]

$$\overline{H}_i - \overline{H}_i^0 = \Phi_L - m\frac{\partial \Phi_L}{\partial m}. \quad (19)$$

A similar expression yields the value of the relative partial molal heat capacity. The heat capacity of the solution is given by[8]

$$C_p = n_u\overline{C}_u^0 + n_2\Phi_{C_p}, \quad (20)$$

where n_u and n_2 refer to the number of moles of solvent (water) and the solute, respectively, and $\overline{C}_u^0$ is the molar heat capacity of pure water. Results from Eq. (20) agree well with the heat capacity data reported by Bromley *et al.*[11]

The density of a salt solution is given by[8]

$$\rho_d = \rho_d^0 + \frac{c}{1000}(M_2 - \Phi_V\rho_d^0), \quad (21)$$

where c is the solute concentration (in moles $liter^{-1}$), Φ_V is the solution apparent molal volume, and ρ_d^0 is the density of pure solvent. Data for Eq. (21) were taken from Ref. 8.

IV. Short-Time Heating of an NaCl Droplet

In this section we calculate the droplet temperature rise resulting from short-time laser heating of an aqueous NaCl droplet. The parameters used in the calculations are given in Table I. During short-time heating the evaporation rate is assumed to be slow enough that the drop's radius and concentration do not change significantly. To compare the drop temperature rise computed here with that given in the literature, we consider conditions similar to those used by other authors.[3,4]

In general, the water content of an aerosol particle depends on both the surrounding relative humidity and the solutes it contains. In the limit of low water vapor pressure (at temperature much lower than the boiling point), the water activity in the drop is approximately equal to the relative humidity (RH). Thus in the case of high RH (e.g., in clouds), the effect of solutes is expected to be minimal. However, at lower RH, or when the heating causes a significant increase in solute concentration, one expects the solute to have an increasing effect on the vaporization rate and temperature rise in the drop. Equation (16) was evaluated for the case of a water drop containing various molalities of sodium chloride. In all cases considered, the salt concentration was low enough that the drop was below the saturation point. (For NaCl the saturation point is reported[9] to be $m \approx 6.1$ at 298 K.)

The temperature rise as a function of the dimensionless heating time predicted by Eq. (16) is shown in Figs. 1 and 2. The main difference between Figs. 1 and 2 is in the magnitude of the heating $I_0\alpha$. Based on

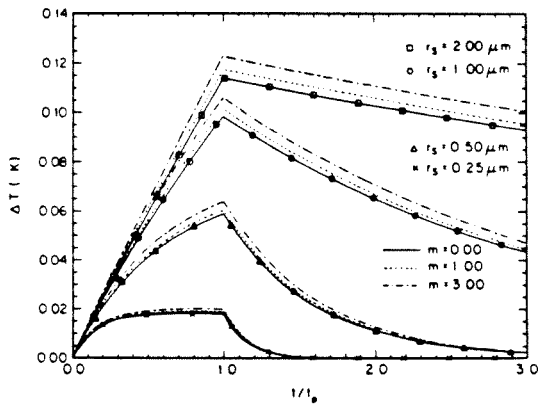

Fig. 1. Temperature rise in a droplet vs dimensionless time at t_p = 5 μsec; r_s = 0.25, 0.5, 1.0, 2.0 μm, and $I_0\alpha = 10^5$ W cm^{-3}.

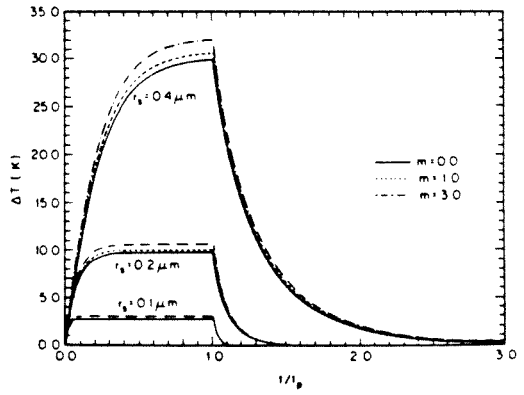

Fig. 2. Temperature rise in a droplet vs dimensionless time at t_p = 5 μsec; r_s = 0.10, 0.20, 0.40 μm, and $I_0\alpha = 10^8$ W cm^{-3}.

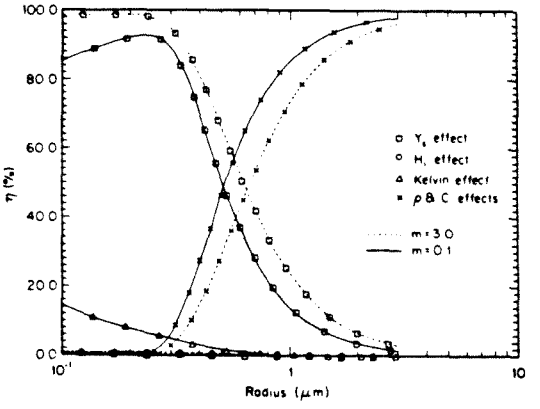

Fig. 3. Contribution of various parameters to the difference between the maximum temperature rise in a solution and that in a pure drop.

index of refraction data in Querry *et al.*,[12] the magnitude of α for an NaCl solution (irradiated by a laser having a wavelength of 9.09 μm) ranges from $\alpha = 595$ cm^{-1} for 1-M solution to $\alpha = 650$ cm^{-1} for 5-M solution (where M is the molar concentration). Thus I_0 was chosen to make $I_0\alpha = 10^8$ and $I_0\alpha = 10^5$ to simulate the heating caused by high and moderate beam intensities.

As seen from Figs. 1 and 2, the main effect of the solute is to increase the drop temperature rise above that which a pure droplet experiences. In all cases shown in Figs. 1 and 2 the maximum difference between the temperature rise of a solution and that in a pure drop is ~10%, a difference that increases with increasing salt concentration. As will be shown shortly, this deviation can be explained in terms of the differences among the densities, the heat capacities, and the vapor pressures of a solution and pure water droplet.

The deviations between the temperature rise in a solution droplet and that in a pure drop, shown in Figs. 1 and 2, are controlled by different parameters depending on the radius and concentration of the drop. To examine the effects of the vapor pressure Y_s, the partial molal quantities ($\bar{C}_l$ and $\bar{H}_l$), the solution density and heat capacity (ρ_d and C_d), and the Kelvin correction term, we define the quantity η as

$$\eta = \frac{T^* - T^0}{T^s - T^0} \times 100\%, \tag{22}$$

where T^0 and T^s are the maximum temperatures achieved in a pure water drop and in a solution, respectively, while T^* is the maximum temperature calculated by including only one of the parameters above in the equation for the temperature rise in a pure droplet. The parameters ρ_d and C_d were lumped together because they appear together in Eq. (4).

The values of η at various radii and molalities are shown in Fig. 3. It is evident that for large drops the difference between the density and heat capacity of a solution droplet and those of a pure droplet is responsible for the extra temperature rise of the solution. This effect occurs because the second term on the right-hand side of Eq. (4) is proportional to $1/r_s^2$, so as r_s increases the second term becomes less significant relative to the first term. In a NaCl solution the product of the density and heat capacity is smaller than the corresponding product in a pure drop; thus when the first term in Eq. (4) dominates (i.e., at large radii), the larger temperature rise in a solution is expected.

It is also apparent that the contribution of the solute partial molal enthalpy to the drop temperature rise is at most 1.0%. The effect of the partial molal heat capacity was <0.1%; therefore, it was omitted from Fig. 3. These results show that neglecting the partial molal terms in Eq. (14) does not lead to a serious error in the calculated temperature rise of the drop.

At the small radii in Fig. 3 the solution vapor pressure is responsible for the increased temperature rise. This pattern occurs because the interaction of solute molecules with the solvent lowers the vapor pressure of the solution. Since the initial vapor pressure over the drop is lower, the change in the vapor pressure during heating is lower. Because the mass flux from the drop is proportional to the change in the vapor pressure (to a first-order approximation), a solution droplet will evaporate less than a pure droplet for the same energy input. As a result of the smaller evaporation, the efficiency of evaporative cooling in a solution is lowered. The heat not dissipated by evaporation must then be removed by conduction; thus the drop's temperature must increase to raise the conduction driving force.

At very small radii (i.e., $r_s \ll 0.1$ μm) the Kelvin effect is expected to control the temperature rise in the drop. However, at these small radii the mean free path of the air molecules becomes comparable with the drop's radius; thus the solution presented here does not apply in that regime.

It should be pointed out that even in the case of a pure droplet the results presented here are slightly different from those reported by Armstrong,[4] because some of the parameters (mainly L and Y^0) were chosen differently. We used data on the heat of vaporization at the ambient temperature rather than at 373 K. We also used a different value of Y^0 because at the value used earlier[4] (Y^0 was 0.0138 at $T_\infty = 296$ K), the relative humidity was ~78%. However, for a pure water droplet to exist in equilibrium (at 298 K), the relative humidity must be 100% at which point $Y^0 \approx 0.020$.

Clearly, as the energy input ($I_0\alpha$) increases for a given drop size, the effects of the large temperature rise in the drop become increasingly important. To evaluate the validity of the analytical solution, we solved the full simultaneous heat and mass transfer equations numerically. A comparison of the analytical and numerical solutions for a 0.8-μm drop is shown in Fig. 4. It is evident from Fig. 4 that the discrepancy between the numerical and analytical solutions increases as the radiation intensity is increased. The top curve in Fig. 4 reveals that large deviations between the analytical and numerical solutions occur when $I_0\alpha r_s^2 = 0.64$ W cm^{-1}. At $I_0\alpha = 10^7$ the deviations occur mainly during the cooling period (at $t_p > 1.0$). It was pointed out by

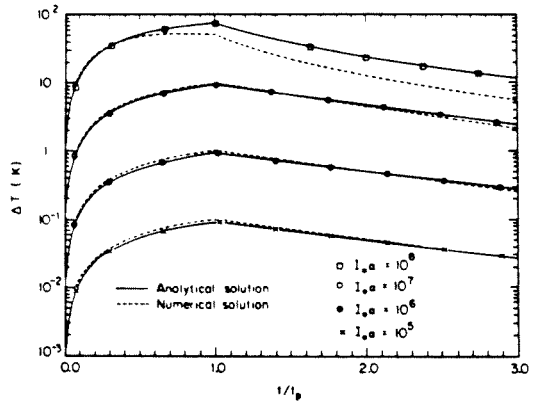

Fig. 4. Discrepancy between the analytical and numerical solutions for the short-time heating of a droplet of $m = 3.0$ and $r = 0.8$ μm.

Armstrong[4] that the analytical solution for a pure droplet is valid when the magnitude of the product $I_0\alpha r_s^2$ is < 0.5. The results of Fig. 4 indicate that the deviations in a solution begin to occur at a smaller value of the product above.

The differences between the heating of a solution and a pure droplet become more pronounced as the heating period increases. In the next section the temperature and radius changes a solution droplet undergoes when heated for a long time period will be discussed.

V. Long-Time Heating of a NaCl Droplet

When a droplet is heated for an extended time period, its radius and molality change with time. As will be shown shortly, the drop pseudo-steady state temperature also changes with time. The initial increase in the drop temperature increases the surface vapor pressure of the drop, thereby inducing a net mass flux from the drop which lowers the drop's water activity. This process continues until a new equilibrium state, determined by Eq. (5), is reached. Hence, during long-time heating, the analytical solution developed earlier is no longer valid. To evaluate the temperature and radius of the drop, the following relation between the mass flux from the drop and the drop radius is used:

$$\frac{\partial r_s}{\partial t} = \frac{1}{\rho_d} J. \tag{23}$$

The temperature changes for various salt concentrations and heating rates were obtained by solving Eqs. (4) and (23) numerically, results of which are shown in Fig. 5. The quantity τ_d used in the nondimensionalization of the temperature corresponds to the time constant for vaporization of a pure water droplet; it is given by[4]

$$\tau_d = \frac{3\rho_d L(k_a + \Gamma)}{I_0\alpha\Gamma}, \tag{24}$$

where

$$\Gamma = \frac{L^2 D_a M_w Y^0}{R(1 - Y^0)T_\infty^2}.$$

The parameter τ_d was chosen to scale the heating time to facilitate the comparison of the long-time heating of a solution droplet with that of a pure droplet.

As seen from Fig. 5, the temperature rise in a solution is quite different from the constant steady state temperature predicted by the analytical solution. This behavior results from the combination of two opposing effects. The first effect on the temperature rise is due to the decrease in the drop radius as a result of evaporation. Equation (16) shows that the temperature rise is proportional to τ_h; however, τ_h is proportional to the drop radius. Therefore, as the drop radius decreases due to evaporation the magnitude of the temperature rise the drop undergoes is expected to decrease as well. The decrease in the temperature during the heating period is also in agreement with results of Caledonia and Teare.[3]

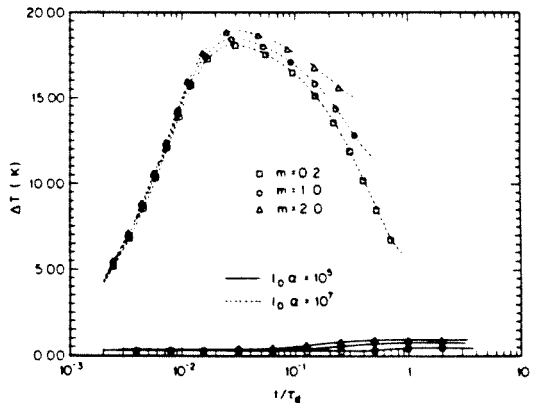

Fig. 5. Temperature rise vs dimensionless heating time for long-time heating of a droplet of initial radius $r_0 = 1.0$ μm, $\tau_d = 0.9435$ sec (at $I_0\alpha = 10^5$ W cm^{-3}), and $\tau_d = 0.009435$ sec (at $I_0\alpha = 10^7$ W cm^{-3}).

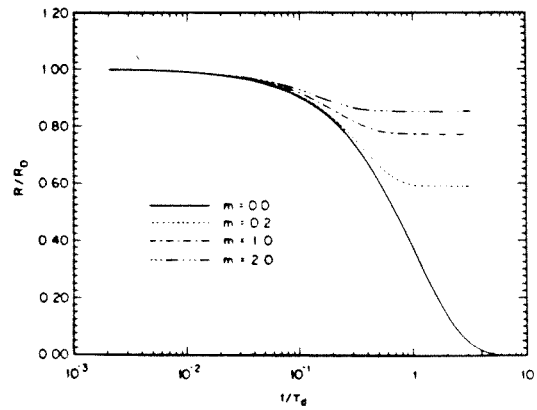

Fig. 6. Dimensionless radius vs dimensionless heating time for $r_0 = 1.0$ μm, and $\tau_d = 0.9435$ sec (at $I_0\alpha = 10^5$ W cm^{-3}).

The second effect on the drop temperature results from the decrease in the vaporization rate from the drop as it approaches a new equilibrium state. Since at equilibrium the net evaporation from the drop is zero, all the heat absorbed by the drop must be dissipated by conduction. The temperature of the drop must, therefore, increase to allow the larger conduction of heat away from the drop.

The two effects above oppose each other, thereby giving rise to the maximum observed in Fig. 5. The vaporization rate effect dominates when the changes in the radius are small and during the initial stage of the heating period. The effect of the decrease in radius begins to dominate only after sufficiently long heating times. The radius effect is less significant for the more concentrated drops simply because these drops undergo a smaller change in radius.

The variation of the drop radius with heating time, shown in Fig. 6, describes the approach of the droplet to its new equilibrium state. Also included in Fig. 6 is the radius change in a pure water droplet calculated from the analytical solution of Armstrong.[4] The radius of the pure droplet decreases continuously, and the process is eventually governed by the Kelvin effect.

As evident from Fig. 6 the dimensionless pure droplet evaporation time constant τ_d is larger than the corresponding time constant in a solution droplet. Additionally, for a given heating rate and drop size, the time required for the solution droplet to reach a new equilibrium size decreases as its salt concentration increases. This occurs because in the more concentrated drops less water needs to evaporate to lower the water activity to the point where a new equilibrium state is established. The smaller fractional change of radius in the more concentrated drops is also clearly demonstrated in Fig. 6.

VI. Conclusions

The laser-induced heating of both a pure water droplet and one containing various concentrations of NaCl has been determined both for short and long heating periods. For the case of short heating times, in which the drop radius does not change appreciably, an analytical solution for the drop temperature rise has been developed. This solution is an extension to Armstrong's[4] analytical solution to the temperature rise in a pure water droplet.

The full governing equations to the heating process were also solved numerically for the case of long heating periods. It was shown that the temperature and radial changes in the drop are strongly influenced by the incident beam intensity and the salt concentration in the drop.

The calculations here were done in terms of the parameter $I_0\alpha$. In a more general solution, the explicit concentration dependence of the bulk absorption coefficient α would be included.

References

1. H. C. van de Hulst, *Light Scattering by Small Particles* (Dover, New York, 1981).
2. A. Ashkin and J. M. Dziedzic, "Observations of Optical Resonances of Dielectric Spheres by Light Scattering," Appl. Opt. **20**, 1803 (1981).
3. G. E. Caledonia, and J. D. Teare, J. Heat Transfer **99**, 281 (1977).
4. R. L. Armstrong, "Aerosol Heating and Vaporization by Pulsed Light Beams," Appl. Opt. **23**, 148 (1984).
5. R. B. Bird, W. E. Stewart, and E. N. Lightfoot, *Transport Phenomena* (Wiley, New York, 1980).
6. F. A. Williams, "On Vaporization of Mist by Radiation," Int. J. Heat Mass Transfer **8**, 575 (1965).
7. A. W. Stelson and J. H. Seinfeld, "Relative Humidity and Temperature Dependence of the Ammonium Nitrate Dissociation Constant," Atmos. Environ. **16**, 983 (1982).
8. S. H. Harned and B. B. Owne, *The Physical Chemistry of Electrolytic Solutions* (Reinhold, New York, 1958).
9. W. J. Hamer and Y. C. Wu, "Osmotic Coefficients and Mean Activity Coefficients of Uni-Univalent Electrolytes in Water at 25°C," J. Phys. Chem. Ref. Data **1**, 1047 (1972).
10. H. F. Gibbard, G. Scatchard, R. A. Rousseau, and J. L. Creek, "Liquid-Vapor Equilibrium of Aqueous Sodium Chloride from 298 to 373 K and from 1 to 6 mole kg^{-1} and Related Properties," J. Chem. Eng. Data **19**, 281 (1974).
11. L. A. Bromley, A. E. Diamond, E. Salami, and D. G. Wilkins, "Heat Capacities and Enthalpies of Sea Salt Solutions to 200°C," J. Chem. Eng. Data **15**, 246 (1970).
12. M. R. Querry, R. C. Waring, W. A. Holand, G. M. Hale, and W. Nijm, "Optical Constants in IR for Aqueous NaCl," J. Opt. Soc. Am. **62**, 849 (1972).

This work was supported by U.S. Environmental Protection Agency grant R-810857. The authors wish to thank Stephen Arnold and Robert L. Armstrong for helpful input.

CHAPTER 3

AEROSOL PARTICLE MOLECULAR SPECTROSCOPY

by :

S. Arnold*

E.K. Murphy*

G. Sageev+

Published in Applied Optics, **24**, 1048, (1985)

*Department of Physics, Polytechnic Institute of New York, Brooklyn, New York, 11201

+Department of Chemical Engineering, California Institute of Technology, Pasadena, CA, 91125

Reprinted from Applied Optics, Vol. 24, page 1048, April 1, 1985

Aerosol particle molecular spectroscopy

S. Arnold, E. K. Murphy, and G. Sageev

The molecular spectroscopy of a solution particle by structure resonance modulation spectroscopy is discussed [S. Arnold and A. B. Pluchino, "Infrared Spectrum of a Single Aerosol Particle by Photothermal Modulation of Structure Resonances," Appl. Opt. 21, 4194 (1982); S. Arnold *et al.*, "Molecular Spectroscopy of a Single Aerosol Particle," Opt. Lett. 9, 4 (1984)]. Analytical equations are derived for time dependence of the particle radius as it interacts with a low intensity IR source (<20 mW/cm^2). This formalism is found to be in good agreement with pulsed experiments. Working equations for the spectroscopy are derived for both constant and periodic IR excitation.

I. Introduction

Recently a means for obtaining the IR absorption spectrum of a single aerosol particle was disclosed. This spectroscopy,[1,2] based on the IR modulation of visible structure resonances, opens a new window for following the molecular nature of a solution particle in the presence of radiation and various gases. A clear application of structure resonance modulation spectroscopy (SRMS)[2] is in elucidating the role of gaseous reactants in the acidification of an aerosol droplet. In addition, since SRMS depends on radiation-induced evaporation from the droplet, the spectroscopy may be used in understanding local processes involved in the propagation of IR radiation through an aerosol.

In what follows we (a) briefly review the SRMS technique, (b) disclose a simple model for explaining the modulation of structure resonances, and (c) show that this model gives good agreement with our present experimental data.

II. Structure Resonance Modulation Spectroscopy

SRMS[2] utilizes the narrow morphological resonances of a single micron sized particle as seen in the visible as a caliper for measuring the size change of the particle in the presence of IR radiation. This technique enables one to obtain a quantitative broadband IR absorption spectrum of the particle[1,2] and to follow temporal effects associated with this absorption. Thus the SRMS approach is distinct from experiments on a polydispersed cloud of submicron particles, because in such a sample the structure resonance caliper is not available and polydispersivity keeps one from understanding the detailed interaction of the IR radiation with a single particle.[1] Nonetheless for a solution droplet the manner in which particle size is changed in the presence of IR radiation was first proposed to understand experimental observations on a polydispersed submicron aerosol.[3] Thus Campillo *et al.*[3] have shown that the heat imparted to an aerosol cloud by a CO_2 laser beam may be used to modulate the visible scattered light produced by a collinear beam from a He–Ne laser. The visible scattered light was modulated apparently because of the local photothermally induced change in particle size. When IR radiation is absorbed by a small solution drop in equilibrium with water vapor, the droplet evaporates slightly; it shrinks in size. The evaporation is caused by the increase in vapor pressure at the surface of the drop as its temperature increases. The new smaller size is stable as long as the radiation is continuous.[2] The mechanism for this phenomenon may be understood for an ideal solution in terms of Raoult's law. Simply stated, the vapor pressure of water at the surface of such a solution is the vapor pressure of pure water P_0 times the mole fraction of water in the solution X_w. When a drop is heated, the vapor pressure P_0 increases; a flux of vapor is emitted into the external medium, and the drop shrinks. Since this shrinkage causes a decrease in the mole fraction of water within the particle, the vapor pressure at the surface of the drop begins to fall. Eventually the particle reaches a vapor pressure equal to the external environment and stabilizes in size.

In the work on a cloud of polydispersed particles,[3] the size-dependent structure associated with the scattered

S. Arnold and E. K. Murphy are with Polytechnic Institute of New York, Physics Department, Brooklyn, New York 11201. The other author is with California Institute of Technology, Department of Chemical Engineering, Pasadena, California 91125.

Received 17 August 1984.
0003-6935/85/071048-06$02.00/0.

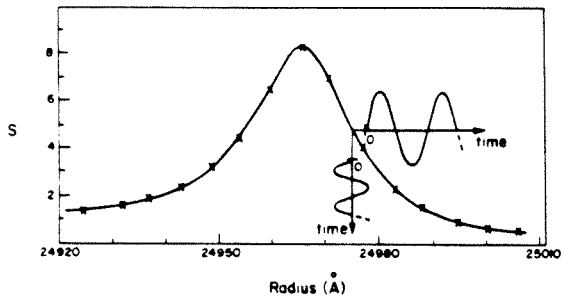

Fig. 1. Back scattered intensity vs particle size for an incident wavelength of 5346 Å. The refractive index is 1.331.

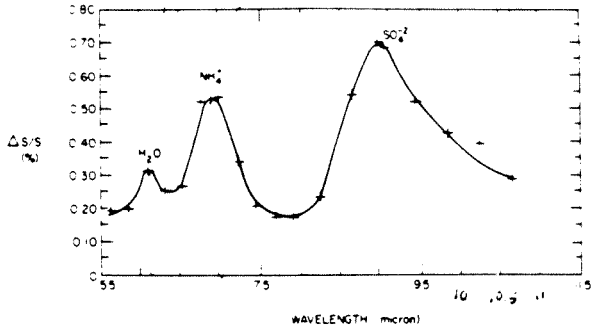

Fig. 2. SRMS spectrum taken on a single solution drop of $(NH_4)_2SO_4$ about 10 μm in diameter.

light was neglected, and consequently interpretation of the scattered light intensity was incomplete. This limits the degree to which one can obtain accurate absorption data. In addition the high intensities needed (>1 W/cm^2) in this case limit the spectral range over which measurements can be made. In SRMS these limitations are overcome by using the properties of structure resonances. The chief advantages of this method are a full accounting for size related effects and a reduction in the IR intensity requirements by more than 3 orders of magnitude.[1] This latter advantage makes possible the use of simple broadband light sources (e.g., Globar) from which a continuous spectrum of the particle may be obtained.[2]

For the weak intensity produced by a monochromatized incandescent IR source (~10-cm^{-1} bandwidth), the size change of a particle 5 μm in diameter may be smaller than 1 Å. However, this size change is easily detected by utilizing the properties of the particle's structure resonances. To do this the narrowband radiation from a tunable dye laser is positioned at the low-wavelength side of a structure resonance of the particle. This resonance, detected through visible scattered light,[4] is a natural electromagnetic mode of the particle.[5] It can be shown[1] that a fractional change in particle radius $\delta a/a$ leads precisely to the same change in resonant wavelength $\delta\lambda_r/\lambda_r$. Thus a given resonance is shifted to shorter wavelength as the particle shrinks. If the incident radiation is positioned at the short-wavelength side of a resonance, a reduction in particle size will lead to an increase in scattered light. Figure 1 shows a Mie calculation of the backscattered light S at 5346 Å from a particle with a refractive index of 1.331 in the size range from 2.4920 to 2.5010 μm. This structure resonance is clear. On the verticle time axis we suppose that the size is made to oscillate harmonically. As a result the scattered light will oscillate as shown on the horizontal time axis. The transfer parameter describing the scattered light change with size is $\beta = (a/S) \cdot (\partial S/\partial a)$. This transfer parameter β is obtained by measuring the excitation spectrum of the scattered light near the wavelength of the dye laser. Due to the pronounced nature of these resonances, the excitation spectrum is virtually a function of optical size $(2\pi a/\lambda)$ near resonance, and as a consequence the wavelength transfer function [i.e. $(\lambda_r/S) \cdot (\partial S/\partial \lambda_r)$] is essentially equal to $-\beta$. Thus the excitation spectrum provides us with a direct measure of β; it calibrates the SRMS technique. The value of β at the point of the harmonic disturbance in the backscattering spectrum in Fig. 1 is −2500. Resonances may also be seen at other scattering angles. In the original work on SRMS by Arnold *et al.*[2] the scattered light was observed normal to the incident light. For this experiment a value for β of −4300 was measured. For such a value a −0.1-Å change in radius out of 2.5 μm (4 ppm) leads to a 1.2% change in scattered light. With periodically modulated IR, a fluctuation in scattered light of ~1% is easily detected.

To obtain an SRMS spectrum we irradiate a levitated microparticle with a temporally chopped IR source and phase sensitively detect the corresponding fluctuation in the visible scattered light.[2] The IR radiation is provided by a Globar followed by a monochromator (bandwidth ~10 cm^{-1}). The visible source is a dye laser (bandwidth ~0.3 Å) with its radiation tuned to a wavelength in the region of a structure resonance (a wavelength which optimizes the transfer parameter β). The resulting SRMS spectrum is a record of the fluctution in visible scattered light vs IR wavelength.

An example of an SRMS spectrum of an $(NH_4)_2SO_4$ drop is shown in Fig. 2. This drop, which was nearly saturated, was 10 μm in diameter. Although the characteristic molecular resonances are broadened by saturation effects due to large particle size in comparison with the absorption depth of the light, the individual vibrational lines for H_2O, NH_4^+, and $SO_4^=$ are evident. To understand both the amplitude and shape of this spectrum one must investigate the physical processes involved. In what follows, we review our current understanding of SRMS, point out its limitations, present a comprehensive model for the spectroscopy, and supply an experimental test of this model.

In earlier work,[1] we gave an equation relating the fractional change in scattered light $\delta S_s/S$ produced by constant IR radiation and measured after the new size equilibrium is reached:

$$\delta S_s(\lambda_2)/S = F_s\beta(\lambda_2)Q_a(\lambda_1)I(\lambda_1), \quad (1)$$

where λ_1 and λ_2 are the infrared (excitation) and visible (probe) wavelengths, Q_a is the particle absorption ef-

ficiency, and I is the infrared intensity. With knowledge of the function F_s, Eq. (1) forms the basis for the measurement of Q_a at a constant IR intensity.[2] The form of F_s given in Refs. 1 and 2 applied to the case of a dilute nonelectrolytic solution and is expected to be a crude approximation when applied to concentrated electrolytic solutions. Our first major goal is to arrive at a more realistic form for the factor F_s.

The static approach to SRMS as described by Eq. (1) is difficult to use in obtaining continuous IR spectra due to the weak intensities available from continuous IR sources. To improve the SNR, it is necessary to use a modulated excitation source and phase sensitively detect the scattered light fluctuations. Consequently, Eq. (1) must be replaced with a dynamical form. Although the dynamical equations governing the coupling between a heated droplet and its vapor field are generally nonlinear, experimental evidence indicates that for the weak intensities used in SRMS ($\langle 20$ mW/cm^2), a simple analytical form can be obtained. Arnold *et al.*[2] have shown experimentally that the amplitude of the scattered light modulation $\delta S_s \bar{S}$ is directly proportional to $\beta(\lambda_2) \cdot Q(\lambda_1) \cdot I_1(\lambda_1)$, where I_1 is the amplitude of the first harmonic of the IR intensity, and $\bar{S}$ is the average scattered light. Thus we define a new factor F_ω through

$$\delta S_\omega(\lambda_2)/\bar{S} = F_\omega \beta(\lambda_2) Q_a(\lambda_1) I(\lambda_1). \tag{2}$$

In the next section we will provide a physical basis for Eqs. (1) and (2) and obtain expressions for F_s and F_ω.

III. Model

The equations describing the detailed coupling between a heated drop and the associated hydrodynamic modes of external gas and vapor are in general nonlinear.[6] Due to this inherent nonlinearity, we lean on experimental evidence in developing a model for the interaction of such a drop with weak radiation. Figure 3 shows a typical oscillogram of the visible light scattered from a particle of $(NH_4)_2SO_4$ 5 μm in diameter in the presence of radiation from a Nernst glower. The particle was held in equilibrium at room temperature above a saturated solution of KCl. Addition of N_2 gas brought the total pressure to 1 atm. The concentration of $(NH_4)_2SO_4$ in the drop was 38% by mass. Although the IR intensity is square wave modulated at 20 Hz one can readily see that the scattered light signal is triangular in form. This different form is not due to a variation in β with size. It is rather the result of a phase boundary relaxation process with a characteristic time which is longer than 1/40 sec, a rate smaller than 40 sec^{-1}.

The rates usually associated with establishing steady state in vapor and thermal transport, β_v and β_t, are

$$\beta_v \sim \frac{3D}{a^2} \qquad \beta_t \sim \frac{K_g}{\rho C_g a^2},$$

where D is the diffusion constant for water vapor through air, and K_g, ρ, and C_g are the thermal conductivity, density, and specific heat of the gas, and a is the particle radius. For a particle 5 μm in diameter in air

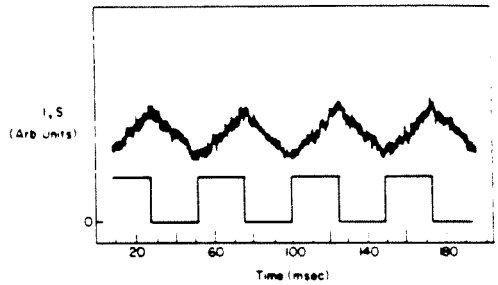

Fig. 3. Oscillogram of both scattered light modulation (above) and incident IR intensity (below) from a $(NH_4)_2SO_4$ particle 5 μm in diameter. The frequency of the incident visible light was positioned on the low-wavelength side of a structure resonance.

at atmospheric pressure and room temperature, each of these rates is of the order of 10^7 sec^{-1}. Since the phase boundary relaxation rate estimate from Fig. 3 is <40 sec^{-1} we will assume that the phenomena described in the previous section may be analyzed with the temperature and vapor fields in steady state. In addition, since the temperature increase over ambient is $<10^{-2}$°C, hydrodynamic influences on heat and mass transport are expected to be negligible.[7] With these reasonable assumptions, the temperature and vapor fields will obey Laplace's equation[7]

$$\nabla^2 C = \nabla^2 T = 0 \tag{3}$$

outside the particle. The radiative power absorbed by the particle P_a is lost through thermal conduction into the ambient gas and through evaporative losses in which each gram lost carries away the appropriate latent heat L:

$$P_a = -\oint (K_g \nabla T + LD\nabla C) \cdot \hat{n} ds. \tag{4}$$

In Eq. (4) the integration is carried out over the surface of the particle. The power absorbed is given properly by Mie theory.[8] In this theory the power absorbed by the particle is an absorption efficiency Q_a times the power incident on the particle's geometrical cross section:

$$P_a = Q_a \pi a^2 I. \tag{5}$$

Energy absorbed is conducted quickly within the particle so that even though the distribution of internal heat sources is anisotropic,[9] this anisotropy almost completely vanishes. Consequently we will assume a condition of spherical symmetry. Combining the assumption of steady state [Eq. (3)] with that of spherical symmetry produces vapor and temperature fields:

$$C(r) = \frac{(C_s - C_\infty)a}{r} + C_\infty \qquad T(r) = \frac{(T_s - T_\infty)a}{r} + T_\infty, \tag{6}$$

respectively, where C_s and T_s are the vapor density and temperature at the particle's surface, and C_∞ and T_∞ are the same quantities far from the particle. Strictly speaking, Eq. (6) should be modified to include the effects of the finite mean free path. In the present case, however, the mean free path is much smaller than the particle size, and the gas is consequently treated as

continuous; mean free path effects are neglected. In what follows $(C_s - C_\infty)$ and $(T_s - T_\infty)$ will alternatively be referred to as δC and δT, respectively.

Since the solution will be electrolytic in the present case, the water vapor concentration at the surface is arrived at by utilizing Raoult's law and the van't Hoff factor.[10] Thus

$$C_s = [1 - i(1 - X_w)]C_p, \tag{7}$$

where X_w is the mole fraction of water in the drop, C_p is the vapor concentration above pure water, and i is the van't Hoff factor. Typical perturbations in particle radius for SRMS are small enough (<1 part in 10^3) to allow the analysis of the change in vapor pressure to be carried out to first order in $\delta a/a$. A corresponding approximation will be made for temperature; the analysis will be carried out to first order in $\delta T/T$. On this basis the change in C_s due to changes in both X_w and C_p is

$$\delta C_s = iC_p\delta X_w + [1 - i(1 - X_w)]\delta C_p. \tag{8}$$

The change in C_p is obtained by combining the Clausius-Clapeyron equation and the ideal gas law. To first order in $\delta T/T$,

$$\delta C_p = C_p\left(\frac{LM}{RT} - 1\right)\frac{\delta T}{T}, \tag{9}$$

where M is the molecular weight of the vapor, and R is the universal gas constant. The change in X_w is obtained from the change in radius of the particle under the assumption of constant particle density to first order in $\delta a/a$:

$$\delta X_w = \frac{3X_w(1 - X_w)}{f_w}\frac{\delta a}{a}, \tag{10}$$

where f_w is the mass fraction of water.

Overall δC_s may be expressed in terms of size and temperature changes by combining Eqs. (8), (9), and (10),

$$\delta C_s = C_p\left\{\frac{3iX_w(1 - X_w)}{f_w}\frac{\delta a}{a} + [1 - i(1 - X_w)]\left(\frac{LM}{RT} - 1\right)\frac{\delta T}{T}\right\}. \tag{11}$$

Ultimately we are after the manner in which the radius shrinks with time. A useful relationship for determining this comes from considering the mass loss of the drop. Simply speaking,

$$\frac{-dm}{dt} = -\oint D\nabla C_{r=a}\cdot\hat{n}ds. \tag{12}$$

On evaluating Eq. (12), using Eqs. (6), we obtain

$$-\rho_p a\dot{a} = D\delta C_s, \tag{13}$$

where ρ_p, the particle density, is assumed to remain constant. Recall that experimentally we are looking at a change in radius of <1 part in 10^3. Consequently, the radius will be considered to be a sum of a constant part a_0 and a time varying part $\epsilon(t)$. Combining Eqs. (13) and (11) we obtain

$$-\dot{\epsilon} = \frac{DC_p}{\rho_p a_0}\left\{[1 - i(1 - X_w)]\left(\frac{LM}{RT} - 1\right)\frac{\delta T}{T} + \frac{3iX_w(1 - X_w)}{f_w}\frac{\epsilon}{a_0}\right\}. \tag{14}$$

This simple linear first-order differential equation [Eq. (14)] is almost our equation of motion. However, we must express δT in terms of the incident intensity and other relevant physical quantities. To do this we return to Eq. (4). Evaluating Eq. (4) [using Eqs. (5) and (6)] we obtain

$$\delta T = \frac{1}{K_g}\left(\frac{Q_a}{4}Ia - LD\delta C_s\right). \tag{15}$$

Substituting for δC_s in Eq. (15) from Eq. (11), we obtain

$$\delta T(1 + LZ) = \frac{1}{K_g}\left[\frac{Q_a Ia}{4} - \frac{3iLDC_pX_w(1 - X_w)}{f_w}\frac{\epsilon}{a_0}\right], \tag{16}$$

where

$$Z = \frac{DC_p}{K_g T}[1 - i(1 - X_w)]\left(\frac{LM}{RT} - 1\right).$$

Finally, by combining Eq. (16) with Eq. (14) we obtain a linearized equation for the motion of the phase boundary:

$$\dot{\epsilon} = -\alpha I - \gamma\epsilon, \tag{17}$$

where

$$\alpha = \left(\frac{Z}{LZ + 1}\right)\frac{Q_a}{4\rho_p},$$

$$\gamma = \frac{3DC_pi}{\rho_p a_0^2 f_w}\cdot\frac{X_w(1 - X_w)}{LZ + 1} + \frac{Q_a IZ}{4a_0\rho_p(LZ + 1)}. \tag{18}$$

For the intensities normally used in SRMS the second term in Eq. (18) is much smaller than the first and may be neglected. For example, in the first experiments by Arnold *et al.*[2] one calculates that the first term in Eq. (18) is more than 100,000 times the second term. Thus the relaxation rate γ in our model is, to within a good approximation, independent of the absorbed energy. This is distinct from the case of pure water (i.e., $1 - X_w = 0$), where the relaxation rate is directly proportional to the absorbed energy, and any imbalance in temperature leads to complete evaporation.[11] It is interesting to compare γ with the vapor relaxation rate β_v. Using Eqs. (1) and (18) we find

$$\gamma = \beta_v\left(\frac{iC_p}{\rho_p f_w}\right)\cdot\frac{X_w(1 - X_w)}{LZ + 1}. \tag{19}$$

Since the ratio of the density of water vapor to the density of liquid water, C_p/ρ_p, near room temperature is 10^{-5}, one immediately can see the large effect which evaporation has on the relative magnitude of γ and β_v. The factor $X_w(1 - X_w)/[LZ(L) + 1]$ further lowers γ with respect to β_v. For the conditions for which the scattered light fluctuations were recorded in Fig. 3 we calculate γ to be 11.6 sec^{-1}. Consequently the phase boundary would take 86 msec to relax, which is consistent with the lower limit estimated from Fig. 3. In what follows we will attempt to test Eq. (19) in a more quantitative fashion.

IV. Experimental

Here we describe the experimental setup and procedure used in measuring the relaxation rate γ. The experimental value of γ obtained here is a direct test of the theoretical development in the previous section.

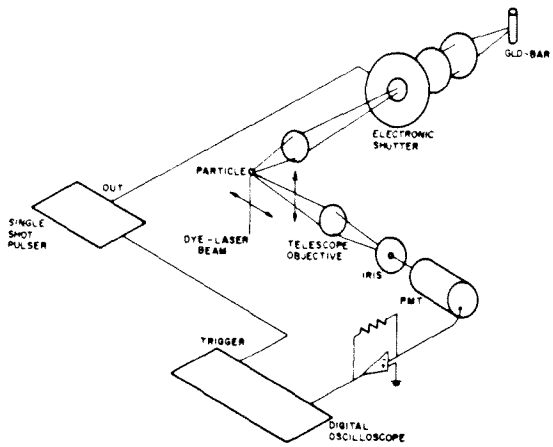

Fig. 4. Experimental setup for transient light scattering measurements.

The particle is electrically suspended within a sealed chamber by use of an electrodynamic trap.[12] This trap is optically servo controlled[13] so that the particle is maintained at the center of the chamber, and its mass is directly monitored. A sample particle was prepared by injecting a dilute solution droplet of ammonium sulfate from an impulse jet into the chamber. Once the drop was trapped, the chamber was evacuated down to a pressure of 1 Torr, at which point the particle consisted of solid ammonium sulfate.

After the evacuation, water vapor was bled into the chamber from a tube attached to the vacuum manifold. The relative humidity in the chamber was maintained at a constant level by utilizing a saturated salt solution as the source of water vapor. Since the relative humidity in the chamber exceeded the deliquescence point of $(NH_4)_2SO_4$, the particle absorbed water. The deliquescence point was observed optically by the gradual appearance of well-defined Mie patterns in the far field. Additionally, the increase in weight of the particle was observed by the increase in balancing voltage. At size equilibrium, the mass fraction of water in the particle was obtained from the levitating voltage before and after the addition of the vapor. At this point N_2 was bled into the chamber so that the experiment was run at a total pressure of 200 Torr. The pressure was raised to decrease the mean free path of the gas molecules so that heat and mass transport processes would be in the realm of low Knudsen numbers, the continuum regime, consistent with our proposed model. After the desired pressure was reached, the positions of a few structure resonances were detected in the frequency spectrum of Mie scattering[4] at 90°. From the measured positions of these resonances, which were found to be stable (consistent with vapor pressure equilibrium), the size of the particle was determined.[5] At this point the sample was irradiated with a square pulse of broadband radiation from a Nernst glower (Fig. 4). The pulse was generated for a specific time by utilizing an electromechanical shutter with opening and closing times of 1 msec.

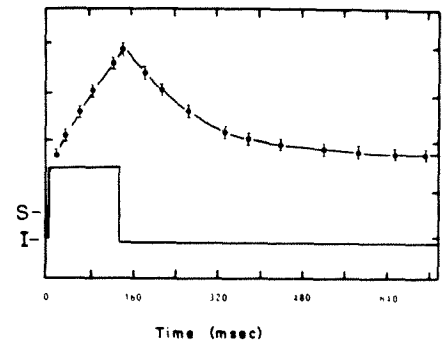

Fig. 5. Light scattering transient from a solution particle of $(NH_4)_2SO_4$ with a radius of 6.2 μm and a water mole fraction of 0.89 ± 0.01. The lower trace shows the measured IR pulse.

For short heating periods and fast relaxation rates the response of the particle to the heat pulse was obtained from the change in the scattered light. In this case, the dye laser was tuned to the low side of a structure resonance where a small fluctuation in the particle size causes a large fluctuation in the scattered light. For longer heating periods and relaxation rates the particle response was observed directly from the changes in the balancing voltage. In all cases, the response of the particle was recorded on a digital oscilloscope. Data from such a recording are shown in Fig. 5. As one can see, the particle relaxed back to its original size once the heat source is turned off.

For the data shown in Fig. 5, the particle size as measured from the position of structure resonances[5] was 6.2 μm. The mole fraction of water in this particle was measured to be 0.89 ± 0.01, consistent with complete saturation at 25°C.[14] From the ambient temperature and associated thermodynamic constants in Eq. (18), we calculate a relaxation rate of 173 msec in good agreement with the measured value of 160 ± 20 msec taken from the logarithmic fit shown in Fig. 6. The

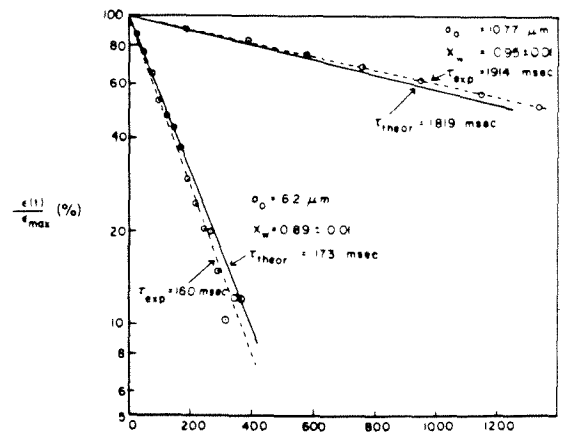

Fig. 6. Scattered light vs time after IR intensity is turned off. The solid lines are theoretical predictions based on Eq. (19). The pressure of N_2 gas plus vapor was 200 Torr.

solid lines in Fig. 6 are theoretical predictions based on Eq. (17). From the other experiment in Fig. 6 we observe that a larger particle containing more water has a smaller relaxation rate, consistent with theory.

V. Discussion

Based on the good agreement between our model and the experimental results shown in Fig. 6, we use the equations developed earlier to calculate the new functionality of the factor F in Eq. (1). For constant excitation, $\dot{\epsilon} = 0$, Eq. (17) gives the particle size change at equilibrium as

$$\epsilon_e = -\frac{I\alpha}{\gamma}. \tag{20}$$

Recalling that $\delta S/S = \beta\epsilon/a_0$, one can substitute Eqs. (18) and (20) into Eq. (1) and obtain the following expression for F_s:

$$F_s = \frac{Za_0 f_w}{12DC_p iX_w(1 - X_w)}. \tag{21}$$

It should be pointed out that Eq. (21) reduces to the earlier expression presented in Refs. 1 and 2 in the limit of dilute nonelectrolytic solutions.

For a periodically modulated excitation source, at angular frequency ω, the factor F in general will depend on ω. If we suppose a harmonic excitation $I = I_1 \exp(j\omega t)$, the corresponding size fluctuation is

$$\epsilon_1(t) = -\frac{\alpha I_1}{(\omega^2 + \gamma^2)^{1/2}} \exp[j(\omega t + \phi)], \tag{22}$$

where $\phi = \tan^{-1}(-\omega/\gamma)$. In practice the quantity I_1 is the first Fourier coefficient of the modulated intensity (e.g., $I_1 = 2I_m/\pi$ for a square wave, where I_m is the maximum intensity). Thus in terms of the amplitude of the first harmonic of the scattering signal (as detected by a phase sensitive detector), we find the value of F_ω to be

$$F_\omega = \frac{Z}{4a_0\rho_p(\omega^2 + \gamma^2)^{1/2}(LZ + 1)}. \tag{23}$$

From Eq. (23) one sees the large effect of the modulation frequency ω on the function F_ω and, therefore, on the scattering light fluctuation. For large particles, where γ may be <1 sec^{-1}, one must go to extremely slow modulations [linear frequency $< (2\pi)^{-1}$ Hz] to optimize the signal. Fortunately, for aerosol size particles near deliquescence, more manageable values for γ are obtained.

VI. Conclusions

In the foregoing, we have presented a simple model for understanding the kinetics of the processes accompanying the structure resonance modulation of a solution droplet. Our experiments indicate that the model contains most of the essential features which are involved. Our assumptions are specific in applying to the case of low intensity and low Knudsen number. The sensitivity of the relaxation rate to size suggests that our model will prove useful in determining the degree of polydispersivity in experiments on the temporal behavior of the photothermal modulation signal from aerosols.[3] Certainly as one reduces ambient pressure further, the importance of finite mean free path will complicate further our model. Wagner[15] has extensively investigated evaporation and condensation in quasi-thermal-equilibrium and finds that the efficiency for water sticking enters both transfer processes as the Knudsen number increases. On this basis one may expect that phase boundary relaxation measurements made in the large Knudsen number regime may be used to investigate water sticking. Such an investigation is currently under way in our laboratory.

We would like to thank M. Neuman (presently at the National Research Council, Manitoba) for taking some preliminary data in this study. We are grateful to Jeff Rosenfeld of the Microparticle Photophysics Laboratory (at the Polytechnic) for his help in computer interfacing. One of us (E. K. M.) was cooperatively supported by a grant from The National Science Foundation and the Chemical Research and Development Center of the Army under NSF grant ATM-8413574. S. Arnold was also supported by this grant and a U.S. Joint Services Electronics contract (F49620-82-C-0084).

References

1. S. Arnold and A. B. Pluchino, "Infrared Spectrum of a Single Aerosol Particle by Photothermal Modulation of Structure Resonances," Appl. Opt. **21**, 4194 (1982).
2. S. Arnold, M. Neuman, and A. B. Pluchino, "Molecular Spectroscopy of a Single Aerosol Particle," Opt. Lett. **9**, 4 (1984).
3. A. J. Campillo, C. J. Dodge, and H.-B. Lin, "Aerosol Particle Absorption Spectroscopy by Photothermal Modulation of Mie Scattered Light," Appl. Opt. **20**, 3100 (1981).
4. A. Ashkin and J. M. Dziedzic, "Observation of Optical Resonances of Dielectric Spheres by Light Scattering," Appl. Opt. **20**, 1803 (1981).
5. P. Chylek, J. T. Kiehl, and M. K. W. Ko, "Optical Levitation and Partial Wave Resonances", Phys. Rev. A **18**, 2229 (1978).
6. G. Sageev and J. H. Seinfeld, "Laser Heating of Aqueous Aerosol Particles" Appl. Opt. **23**, 4368 (1984).
7. L. D. Landau and E. M. Lifshitz, *Fluid Dynamics* (Pergamon, London, 1959).
8. G. Mie, "Beitrage zur Optik tüber Medien Speziell Kolloidaler Metallösungen," Ann. Phys. **25**, 377 (1908).
9. P. W. Dusel, M. Kerker, and D. D. Cooke, "Distribution of Absorption Centers Within Irradiated Spheres," J. Opt. Soc. Am. **69**, 55 (1979); A. B. Pluchino, "Photophoretic Force on Particles for Low Knudsen Number," Appl. Opt. **22**, 103 (1983); S. Arnold and M. Lewittes, "Size Dependence of the Photophoretic Force," J. Appl. Phys. **53**, 5314 (1982).
10. See, for example, E. A. Moelwyn-Hughes, *Physical Chemistry* (Pergamon, London, 1957), p. 823.
11. M. B. Baker, "Energy Absorption by Volatile Aerosol Particles," Atmos. Environ. **10**, 241 (1976).
12. M. A. Philip, F. Gelbard, and S. Arnold, "An Absolute Method for Single Aerosol Particle Mass Measurement ," J. Colloid Interface Sci. **91**, 507 (1982).
13. S. Arnold, Y. Amani, and A. Orenstein, "Photophoretic Spectrometer," Rev. Sci. Instrum. **51**, 1202 (1980).
14. B. F. Wishaw and R. H. Stokes, "Activities of Aqueous Ammonium Sulphate Solutions at 25°C," Trans. Faraday Soc. **50**, 952 (1954).
15. P. E. Wagner, "Aerosol Growth by Condensation," in *Aerosol Microphysics II* W. H. Marlow, Ed. (Springer, Berlin, 1982), Chap. 5, pp. 129–178.

CHAPTER 4

CONDENSATION RATES OF WATER ON AQUEOUS DROPLETS IN THE TRANSITION REGIME

By :

Gideon Sageev*

Richard C. Flagan*

John H. Seinfeld*

Stephen Arnold+

Published in the J. Coll. Int. Sci., **113**, 421, (1986).

*Department of Chemical Engineering, California Institute of Technology, Pasadena, CA 91125

+Department of Physics, Polytechnic Institute of New York, Brooklyn, New York, 11201

ABSTRACT

The rate of condensation of water on single aqueous solution drops in the transition regime is measured with an electrodynamic balance. Observed characteristic relaxation times are compared with those predicted theoretically to determine the thermal accommodation coefficient, which is found to be unity (consistent with the accepted value in the literature). Due to the large heat of vaporization of water and the experimental conditions used, the relaxation time is relatively insensitive to the water mass accommodation coefficient, although the data would support a value close to unity.

1. INTRODUCTION

There has long been a concern in aerosol science with understanding heat and mass transfer processes to single particles in the non-continuum regime. Several theoretical treatments are available for transport to particles in the non-continuum regime, in which flux expressions are derived that predict transport rates from the free molecule, through the so-called transition regime, to the continuum regime. The crux of these flux theories is their dependence on the Knudsen number, $Kn = \lambda / R_p$, where λ is an appropriately defined mean free path and R_p is the particle radius. In addition, the heat and mass transfer processes are characterized by the thermal and mass accommodation coefficients, α_T and β_M, respectively. The thermal accommodation coeficient α_T can be considered as the ratio of the actual heat transfer flux to that predicted if every molecule thermally accommodates at the surface of the particle. The mass accommodation, or sticking, coefficient β_M is just the fraction of molecules that strike the surface of the particle that adhere to it. The object of the present work is to measure the rate of condensation of water on single aqueous aerosol particles in the transition regime so as to evaluate, if possible, the applicability of existing transition regime flux theories as well as thermal and mass accommodation coefficients.

In the present work water condensation rates are measured on single $(NH_4)_2SO_4$ aqueous solution droplets suspended in an electrodynamic balance, or quadrupole. The medium surrounding the particles consists of an air/water vapor or N_2/water vapor mixture. Two related studies have recently been presented. Arnold et al[1] described similar experiments on suspended aqueous solution droplets in which the transport processes were in the continuum regime. The present work extends the experiments

into the transition regime. Richardson et al[2] have reported measurements of growth rates of NaCl solution droplets in a background of water vapor. The absence of non-condensing gas molecules (i.e., O_2 and N_2) enabled the use of self-diffusion theory in analyzing mass transfer to the droplets. The presence of non-condensing gas molecules in the current system necessitates the use of binary diffusion theory, in describing the mass transport.

In section 2 we describe the experimental system and how particle growth rate measurements were obtained. Section 3 is devoted to a brief summary of applicable transition regime theoretical results for heat and mass transfer rates. Finally, we present in Section 4 the experimental data obtained and their interpretation in light of the theory.

2. EXPERIMENTAL SYSTEM

2.1 The Electrodynamic Balance

The experiments described here were carried out in an electrodynamic balance. As shown in Figure 1, the balance consists of two hyperboloidal endcap electrodes between which a DC potential is held, and a hyperbolic torus to which an AC voltage is applied. The use of this apparatus, as well as its historical development, has been documented by Davis[3] . The dynamic behavior of a charged particle in the electric field inside the chamber has been presented elsewhere[4,5,6] , thus here it will suffice to mention that a charged particle can be stably levitated in the device by applying a DC voltage between the endcaps, V_{dc} , such that

$$q\, C \frac{V_{dc}}{2\, Z_o} = m\, g \qquad [1]$$

where q and m are the particle charge and mass, g is the gravitational constant, Z_o is the distance between the center of the chamber and the endcaps, (which equals 4.49 mm in our case), and C is a geometric constant for the hyperbolic geometry of Figure 1. The value of the geometric constant has been determined theoretically by several authors[4,5]. Phillip et al obtained a value of 0.80 by computing the internal field numerically. Davis et al[4] evaluated C by obtaining an analytical solution to the approximated field in the chamber (by neglecting the presence of the ring electrode). The theortical value for C calculated by Davis is 0.8768. In the theoretical studies above the effect of the ring or the effect of holes in the ring electrode has been ignored; thus, as Davis points out, the value of the geometric constant must be determined experimentally.

As shown in Figure 1, the electrodes (made of stainless steel), are

positioned within a stainless steel container. The electrical connections to the electrodes are made through the bottom plate, along the supporting legs of the electrodes. The particle is illuminated with a HeNe laser the beam which enters through the bottom window of the container and runs vertically through the chamber. The pressure in the chamber is measured with a capacitative manometer, and the temperature is monitored by a thermistor. Additionally, the chamber is held at a constant humidity through a connection to a glass bulb containing a saturated salt solution, ($(NH_4)_2PO_4$ solution in the present case).

In order to facilitate the continuous monitoring of the particle balancing voltage, we have incorporated an automatic servo system into the apparatus, the basic design of which has been described by Arnold et al[8]. As shown in Figure 1, the servo system functions by re-imaging the particle on the edge of a 45° mirror. One photomultiplier tube is placed directly above the edge, while the other is positioned in the direction of the incident light. The optics are adjusted so that when the particle is in the center of the chamber, its image is split across the edge of the mirror. In this fashion, small vertical displacements of the particle result in different current outputs from the two photomultiplier tubes. By feeding the current output of the photomultiplier tubes into a log-ratio amplifier, a correcting signal to the balancing voltage is generated.

2.2 Particle Insertion and Sizing

Particles are introduced into the electrodynamic balance by first removing the top cap (including the Brewster window), and then positioning a droplet impulse jet over the top electode. In the jet (made by Uni Photon System, Inc., model 1), a fluid displacement is achieved by pulsing

a piezoelectric crystal. The purity of the drop is ensured by first flushing the jet with purified water, and then backfilling a minute quantity of salt solution through its glass tip. The droplets are charged inductively as they leave the jet and enter the chamber.

After a particle has been trapped, the chamber is evacuated down to a pressure of about 1 torr in order to dry out the particle and measure the balancing voltage needed to levitate the dried particle. Once this voltage is found, water vapor is bled into the the chamber by opening a valve connecting the chamber to a saturated salt solution. At a particular water vapor concentration the dry particle deliquesces. The final particle size is determined by the relative humidity in the chamber which is governed by the saturated salt solution. The water content of the droplet is computed from the relative voltages of the dry and the deliquesced particle. After the droplet size has stabilized, either air or N_2 is bled slowly into the chamber, raising the pressure to a desired level.

At this point the particle size (which is needed in the subsequent rate calculations) is determined either by its sedimentation rate, or from its "spring-point" potential[6] . When using the sedimentation method, the particle initial balancing voltage, V_{dc}^{o} , is first changed to a new value, V_{off} . The AC field is then turned off and the particle begins to move under the combined influence of gravity and the electric field. In this case a force balance on the particle yields:

$$mg - \frac{q\,C}{2\,Z_o} V_{off} = \frac{6\,\pi\,R_p\,\mu}{C_c} v \qquad [2]$$

where R_p and v are the particle radius and terminal velocity, C_c is the Cunningham correction factor to Stokes drag, and μ is the gas viscosity. Since the particle charge to mass ratio is known from the initial

balancing voltage, the radius R_p can be found by straightforward manipulation of equation [2] resulting in:

$$R_p = \left(\frac{9\,\mu\,v}{2\,C_c\,\rho_p\,g}\left[\frac{V_{dc}^{\circ}}{V_{dc}^{\circ} - V_{off}}\right]\right)^{1/2} \qquad [3]$$

It should be pointed out that when using this method the particle was only allowed to fall about 1 mm around the center of the chamber where the field is relatively uniform. For particles under current investigation (10-20 microns in diameter), an offset of ≈ 2% from the initial voltage, resulted in fall times of 2-5 seconds. The falling particles were observed through a calibrated reticle of a 30 × microscope, and timed manually as they passed through a given distance on the reticle. With the balancing voltage known to 0.1% and asuming that human response time is ≈ 100 msec, the uncertainty in the velocity measurment is ≈ 5%, while for a 2% offset voltage, the uncertainty in the term $\left[\frac{V_{dc}^{\circ}}{V_{dc}^{\circ} - V_{off}}\right]$ is also 5%. Thus the uncertainty in the radius evaluation at atmospheric pressure (where $C_c \approx 1$) is about 5% for a single measurement.

When using the "spring-point" method, the AC trapping voltage is increased to the point at which the particle becomes unstable and begins to oscillate at half the driving frequency[6]. Instability diagrams for the hyperbolic geometry, which show the regions of stable and unstable levitation, have been presented elsewhere[4] . In these diagrams, the instability envelope is expressed as a function of the drag and electric field parameters, $\bar{k}$ and Q ; where $\bar{k} = \frac{12\,\pi\,R_p\,\mu}{C_c\,m\,\omega}$ (for a sphere), and $Q = \frac{8\,V_{ac}^{\bullet}\,g}{\omega^2\,Z_o\,V_{dc}^{\circ}\,C}$ in which $V_{ac}^{\bullet}$ is the spring-point voltage and ω is the driving frequency, (60 Hz in this case). As evident from the equation above,

the calculation of Q requires knowledge of the cell constant C. The value of C for our chamber was found experimentally by placing PSL particles in the chamber and measuring their size from the fall rate and the spring-point method. Since the radius obtained by the fall rate is independent of C, we used results of that method to calibrate the particle. Knowing the radius of the particle, the value of C was varied until the radii obtained by both methods were equal. Our experimental value of C is 0.71, about 10% lower than the theoretical value. This reduction is also in agreement with data presented by Phillip[7] which were obtained in an identical chamber. Thus by measuring $V_{ac}^{\bullet}$, Q can be calculated and the radius is found from the corresponding value of the drag parameter. It should be mentioned that this sizing technique has also been used by Richardson et al[2].; however in the case in which the particles are solid crystals a shape factor multiplying the Stokes drag is required.

2.3 The Growth-Rate Measurement

Particle growth rates were measured by the method of Arnold et al[1]. For completeness a short description of the method is included in what follows. Once the particle diameter is determined, the particle size is decreased slightly from its equilibrium value by heating the droplet, and the rate at which it grows back to its original size once the heating is terminated is recorded. In the first step in the growth rate measurement the automatic servo system is turned on and the microscope eyepiece (Figs. 1 & 2) is replaced with a photomultiplier tube. As is evident from Figure 1, the photomultiplier tube is positioned so as to receive the 90° scattered light from the particle. At this point the shutter, shown in Figure 2, is opened for 1/4 - 1/32 second, thereby exposing the particle to an IR heat source (consisting of a coiled Nicrome wire). During the

heating the particle evaporates slightly and the change in size is reflected by a change in the scattering signal from the photomultiplier tube. The scattering signal is recorded either on a storage scope or on an X-Y recorder from which the particle relaxation time may be determined.

The relationship between the change in the scattered light intensity S from the particle and the change in its diameter is[1,10]

$$\frac{\Delta S}{S} = \beta \frac{\Delta R_p}{R_p} \qquad [4]$$

where β is a transfer function which can become very large ($> 10^3$) near resonance. In converting the scattering signal to growth rates it is crucial that the value of β remains constant. As long as β remains constant, the size relaxation time constant is equal to the scattered light relaxation time constant; thus an exact knowledge of the value of β is not nesecary. To ensure a constant β, we produce only small size fluctuations by heating the particle for a short period. Additionally, the same particle is heated for several different times to check that the relaxation rate remains constant for different changes in the radius. For each reported measurement the decay in the scattered light fluctuation, following heating, was found to be exponential, which as shown by Arnold et al[1] is consistent with a constant value for β.

3. RESPONSE OF AN AQUEOUS DROP TO HEATING AND COOLING

When describing the dynamic behavior of a droplet, initially in equilibrium with its surroundings, whose temperature is suddenly perturbed, one must account for both heat and mass transfer from the drop. In an earlier work, Sageev and Seinfeld obtained both analytical and numerical solutions for the temperature and size of an evaporating drop under the influence of an intense heat source[11]. Those solutions are not applicable here as we are interested in the cooling period, after the heat source is turned off. The description of this process has been addressed by several authors[1,12,13,14], the most comprehensive treatment of which is that of Wagner[12]. The theoretical development Arnold et al[1] can form the basis for extension of the theory of particle growth into the transition regime. We also have noted in the Introduction that another goal of the present study is to obtain estimates of the thermal accommodation coefficient, α_T, and the condensation coefficient, β_M for water. These coefficients arise in the correction terms describing the deviation of the growth rate from that in the continuum regime. As pointed out by Wagner[12], since these correction terms become more dominant as the Knudsen number Kn is increased, it is best to work in either the free molecule or transition regimes in order to obtain estimates of the α_T and β_M.

The mass flux from a drop can be expressed as

$$J_M = \varphi_M D_g \left(\frac{\partial C}{\partial r}\right)_{r=R_p} \qquad [5]$$

where C ic the mass concentration of the diffusing species, D_g is the binary diffusion coefficient of the diffusing species in the background gas, and φ_M is the non-continuum correction to the mass flux. Various forms of φ_M have appeared in the literature[3]. For example, by an approximate

solution to the Boltzmann equation, Sitarski and Nowakowski[15] obtained the following expression for φ_M,

$$\varphi_M = \frac{1 + 3\,\beta_M\,(1 + Z_{ij})^2\,Kn/4\,(3 + 5\,Z_{ij})}{1 + \frac{15\,\pi\,(1 + Z_{ij})^2}{4\,(9 + 10\,Z_{ij})}\left[\left(\frac{\beta_M\,(1 + 2\,Z_{ij})}{\pi\,(3 + 5\,Z_{ij})} + \frac{1}{2\,\beta_M}\right)Kn + \frac{9\,(1 + Z_{ij})^2}{8\,(3 + 5\,Z_{ij})}\,Kn^2\right]} \qquad [6]$$

where Z_{ij} is the ratio of the molecular weight of the diffusing species to that of the background gas. We use the equation above to describe φ_M because in an earlier work by Davis[16,17], mass transfer data was modeled accurately using the same expression.

It should be pointed out that when there exist several vapor species in the system the mean free path for thermal transport λ_T differs from that for mass transport λ_M. The reason for this difference is that heat conduction is carried out by both the diffusing species and the background gas, whereas mass transfer results from the transfer of the diffusing species alone. Therefore we consider λ_T to be the average distance between collisions in the gas mixture, while λ_M is taken as the distance the diffusing species, in our case water molecules, travel between collisions. In the present work we will base the calculations of the Knudsen number on λ_T because, as will be shown in the next section, due to the large heat of vaporization of water the thermal correction φ_T dominates the growth rate of the drop. The computation of λ_T was based on the average properties of the gas mixture through the equation[18],

$$\lambda_T = \frac{\mu}{0.499\,\rho\,\bar{c}} \qquad [7]$$

where $\bar{c}$ is the average molecular velocity in the gas.

Since heat conduction through the drop is much faster than that through the gas, the Biot number for the drop/gas system is much less than unity. Under these circumstances the temperature profile inside the drop can be considered to be uniform and the energy balance on the drop is then given by,

$$\rho_p C_p \frac{R_p}{3} \frac{dT}{dt} = - \frac{Q_a I}{4} - [\varphi_T k (\frac{\partial T}{\partial r})_{r=R_p} + \varphi_M L D_g (\frac{\partial C}{\partial r})_{r=R_p}] \qquad [8]$$

where Q_a and I are the particle absorption coefficient and the incident light intensity respectively, k is the gas thermal conductivity, C_p is the drop heat capacity, L is the water latent heat of vaporization, , and φ_T is the correction to the continuum Fourier heat flux to account for non-continuum conditions. The correction above can be computed by assuming that inside the thermal boundary layer surrounding the drop heat transfer is described by Knudsen flow, while outside the boundary layer heat transfer follows the continuum conduction equation. By matching these two heat fluxes at the boundary layer the following expression can be obtained for φ_T[13],

$$\varphi_T = \frac{R_p}{R_p + l_T} \qquad [9]$$

where

$$l_T = \frac{k (2 \pi M R T)^{1/2}}{\alpha_T P (C_v + R/2)} \qquad [10]$$

where α_T is the thermal accommodation coefficient, P and C_v are the gas pressure and heat capacity, respectively, and R is the gas constant.

Noting that the temperature and concentration fields in the gas phase are established much more quickly than the mass relaxation[1,11]

allows one to approximate the system as if in quasi-steady state. Equations [5] and [8] reduce to:

$$\rho_p \frac{dR_p}{dt} = -\varphi_M D_g \frac{(C_s - C_\infty)}{R_p} \qquad [11]$$

and

$$\frac{Q_a I}{4} = \varphi_T k \frac{(T_s - T_\infty)}{R_p} + \varphi_M L D_g \frac{(C_s - C_\infty)}{R_p} \qquad [12]$$

where C_s and C_∞ are the vapor mass concentrations at the surface and far away from the drop, respectively.

Utilizing Raoult's Law and the Van't Hoff factor i to relate the vapor concentration over the surface of the salt solution to that of pure water gives,

$$C_s = [\,1 - i(\,1 - X_w)\,]\, C^\circ \qquad [13]$$

where X_w is the water mole fraction, and C° is the pure water concentration (on a mass basis).

The variation in water vapor concentration, C_s, with temperature is related to the temperature variation through the Clausius-Clapeyron equation:

$$\frac{dC^\circ}{C^\circ} = \left(\frac{L M}{R T} - 1\right) \frac{dT}{T} \qquad [14]$$

By considering only small changes in the radius we let $R_p(t) = R_{po} + \varepsilon(t)$ where $\varepsilon \ll R_{po}$. Finally substitution of equations [12], [13], and [14] into equation [11] yields the following expression describing the growth rate of the particle,

$$\frac{d\varepsilon}{dt} = -\alpha' I - \gamma' \varepsilon$$

[15]

where α' and γ' are,

$$\alpha' = \left(\frac{Z}{1 + \frac{\varphi_M}{\varphi_T} L Z}\right) \frac{\varphi_M}{\varphi_T} \frac{Q_e}{4 \rho_p} \qquad [16]$$

$$\gamma' = \frac{3 D_g C^\circ i X_w (1 - X_w) \varphi_M}{\rho_p R_{po}^2 f_w (1 + \frac{\varphi_M}{\varphi_T} L Z)} + \frac{Q_e I Z}{4 \rho_p (1 + \frac{\varphi_M}{\varphi_T} L Z)} \frac{\varphi_M}{\varphi_T} \qquad [17]$$

with

$$Z = \frac{D_g C^\circ}{k T} [1 - i (1 - X_w)] [\frac{L M}{R T} - 1] \qquad [18]$$

It should be noted that γ' reduces to that of Arnold et al[1] in the continuum regime (i.e., for $\varphi_M = \varphi_T = 1.0$). Just as in that work, the second term in the equation for γ' may be neglected in comparison with the first term for the intensities used in this experiment.

At the low intensities used in the experiment the second term in equation [17] (involving Q_e and I) is much smaller than the first term and can therefore be neglected. The relaxation rate of the particle radius is given by γ', and its inverse is the charateristic relaxation time τ of the particle. The ratio of the relaxation time to that in the continuum regime τ_c is obtained directly from equation [17] as

$$\frac{\tau}{\tau_c} = \frac{1 + \frac{\varphi_M}{\varphi_T} L Z}{(1 + L Z) \varphi_M} \qquad [19]$$

1. RESULTS AND DISCUSSION

The experimental relaxation times divided by the times predicted by the continuum theory are shown in Figure 3. We also show the ratio of the

theoretical non-continuum relaxation time divided by the theoretical continuum time as expressed by equation [19]. In the theoretical line both α_T and β_M were assumed to be unity. The proximity of the experimentally measured relaxation times and those predicted theoretically indicates that the experimental behavior matches the theoretical prediction quite well over the entire range under study. A summary of the conditions and the results of the experiments is shown in Table 1. The differences in droplet composition seen in Table 1 are caused by small variations in the relative temperature of the chamber and the humidification bulb. It should be pointed out that we have attempted to obtain data at higher Knudsen numbers; however at those conditions the scattered light signal became noisy due to oscillation of the droplet, therefore that data were not analyzed.

To probe the sensitivity of these results to changes in the thermal accommodation and condensation coefficients, we first consider the value of the product (LZ) in the denominator of equation [19]. Under the experimental conditions shown in Table 1, Z ranged from 0.15 to 0.015 g/cal while L is on the order of 580 cal/g. Since both α_T and β_M appear to be of order unity in our case, the condition $\frac{\varphi_M}{\varphi_T} L Z \gg 1$ holds. Looking back at equations [17] and [19], one immediately sees that, due to the large heat of condensation of water, the relaxation rate γ' is more or less independent of the non-continuum correction factor φ_M. Since φ_M contains the water condensation coefficient β_M, the relaxation rate is therefore largely independent of the water condensation coefficient. Thus under these conditions $\tau / \tau_c \approx \varphi_T^{-1}$, and the ratio of the relaxation times equals the thermal non-continuum correction factor.

In Figure 4 we show the theoretical relaxation time divided by the continuum relaxation time as a function of Kn for a thermal accommodation coefficient $\alpha_T = 1.0$ and water vapor condensation coefficient of $\beta_M = 1.0$ and 0.1. The results in Figure 4 indicate that it is not possible to determine conclusively the value of β_M from our data. The closeness of $\beta_M = 1.0$ and 0.1 curves was to be expected from our discussion above. In Figure 5 we show the theoretical relaxation time divided by the continuum time as a function of Kn for a water vapor condensation coefficient $\beta_M = 1.0$ and thermal accommodation coefficient $\alpha_T = 1.0$, 0.8, and 0.5. As expected the relaxation time is more sensitive to the value of α_T than to the value of β_M. Moreover, the experimentally determined relaxation rates indicate that the value of the thermal accommodation coefficient is indeed close to unity.

In order to obtain a better estimate of the sticking coefficients for water in this system, the condition $\frac{\varphi_M}{\varphi_T} L Z \leq 1$ must hold. This condition can be achieved by repeating the experiments at a higher Knudsen number. Assuming we work at a pressure of 25 torr, a temperature of 25° C and a value of Z of about 0.05 g/cal implies that we need to achieve a Knudsen number of order 10.

5. CONCLUSIONS

We have reported the results of an experimental study of the growth of single aqueous solution droplets in the transition regime of heat and mass transfer. In the experiments $(NH_4)_2SO_4$ droplets of diameter between 10 μm and 20 μm were charged and levitated in an electrodynamic balance of quadrupole design, briefly heated from an IR radiation source to induce water evaporation, and then followed by light scattering as they relaxed back to their original equilibrium size. Knudsen numbers were varied between 0.23 and 0.0057 by controlling the total pressure in the system between 21.6 and 736.1 mm Hg.

The object of the experiments was twofold. First, it was desired to evaluate the extent of agreement between the measured relaxation times and those predicted by transition regime heat and mass transfer theories. Second, by comparison of the measured and predicted relaxation times in the transition regime we wished to assess the ability to infer values of the thermal and mass accommodation coefficients, α_T and β_M, respectively, from such relaxation growth experiments.

We have found that the dependence of the measured relaxation times on Knudsen number is well represented by the available theories of heat and mass transfer in the continuum regime. Because of the large latent heat of vaporization of water, the growth process is controlled more by the heat transfer process than by mass transfer of water molecules to the drop. Consequently it was not possible to infer a value of β_M from the data, although the data suggest that a value of β_M close to unity would not be an inconsistent interpretation. The data do afford a determination of α_T, and it was found that the data clearly support a value of $\alpha_T = 1$. This

experimental determination supports the commonly made assumption that the thermal accommodation coefficient for aerosol particles is unity.

6. ACKNOWLEDGEMENTS

This work was supported by U.S. Environmental Protection Agency grant R-810857. S. Arnold was supported by a Chevron Visiting Professorship at the California Institute of Technology and by a National Science Foundation grant ATM-8413574. The authors wish to thank Anthony B. Pluchino of the Aerospace Corporation and Thomas Dunn for their advice during this work.

7. REFERENCES

[1] Arnold S., Murphy E.K., and Sageev G., Appl. Opt., **24**, 1048, (1985)

[2] Richardson C.B., Lin H.B., and Tang I.N., Submitted.

[3] Davis E.J., Aeros. Sci. Tech., **2**, 121, (1983)

[4] Davis E.J., Langmuir, **1**, 379, (1985)

[5] Phillip M.A., Gelbard F., and Arnold S., J. Col. Int. Sci., **91**, 507, (1983)

[6] Frickel R.H., Shaffer R.E. and Stamattoff J.B., Technical report ARCSL-TR-77041, U.S. Arm Armament Research and Development Command, Chemical Systems Laboratory, Aberdeen Proving Ground, Maryland (1978)

[7] Phillip M.A., "An Absolute Method for Aerosol Particle Mass Measurement", M.S. Thesis, MIT, October (1981), page 47.

[8] Arnold S., J. Aerosol Sci, **10**, 49, (1979); Arnold S., Amani Y., Opt. Lett., **5**, 242, (1980); Arnold S., Amani Y. and Orenstein A., Rev. Sci. Inst., **51(9)**, 1202, (1980)

[9] Hamer W. J. and Wu Y. C., J. Phys. Chem. Ref. Data, **1**, 1047, (1972)

[10] Arnold S. and Pluchino A.B., Appl. Opt., **21**, 4194, (1982); Arnold S., Newman M. and Pluchino A.B., Opt. Soc. Am., **9**, 4, (1984)

[11] Sageev G. and Seinfeld J.H., Appl. Opt., **23**, 4368, (1984)

[12] Wagner P.E., in Particle Microphysics II (W.H. Marlow ed.) Springer-Verlag, Berlin P. 129-178

[13] Fukuta N. and Walter L.A., J. Atm. Sci., **27**, 1160, (1970)

[14] Armstrong R.L., Appl. Opt., **23**, 148, (1984)

[15] Sitarski M. and Nowakowski, J. Coll. Int. Sci., **72**, 113, (1979)

[16] Davis E.J. and Ray A.K., J. Aerosol Sci., **9**, 411, (1978)

[17] Davis E.J., Ravindran, P. and Ray A.K., Adv. Coll. Int. Sci., **15**, 1, (1981)

[18] Seinfeld J.H., "Atmospheric Chemistry and Physics of Air Pollution", Wiley, (1985)

Table 1. A summary of the experimental conditions during various runs.

No.	Pressure (mm)	Xw	Temp. (C)	Diameter (microns)	Kn	Relaxation time (msec)
1	21.6	0.91	23.70	13.6	0.239	600
2	34.9	0.91	24.31	12.6	0.172	280
3	43.7	0.89	25.01	11.8	0.150	230
4	51.4	0.88	25.92	11.7	0.132	155
5	48.8	0.92	23.85	19.3	0.079	930
6	79.9	0.92	23.85	19.3	0.052	900
7	121.5	0.91	24.06	18.8	0.035	610
8	203.9	0.90	24.25	18.8	0.021	575
9	736.1	0.90	23.25	19.3	0.0057	735

FIGURE CAPTIONS

Figure 1. A schematic diagram showing the cross section of the electrodynamic balance system.

Figure 2. A schematic diagram of the top view of the electrodynamic balance system.

Figure 3. Experimental relaxation times divided by the calculated theoretical time in the continuum regime, as a function of the Knudsen number. The solid line is the theoretically predicted ratio assuming α_T and $\beta_M = 1.0$.

Figure 4. The effect of the value of the mass condensation coefficient on the relaxation time, for $\alpha_T = 1.0$.

Figure 5. The effect of the value of the thermal accommodation coefficient on the relaxation time, for $\beta_M = 1.0$.

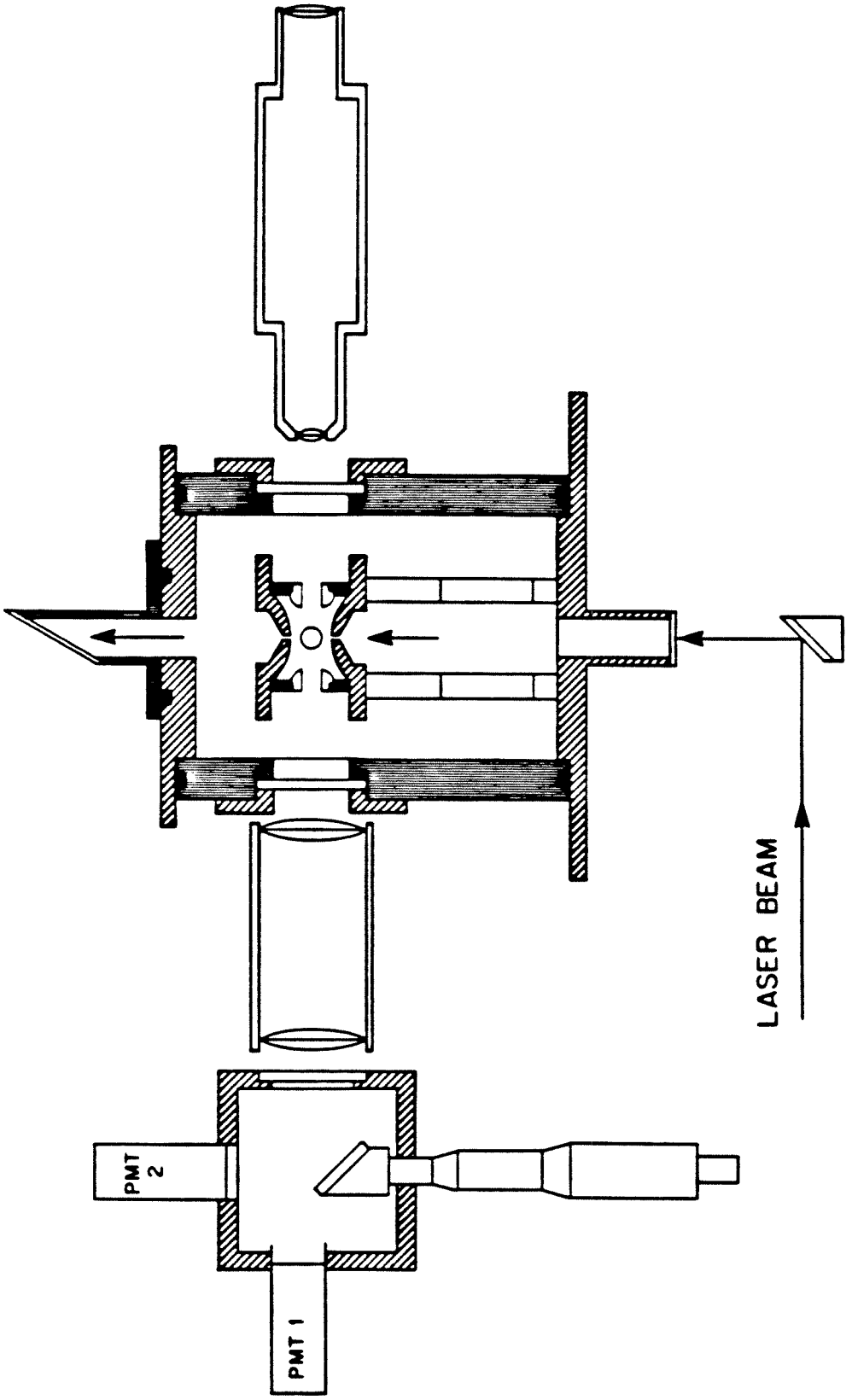

Figure 1. A schematic diagram showing the cross section of the electrodynamic balance system.

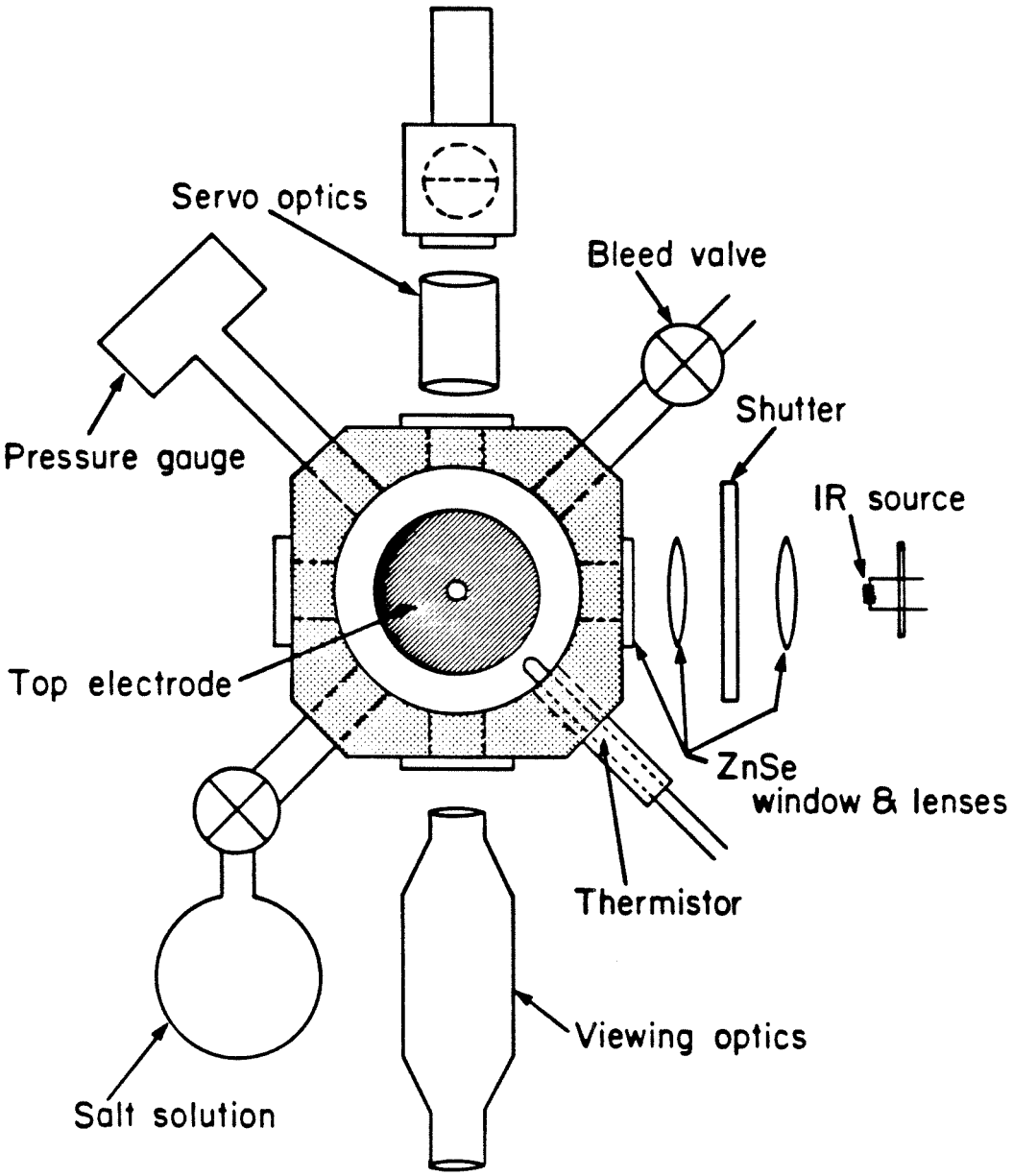

Figure 2. A schematic diagram of the top view of the electrodynamic balance system.

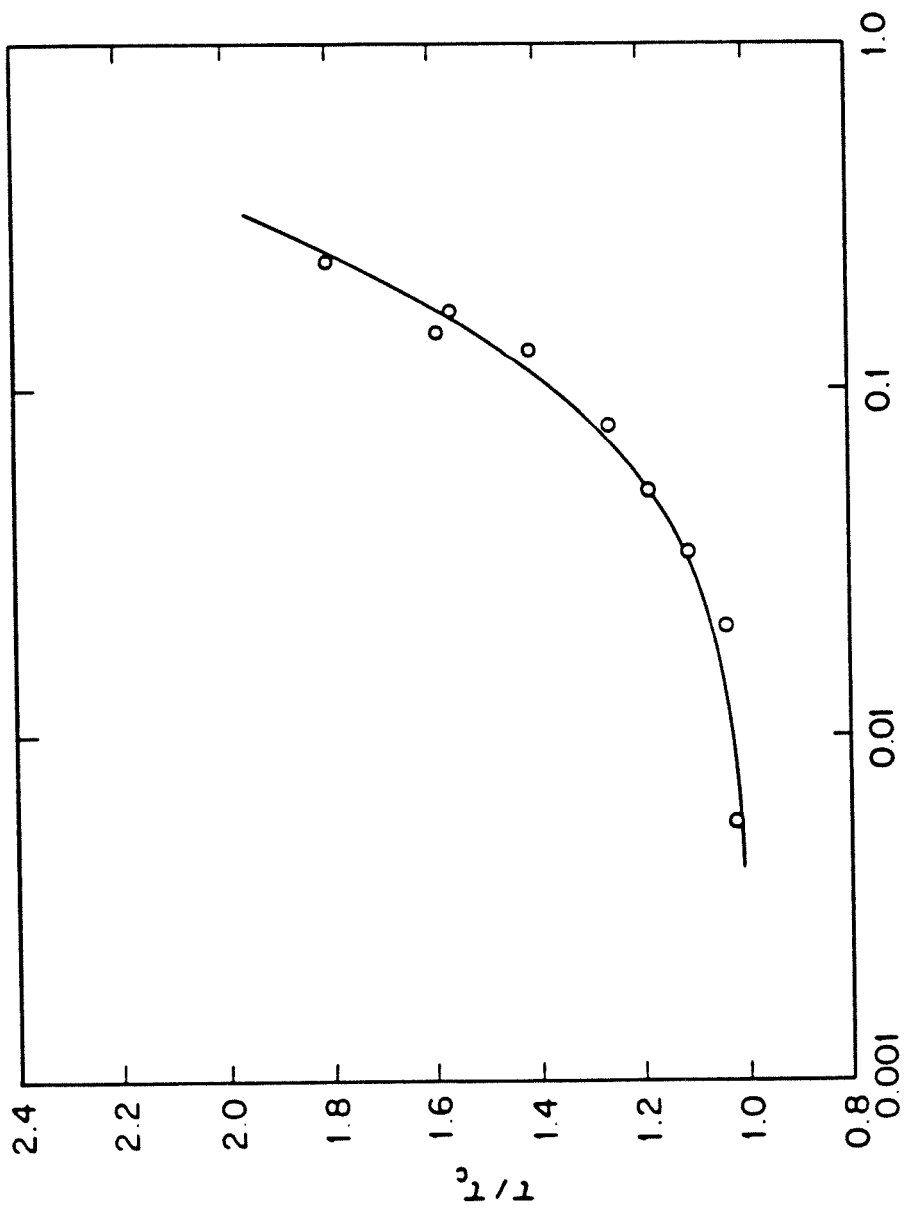

Figure 3. Experimental relaxation times divided by the calculated theoretical time in the continuum regime, as a function of the Knudsen number. The solid line is the theoretically predicted ratio assuming α_T and $\beta_M = 1.0$.

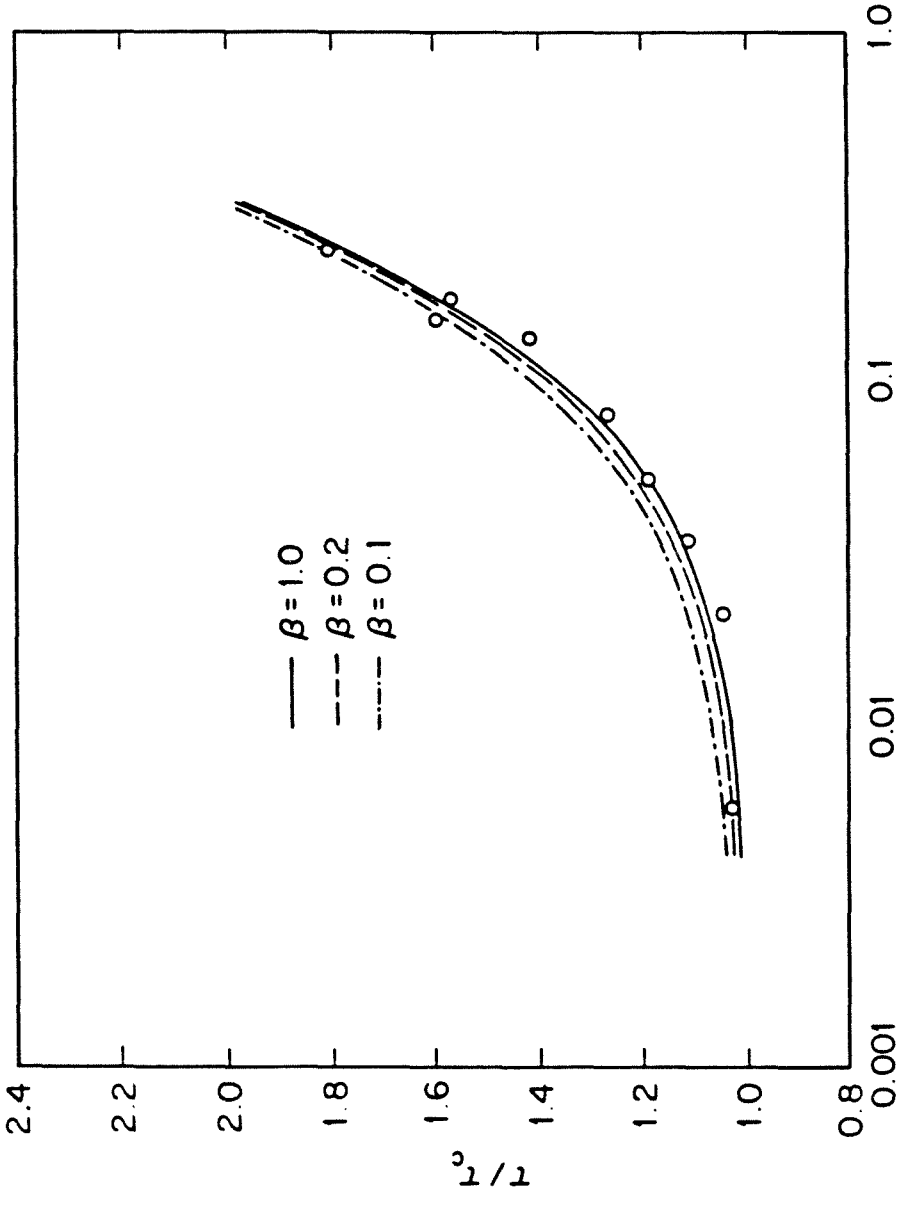

Figure 4. The effect of the value of the mass condensation coefficient on the relaxation time, for $\alpha_T = 1.0$.

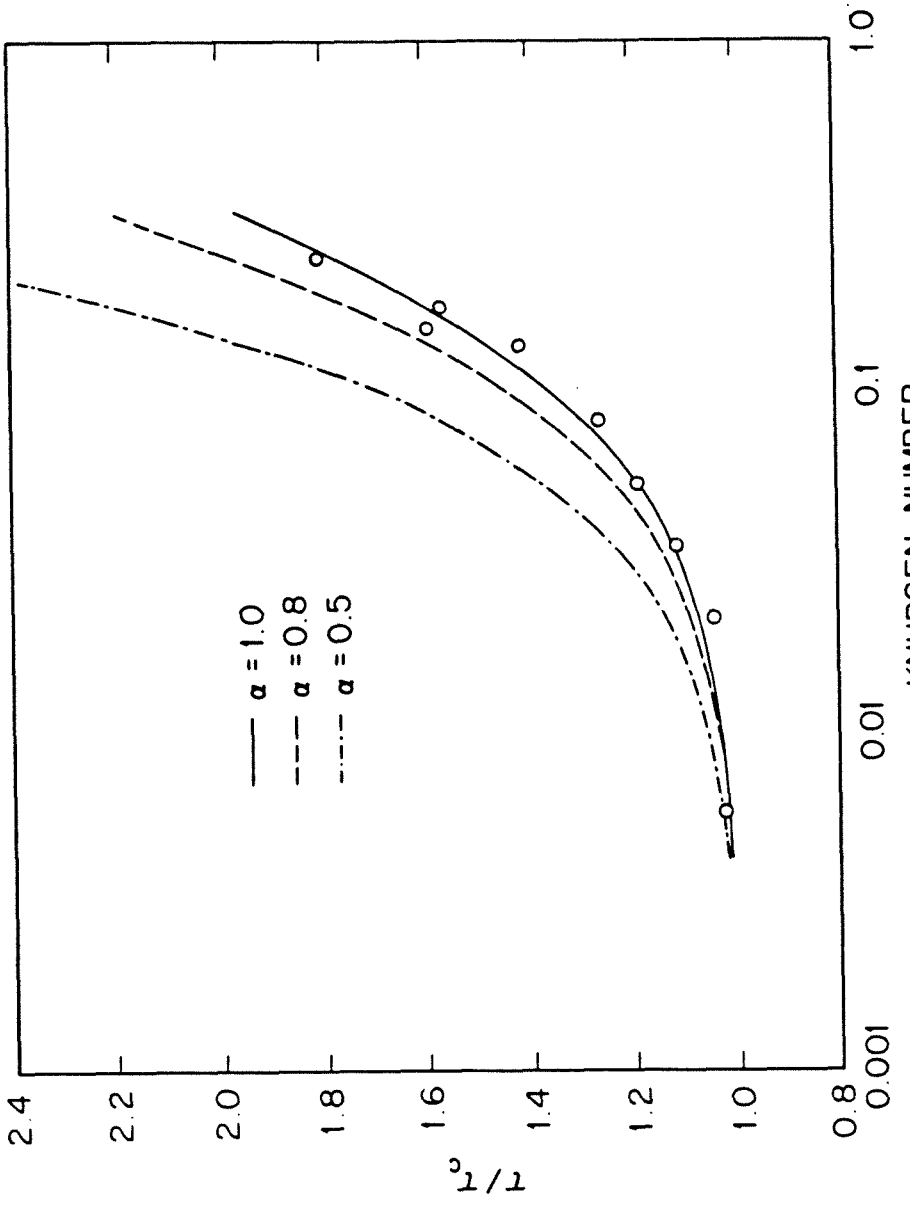

Figure 5. The effect of the value of the thermal accommodation coefficient on the relaxation time, for $\beta_M = 1.0$.

CHAPTER 5

PARTICLE SIZING IN THE ELECTRODYNAMIC BALANCE

By :

Gideon Sageev

John H. Seinfeld

Richard C. Flagan

Published in Rev. Sci. Instr., **57**, 933, (1986).

ABSTRACT

We report here a new technique for sizing particles in the electrodynamic balance. In this technique, the trajectory of a falling particle is followed with a photomultiplier tube. Particle velocities are measured by placing a mask between the particle and the detector. The masked region in the particle trajectory is roughly 0.6 mm wide. Output from the PMT is sampled every milisecond by a A/D converter and stored in a computer. Flight times of several hundred miliseconds are measured and the size is then computed from the particle's terminal velocity. With a modification of the mask, the technique is used to verify the uniformity of the electric field through which the particle is falling. In the present work we use the technique to determine size of polystyrene latex microspheres having nominal diameters of 10 and 20 microns. The technique can be used on any size particle, independent of its charge to mass ratio, and provides the size information in a short time.

1. INTRODUCTION

The electrodynamic balance is an instrument in which single micron-sized particles can be levitated and studied. The historical development of the electrodynamic balance, as well as the behavior of charged particles in its electric field, has been documented by several authors[1-3]. This device has found application in many research areas such as photoemission from single particles[4], energy transfer in single droplets[5], particle laser heating[6], condensation rates[7-8], and aerosol spectroscopy[9]. In some cases the analysis of the experimental data obtained from the electrodynamic balance requires an estimate of the particle size. Numerous sizing techniques have been used in the past, for example the sedimentation method, the matching of scattered light from the particle to that predicted by Mie theory, the "spring-point" method[10] and the electron stepping technique[11].

Among the sizing methods sedimentation is probably the oldest. The sedimentation method requires measurement of the terminal velocity of a moving particle, from which the particle radius can be calculated. This technique has the advantage that it is independent of both the electric field and the particle's charge. However, for particles on the order of 10 microns and falling distances of order one millimeter, (typical values in the present work), the uncertainty in the fall time becomes large when measured manually. This shortcoming was the impetus for the development of a new technique in which the particle trajectory is followed electronically. This technique, which is reported here, reduces the uncertainty of the fall time measurement from that carried out manually and thus provides an accurate and reproducible sizing method for particles in the electrodynamic balance.

2. EXPERIMENTAL SYSTEM

A detailed description of the electrodynamic balance has been provided earlier[8]. During an experiment, a charged particle is levitated between a set of hyperbolic electrodes, the schematic diagram of which is shown in Figure 1. There are two endcap electrodes between which a DC potential is held, as well as a ring electrode to which an AC voltage is applied. The DC potential across the endcaps balances the particle against gravity, while the AC voltage on the ring provides for the focusing of the particle towards the center of the chamber. The particle is illuminated by a HeNe laser beam that traverses the chamber vertically through holes drilled into the center of the endcap electrodes. As shown, the 90° scattered light from the particle is observed through holes in the ring electrode.

At the geometric center of the device there is no AC field. Therefore when the electric force produced by the DC field just balances the gravitational force on the particle, the center of the chamber becomes a stable equilibrium point for the particle. Stated differently, whenever a balanced particle drifts away from the center it "feels" a net force towards the center of the chamber. For a balanced particle in the apparatus,

$$q\,C\frac{V_{dc}}{2\,Z_o} = m\,g \qquad [1]$$

where q and m are the particle charge and mass, g is the gravitational constant, Z_o is the distance between the center of the chamber and the endcaps, (which equals 4.49 mm in our case), and C is a geometric constant for the hyperbolic geometry of Figure 1. The theoretical value of C has been evaluated both numerically[11] and analytically[10]. The numerical result was found to be 0.8, however the calculation did not take into

account the holes in the ring electrode. The analytical solution neglected the presence of the ring electrode and yielded a value for C which is ≈ 10% larger than the numerical result. Since the holes in the electrodes distort the field somewhat[10] from that in their absence, it is necessary to determine C experimentally.

We have determined the value of cell constant[8] by first measuring the size of PSL particles with the spring-point method[10] using the theoretical cell constant of 0.8 . We then manually measured the fall rate of the same particles and evaluated their size, as described below, independent of the value of C. Knowing the size of the particles, the value of C was varied until the sizes obtained by both methods were equal. The experimental value of C is 0.71, about 10% lower than the theoretical value.

When using the sedimentation method, the particle initial balancing voltage, V_{dc}^{0} , is first changed to a new value, V_{dc}^{1} . The AC field is then turned off and the particle begins to move under the combined influence of gravity and the electric field. In this case a force balance on the particle yields[8]:

$$R_p = \left(\frac{9\,\mu\,v}{2\,C_c\,\rho_p\,g}\left[\frac{V_{dc}^{0}}{V_{dc}^{0} - V_{dc}^{1}}\right]\right)^{1/2} \qquad [2]$$

where R_p and v are the particle radius and terminal velocity, C_c is the Cunningham correction factor to Stokes drag, and μ is the gas viscosity. It should be pointed out that when using this method the particle is only allowed to fall about 1 mm around the center of the chamber where the field is relatively uniform.

It can be shown that the time constant for a falling particle to reach

terminal velocity is m/C_d, where C_d is the drag coefficient. Using Stoke's law to compute C_d, a 20 micron polystyrene latex sphere has a time constant of $\approx$ 1 millisecond. In the present study all particles were allowed to fall 100-200 milliseconds prior to measuring their velocity, thereby ensuring that the terminal velocity was reached.

The method by which the particle motion is detected is shown in Figure 2. In the first step the particle is brought into the focus of a 45× microscope. The microscope eyepiece contains a reticle on which a 0.916 mm wide strip of opaque material is placed. The strip was formed by photolithography where a precoated glass plate was first illuminated by UV light and then treated by a negative photoresist solution. The edges of the mask were observed under a microscope and found to have less than 1 micron fluctuations. The particle fall distance, masked by this strip, was calibrated by focusing the microscope on a reticle scale, having 0.01 mm divisions. Thus when a particle is focused on the mask, the distance it travels crossing the mask is known.

As shown in Figure 2, the time it takes the particle to cross the mask is measured by placing a photomultiplier tube behind the eyepiece and recording the scattered light signal from the particle. The photomultiplier tube we used is an RCA 4818 operated at about 750 volts. The scattered light signal was first preamplified and then fed into a 16-bit A/D converter (Burr Brown ADC76KG). The A/D converter was triggered to convert every millisecond and its parallel output was latched and stored directly into the memory of a Zenith Z-120 computer.

The computation of the velocity from the time measurement relies on the assumption that the field is uniform near the center of the

chamber. Clearly , if the field is not uniform, the particle velocity will not remain constant as the particle falls. In order to determine the uniformity of the field, a second mask was prepared, consisting of two thin strips of aluminum (0.297 mm wide), separated by a 0.297 mm gap. Like the previous mask, this mask was prepared by photolithography. Since the two masked areas are equal in width, yet spatially separated from each other, a measurement of the time it takes a particle to cross each mask gives a clear indication of the field uniformity. Additionally, the signal from a particle passing through this mask yields the falling time over six different intervals. (A mask with n opaque strips would have [2n-1]! separate intervals). By normalizing the fall time over the different intervals to that over a single strip, one obtains an accurate average of the time it takes a particle to cross each strip.

3. RESULTS

The scattered light signal obtained from a spherical (nominally 19.1 micron) polystyrene latex particle is shown in Figure 3. The first and second steep changes in the signal correspond to the times when the the particle was first obscured by the front edge of the mask and when it reappeared on the other side, respectively. The other sharp dip in the signal is caused by the particle's quick return to the center of the electrodynamic balance once the AC field is turned back on.

An expanded view of the area of interest is shown in Figure 4. As seen in Figure 4, the scattered light signal does not drop instantaneously as the particle moves behind the mask. This is due to the finite size of the particle. The question then arises as to which point along the steep portion of the curve should be taken as the cross-over point, (by cross-over we mean the the time at which half the particle is behind the mask). For the purpose of calculation we assume that the cross-over occurs midway along the steep parts of the curve. The points along each of the steep parts as well as the bottom and shoulder regions were fit to straight lines by a least-squares program. The lines thus generated were plotted and the four intersection points of the five straight lines were computed. The fall time is then computed from the midpoints of the two steep lines. The terminal velocity was then found from the the fall time and distance, from which the particle diameter was computed. It should be pointed out that the mask is not 100% opaque, especially near the edges; this gives rise to the rounded corners around the break points of the scattered light signal.

In order to test the assumption about the cross-over point we also

measured the size of some particles by the spring-point method. When using the spring-point method, the AC trapping voltage is increased to the point at which the particle becomes unstable and begins to oscillate at half the driving frequency[2,10]. We have found that the diameter resulting from the spring-point method was 2-3 percent larger than that computed with the current technique. Since the velocity is proportional to the square of the particle diameter the larger size inferred from the spring-point measurement would correspond to a 4-6 percent higher velocity. The difference between the two results is partially due to the uncertainty in the earlier determination of the cell constant; however, it highlights a limitation in the precision of the current technique.

The voltage offset for the particle of Figures 3-5 was about 12% and the resulting diameter was 18.9 μm . In Figure 5 we show the scattered light signal from a 9.96 μm polystyrene latex particle. (The nominal diameters of the particles were 19.1 μm , and 9.6 μm with 5.8% standard deviation). Even though the offset voltage of $\approx$ 22% was used on this particle, the fall time is longer than that of the larger particle. This is a result of the drag being inversely proportional to the square of the diameter.

It must be mentioned that particle sizes can also be obtained accurately by fitting the angular scattered light from the particle to that predicted by Mie theory[12]. We have not used this technique due to the geometric limitations of our present chamber. Although the Mie scattering technique is more precise than the present sizing method, the former technique only applies for homogeneous spheres whereas the method presented here could also be applied to nonspherical particles provided the shape correction factor to Stokes law is available. Additionally the Mie scattering method requires knowledge of the particle's refractive

index, whereas the current method is independent of this parameter.

The scattered light from a particle crossing the double mask reticle is shown in Figure 6. Using all six time measurements in Figure 6, we obtain an average time of 197 milliseconds with a standard deviation of 1.2%. Therefore the assumption of uniform field near the center of the chamber is valid with an uncertainty of about 1%. This variation is consistent with that predicted for electrodes having no holes.

Referring again to Figure 3, it is evident that there are some small peaks in the scattered light signal on both sides of the mask. These peaks may be caused by diffraction effects and may, therefore, also contain particle size information. This additional structure does not directly affect our current results.

4. ACKNOWLEDGEMENTS

This work was supported by U.S. Environmental Protection Agency grant R-810857. The authors wish to thank John Lee and Wade Regehr of Caltech for their help during this project.

5. REFERENCES

[1] E.J. Davis, Aeros. Sci. Tech., **2**, 121, (1983).

[2] R.H. Frickel, R.E. Shaffer and J.B. Stamattoff, Technical report ARCSL-TR-77041, U.S. Army Armament Research and Development Command, Chemical Systems Laboratory, Aberdeen Proving Ground, Maryland (1978).

[3] R.F. Weurker, H. Shelton, and R.V. Langmuir, J. Appl. Phys., **30**, 342, (1959).

[4] S. Arnold and N. Hessel, Rev. Sci. Inst., **56**, 2066, (1985).

[5] L.M. Folan, S. Arnold, and S.D. Druger, Chem. Phys. Lett., **118**, 322, (1985).

[6] R.E. Spjut, A.F. Sarofim, and J.P. Longwell, Langmuir, **1**, 355, (1985).

[7] E.J. Davis and A.K. Ray , J. Aerosol Sci., **9**, 411, (1978).

[8] G. Sageev, R.C. Flagan, J.H. Seinfeld and S. Arnold, J. Coll. Int. Sci. (in press).

[9] S. Arnold , E.K. Murphy , and G. Sageev , Appl. Opt., **24**, 1048, (1985).

[10] E.J. Davis , Langmuir, **1**, 379, (1985).

[11] M.A. Phillip , F. Gelbard , and S. Arnold, J. Col. Int. Sci., **91**, 507, (1983).

[12] R. Chang and E.J. Davis , Langmuir, J. Col. Int. Sci., **54**, 352, (1976).

FIGURE CAPTIONS

1. Schematic diagram of the electrodynamic balance.

2. Experimental arrangement for measuring particle fall times.

3. Scattered light signal from a 19.5 micron polystyrene latex particle crossing an opaque strip (0.9 mm wide).

4. Expanded view of the region where the 19.5 micron particle crosses the mask, and determination of the particle fall time by a least squares fit of the data.

5. Scattered light signal and fall time of a 10.15 micron polystyrene latex particle.

6. Expanded signal from a 19.5 micron PSL particle crossing a mask with two opaque strips (each 0.3 mm wide).

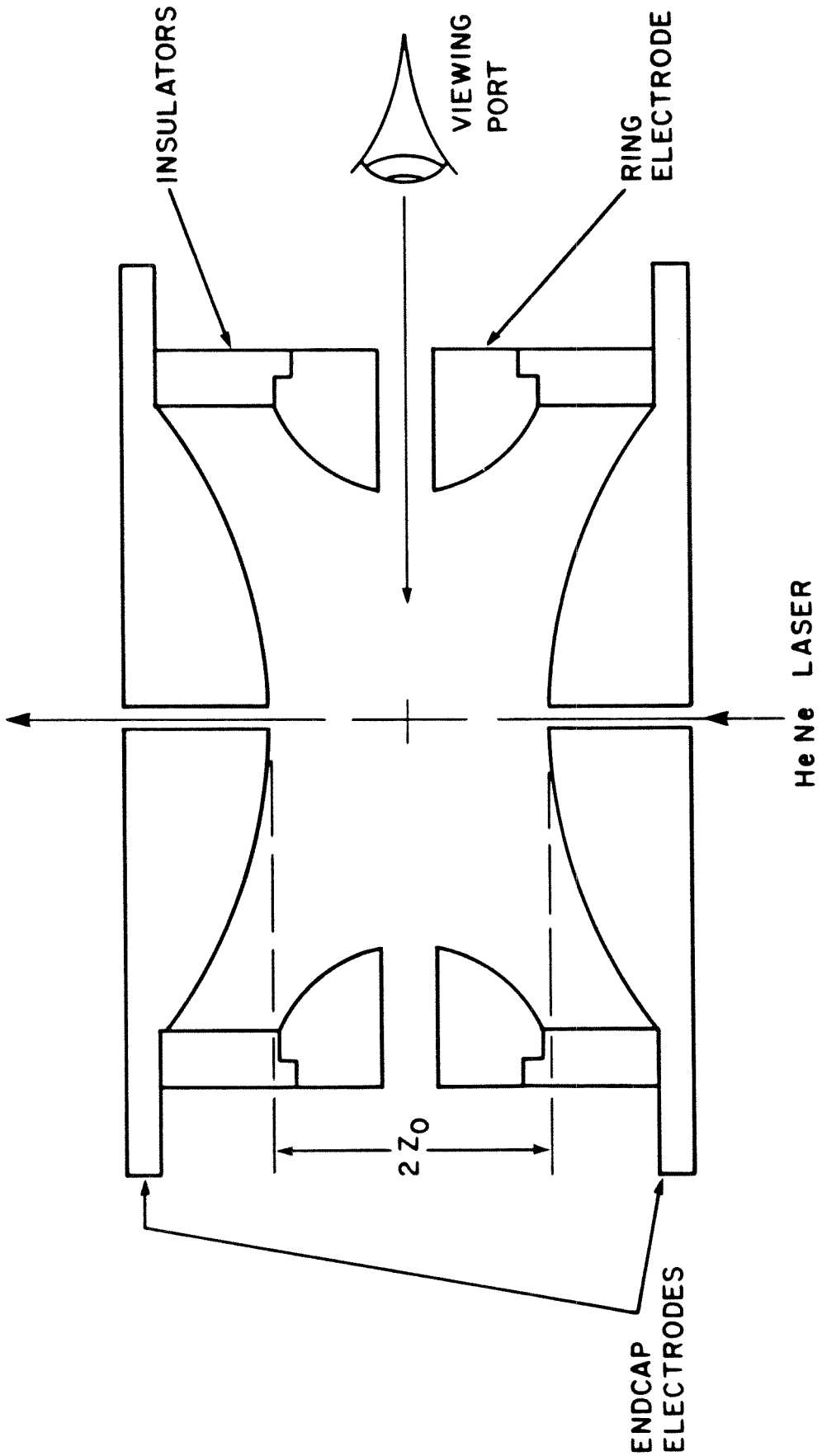

Figure 1. Schematic diagram of the electrodynamic balance.

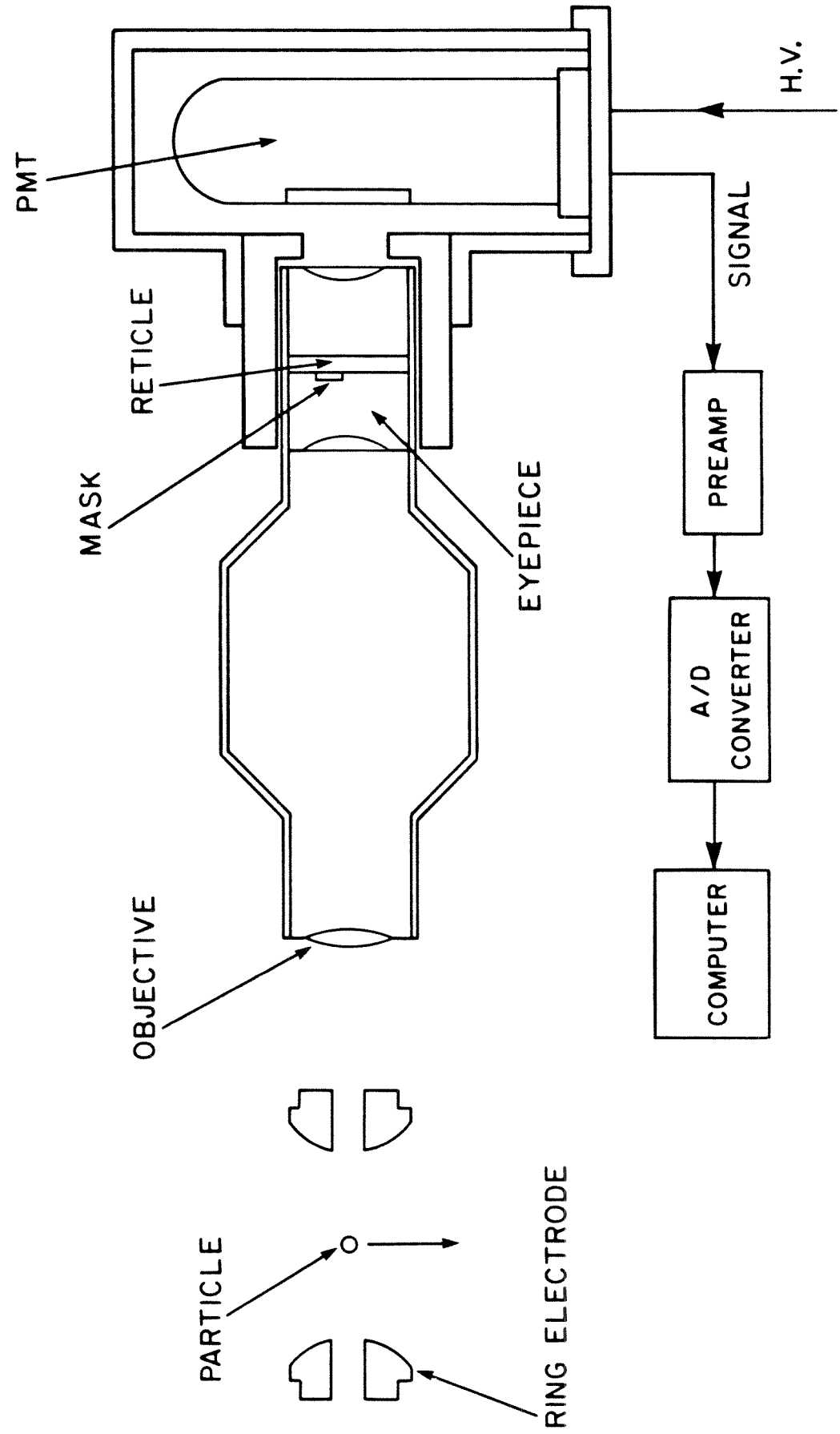

Figure 2. Experimental arrangement for measuring particle fall times.

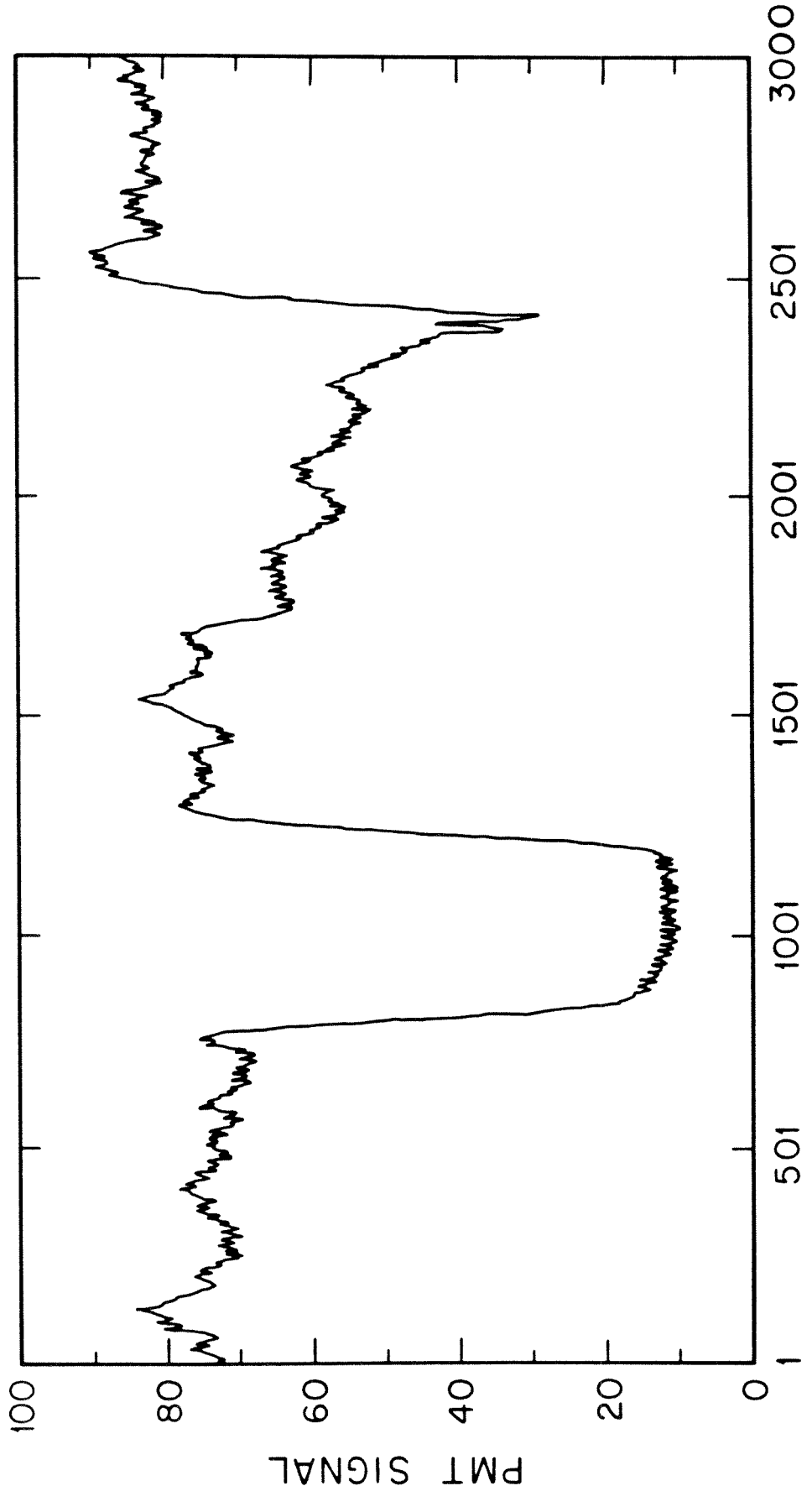

Figure 3. Scattered light signal from a 19.5 micron polystyrene latex particle crossing an opaque strip (0.9 mm wide).

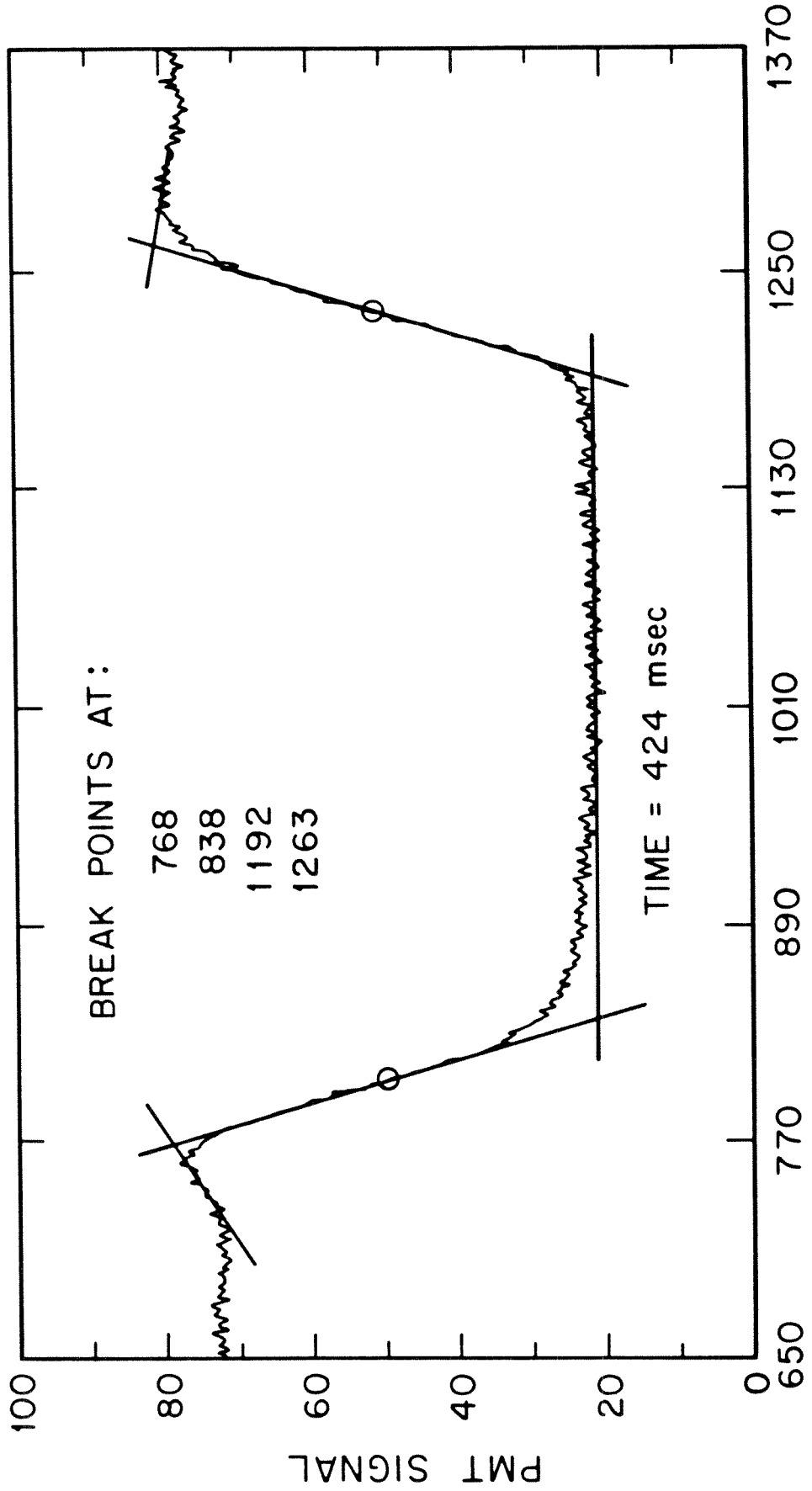

Figure 4. Expanded view of the region where the 19.5 micron particle crosses the mask, and determination of the particle fall time by a least squares fit of the data.

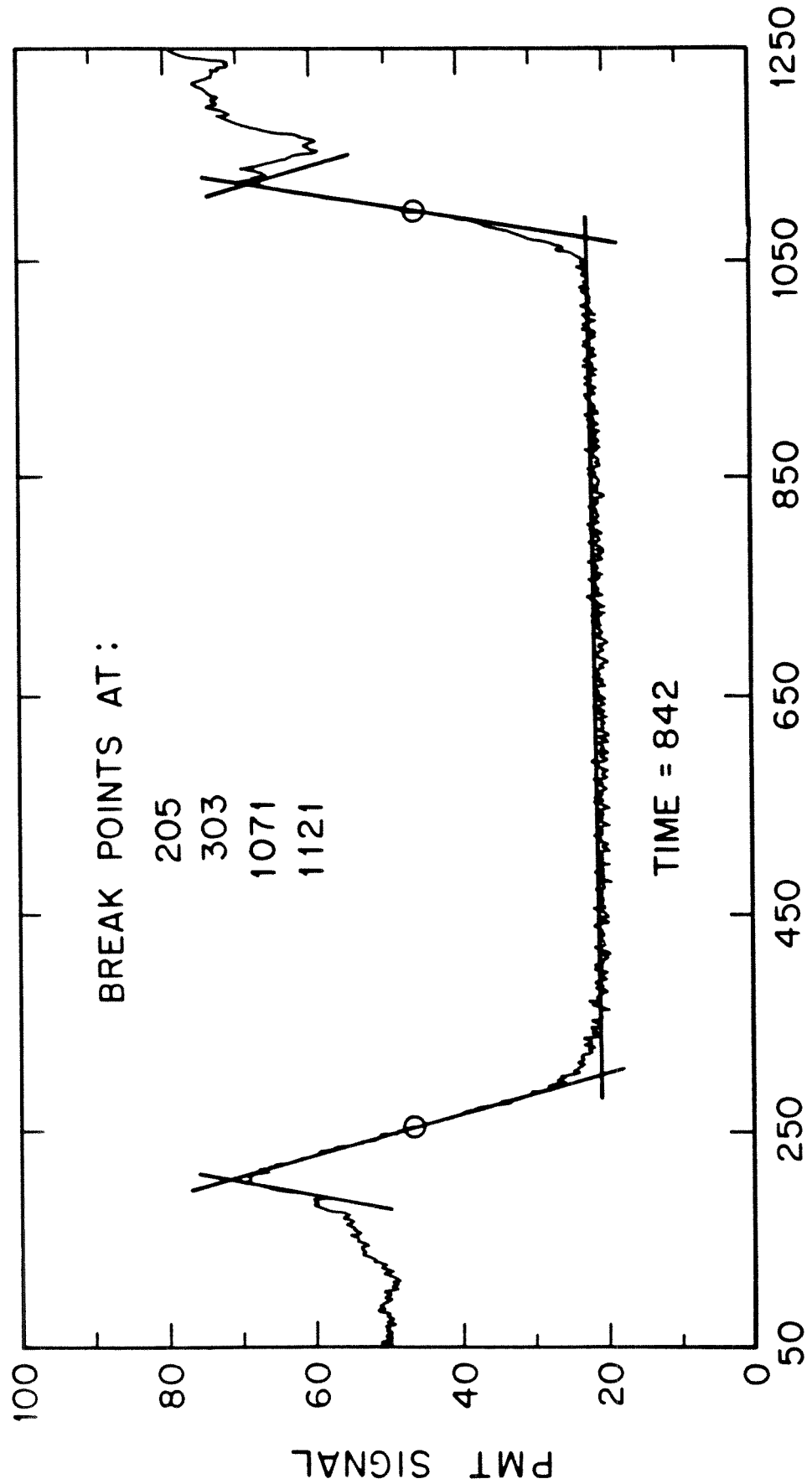

Figure 5. Scattered light signal and fall time of a 10.15 micron polystyrene latex particle.

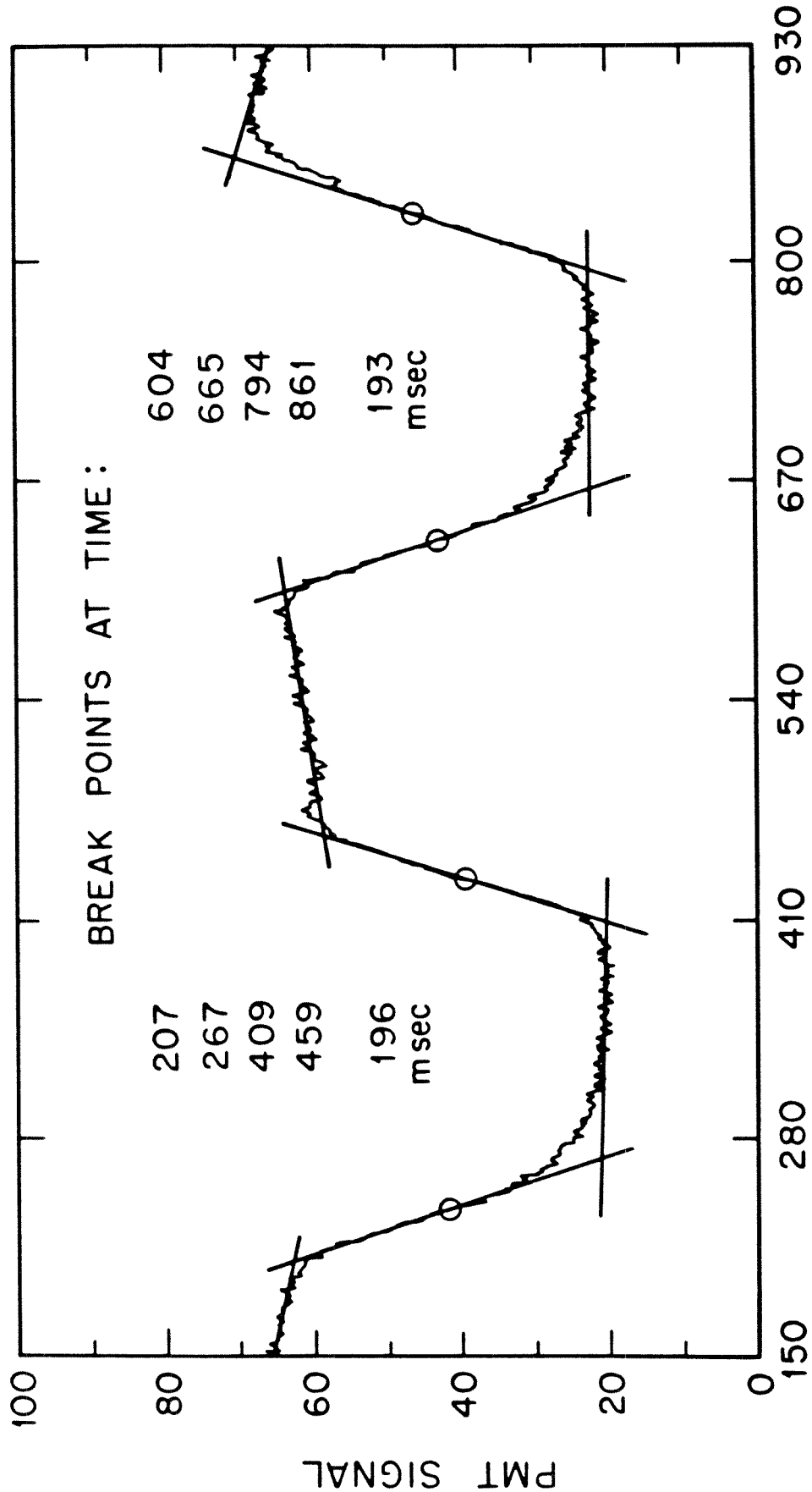

Figure 6. Expanded signal from a 19.5 micron PSL particle crossing a mask with two opaque strips (each 0.3 mm wide).

CHAPTER 6

FOURIER TRANSFORM INFRARED SPECTROSCOPY OF A SINGLE AEROSOL PARTICLE

By :

Gideon Sageev Grader*

Stephen Arnold+

Richard C. Flagan*

John H. Seinfeld*

Submitted to the Journal of Chemical Physics.

*Department of Chemical Engineering, California Institute of Technology, Pasadena, CA 91125

+Department of Physics, Polytechnic Institute of New York, Brooklyn, New York, 11201

ABSTRACT

A method is developed for obtaining the molecular composition of a single suspended microparticle by Fourier transform infrared spectroscopy. The particle is held in an electrodynamic balance and irradiated simultaneously by the infrared output from a Michelson interferometer and the visible light from a dye laser. The laser is tuned to an edge of an optical resonance of the particle while the IR beam is chopped. Through evaporation and condensation the chopped IR beam causes a size modulation of the droplet, which inturn induces a fluctuation in the laser light scattered from the particle. The scattered light is detected at 90^o with a photomultiplier, and the amplitude of the light fluctuation is measured with a lock-in amplifier. The lock-in signal is then inverted by a discrete fast Fourier transform routine (FFT), to yield the particle absorption spectrum. Spectra of $(NH_4)_2SO_4$ droplets at different solute concentrations are presented. The data shown includes the first infrared spectrum of a highly supersaturated solution.

1. INTRODUCTION

A long-standing goal in aerosol science has been to develop methods to probe the molecular composition of a single micro-particle. One approach to isolate a single particle is to use an electrodynamic balance[1,2,3], (also called a quadrupole), within which a micron-sized, charged particle can be levitated virtually indefinitely. The electrodynamic balance offers the additional advantage of affording a well-controlled gaseous environment for studying the response of the particle to temperature variations and changes in its surrounding vapor. For a liquid particle, for example, the lack of physical contact with foreign surfaces and other particles makes the system very suitable for the study of solution-phase phenomena such as vapor-liquid equilibrium[4,5], particle-phase chemical reactions[6], and deliquescence-crystallization[7].

A number of methods have recently been reported for determining the molecular composition of a single liquid particle including ones based on the fluorescence[8] and Raman[9,10] emission from the particle and on the infrared absorption[11,12] of the particle. When applied to a micron-sized particle, the excitation wavelength in both the fluorescence and Raman techniques is small compared with the particle diameter. Therefore the spectra, obtained via the scattered light from the particle, are complicated by the resonant nature of the scattering in the Mie regime. The spectra may also be affected by a nonhomogeneous distribution of scatterers inside the particle. In contrast, when infrared light is used to excite the particle, the wavelength is comparable with the particle size. Therefore under this condition the particle will appear almost Rayleigh like[12], where the absorption is uniform and

can be related to the average composition.

The absorption spectrum of an aqueous droplet may be obtained by heating with an IR source, and simultaneously illuminating the droplet with a visible laser[11]. When an aqueous solution droplet is suspended in a humid environment its water activity equals the ambient relative humidity and, as long as the the relative humidity is held constant, the particle size remains constant (provided the solute in the drop is nonvolatile). Upon heating, the droplet evaporates due to the increase of the water vapor pressure with temperature. This evaporation is restrained, however, by the increase in the ionic strength in the particle accompanying water loss. When the heating is stopped, the particle returns to its initial temperature and its original size. Therefore periodically exposing the particle to an infrared beam will cause a periodic fluctuation in the particle size.

Since the visible scattered light from a particle is a strong function of its size, size fluctuations cause a corresponding modulation in the scattered light from the particle. Arnold et al[11,12,13] have shown that this modulation may be enhanced if the light scattering is measured near a structure resonance of the particle. If,in addition, the particle is heated by selected wavelengths in the IR, larger modulations in the size and light scattering will occur at wavelengths where species in the particle absorb the incident radiation. By correlating the magnitude of the scattered light fluctuation with the incident IR wavelength, the absorption spectrum of the particle can be obtained. In Arnold, Neuman and Pluchino's technique[11] the wavelength in the IR was selected with a wedge monochromator. The advantages of this technique are its simplicity, and ability to monitor the absorption at a particular wavelength

continuously. However the spectral resolution is limited to the bandwidth at a given position of the wedge. In addition, the monochromator acts as a filter which limits the amount of intensity deliverad to the particle.

This paper introduces a Fourier transform technique for obtaining the composition of a single suspended aerosol particle similar to that proposed by Arnold and Pluchino[12]. In the present technique the entire IR beam is passed through a Michelson interferometer consisting of a beam splitter and two mirrors. At the beam splitter different wavelengths undergo constructive and destructive interference depending on the relative separation between the mirrors and the beam splitter. As a result the FTIR technique offers a greater energy throughput to the sample. Since the resolution in FTIR spectroscopy is inversely proportional to the scan length of the interferometer mirror, this method can reach higher resolution than the previous technique. For example, a one centimeter mirror scan can potentially yield a resolution of 1 cm^{-1}, which is an order of magnitude smaller than the resolution of the wedge monochromator. Although the added resolution has limited application in aqueous solutions in which the vibrational resonances are broad[14] ($\geq$ 50 cm^{-1}), in future applications the higher potential resolution could prove useful.

In the next section the theory of the FTIR technique will be developed. Then the apparatus and experiment will be described. Finally results of application of the technique to ammonium sulfate droplets will be presented.

2. THEORY

The IR spectroscopy developed here is based on two fundamental processes: evaporation and condensation due to particle heating and cooling, and fluctuations in the light scattering resulting from particle size changes. The evaporation and subsequent relaxation back to its original size of a particle momentarily heated can be used to provide data on the simultaneous heat and mass transfer processes in the continuum[13] as well as the transition[15] regime. In such processes, if the size change is small relative to its initial size, for a particle with an initial radius a_o, the pertubation in the radius, $\epsilon(t) = a(t) - a_o$, can be shown to be governed by[13,15]

$$\frac{d\epsilon}{dt} = -\int_0^\infty \alpha(k) I_o(k) dk - \gamma\epsilon \tag{1}$$

where $I_o(k)dk$ is the incremental IR intensity at wavenumber k. $\alpha(k)$ is related to the particle absorption coefficient, $Q_a(k)$, and is given by,

$$\alpha(k) = \frac{Z}{LZ+1}\frac{Q_a(k)}{4\rho_p} \tag{2}$$

where L and ρ_p are the water latent heat of vaporization and the particle density respectively, and Z is a constant that depends on the water diffusivity in the gas, the heat transfer properties of the particle, and the salt concentration. Finally, γ in equation (1) is the particle relaxation rate (when the heating is stopped), and is given by,

$$\gamma = \frac{3D_g C^o i X_w (1 - X_w)}{\rho_p a_o^2 f_w (1 + LZ)} \tag{3}$$

where D_g and C^o are the water diffusivity in the gas, and the pure water vapor pressure respectively. X_w and f_w are the water mole fraction and weight fraction in the droplet, respectively, and i is the Van't Hoff factor.

The incremental radius change resulting from heating and cooling, $\epsilon(t)$, can be related to a fluctuation, $\delta S(t)$, in the scattered light from the particle in terms of an amplification factor β,[12],

$$\frac{\delta S(t)}{S_o} = \beta \frac{\epsilon(t)}{a_o} \tag{4}$$

where S_o is the scattering signal from the particle before the size modulation.

If the infrared source is from a Michelson interferometer, the incremental intensity in the wavenumber range $(k, k + dk)$ at a mirror distance l from its equal arm point is given by,

$$I_o(l,k)dk = e^{j2kl}T(k)I_s(k)dk \tag{5}$$

where the wavenumber of the infrared light is related to its wavelength by , $k = \frac{2\pi}{\lambda}$, $T(k)$ is the transmission function of the optical elements in the IR pathway, between the source and the particle, and $I_s(k)dk$ is the incremental source intensity between k and $k + dk$. If the output intensity is chopped at a frequency ω, equation (5) becomes,

$$I_o(l,k,t)dk = e^{j(2kl+\omega t)}T(k)I_s(k)dk \tag{6}$$

The time dependent IR excitation can be employed to drive the particle size change as expressed in equation (1). Note that the total intensity received by the particle is the integral of equation (6) over all wavelengths. Since the particle responds at the same frequency as the driving heat source, the solution to equation (1) can be expressed as

$$\epsilon(t,l) = \int_{-\infty}^{\infty} A(k)e^{j(\omega t+\phi)}dk \tag{7}$$

where ϕ is the phase of the particle response with respect to the driving force. Substituting equations (5) and (7) into equation (1) yields the values of $A(k)$ and ϕ. The resulting size fluctuation is given by,

$$\epsilon(t,l) = -\int_{-\infty}^{\infty} \frac{\alpha(k) I_s(k)\ T(k)}{(\omega^2+\gamma^2)^{1/2}} e^{j(\omega t+\phi)} dk \tag{8}$$

where $\phi(k) = 2kl - \frac{\omega}{\gamma}$. The change in the radius is seen to be a function of the mirror position and time. Using equation (4), the corresponding scattered light fluctuation is,

$$\frac{\delta S(t,l)}{S_o} = -\int_{-\infty}^{\infty} \frac{\beta}{a_o} \frac{\alpha(k) I_s(k)\ T(k)}{(\omega^2+\gamma^2)^{1/2}} e^{j(\omega t+\phi)} dk \tag{9}$$

The equation above represents the incremental time dependent scattering signal resulting from the chopped IR heating of the particle. We desire the magnitude of the AC component of the scattered light fluctuation. To obtain a DC level from equation (9) we detect the scattered light signal with a lock-in amplifier, referenced to the IR chopper frequency. At the output of the lock-in amplifier the scattered light signal at any mirror position l is,

$$\frac{<\delta S(t,l)>}{S_o} = -\int_{-\infty}^{\infty} B(k) e^{j(kl+\theta)} dk \tag{10}$$

where

$$B(k) = \frac{\beta}{a_o} \frac{\alpha(k) I_s(k) T(k)}{(\omega^2+\gamma^2)^{1/2}} \tag{11}$$

, $\theta = -\frac{\omega}{\gamma}$, and $< \delta S(l) >$ is the measured signal in the present experiment. The chemical information that is of interest is in the absorption coefficient $\alpha(k)$, which is contained in $B(k)$. Multiplying equation (10) by $e^{-jk'l} dl$ and integrating over all

mirror positions yields,

$$\frac{1}{2\pi}\int_{-\infty}^{\infty}\frac{<\delta S(l)>}{S_o}e^{-jk'l}dl = B(k') \tag{12}$$

which is recognized as the inverse Fourier transform of the data which can be carried out with a discrete fast Fourier transform (FFT) routine[16]. Since γ and ω are known constants, and $I_s(k)$ and $T(k)$ are determined for the particular source and intrferometer optics, the evaluation of $B(k)$ allows us to obtain $\alpha(k)$ which depends directly on the particle absorption coefficient $Q_a(k)$.

3. EXPERIMENTAL SYSTEM

In this experiment a single charged particle is held by the electric field generated with a quadrupole trap. As shown in Figure 1, the trap consists of top and bottom electrodes between which a DC voltage is held, and a ring electrode to which an AC voltage is applied. The exact geometry of the trap has been described earlier[15,17], and for now it suffices to know that the device can hold a charged particle virtually indefinitely. The historical development of this technique and the behavior of charged particles in its electric field have been documented elsewhere[1-3]. The trap is encased inside a sealed chamber that can be evacuated and filled back with the gases of interest. Particles are introduced into the chamber by opening the top seal and lowering a particle jet above the top electrode. The jet (Uni Photon System model 1) works on the following principle[18]. By applying an electrical pulse to a piezoelectric crystal, a pressure wave is generated that forces a droplet out a small opening in the glass tip (see Figure 1). The droplet is charged inductively as it leaves the tip of the jet and is then trapped by the AC field. The whole jet assembly is enclosed inside a teflon bag through which filtered dry air is continuously passed. In so doing we prevent room-air particles from entering the chamber and contaminating the particle. The relative humidity inside the chamber is controlled through a connection of the chamber to a water reservoir positioned in a constant temperature bath.

A schematic of the experimental system is shown in Figure 2, where the electrodes and chamber are omitted for the sake of clarity, (the particle in the figure is not drawn to scale). In describing the apparatus the IR pathway will first be

traced, and then the laser and associated electronics will be discussed. The infrared beam is generated in a commercial Michelson interferometer (Advanced Kinetics), and consists of a 2-mm wide glowbar (Perkin Elmer), collimated by f/3 optics. The instrument is supplied with a geared-down DC motor coupled to a micrometer. The motion of the mirror is followed with a Moire' encoder. The interferometer is designed to scan continuously, however the instrument was modified to step the mirror in equal intervals, allowing integrating of the signal at each of the mirror positions. The reason for this modification is that at each mirror position time must be allowed for the droplet to relax to its preheated size. If the interferometer mirror is driven continuously, (without the chopper), the rate of the IR signal modulation depends on the mirror speed. For example at the slowest mirror speed of 10 μm sec^{-1} and wavelength of 5 μm, an IR fringe will pass every 0.5 seconds. Recording the scattered light level at every micron of the mirror travel will allow 100 milliseconds between readings. Under this condition not only must the droplet respond at a faster rate, but also the signal to noise ratio must be sufficiently large in that bandwidth. For the particles considered in this study a 10-30 second integration time constant was needed to obtain a sufficiently clean signal. Being able to step the interferometer mirror and chop the IR was critical as it enabled signal averaging for as long as neccesary.

The output beam is first focused on a iris and then chopped at 5-10 Hz. Since the particle absorbs only a minute fraction of the beam, preventing the major part of the beam from entering the system avoids excessive heating of the chamber. This fact is important in maintaining the relative humidity surrounding the particle

constant during the experiment. The diverging beam is then refocused on the particle. After passing the particle, the beam exits through an opposite window. The mercury cadmium teluride (MCT) detector shown in line with the IR beam is used for the initial alignment and continuous monitoring of the interferometer output during an experiment.

Simultaneously with the IR beam the particle is also illuminated with a visible dye laser in the vertical direction. The dye laser used is a Spectra Physics model 375, pumped with their argon ion laser model 2020-5. The 90° visible scattered light from the particle is collected through a microscope objective and coupled into a photomultiplier tube. The PMT signal is measured with a picoammeter and is then fed to the input stage of a lock-in amplifier. As mentioned earlier, the PMT signal contains a fluctuation resulting from the size modulation of the droplet. The amplitude of this fluctuation is measured by referencing the lock-in to the chopper output. The lock-in output is sent to a 16-bit A/D converter and read by a computer. As shown, the computer (Zenith 120) also synchronizes the stepping of the interferometer mirror. Depending on the lock-in time constant, the computer is programmed to allow enough time between moving the mirror and taking a new A/D reading. At the end of a scan the data are inverted by FFT to yield the absorption spectrum.

In this experiment we make use of the optical resonances occurring in the scattered light from a small particle. An example of such resonances for a $(NH_4)_2SO_4$ particle is shown in Figure 3. These resonances were predicted by Mie[19], and were first observed by Ashkin[20]. For a given particle of radius a, and incident radia-

tion of wavelength λ, the optical parameter, $\frac{2\pi a}{\lambda}$, remains constant for a particular resonance. It then follows that pertubations in the radius, $\delta a (= \epsilon)$, and in the wavelength, $\delta\lambda$, for such a resonance are related by $\frac{\delta a}{a} = \frac{\delta\lambda}{\lambda}$,[11]. Therefore in a region where the scattered light changes linearly with wavelength (i.e., on the edge of an optical resonance), it also changes linearly with the size fluctuations of the particle.

It is critical that during an experiment, we remain on the linear portion of the scattering curve so that size fluctuations are linearly related to the scattered light fluctuation. At the start of an experiment we first tune the dye laser to the edge of an optical resonance (see Figure 3), thereby turning the resonance into an optical amplifier for small size changes in the droplet. The amplification factor, β in equation (2), can exceed 4000,[11]. Once the laser is tuned, the chopper is turned on and the scattered light fluctuations are observed on an X-Y recorder. Small drifts in the particle size due to changes in the relative humidity in the chamber as a result of slow heating of the chamber will cause the system to drift off the edge of the resonance. These drifts are compensated by re-tuning the dye laser. In this fashion the amplification factor β, remains constant during an experiment.

While scanning the interferometer the mirror is moved in equal steps from one side of the equal arm point to the other. The lock-in time constant normally used was 10 seconds; and 140 data points were usually taken each scan, separated by roughly 1 μm and centered about the equal arm point. Increasing the resolution by taking longer scans did not prove useful because of low signal to noise ratio in the wings of the interferogram. This problem could be avoided by increasing the

lock-in time constant. We have used a 30-second time constant; however, increasing it any further would make the time neccessary for a single scan prohibitively large. It should be pointed out that after turning the system on, we allow about an hour for all the components to stabilize before taking the first scan.

4. RESULTS AND DISCUSSION

An example of the recorded scattered light signal, $< \delta S(l) >$, as a function of mirror position is shown in Figure 4. The zero point on the x-axis corresponds to the position where the two interferometer mirrors are at equal distances from the beam splitter. Only at this position are all the waves recombining at the beam splitter in phase with each other. Therefore at this point all those bonds of species inside the droplet absorbing in the IR, are excited. This gives rise to a maximum size modulation signal at the equal arm point. Hence at this position the scattered light modulation reaches the maximum shown in Figure 4. As the mirror is moved on either side of the equal arm point, some wavelengths undergo destructive interference at the beam splitter, giving rise to a smaller absorption that is reflected in a smaller scattered light fluctuation. As the mirror is moved further from the equal arm point some of the waves combine at the beam splitter incoherently. The incoherent recombination reduces the intensity modulation at all wavelengths which shows up as smaller modulation signals in Figure 4. For the scan shown in Figure 4, the particle consisted of a 24.4% (by mass) aqueous solution of ammonium sulfate. The particle radius was 3.14 $\pm 0.03 \mu$m . The data shown in Figure 4 represent the first infrared interferogram reported for a single aqueous droplet.

By inverting the data in Figure 4 by FFT, the resulting $B(k)$ spectrum shown in Figure 5 is obtained. From equation (11) we note that $B(k)$ contains the instrument line function $T(k)I_s(k)$. $T(k)$ was obtained independently by measuring the transmission of each optical element with a spectrometer. $I_s(k)$ was not obtained directly due to a lack of instrumentation at the present time. However we estimated

$I_s(k)$, by measuring the temperature of the source with an optical pyrometer and computing the black body emission at that temperature. (The black body behavior of the source was assured by the manufacturer). We then normalized $I_s(k)$ to its value at the highest wavenumber. The normalized absorption of the particle, shown in Figure 6, was obtained by dividing $B(k)$ in Figure 5 by the instrument line function. Therefore the spectrum in Figure 6 exhibits the wavenumber behavior of the particle absorption. The peaks identified in Figure 6 are the sulfate, the ammonium and the water lines. Note that the water peak, more pronounced in Figure 5, is now a shoulder on the side of the ammonium peak. The theoretical resolution of this scan was ≈ 70 cm^{-1}, however fluctuations in β during the time of the scan are most probably responsible for the enhanced width of the peaks shown by the data. The position of these peaks agree with previous work on a levitated particle[13], and also with data taken on bulk solutions[21,22]. Both the sulfate and the ammonium peaks are positioned above a broad absorption baseline. This is consistent with the data for water and ammonium sulfate absorption presented by Volz[22] and is considered to be associated with hydrogen bonding.

To show the effect of the water concentration we repeated the experiment at a smaller relative humidity (a higher salt concentration). At this condition the salt weight fraction was 63.3% and the particle radius was 2.25 $\pm 0.02\mu$m. The result is shown as the solid line in Figure 7, where for comparison we also include the spectrum from Figure 6 (shown in the dotted line). The effect of the different particle radii, as well as different amplification factor, β, was accounted for in equation (11). The effect of the reduced amount of water in the drop on the spectrum

is clearly seen by the fall of the absorption baseline near 1280 cm^{-1}. The 63.3% $(NH_4)_2SO_4$ solution is highly concentrated (13 molal), where the ratio of water molecules to salt ions is roughly 1.4 to 1. In contrast, the corresponding ratio at the solute weight fraction of 24.4% is 7.6 to 1. Due to the substantial decrease in the amount of water in the particle, one would expect a reduction in the degree of hydrogen bonding in the concentrated solution. By looking at the water peak in Figure 7, it is apparent that its position was shifted upward in the supersaturated state. This may be due to the greater average proximity of the water molecules to the ions in the solution which can restrict the water bending mode. Note also that the saturation point for ammonium sulfate at room temperature is about 5 molal, and thus the spectrum shown in Figure 7 represents that of a supersaturated solution. This is apparently the first reported spectrum for an ammonium sulfate solution at this degree of saturation.

As mentioned above, the resolution of the spectra in Figures 5 and 6 was $\approx$ 70 cm^{-1}. Increasing the resolution by moving the interferometer mirror a greater distance did not prove useful due to the poor signal-to-noise ratio in the wings of the interferogram. An important contribution to this noise is the particle size drift due to temperature variations in the chamber during the run. The main causes of these variations are the heating of the chamber by the IR source, and the heating or cooling of the chamber due to changes in the ambient temperature. These temperature changes alter the relative humidity in the chamber which forces the particle to change its size accordingly. The manifestation of this drift is that β is not absolutely constant during the experiment. Since the scattered light signal is

directly proportional to β, the temperature fluctuations contribute strongly to the noise in the interferogram.

The drift problem mentioned above could be reduced by using smaller particles. The advantage of using smaller particles is that their resonances are wider. Although wider resonance implies that the amplification factor β is smaller, (the resonance curve is less steep), the scattered light becomes less sensitive to small drifts in the particle size. To overcome the problem of decrease in modulation signal the IR chop rate can be reduced. Since the particle relaxation time constant decreases with the square of the radius[13,14], the response time of the detector, (the particle in our case), improves. The faster response assures that the particle returns back to its original size quickly thereby yielding a cleaner size modulation and lower noise.

5. CONCLUSIONS

We have reported here a new method based on Fourier transform spectroscopy to obtain a complete molecular spectrum of a single suspended aqueous microparticle. The first interferogram of a 3.14 μm radius ammonium sulfate droplet has been presented. We have also presented a spectrum of a particle in a highly supersaturated state. The differences between the two spectra show the effect of reduced hydrogen bonding in aqueous solutions.

6. ACKNOWLEDGEMENT

This research was supported by U.S. Environmental Protection Agency grant R-810857 and by gifts from General Motors Corporation and Mobil Oil Corporation. S. Arnold was supported by a Chevron Visiting Professorship at the California Institute of Technology and by National Science Foundation Grant ATM-8413574. The authors thank Anthony B. Pluchino of the Aerospace Corporation and Ralph Waniak of Advanced Kinetics for helpful advice during this work.

7. REFERENCES

1. R.H. Frickel, R.E. Shaffer, and J.B. Stamatoff, Technical Report ARCSL-TR-77041 U.S. Army Armament Research and Development Command, Chemical Systems Laboratory, Aberdeen Proving Grounds, Maryland, (1955).
2. R.F. Weurker, H. Shelton, and R.V. Langmuir, J. Appl. Phys.,**30**, 342, (1959).
3. E.J. Davis, Langmuir, **1**, 379, (1985).
4. E.J. Davis, P. Ravindran, and A.K. Ray, Adv. Coll. Int. Sci., **15**, 1, (1981).
5. G.O. Rubel, J. Coll. Int. Sci., **85** , 549, (1982).
6. G.O. Rubel and J.W. Gentry, J. Aerosol Sci., **15**, 661, (1984).
7. M.C. Cohen, R.C. Flagan, and J.H. Seinfeld, submitted for publication.
8. L.M. Folan, S. Arnold and S.D. Druger, Chem. Phys. Lett. **118** , 322, (1985).
9. R. Thurn and W. Kiefer, Applied Optics **24** , 1515, (1985).
10. R.E. Preston, T.R. Letteri, and H. Semerjian, Langmuir **1** , 365, (1985).
11. S. Arnold, M. Neuman, and A.B. Pluchino, Optics Lett. **2**, 4, (1984).
12. S. Arnold and A.B. Pluchino, Appl. Opt. **21**, 4199, (1982).
13. S. Arnold, E.K. Murphy and G. Sageev, Appl. Opt. , **7**, 1048, (1985).
14. M.R. Querry, R.V. Waring, W.E. Holland, L.M. Earls, M.D. Herrman, W.P. Nijm, and G.M. Hale, J. Opt. Soc. Am., **64** , 39, (1974).
15. G. Sageev, R.C. Flagan, J.H. Seinfeld, and S.Arnold, J. Coll. Int. Sci., **113** , 421, (1986).
16. R.G. Bell, "Introductory Fourier Transform Spectroscopy", Academic Press, N.Y., (1972).
17. G. Sageev, J.H. Seinfeld, and R.C. Flagan, Rev. Sci. Inst., **57**, 933, (1986).

18. S. Arnold and L.M. Folan, Rev. Sci. Inst., **57**, 2250, (1986).

19. G. Mie, Ann. Physik, **25**, 377, (1908).

20. A. Ashkin and J.M. Dziedzic, Phys. Rev. Lett., **38**R, 1351, (1977).

21. E.E. Remsberg, Appl. Opt., **12**, 1389, (1973).

22. F.E. Volz, Appl. Opt., **12**, 565, (1973)

8. FIGURE CAPTIONS

Figure 1. A schematic diagram of the single particle levitation system, the vacuum chamber,and the particle jet.

Figure 2. The experimental layout for single particle Fourier transform infrared spectroscopy.

Figure 3. The scattered light intensity at 90° from a single $(NH_4)_2SO_4$ particle, illuminated by a dye laser, as a function of the laser wavelength.

Figure 4. The amplitude of the scattered light modulation, obtained with a lock-in amplifier, as a function of the interferometer mirror position for a 24.4% (by mass) $(NH_4)_2SO_4$ - H_2O particle, 3.14 μm radius.

Figure 5. The convolution of the instrument line function and the particle absorption spectrum, $B(k)$, as a function of wavelength, obtained by a discrete FFT inversion of the data shown in Figure 4.

Figure 6. The relative absorption spectrum, $B(k)/I_s(k)T(k)$, of the $(NH_4)_2SO_4$ particle in Figure 5.

Figure 7. The effect of a reduction in the particle water content on the absorption spectrum, obtained for a 13 molal (solid line) and a 2.5 molal (dashed line) $(NH_4)_2SO_4$ particles.

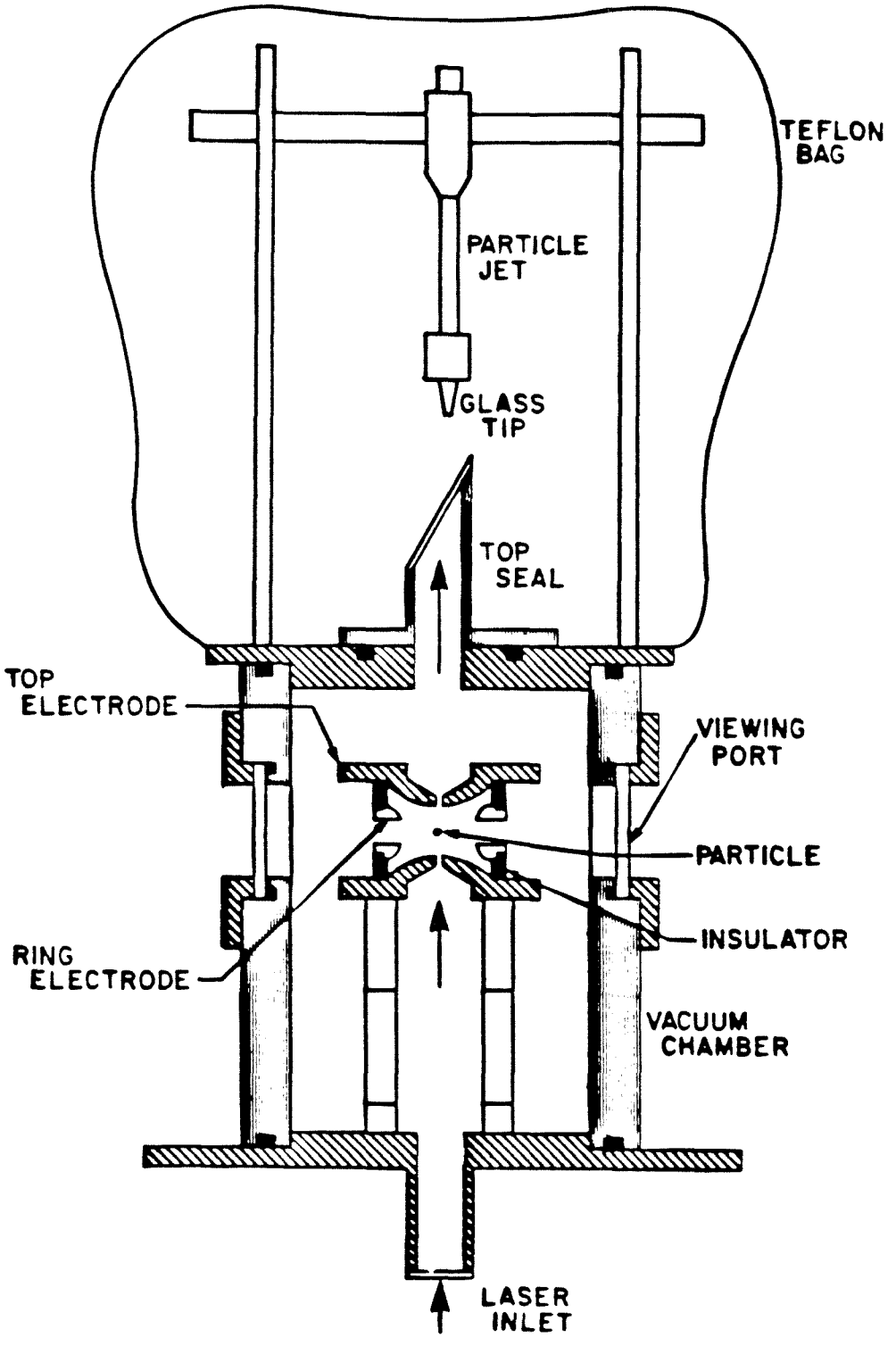

Figure 1. A schematic diagram of the single particle levitation system, the vacuum chamber,and the particle jet.

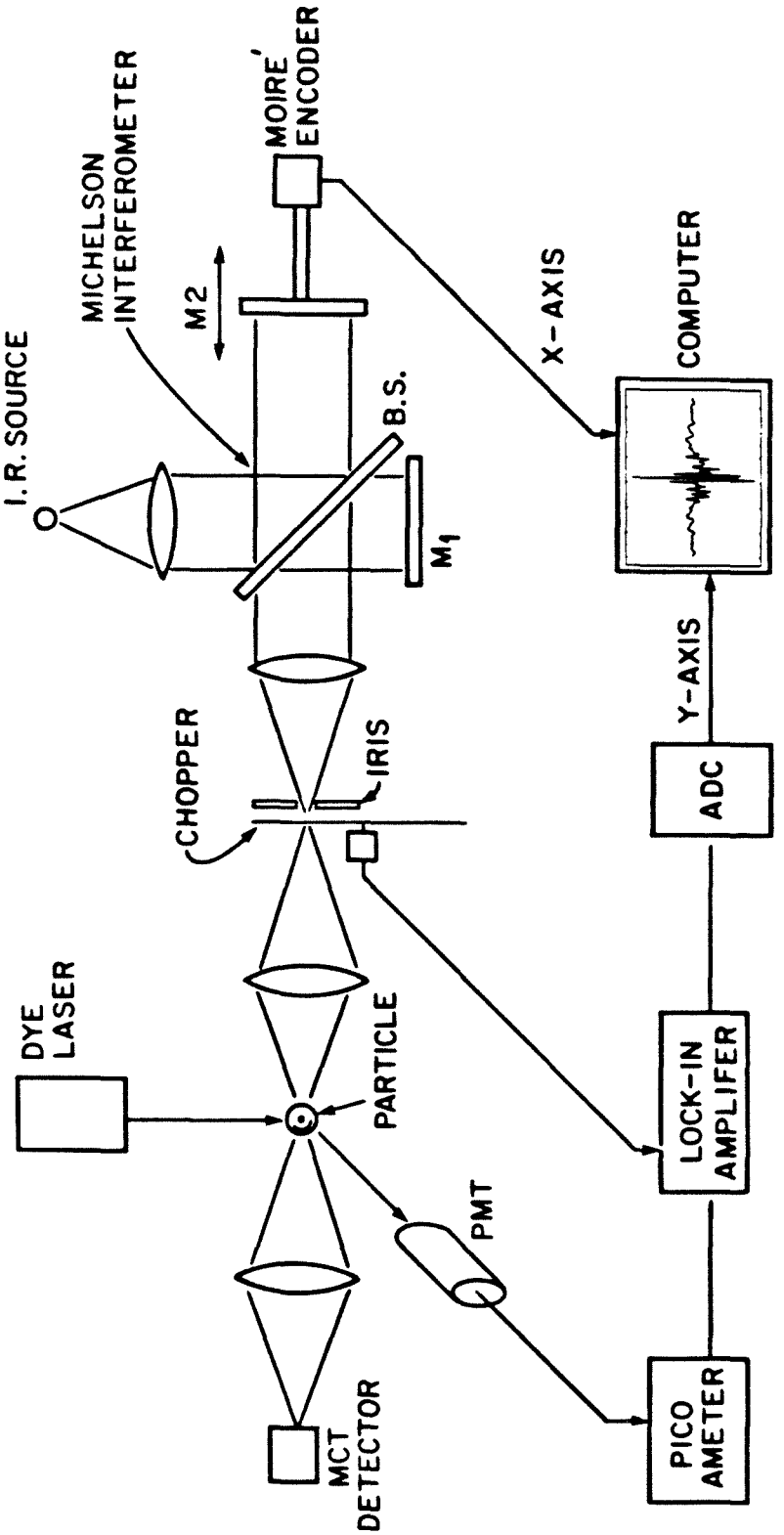

Figure 2. The experimental layout for single particle Fourier transform infrared spectroscopy.

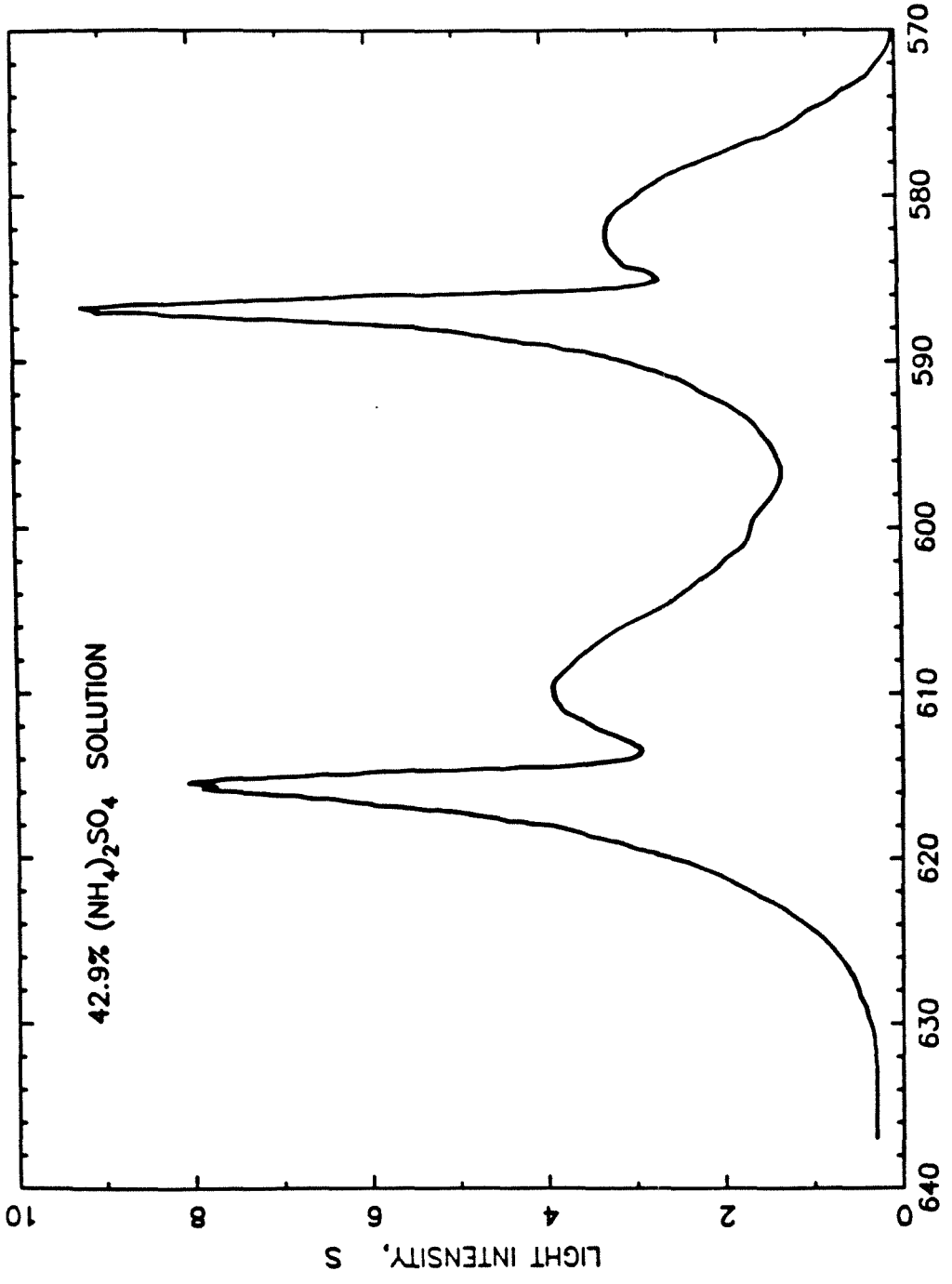

Figure 3. The scattered light intensity at 90° from a single $(NH_4)_2SO_4$ particle, illuminated by a dye laser, as a function of the laser wavelength.

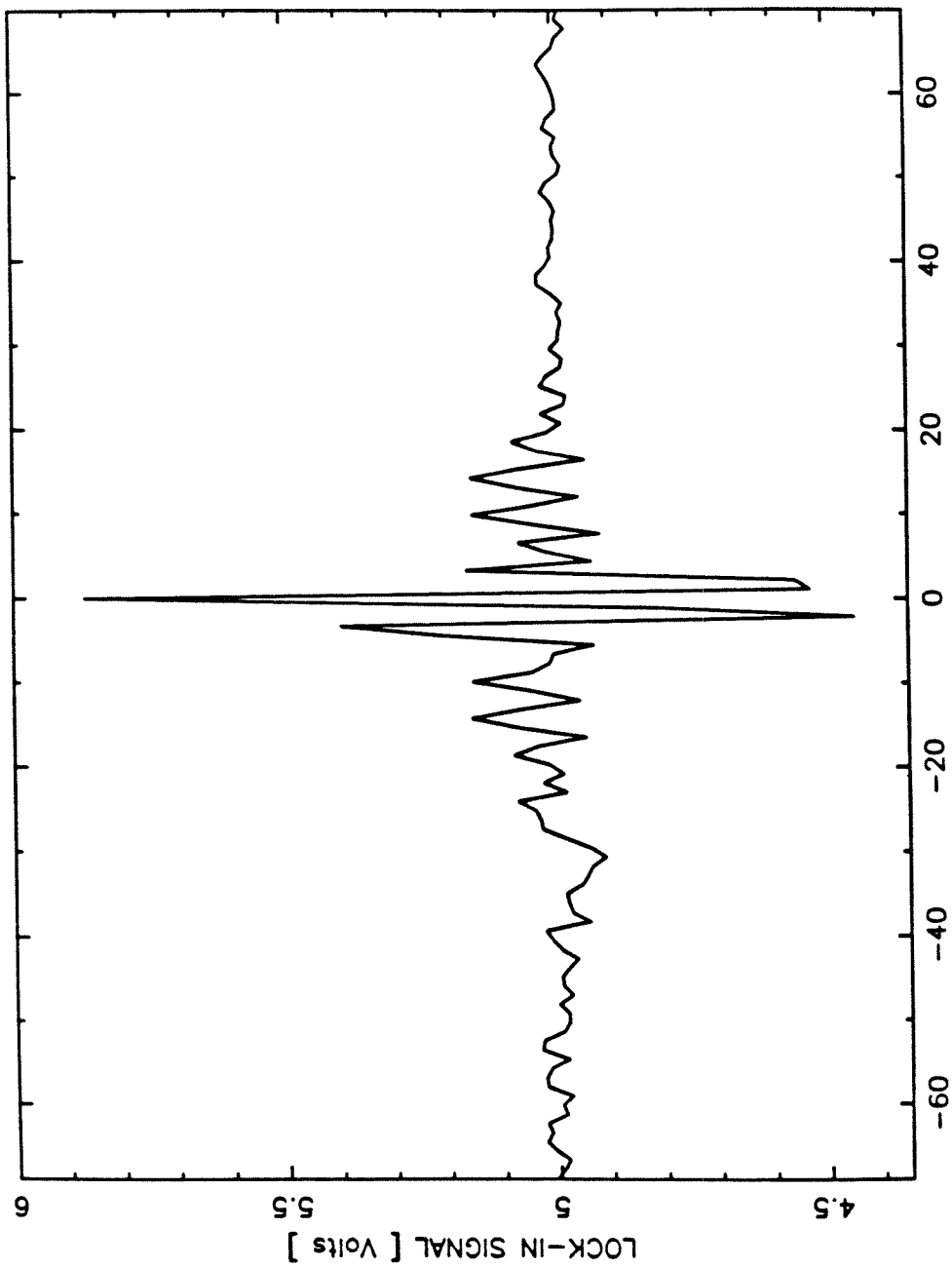

Figure 4. The amplitude of the scattered light modulation, obtained with a lock-in amplifier, as a function of the interferometer mirror position for a 24.4% (by mass) $(NH_4)_2SO_4$ - H_2O particle, 3.14 μm radius.

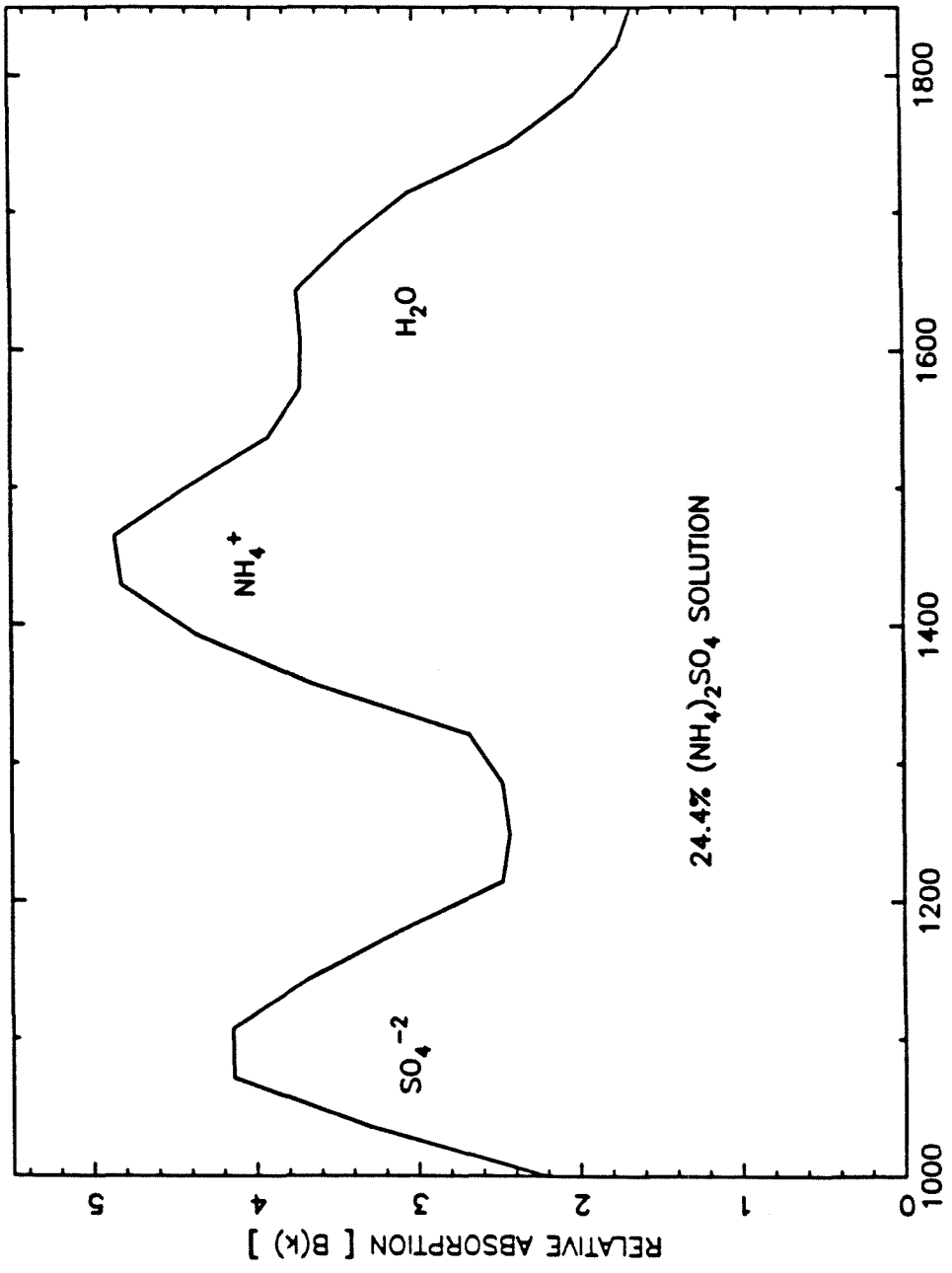

Figure 5. The convolution of the instrument line function and the particle absorption spectrum, $B(k)$, as a function of wavelength, obtained by a discrete FFT inversion of the data shown in Figure 4.

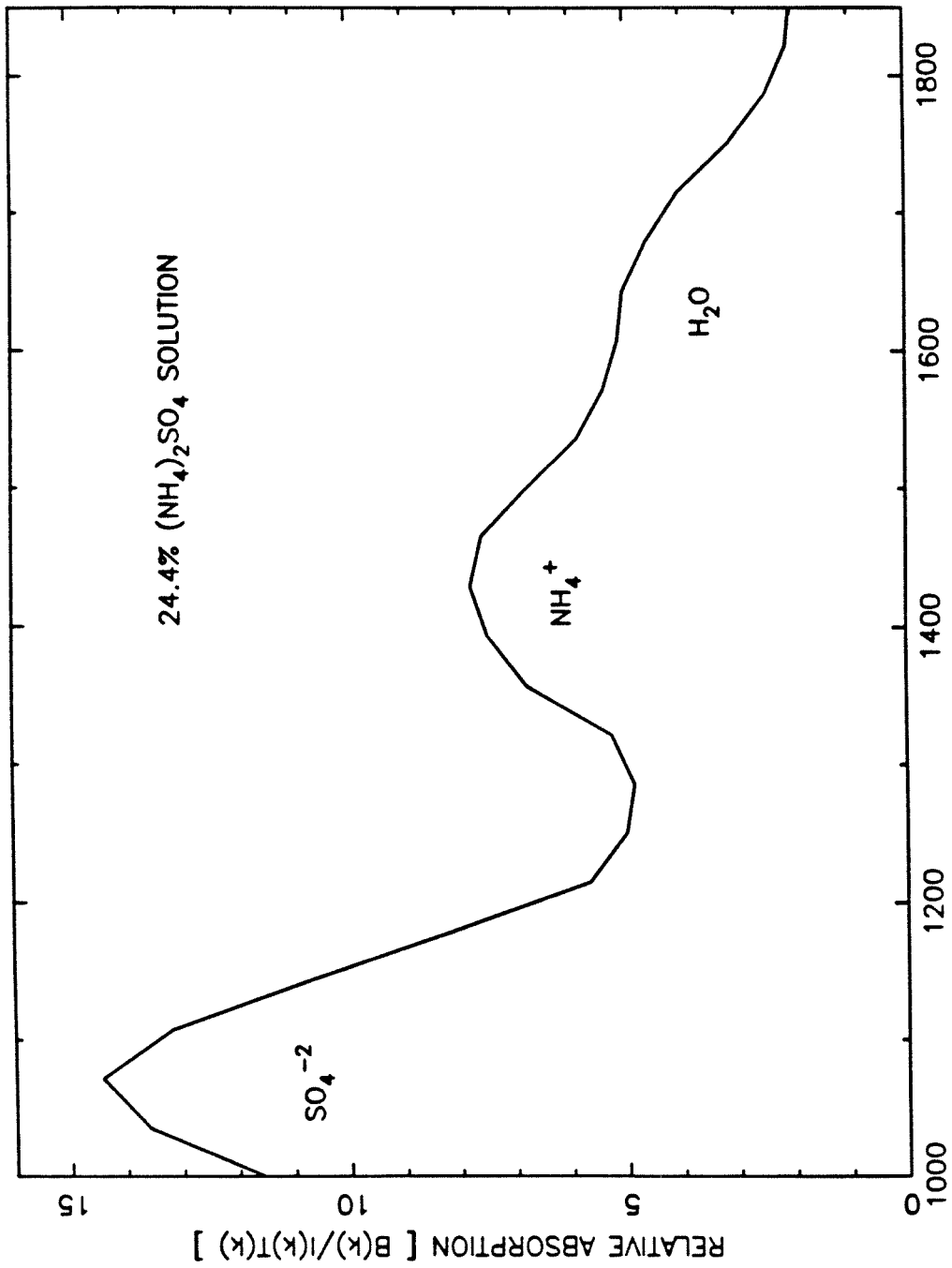

Figure 6. The relative absorption spectrum, $B(k)/I_s(k)T(k)$, of the $(NH_4)_2SO_4$ particle in Figure 5.

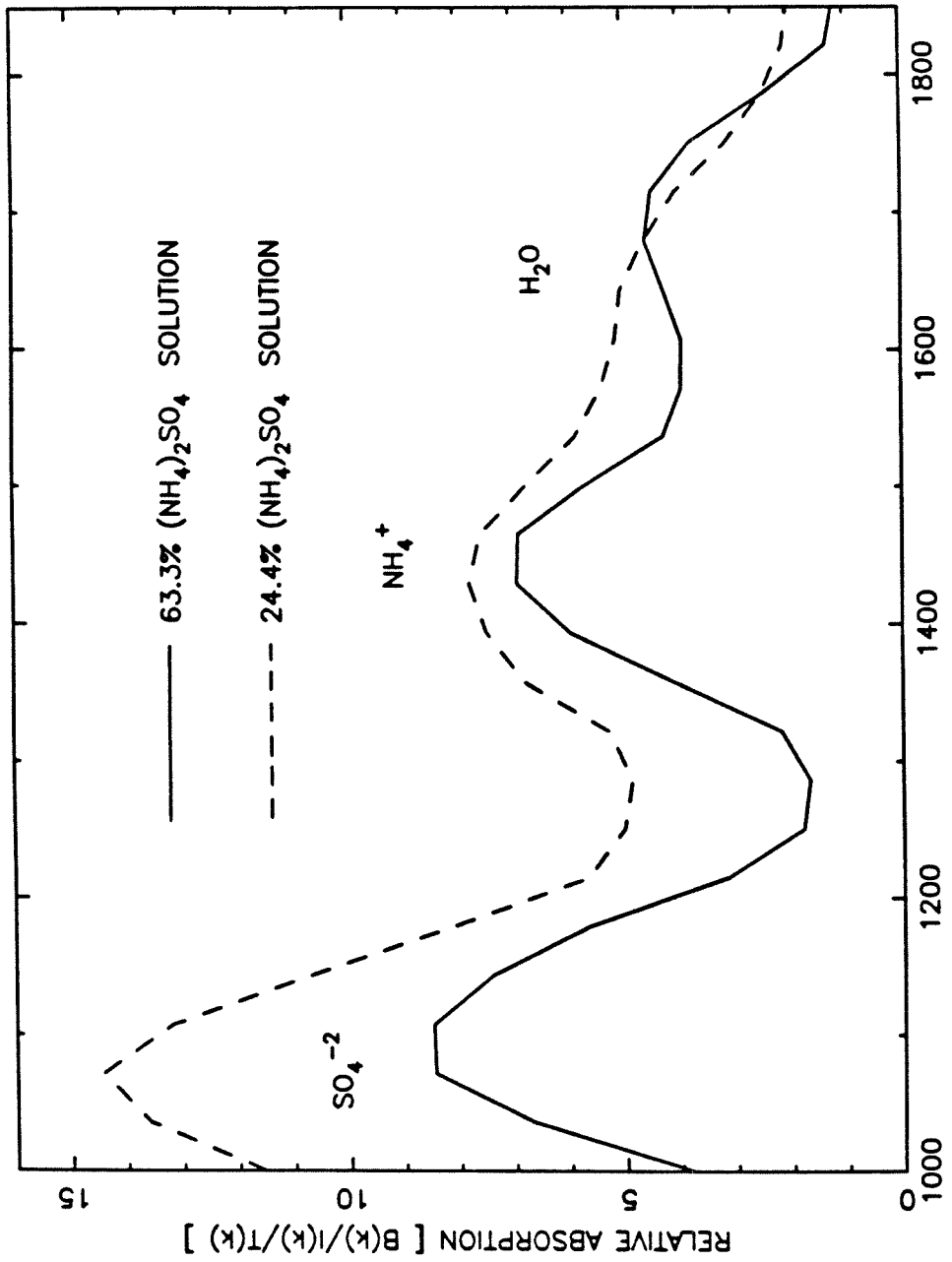

Figure 7. The effect of a reduction in the particle water content on the absorption spectrum, obtained for a 13 molal (solid line) and a 2.5 molal (dashed line) $(NH_4)_2SO_4$ particles.

CHAPTER 7

FTIR SPECTROMETER FOR A SINGLE AEROSOL PARTICLE

By :

Gideon Sageev Grader*

Richard C. Flagan*

Stephen Arnold+

John H. Seinfeld*

Submitted to Review of Scientific Instruments, November, 1986.

*Department of Chemical Engineering, California Institute of Technology,

Pasadena, CA 91125

+Department of Physics, Polytechnic Institute of New York, Brooklyn,

New York, 11201

ABSTRACT

A spectrometer is reported here for obtaining the infrared spectrum of a single aqueous aerosol particle by a Fourier transform technique. The particle is held in an electrodynamic balance and irradiated simultaneously by the infrared output from a Michelson interferometer and the visible light from a dye laser. The size of the particle is modulated by chopping the IR beam, and the resulting visible scattered light fluctuation is detected at 90° with a photomultiplier tube. The amplitude of the scattered light fluctuation is measured with a lock-in amplifier at each interferometer mirror position. The electronic cicuitry for stepping the interferometer mirror is presented and discussed. Inverting the lock-in signal by a discrete fast Fourier transform routine (FFT) yields the particle absorption spectrum. The resulting spectrum for an $(NH_4)_2SO_4$ droplet is presented.

1. INTRODUCTION

The ability to characterize and chemically analyze aerosol particles has been of great interest in aerosol research. This effort has been pursued along two main streams; in one direction attention is directed to a whole assembly of particles, and in the other a single particle is isolated and studied. The advantage of the first approach is that the number of particles under study can be made large, and thus various conventional analytical techniques can be used to characterize them. On the other hand, the single particle technique has become a versatile tool for studying fundumental processes occurring within an aerosol particle. Among the various applications of the single particle technique are evaporation and condensation phenomena[1,2], chemical reactions[3], photoemission from a single particle[4], photophoretic spectroscopy[5], material phase transitions[6], and energy transfer within a microparticle[7]. The versatility of the single particle approach arrises from the ability to monitor continuously the charge-to-mass ratio as well as the scattered light from the particle. Hence any changes in the particle size or its refractive index can be readily observed. In addition, nonlinear phenomena such as the optical resonances[8] in the scattered light from a single particle can be be employed to detect small changes in the size or refractive index of a microparticle.

Recently a method for obtaining the infrared spectrum of a single particle was conceived[9] and demonstrated[10,11]. In the method a single charged particle is levitated in an electrodynamic balance by the fields generated in quadrupolar geometry[12,13,14]. The infrared spectrum was obtained by illuminating the particle with a dye laser, and simultaneously heating the particle periodically with an IR

source. The excitation wavelength in the IR is selected with a wedge monochromator. Heating the particle periodically causes a modulation in its size, which induces a corresponding fluctuation in the scattered light from the particle. This scattered light fluctuation is measured at 90^o (for geometrical simplicity), using a photomultiplier tube (PMT). By phase sensitively detecting the amplitude of the scattered light fluctuation as a function of the IR wavelength, an absorption spectrum of the particle is obtained.

We have recently reported a variation of the above method, where the the IR spectrum of an aqueous droplet is obtained by a Fourier transform technique[15], similar to that suggested earlier[9]. In this method the particle is irradiated by the output from a Michelson interferometer. The amplitude of the scattered light fluctuation is measured as a function of the interferometer mirror position. The resulting scan (called an interferogram), is stored in a computer and the spectrum is obtained by inverting the scattered light data by a discrete fast fourier transform (FFT) routine. The purpose of the present paper is to describe the Fourier transform spectrometer, show a spectrum for an $(NH_4)_2SO_4$ particle, discuss the performance of the instrument, and outline where simplifications can be made.

2. THE APPARATUS

In the technique described here a single aqueous solution microparticle is levitated in an electrodynamic balance (also called a quadrupole trap). The trap consists of top and bottom electrodes between which a DC potential is held, and a ring electrode to which an AC voltage is applied[2,16]. Once trapped in this device, a charged particle can be held almost indefinitely. The trap is positioned inside a vacuum chamber which allows for accurate control of the pressure and vapor phase surrounding the particle.

A schematic diagram of the single-particle FTIR spectrometer is shown in Figure 1, where for clarity the vacuum chamber is omitted. As indicated the particle is illuminated simultaneously by a dye laser and the IR output from a Michelson interferometer. The 90^o scattered light from the particle falls on a photomultiplier tube, and the resulting PMT current is measured with a picoammeter. The laser is tuned to an edge of an optical resonance[8] where the scattered light from the particle is sensitive to changes in the particle size[9]. From Figure 1 it is also noted that the IR output of the interferometer is chopped prior to falling on the particle. When the IR radiation falls on the particle, its effect is to heat the particle slightly, causing evaporation of a small amount of water from the drop. Continued evaporation upon heating is restrained by the increase in the water activity of the droplet accompanying water loss. When the chopper shields the particle from the IR, water vapor recondenses on the particle and the droplet returns to its original size. Since the scattered light from the particle is highly sensitive to size changes, the size modulation caused by the periodic IR heating induces a corresponding fluc-

tuation in the scattered light from the particle. This fluctuation is measured with a lock-in amplifier.

In conventional near IR interferometery, the interferometer mirror is moved continuously because the detector used has a fast response time compared with the modulation rate of the IR intensity. However in our experiment the detector is a single droplet whose response time is governed by the rate of water evaporation and condensation on the surface of the droplet. As earlier work showed[2,11], this rate is in general slow because of the large heat of vaporization of water. In addition, we have found that the signal-to-noise ratio of the scattered light signal from the particle was poor near the optical resonances. In order to increase the S/N ratio, we move the interferometer mirror in steps. This approach allows us to chop the IR beam and detect the scattered light modulation signal with a lock-in amplifier. By increasing the lock-in time constant, the S/N ratio of the scattered light signal can be improved. Thus a key to this experiment is the ability to accurately move the interferometer mirror in equal steps, (down to ≈ 0.5 μm per step), over a distance ranging from a few hundred microns to a few millimeters. The steps must be of equal length because the discrete FFT inversion routine relies on this factor. The existing piezoelectric drivers capable of this step resolution usually have a range that is smaller than 100 μm. A possible solution would have been to use an inch-worm type of driver, however to make use of available equipment, we decided to modify a conventional interferometer in which the moving mirror is mounted on air bearings and is driven by a geared down DC motor. The stepping of the mirror is achieved by applying a train of pulses to the motor and disabling the motion when

the desired distance has been covered. The travel of the mirror is tracked with a moire' encoder that outputs a pulse every time the mirror travels ≈ 0.5 μm.

A schematic diagram of the circuit used to control the mirror motion is presented in Figure 2. To achieve equal repetitive steps, it is critical to disable the mirror motion immediately when the encoder signal arrives. For flexibility, the pulse rate and length were computer controlled; however, to achieve quick switch-off times the computer pulse was disabled by hardware. As shown in Figure 2, an enable pulse from the computer triggers a 1 μsec pulse (from a monostable) that presets a J-K flip flop. The Q output of the flip flop and the computer enable pulse are sent to the inputs of an AND gate, the output of which forms the mirror step signal. The encoder signal is optically isolated from the driving electronics to avoid grounding problems. To shorten the rise and fall times of the optical isolator output pulse, the signal was sent to a Schmitt trigger followed by an FET transistor. The main purpose of the FET output is to stop the mirror enable signal by clocking the flip flop that turns the Q output low. In addition the rising edge of the FET signal triggers a monostable, the output of which is sent to the computer and tells the program to stop the current enable pulse.

After the mirror was stepped to a new postion, enough time must be allowed for the lock-in signal to stabilize before a new data point is taken. This can be done either manually or automatically. The delay time between moving the mirror and taking a new A/D reading depends on the lock-in time constant. In most cases the lock-in time constant was 10 to 30 seconds, and 140 data points were taken. Thus it usually took 1-2 hours to record a complete scan.

3. THEORY

The measured signal in this experiment is the lock-in output (which is proportional to the amplitude of the scattered light fluctuation), as a function of the interferometer mirror position, l . For a particle with an initial radius a_o, and an initial scattered light intensity S_o, the signal measured at the output of the lock-in amplifier is given by[15],

$$\frac{< \delta S(l) >}{S_o} = - \int_{-\infty}^{\infty} B(k) e^{j(kl+\theta)} dk \tag{1}$$

where $\delta S(l)$ is the scattered light fluctuation, k is the infrared wavenumber, $2\pi/\lambda$, and $B(k)$ is given by[11],

$$B(k) = \frac{\beta}{a_o} \frac{\alpha(k) I_s(k) T(k)}{(\omega^2 + \gamma^2)^{1/2}} \tag{2}$$

where $T(k)$ is the transmission of the optical elements in the IR pathway, $I_s(k)$ is the IR source intensity, ω is the IR chop rate, and γ is the relaxation rate of a heated particle to its unheated original size. In equation (1) θ is given by $\theta = -\frac{\omega}{\gamma}$. β is the amplification factor that allows one to relate the changes in the particle size to the measured fluctuations in the scattered light and is given by[9],

$$\frac{\delta S}{S_o} = \beta \frac{\delta a}{a_o} \tag{3}$$

Finally, $\alpha(k)$ is proportional to the particle absorption coefficient, Q_a, and therefore contains the desired chemical information about the particle.

4. RESULTS

An example of a scattered light interferogram taken on an aqueous $(NH_4)_2SO_4$ particle is shown in Figure 3. The chopping frequency during this scan was 4 Hz, and the mirror was stepped 140 times with a separation of $\approx$ 1 μm between successive steps. The zero point of the mirror position in Figure 3 is at the equal arm point of the Michelson interferometer. Recall that the interferometer consists of a beam splitter and two mirrors that reflect the splitted beam back towards the beam splitter where they recombine. Therefore at the equal arm point all the wavelengths recombine constructively. Hence only at this point are all the absorbing species in the droplet excited simultaneously. Thus the energy absorbed by the droplet is higher, and the resulting scattered light fluctuation is larger than at any other point in the interferogram. As the mirror is stepped away from the zero point, the amplitude of the fluctuation drops since some of the wavelengths at which the droplet absorbs undergo destructive interference.

The spectrum of the particle is obtained from the interferogram by a discrete fast Fourier transform (FFT) routine. The resulting relative absorption spectrum, $B(k)/I_s(k)T(k)$, is shown in Figure 4. This particular spectrum was obtained from a 3.0 μm solution droplet of 35 % (by weight) ammonium sulfate. The absorption peaks of the sulfate, ammonium, and water are indicated. The position of the peaks agrees with previous results for a single particle[11], as well as with spectra obtained from bulk solutions[17,18].

5. DISCUSSION

The spectrum shown in Figure 4 was obtained by moving the mirror about 140 μm, giving rise to a theoretical resolution of $\approx$ 70 cm^{-1} in the displayed spectrum. It took roughly 2 hours to obtain the scan displayed in Figure 3 which means that at present the technique is suitable only for the study of static chemical systems. In order to facilitate the study of systems where chemical reactions might be occurring, the time necessary for a single scan must be shortened. One approach towards this goal is reducing the particle size, thereby reducing the particle relaxation time[2,11]. The shorter relaxation time allows a faster chop rate of the IR, which in turn can reduce the required lock-in time constant and yield a shorter scan time.

Another approach to shortening the scan time, first proposed by Arnold and Pluchino[9], is to move the mirror continuously as in conventional IR interferometers. By moving the mirror continuously the use of the chopper and the lock-in amplifier is eliminated (thus simplifying the experiment). The modulation in the IR intensity at the droplet is now governed by the velocity v of the mirror. The resulting inverse transform $B(k)$ is given by,

$$B(k) = \frac{\beta}{a_o} \frac{\alpha(k) I_s(k) T(k)}{((2kv)^2 + \gamma^2)^{1/2}}. \tag{4}$$

As mentioned earlier the main difficulty in this approach is overcoming small signal-to-noise ratio in the scattered light from a particle near the optical resonance. The signal can be increased by using smaller particles and by increasing temperature of the IR source. For example a Nurnst glower may be operated at temperatures above 2000°C, whereas the glow bar used here was operated at 1250°C. Among the possible sources of this noise are a small amount of dirt in the particle (or on

its surface), which alters the amount of light scattered towards the photomultiplier tube as the particle rotates; another source of noise is the fluctuations in intensity associated with the dye laser. However if the signal to noise ratio can be improved, a continuous scan could be implemented which will both simplify the experiment as well as shorten the time required to obtain the spectrum of a single particle.

6. CONCLUSIONS

We describe here an instrument with which the IR spectrum of a single aerosol particle can be obtained by Fourier transform spectroscopy. The absorption spectrum of an aqueous $(NH_4)_2SO_4$ solution particle is shown and the performance of the current instrument is discussed.

7. ACKNOWLEDGEMENT

This research was supported by U.S. Environmental Protection Agency grant R-810857 and by gifts from General Motors Corporation and Mobil Oil Corporation. S. Arnold was supported by a Chevron Visiting Professorship at the California Institute of Technology and by National Science Foundation Grant ATM-8413574. The authors thank Anthony B. Pluchino of the Aerospace Corporation and Ralph Waniak of Advanced Kinetics for helpful advice during this work.

8. REFERENCES

1. E.J. Davis, P. Ravindran, and A.K. Ray, Adv. Coll. Int. Sci., **15** , 1, (1981).
2. G. Sageev, R.C. Flagan, J.H. Seinfeld, and S.Arnold, J. Coll. Int. Sci., **113** , 421, (1986).
3. G.O. Rubel and J.W. Gentry, J. Aerosol Sci., **15** , 661, (1984).
4. S. Arnold and S. Hessel, Rev. Sci. Inst., **56** , 2066, (1985).
5. S. Arnold and Y. Amani, Opt. Lett., **5**, 242, (1980).
6. C.A. Kurtz and C.B. Richardson, Chem. Phys. Lett., **109**, 190, (1984).
7. L.M. Folan, S. Arnold and S.D. Druger, Chem. Phys. Lett. **118** , 322, (1985).
8. A. Ashkin and J.M. Dziedzic, Phys. Rev. Lett., **38** , 1351, (1977).
9. S. Arnold and A.B. Pluchino, Appl. Opt. **21**, 4199, (1982).
10. S. Arnold, M. Neuman, and A.B. Pluchino, Optics Lett. **2** , 4, (1984).
11. S. Arnold, E.K. Murphy and G. Sageev, Appl. Opt. , **7** , 1048, (1985).
12. E.J. Davis, Langmuir, **1**, 379, (1985).
13. R.H. Frickel, R.E. Shaffer, and J.B. Stamatoff, Technical Report ARCSL-TR-77041 U.S. Army Armament Research and Development Command, Chemical Systems Laboratory, Aberdeen Proving Grounds, Maryland, (1955).
14. R.F. Weurker, H. Shelton, and R.V. Langmuir, J. Appl. Phys., **30**, 342, (1959).
15. G. Sageev-Grader, S. Arnold, R.C. Flagan, and J.H. Seinfeld, submitted for publication.
16. G. Sageev, J.H. Seinfeld, and R.C. Flagan, Rev. Sci. Inst., **57** , 933, (1986).
17. E.E. Remsberg, Appl. Opt., **12**, 1389, (1973).
18. F.E. Volz, Appl. Opt., **12**, 565, (1973)

8. FIGURE CAPTIONS

Figure 1. Experimental system for single particle Fourier transform infrared spectroscopy.

Figure 2. Electronic circuitry for stepping the interferometer mirror.

Figure 3. The amplitude of the scattered light modulation, obtained with a lock-in amplifier, as a function of the interferometer mirror position for a 35 % (by mass) $(NH_4)_2SO_4 - H_2O$ solution particle, 3.0 μm radius.

Figure 4. The relative absorption spectrum, $B(k)/I_s(k)T(k)$, of the $(NH_4)_2SO_4$ particle in Figure 3.

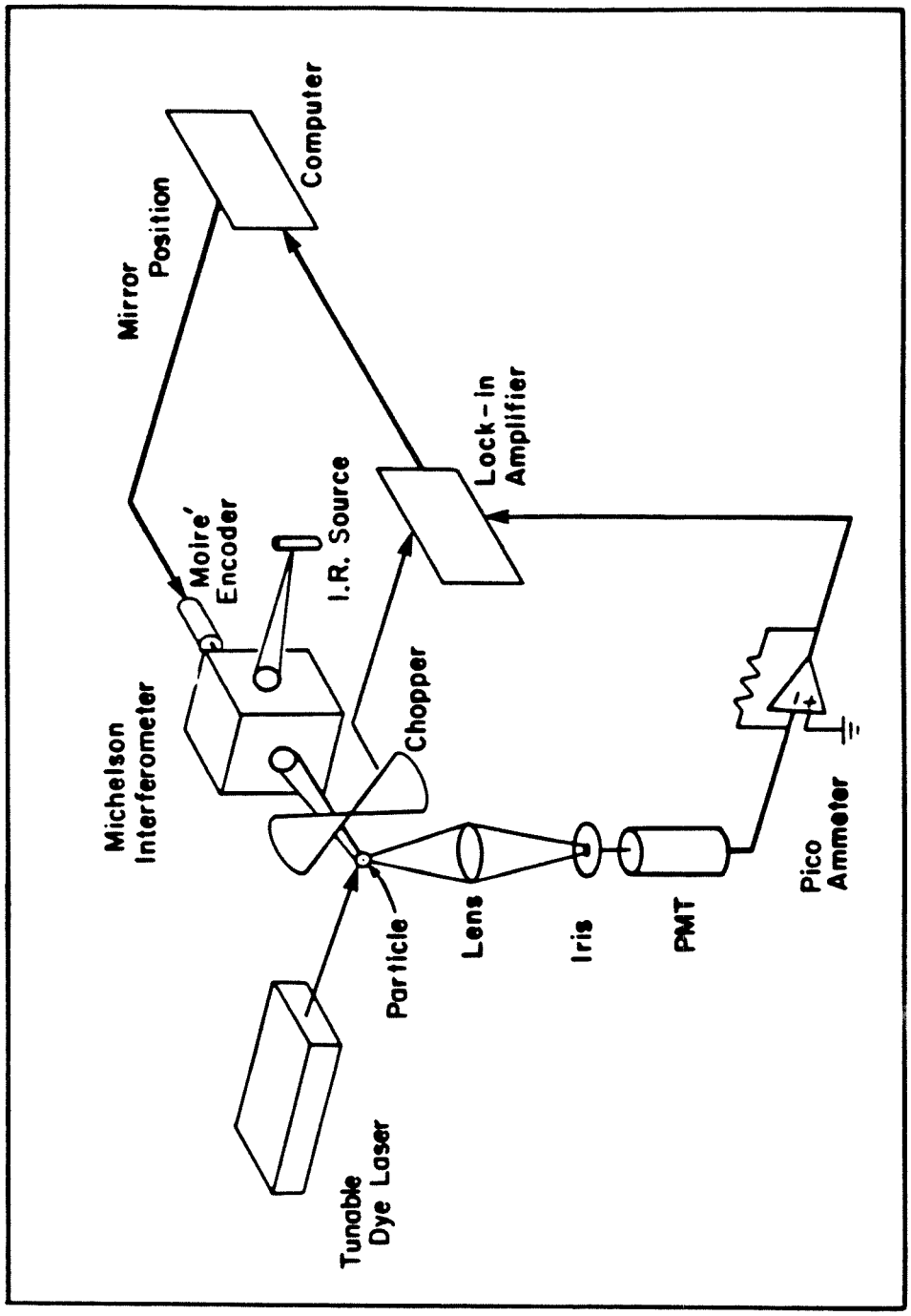

Figure 1. Experimental system for single particle Fourier transform infrared spectroscopy.

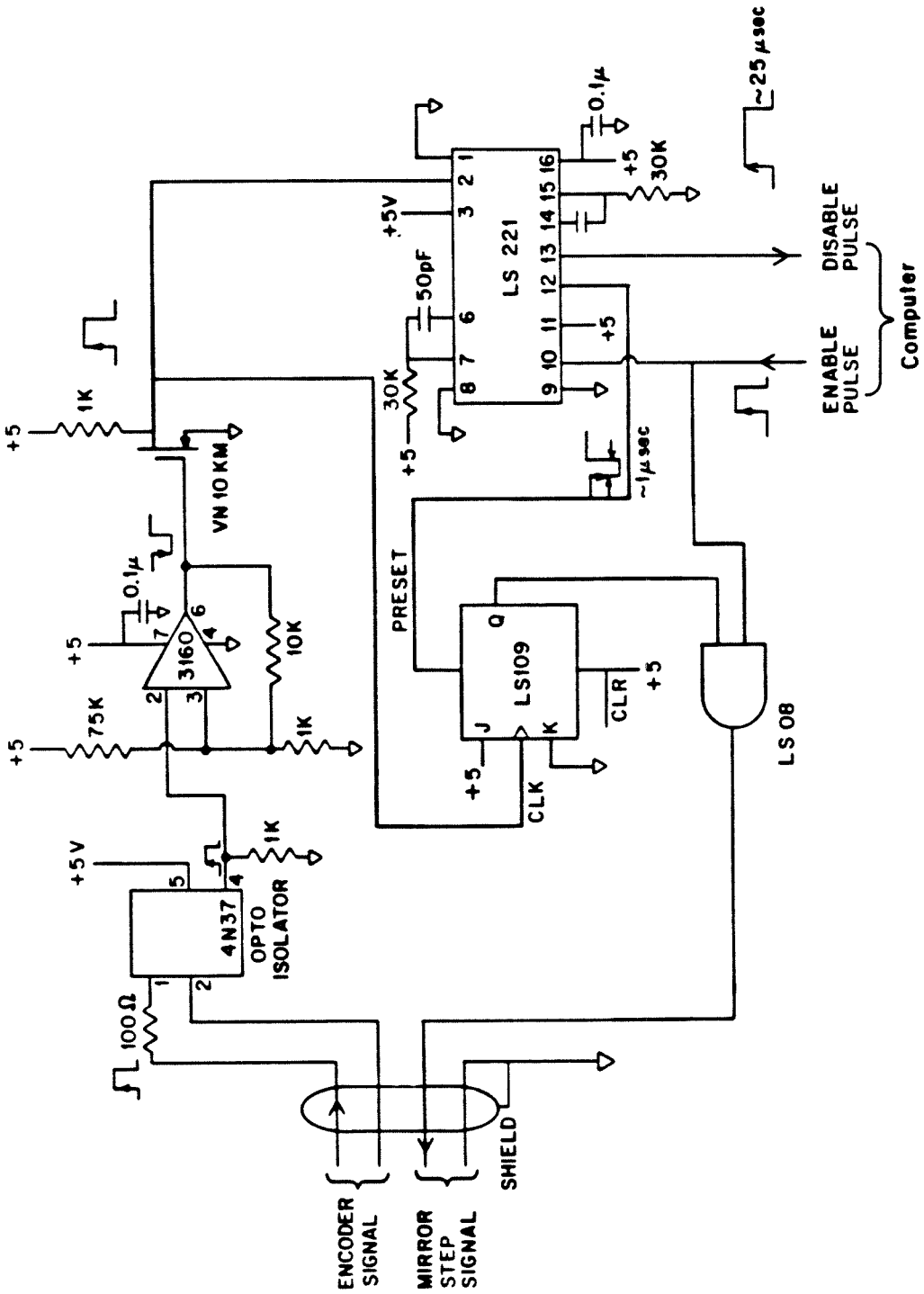

Figure 2. Electronic circuitry for stepping the interferometer mirror.

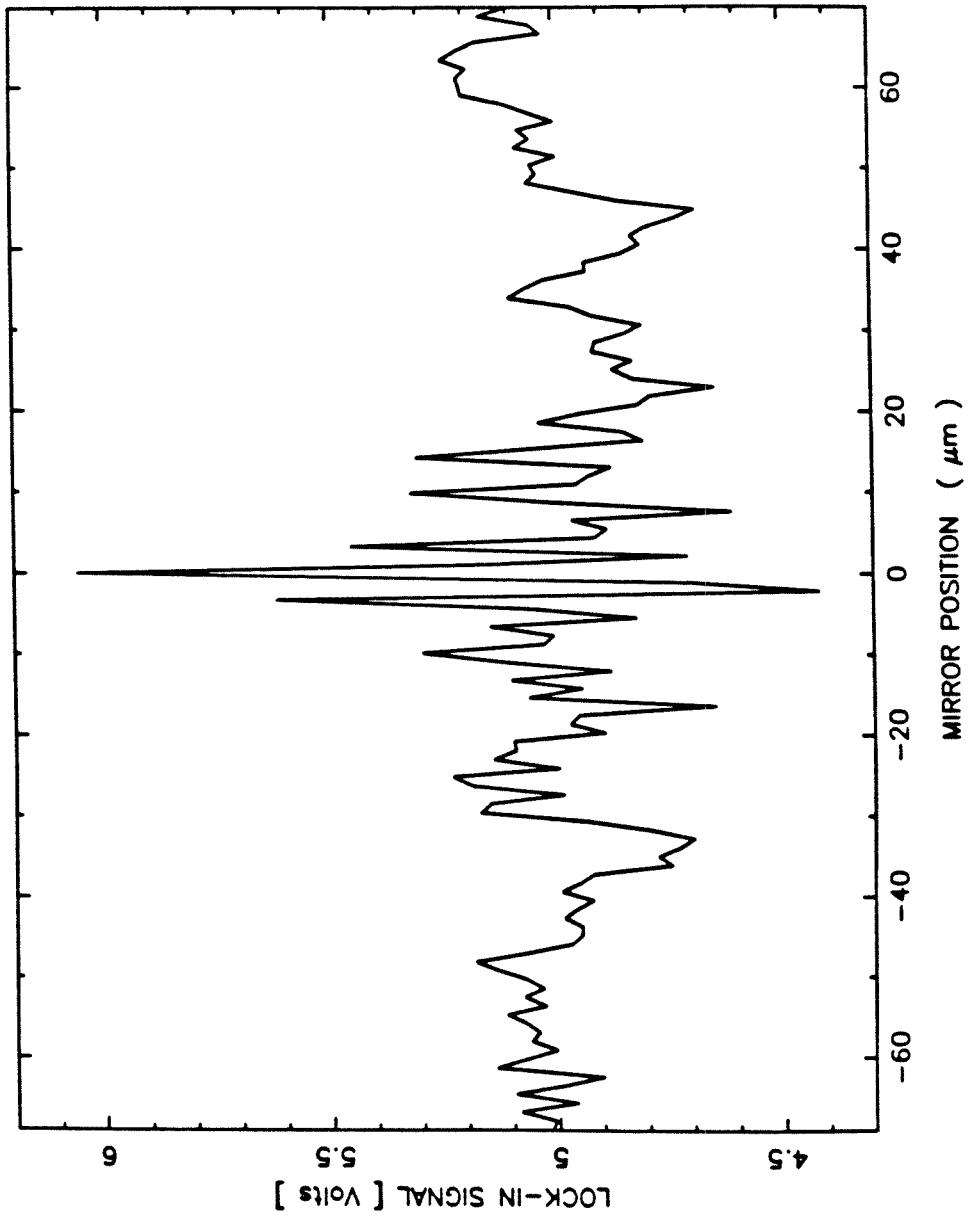

Figure 3. The amplitude of the scattered light modulation, obtained with a lock-in amplifier, as a function of the interferometer mirror position for a 35 % (by mass) $(NH_4)_2SO_4 - H_2O$ solution particle, 3.0 μm radius.

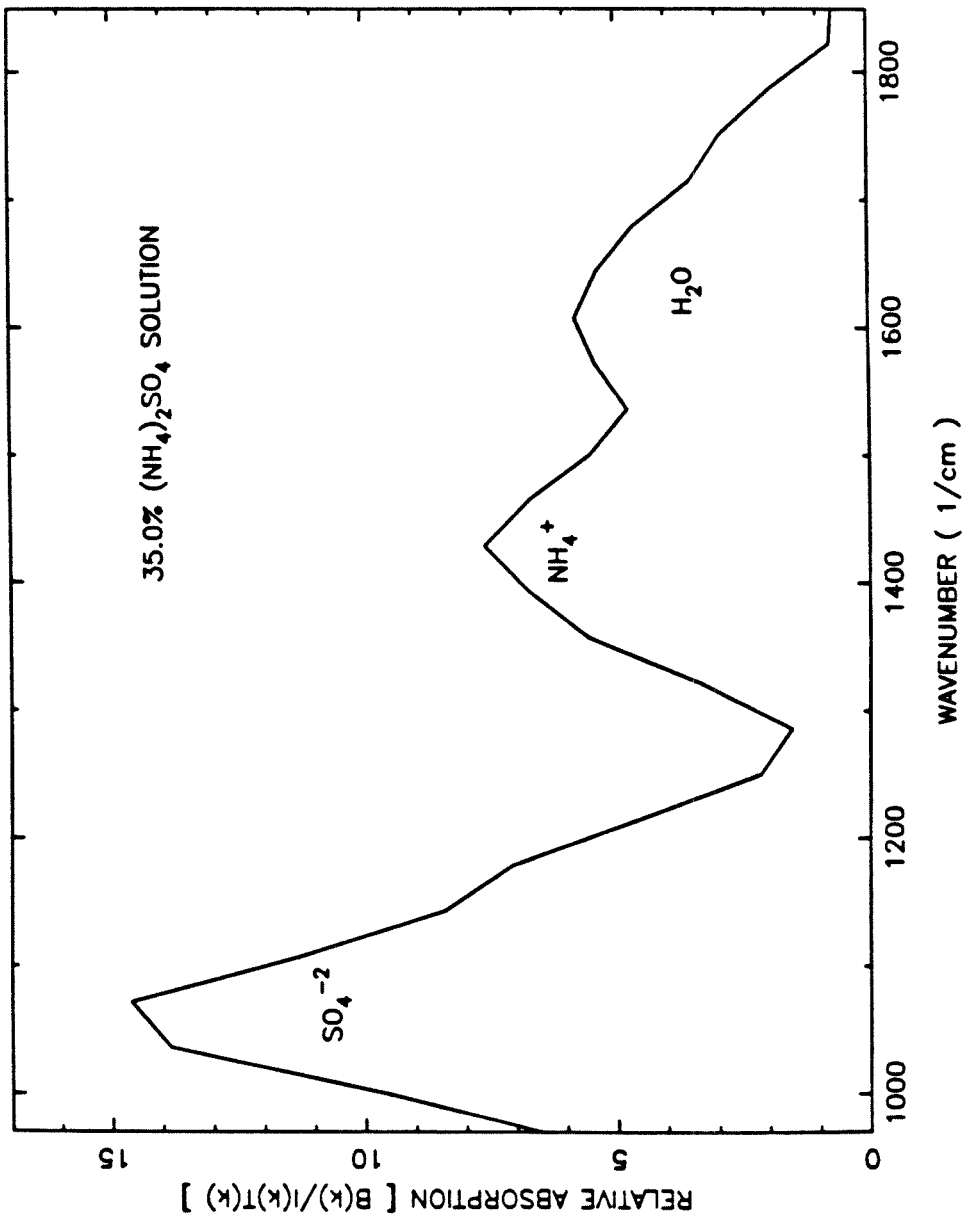

Figure 4. The relative absorption spectrum, $B(k)/I_s(k)T(k)$, of the $(NH_4)_2SO_4$ particle in Figure 3.

CHAPTER 8

CONCLUSIONS

CONCLUSIONS

During this project the effect of energy absorption in aqueous solutions of non-volatile salts was studied both theoretically and experimentally. By heating a charged particle, suspended in an electrodynamic balance, we measured the rates of evaporation and condensation on the particle. The theory developed to describe the water loss and gain processes was shown to agree with the experimental results. In these studies we also attempted to determine the value of both the thermal and mass accommodation coefficients of the water molecule. Results for the thermal accommodation show that its value is close to unity. However the results for the mass accommodation were not conclusive because the thermal effect was dominant due to the large heat evaporization of water.

The main thrust of this research was aimed at employing the particle size changes, associated with heat absorption, in the development of an FTIR technique for obtaining the particle chemical composition. At present we have applied the FTIR spectroscopy to solution droplets of ammonium sulfate. By changing the relative humidity surrounding the droplet, we obtained spectra at various droplet concentrations. The results show changes in the chemical nature of the droplet as the salt concentration changes. For example, the water bending mode which occurs around 1640 cm^{-1}, seems to be shifted upward towards the 1700 cm^{-1} region. This points to the confinement of the hydrogens in the bending mode. It therefore follows that a natural application of this device is to study the chemistry of concentrated (supersaturated) electrolyte solutions.

In an attempt to demonstrate the technique on chemical systems other than

ammonium sulfate, several systems were tried. One system consisted of organic salts such as sodium acetate and sodium formate. In these particles the carbonyl stretch absorbs strongly $\approx$ 2000 cm^{-1}, however we were unable to obtain spectra for these solutions because roughly 10-20 minutes after the droplets were trapped the scattered light from the initially clean particles suddenly became noisy. To demonstrate this problem we show the results obtained from a sodium formate particle. Figure 1 demonstrates the initial resonance curve of the particle, while in Figure 2 the curve for the same particle 20 minutes later. The origin of the sudden change in scattering of the particle shown in Figure 2 is at present unknown.

Another solution with which we tried to demonstrate the technique was sodium nitrate. Here one expects several IR active absorption bands in the 1000-1500 cm^{-1} region. The interferogram obtained from a sodium nitrate droplet is shown in Figure 3, while the inverted result is presented in Figure 4. The results shown here are only initial and the experiments need to be repeated to ensure the reproducibility of the peaks.

It is natural at this point to evaluate the technique developed here and point out how it may be improved. As stated in Chapters 6 and 7, the theoretical resolution of the scans obtained thus far was 70 cm^{-1}. The potential resolution of the instrument is however much lower than the one achieved here. In order to reduce the resolution the signal-to-noise ratio during the scan must be improved. In addition, the time required for a single scan needs to be shortened, to render the technique more useful in reaction studies. As pointed out in Chapter 7 both the scan speed, and the enhanced resolution of the spectrum could be aided by scanning the interferometer

mirror continuously.

The results could also be improved by changing the IR source. In particular, if a hotter source (i.e., a Nurnst glower) is used, the energy throughput in the sample will increase. The increase in energy would enlarge the particle size fluctuation, and thus improve the signal-to-noise ratio directly. Unlike the present instrument, where the IR glow bar is positioned at the focal point of the interferometer optics, the source should be re-imaged on a diaphragm (using an eliptical mirror for example), before entering the interferometer. This would limit the IR energy that enters the chamber, and thus prevent the excessive heating of the chamber during an experiment. As mentioned in Chapter 6 the effect of chamber heating is to slowly change the relative humidity in the chamber, thereby causing a drift in the particle size. The drift in the particle size forces the periodic readjustment of the dye laser, and induces a variation in β, (the amplification factor), during the experiment. Since the variation in β adds directly to the noise in the interferogram, any stabilization of β during the scan will improve the signal-to-noise ratio in the experiment.

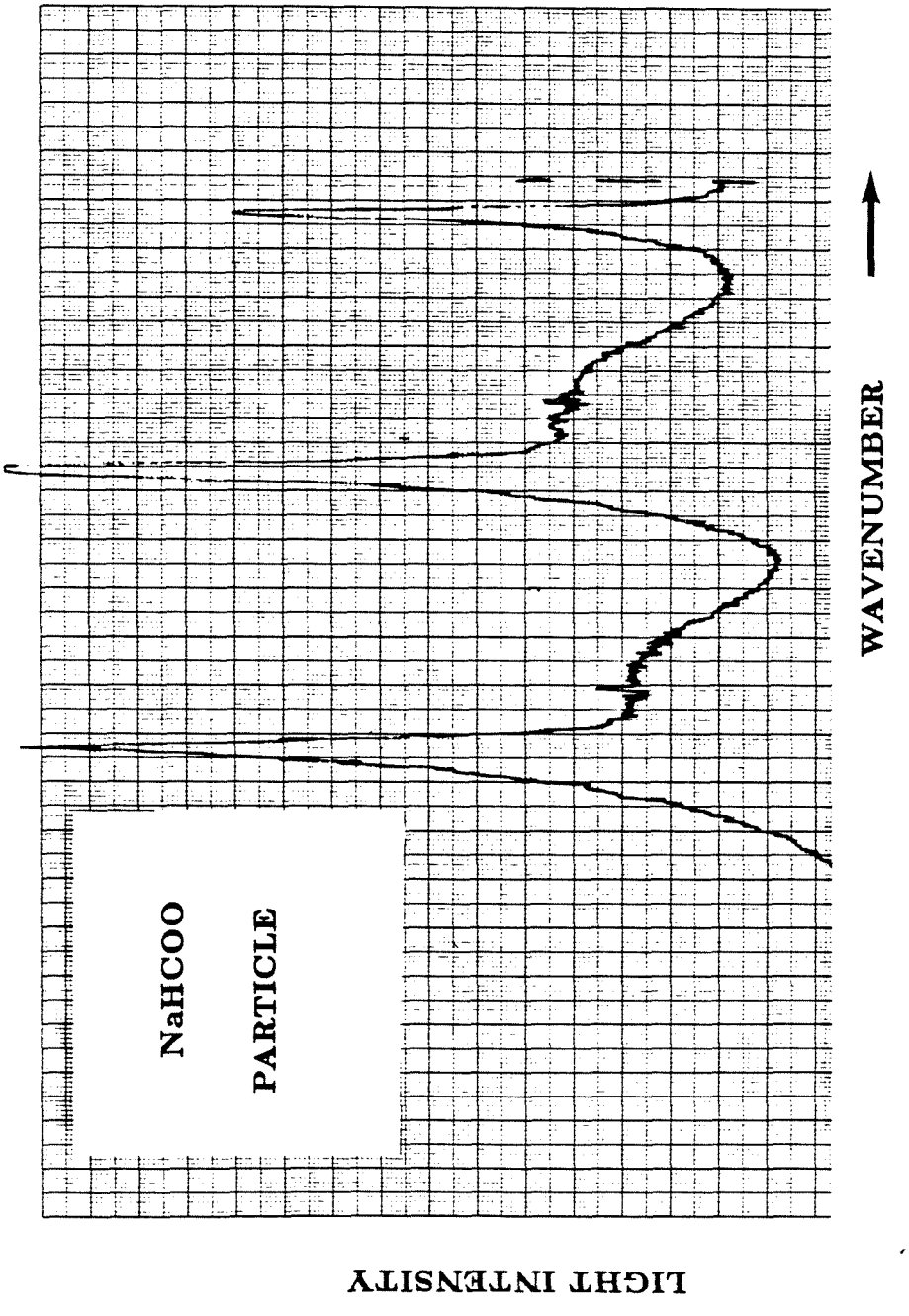

Figure 1. The scattered light intensity from an NaHCOO solution droplet as a function of the dye laser wavelength, measured immediately after the particle was trapped.

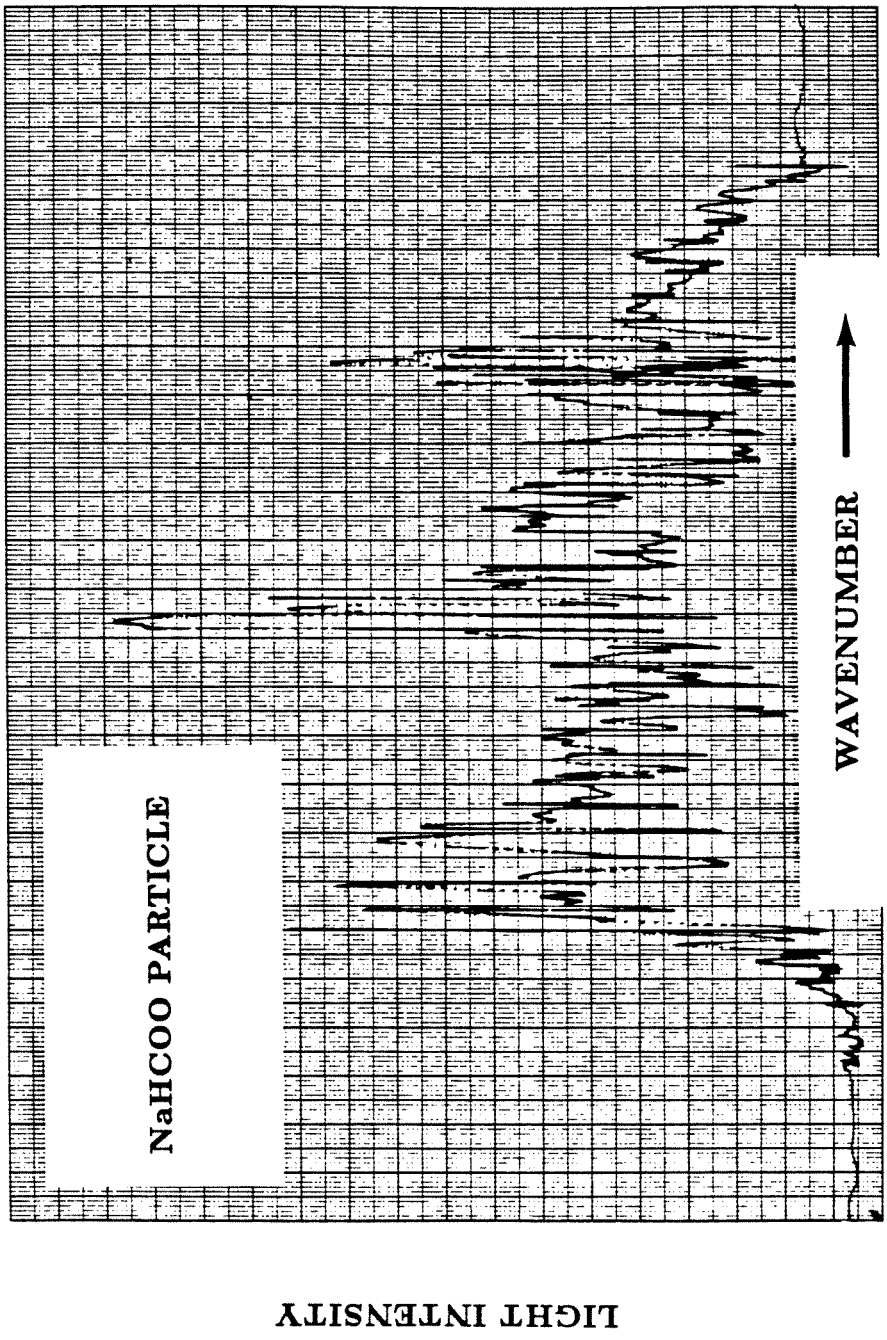

Figure 2. The scattered light intensity from an NaHCOO solution droplet, whose initial clean signal is seen in Figure 1, about 20 minutes after the particle was trapped.

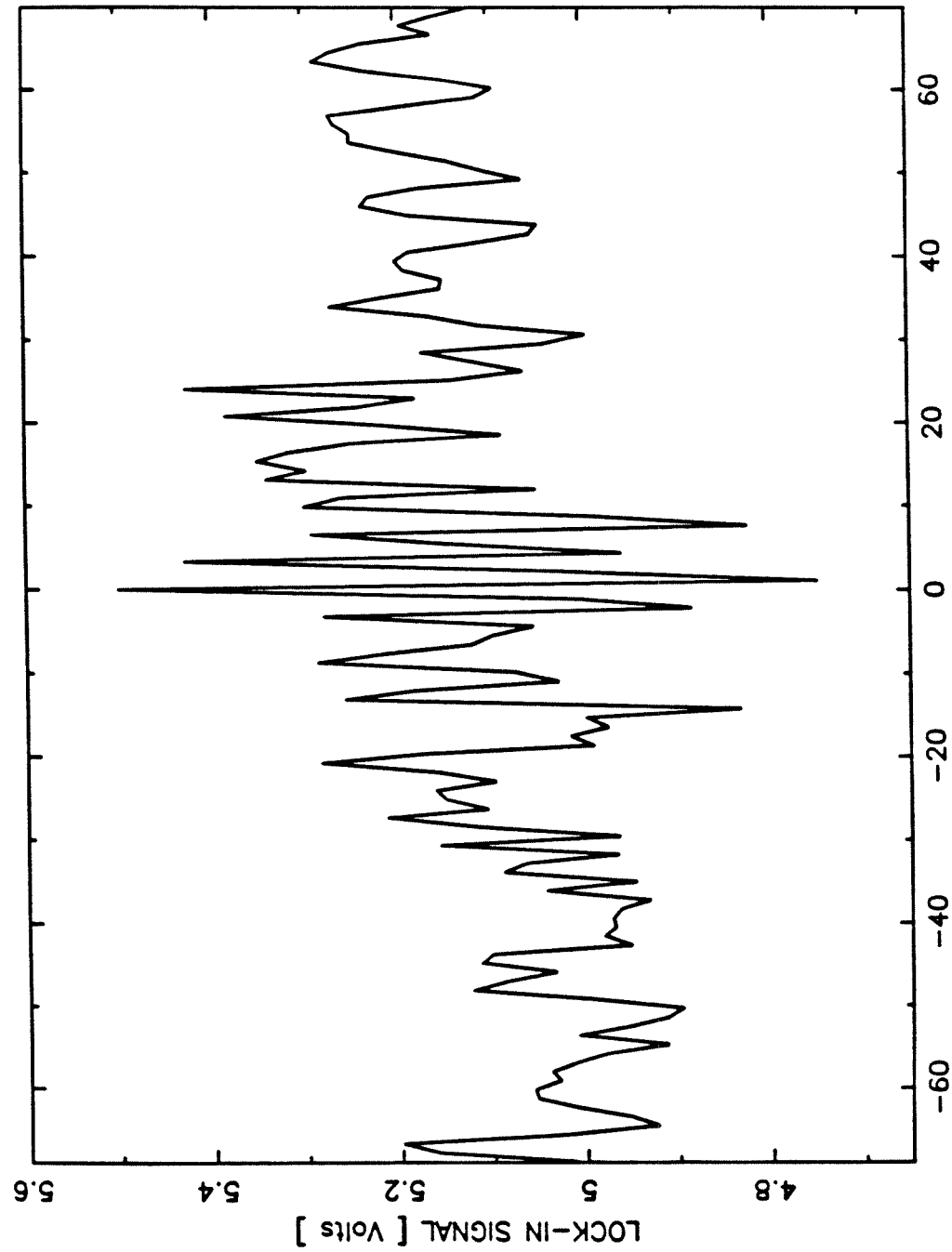

Figure 3. The interferogram obtained from an $NaNO_3$ solution droplet.

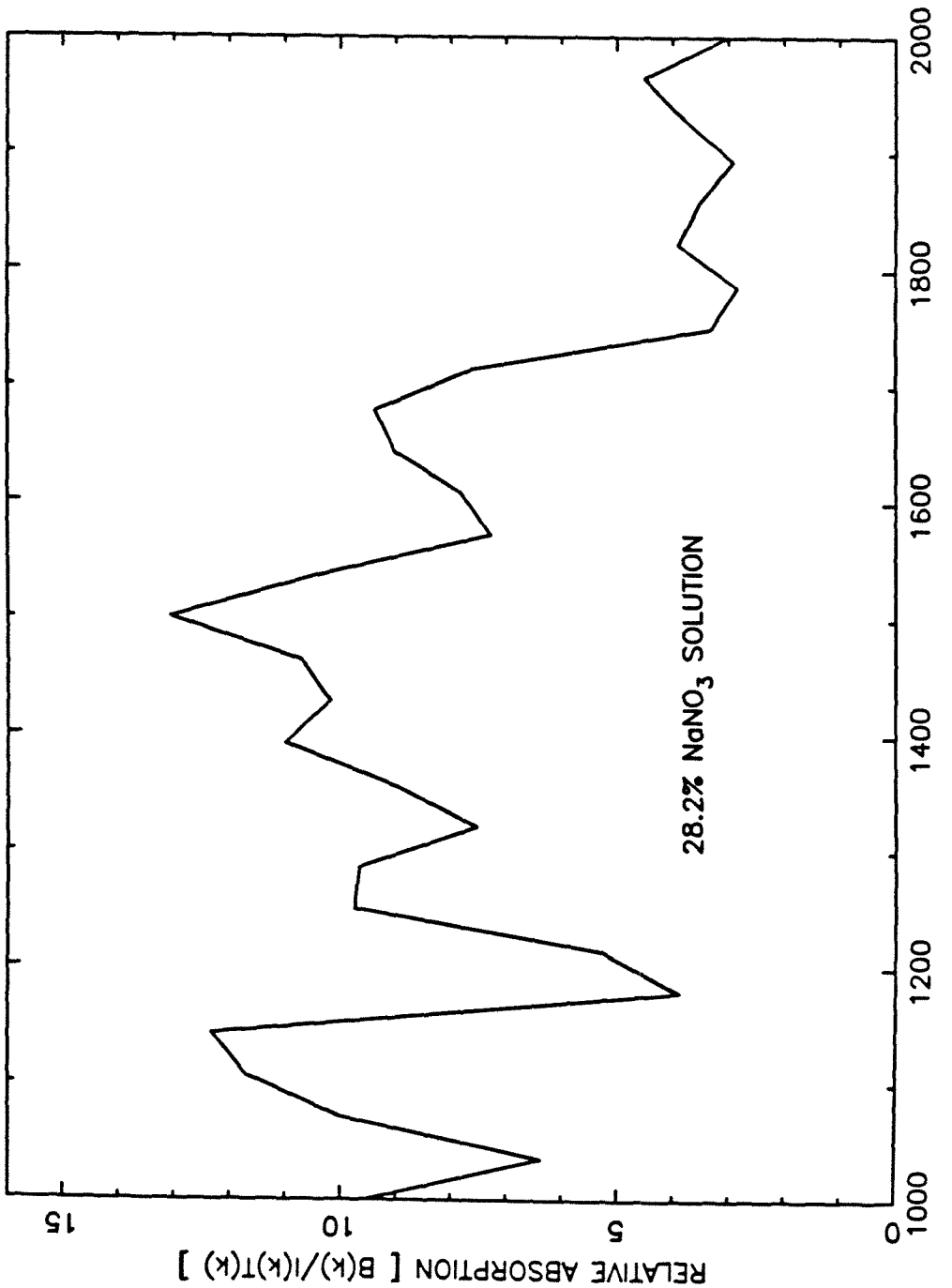

Figure 4. The relative absorption spectrum of an $NaNO_3$ droplet, obtained by inverting the data of Figure 3.

APPENDIX A

COMPUTER PROGRAMS

```
10    REM       FLY.BAS
20    REM
30    REM       WRITTEN             7-JUL-86
40    REM       REVISED             6-NOV-86
50    REM
60    REM ************************************************************************
70    REM
80    REM         PROGRAM FOR MOVING THE INTERFEROMETER MIRROR CONTINUOUSLY
90    REM         TAKING READINGS FROM THE A/D CONVERTER ACCORDING TO THE
100    REM         MOIRE ENCODER.
110    REM
120   REM         PROGRAM EMPLOYS ASSEMBLY ROUTINE:
130   REM
140   REM         MCFLY.ASM - MOVES THE INTERFEROMETER MIRROR AND READS THE
150   REM                     A/D IN MULTIPLES OF  0.5 microns.
160   REM
170   REM ************************************************************************
180   IAVG=0
190   DEFINT I,J,K,L
200   EX=0                                :REM    EXPANSION FACTOR
210   CLEAR ,&HC000
220   DEF USR0=&H0
230   REM
240   DEF SEG=&H1F00 : GOSUB 3950: DEF SEG
250   OUT &H3C, 5
260   CLS
270   DEF SEG=&H1F00
280   I3=PEEK(5) : I4=PEEK(6)
290   MPOINTS=256*I4 + I3
300   I3=PEEK(11) : I4=PEEK(12)
310   FRINGE=256*I4 + I3
320   REM ************************************************************************
330   REM
340   REM           INTERFEROMETER SET POINTS MENU
350   REM
360   REM      1 -- SET THE TOTAL NUMBER OF POINTS.
370   REM      2 -- SET THE FRINGE SPACING OR MIRROR STEP SIZE.
380   REM      3 -- REVERSE THE INTERFEROMETER DIRECTION TO ENABLE
390   REM           A MANUAL RETURN TO THE STARTING POINT.
400   REM      4 -- TURN THE MOTOR DIRECTION FORWARD TO ENABLE A
410   REM           FORWARD STEPPING OF THE MIRROR.
420   REM
430   REM ************************************************************************
440   CLS
450   LOCATE 1,30,1:PRINT" MAIN PROGRAM MENU "
460   LOCATE 3,10,1:PRINT" 1. TOTAL NUMBER OF DATA POINTS   : ", MPOINTS
470   LOCATE 4,10,1:PRINT" 2. FRINGE STEPS                  : ", FRINGE
480   LOCATE 5,10,1:PRINT" 3. REVERSE MOTOR                 : "
490   LOCATE 6,10,1:PRINT" 4. FORWARD MOTOR                 : "
```

```
500   REM
510   MENU0=0
520   LOCATE 10,59,1 :PRINT"                    "
530   LOCATE 10,10,1
540   INPUT" ENTER : [RUN=0]   SETUP : type 1-4 & <RET> ",MENU0
550   LOCATE 10,10,1
560   PRINT"                                                                    "
570   IF MENU0=0 THEN GOTO 830
580   LOCATE 15,10,1
590   ON MENU0 GOTO 640, 750,610, 620
600   GOTO 510
610   OUT &H3C,0 : GOTO 510
620   OUT &H3C,5 : GOTO 510
630   REM
640   INPUT " ENTER NUMBER OF DESIRED DATA POINTS : ",MPOINTS
650   I5=MPOINTS
660   I1=INT(I5/256) : I2=INT(I5-I1*256)
670   POKE 5 , I2 : POKE 6 , I1
680   LOCATE 15,1,1
690   PRINT "                                                                   "
700   LOCATE 3,10,1:PRINT" 1. TOTAL NUMBER OF DATA POINTS    : ", MPOINTS
710   GOTO 510
720  REM
730  REM               SET THE NUMBER OF MULTIPLE STEPS
740  REM
750  INPUT " ENTER THE DESIRED FRINGE STEPS : ",FRINGE
760  I5=FRINGE
770  I1=INT(I5/256) : I2=INT(I5-I1*256)
780  LOCATE 15,1 ,1
790  PRINT"                                                                    "
800  POKE 11,I2 : POKE 12, I1
810  LOCATE 4,10,1:PRINT" 2. FRINGE STEPS                : ", FRINGE
820  GOTO 510
830  REM
840  X1=65535!
850  N0=0
860  DIM Y(1150)
870  I0=100
880  TOTAL = INT(MPOINTS)
890  F1=1                                  :REM    BOTTOM LIMIT
900  F2=MPOINTS                            :REM    TOP LIMIT
910  INAME=0                               :REM    TITLE OF PLOT HAS BEEN STORED
920  GOSUB 2270              :REM PLOT THE COORDINATES OF THE INTERFEROGRAM
930  GOSUB 1900                            :REM    PLOT COORDINATES
940  LOCATE 25,35,1 : PRINT" FLYING "
950  DEF SEG=&H1F00
960  DUMMY=USR0(0)
970  GOSUB   3790                    :REM   PLOT A/D DATA
980  LOCATE 25,20,1 :PRINT"                                "
```

```
990    REM ************************************************************************
1000    REM
1010    REM                        MANIPULATE THE DATA
1020    REM
1030    REM      ZOOM - 1 --- ZOOM IN ON THE DESIRED INTERVAL ( BY LIMITING
1040    REM                   POINTS : N1, N2 ).
1050    REM      EXP  - 2 --- EXPAND THE PLOT VERTICALLY.
1060    REM      CORR - 3 --- CORRECT THE A/D DATA FOR ITS OFFSET (FOUND BY
1070    REM                   MEASURING THE VOLTAGE VS. A/D READING).
1080    REM      ORG  - 4 --- REPLOT THE ORIGINAL SCAN DATA.
1090    REM      DUMP - 5 --- DUMP THE SCREEN ONTO A PLOTTER.
1100    REM      DSK  - 6 --- STORE THE SCAN ON A DISK UNDER A FILE CALLED
1110    REM                   "DATA".
1120    REM      NEW  - 7 --- ZERO ALL THE FLAGS AND RESTART A FRESH SCAN.
1130    REM
1140    REM ************************************************************************
1150    INAME=0
1160    EX=0                                  :REM    EXPANSION FACTOR
1170    REM
1180    IFLAG=0
1190    MENU=0
1200    LOCATE 25,1,1
1210    INPUT"ZOOM=1  EXP=2  CORR=3  ORG=4  DUMP=5  DSK=6  NEW=7  ";MENU
1220    IF MENU=0 THEN GOTO 1170
1230 LOCATE 25,1,1:PRINT"                                                          "
1240    ON MENU GOTO 1460, 1490, 1390, 1260, 1310, 1350, 180
1250    GOTO 1170
1260    REM
1270    CLS : F2=MPOINTS
1280    GOSUB 2270              :REM PLOT THE COORDINATES OF THE INTERFEROGRAM
1290    GOSUB 3790                    :REM   PLOT A/D DATA
1300    GOTO 1170
1310    REM
1320    GOSUB 1670                 :REM    DUMP THE SCREEN ON PRINTER
1330    INAME=1
1340    GOTO 1170
1350    REM                                 STORE IN DISK
1360    GOSUB 1570
1370    GOTO 1170
1380    REM
1390    REM                                 CORRECT THE DATA FOR A/D OFSET
1400    PRINT "                                                                    "
1410    INPUT" Y-INTERCEPT and SLOPE : ", YINT, SLOPE
1420    FOR I=1 TO MPOINTS
1430            Y(I)= Y(I)*SLOPE + YINT
1440    NEXT I
1450    GOTO 1160                   :REM    PLOT THE CORRECTED DATA
1460    REM
1470    GOSUB 2990                :REM    ZOOM ON THE INTERVAL
```

```
1480   GOTO 1170
1490   REM
1500   GOSUB 3370              :REM     EXPAND THE PLOT
1510   GOTO 1170
1520   REM
1530   LOCATE 1,5,1: STOP : END
1540   REM ************************************************************************
1550   REM               OUTPUT THE DATA ONTO A DISK
1560   REM ************************************************************************
1570   POINTS=INT(F2-F1+1)
1580   OPEN "O",#1,"DATA"
1590   PRINT #1,POINTS
1600   PRINT #1,FRINGE
1610   FOR I=F1 TO F2
1620            PRINT #1, Y(I)
1630   NEXT I
1640   CLOSE #1
1650   DEF SEG
1660   RETURN
1670   REM ************************************************************************
1680   REM                                DUMP SCREEN TO THE TERMINAL
1690   REM ************************************************************************
1700   IF INMAE=1 THEN GOTO 1740        :REM    SKIP IF NAME WAS ALREADY STORED
1710   LOCATE 25,1,1
1720 PRINT"                                                                       "
1730   INPUT " ENTER THE DATE & NAME [i.e. 15-AUG-85-name] : "; DAY$
1740 PRINT"                                                                       "
1750   LOCATE 25,30,1
1760   PRINT"DATA POINTS " , DAY$
1770   REM
1780   REM  Have the printer work during one direction only
1790   LPRINT CHR$(27)+"["
1800   IF INKEY$=CHR$(3) THEN GOTO 1830
1810   FOR I=1 TO 1000 : I=I+1 : NEXT I : BEEP
1820   GOTO 1800
1830   LPRINT CHR$(27)+"]"
1840   LOCATE 25,1,1
1850   LPRINT "       "
1860   RETURN
1870   REM ************************************************************************
1880   REM                          NUMBER THE Y-AXIS COORDINATES
1890   REM ************************************************************************
1900   IF EX <> 0 THEN GOTO 2050  :REM    IF EXP=0 PLOT THE ORIGINAL DATA
1910   YAX=1000.001/100
1920   L=1
1930   YAXT=INT(YAX*1000.1)
1940   YAX=YAXT/1000
1950   LOCATE L,2 : PRINT YAX
1960   L=L+4.2
```

```
1970   YAX=YAX-2.00001
1980   IF YAX<1.9999  THEN GOTO 2020
1990   IF YAX>4.00001 THEN GOTO 1930
2000   L=L+1
2010   GOTO 1930
2020   YAX=.001
2030   LOCATE 22,3 : PRINT YAX
2040   RETURN
2050   REM
2060   GOSUB 2690                          :REM    AVERAGE THE DATA
2070   VMAX=Y(IMAX) : VMIN=Y(IMIN)         :REM    MIN/MAX DATA POINTS
2080   RANGE=ABS((VMAX-VMIN)*100/EX)       :REM    OVERALL Y-AXIS RANGE
2090   YSTEP=RANGE/5                       :REM    Y-AXIS STEPS
2100   YAX=VMAX+(RANGE-(VMAX-VMIN))/2      :REM    TOP COORDINATE
2110   YMIN=YAX-RANGE                      :REM    TOP COORDINATE
2120   L=1
2130   YAXT=INT(YAX*1000.1)
2140   YAX=YAXT/1000
2150   LOCATE L,2 : PRINT YAX
2160   L=L+4.2
2170   YAX=YAX-YSTEP
2180   IF YAX<YMIN+.9*(YSTEP) THEN GOTO 2220
2190   IF YAX>YMIN+(YSTEP)*2   THEN GOTO 2130
2200   L=L+1
2210   GOTO 2130
2220   YAXT=INT(YMIN*1000)
2230   YAX=YAXT/1000
2240   LOCATE 22,2 : PRINT YAX
2250   RETURN
2260   REM ************************************************************************
2270   REM                        Plot the coordinates
2280   REM ************************************************************************
2290   CLS :PI=4*ATN(1)
2300   LINE (0,0)-(640,200),,B
2310   TOTAL = F2-F1+1
2320   FOR J=0 TO 60 : W=640/60
2330          LINE(J*W,200)-(J*W,198)
2340   NEXT J
2350   FOR J=1 TO 6 : W=640/6
2360          LINE(J*W,200)-(J*W,195): NEXT J
2370   FOR J=0 TO 200 STEP 20
2380          LINE (0,J)-(7,J)
2390   NEXT J
2400   FOR J=0 TO 200 STEP 5
2410          LINE (0,J)-(3,J)
2420   NEXT J
2430   FOR J=0 TO 200 STEP 20
2440          LINE (633,J)-(640,J)
2450   NEXT J
```

```
2460   FOR J=0 TO 200 STEP 5
2470           LINE (637,J)-(640,J)
2480   NEXT J
2490   W=640/TOTAL
2500   XLAB=TOTAL/6
2510   A0= 640/6
2520   L=23
2530   XAX=A0
2540   LOCATE 23,1,1:PRINT F1
2550   FOR I=1 TO 6
2560   XAX=A0* I
2570   N=XAX/8.600001
2580   XL% = F1+XLAB*I - .5
2590   IF I<3 THEN GOTO 2610
2600           N=N+1
2610   IF I<5 THEN GOTO 2630
2620           N=N+1
2630   IF I<5.9 THEN GOTO 2660
2640           XL% = F2
2650           N=N-1
2660   LOCATE L,N : PRINT XL%
2670   NEXT I
2680   RETURN
2690   REM ************************************************************************
2700   REM                          AVERAGE THE DATA
2710   REM ************************************************************************
2720   SUM=0!
2730   FOR I=F1 TO F2
2740          SUM=SUM+Y(I)
2750   NEXT I
2760   AVJ=SUM/(F2-F1+1)
2770   AMAX =AVJ
2780   AMIN =AVJ
2790   FOR I=F1 TO F2
2800          IF Y(I) < AMAX  THEN GOTO 2840
2810                  AMAX = Y(I)
2820                  IMAX=I
2830                   GOTO 2870
2840          IF Y(I) > AMIN THEN GOTO 2870
2850                  AMIN= Y(I)
2860                   IMIN=I
2870   NEXT I
2880   AMAX=200-20*AMAX
2890   AMIN=200-20*AMIN
2900   RETURN
2910   FOR I=IL1 TO IL2
2920           W=640/(F2-F1):J=W*(I-F1)
2930           YY=YYINT+SL*I
2940           YY=200-20*YY
```

```
2950          YY=BOT-CC*(AMIN-YY)
2960          PSET(J,YY)
2970   NEXT I
2980   RETURN
2990   REM ************************************************************************
3000   REM                        ZOOM IN ON DESIRED INTERVAL
3010   REM ************************************************************************
3020   LOCATE 25,1,1
3030 PRINT"                                                                        "
3040   PRINT "OLD LIMITS: ",F1,F2
3050   LOCATE 25,40:INPUT"F1 , F2 = ", F1,F2
3060   GOSUB 2270                          :REM    PLOT THE GRAPH
3070   GOSUB 1870                           :REM    PLOT THE Y-AXIS
3080   IF EX<>0 THEN GOTO 3150
3090   FOR I=F1 TO F2
3100         W=640/(F2-F1):J=W*(I-F1)
3110        AA=200-20*Y(I)
3120         PSET(J,AA)
3130   NEXT I
3140   RETURN
3150   GOSUB 2690                : REM   AVERAGE THE DATA
3160   EXABS=ABS(EX)
3170   CC=2*EXABS/(AMIN-AMAX)
3180   BOT = 100+EXABS
3190   TOP = 100-EXABS
3200   IF EX > 0 THEN GOTO 3300
3210   FOR I=F1+1 TO F2
3220          W=640/(F2-F1):J=W*(I-F1)
3230          AA0=200-20*Y(I-1)
3240          AA0=BOT-CC*(AMIN-AA0)
3250          AA1=200-20*Y(I)
3260          AA1=BOT-CC*(AMIN-AA1)
3270          LINE(J-W ,AA0)-(J,AA1)
3280   NEXT I
3290   RETURN
3300   FOR I=F1 TO F2
3310          W=640/(F2-F1):J=W*(I-F1)
3320          AA=200-20*Y(I)
3330          AA=BOT-CC*(AMIN-AA)
3340          PSET(J,AA)
3350   NEXT I
3360   RETURN
3370   REM ************************************************************************
3380   REM                      EXPAND THE DATA VERTICALLY
3390   REM ************************************************************************
3400   LOCATE 25,1,1
3410   EX = 0
3420 PRINT"                                                                        "
3430   INPUT"% OF Y-AXIS EXPANSION : (100-0)%=PNT, -(1-100)%=LINE   ";EX
```

```
3440   GOSUB 2270                : REM    PLOT THE X-AXIS
3450   GOSUB 1870                : REM    PLOT THE Y-AXIS
3460   GOSUB 2690                : REM   AVERAGE THE DATA
3470   EXABS=ABS(EX)
3480   CC=2*EXABS/(AMIN-AMAX)
3490   BOT = 100+EXABS
3500   TOP = 100-EXABS
3510   IF EX > 0 THEN GOTO 3610
3520   FOR I=F1+1 TO F2
3530           W=640/(F2-F1):J=W*(I-F1)
3540           AA0=200-20*Y(I-1)
3550           AA0=BOT-CC*(AMIN-AA0)
3560           AA1=200-20*Y(I)
3570           AA1=BOT-CC*(AMIN-AA1)
3580           LINE(J-W ,AA0)-(J,AA1)
3590   NEXT I
3600   RETURN
3610   FOR I=F1 TO F2
3620           W=640/(F2-F1):J=W*(I-F1)
3630           AA=200-20*Y(I)
3640           AA=BOT-CC*(AMIN-AA)
3650           PSET(J,AA)
3660   NEXT I
3670   RETURN
3680   REM
3690   SUMY=0
3700   INPUT "INTERVAL = ", INT1, INT2
3710   FOR I=INT1 TO INT2
3720           SUMY=Y(I)+SUMY
3730   NEXT I
3740   YAV=SUMY/(INT2-INT1+1)
3750   REM               WRITE THE Y-LEVEL ON THE SCREEN
3760   L=22
3770   RETURN
3780   REM                      DATA PLOTTING
3790   DEF SEG=&H2000
3800   FOR I=F1 TO F2
3810           N=N0+2*(I+1)
3820           A=PEEK(N)
3830           B=PEEK(N+1)
3840           C=A+256*B
3850           YY=-(C-X1)*10/X1
3860           Y(I)=YY
3870           X=I*W
3880           YY=200 - 20*YY
3890           PSET(X,YY)
3900   NEXT I
3910   RETURN
3920   REM ************************************************************************
```

```
3930   REM                      ASSEMBLY DATA-TAKING ROUTINE
3940   REM ************************************************************
3950   FOR X= 0 TO  96:READ Y:POKE X,Y:NEXT X
3960   DATA 250,252,30,6,187,44,1,184,0,32,185,1,0,81,142
3970   DATA 192,191,0,0,186,61,0,176,5,230,60,185,4,0,226
3980   DATA 254,176,7,230,60,176,23,230,60,89,81,228,60,60,4
3990   DATA 117,250,73,227,9,81,185,60,0,226,254,89,235,238,176
4000   DATA 7,230,60,185,4,0,226,254,237,171,75,139,203,227,7
4010   DATA 185,40,0,226,254,235,209,176,2,230,60,144,176,10,230
4020   DATA 60,89,7,31,251,203,0
4030   RETURN
```

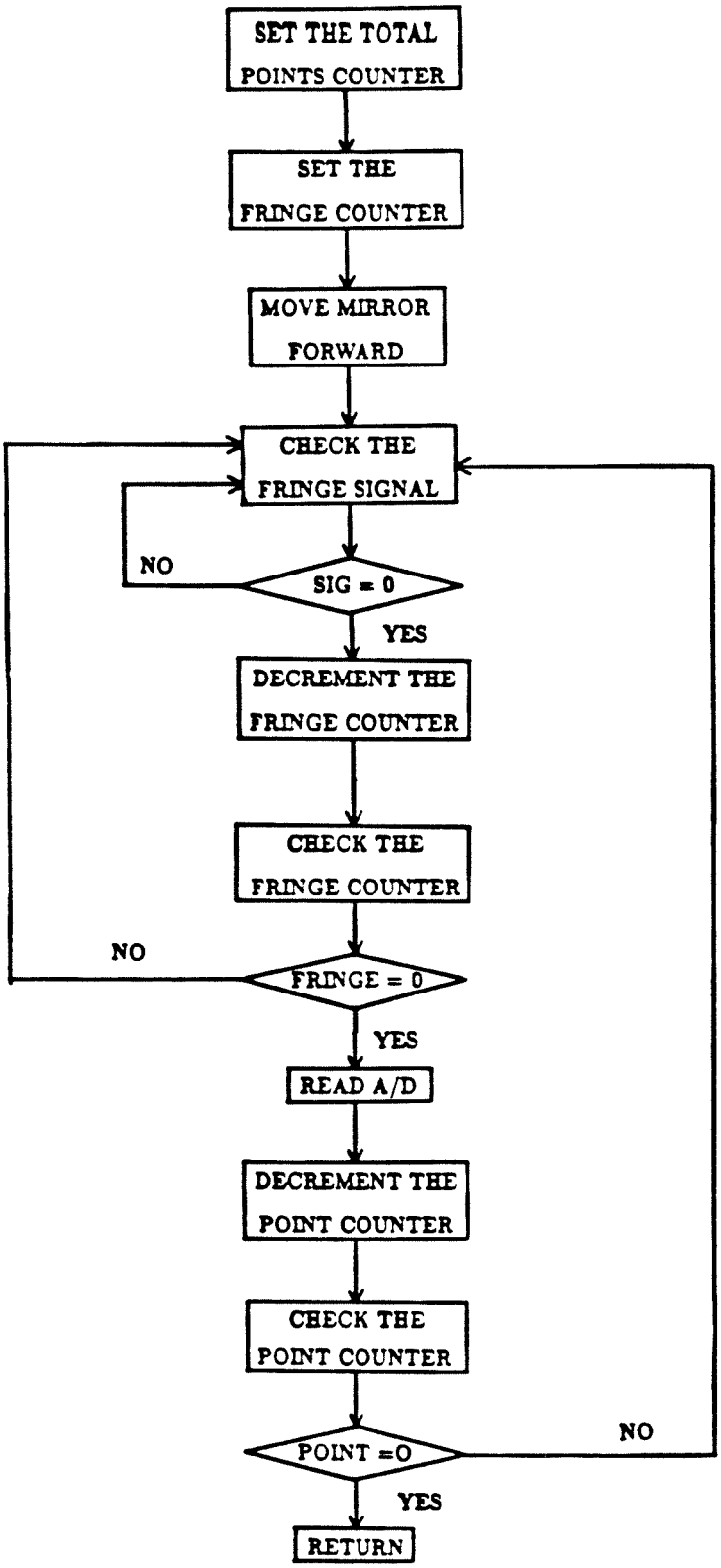

Figure 1. A flow chart of the assembly code MCFLY.ASM, (which moves the mirror continuously), (used in the program FLY.BAS).

```
;               MCFLY.ASM
;
;               WRITTEN:        30-MAY-86
;               REVISED:         8-JUL-86
;
;               TO BE USED IN    FLY.BAS  PROGRAM
;
;       1.      PROGRAM TO READ THE A/D ACCORDING TO THE SIGNAL
;               FROM THE MOIRE ENCODER. PROGRAM IS INTENDED TO BE USED
;               FOR CONTINUOUS SCAN OF THE INTERFEROMETER.
;       2.      ONCE THE M.C. SIGNAL IS READ, THE A/D IS TRIGGERED
;               AND THE DATA IS TAKEN.
;       3.      AFTER DATA IS TAKEN, MOTOR IS REVERSED AND LOWER LIMIT
;               IS SEARCHED.
;
ADCODE          SEGMENT
                ASSUME  CS:ADCODE
START           PROC    FAR
                CLI                             ; CLEAR INTERUPT FLAG
                CLD                             ; CLEAR DIRECTION FLAG
                PUSH    DS
                PUSH    ES
                MOV     BX, 200                 ; GET NUMBER OF DATA POINTS
                MOV     AX,2000H                ; LOAD A REG: AH=32, AL=0
                MOV     CX,1                    ; NO. OF FRINGE SPACING
                PUSH    CX                      ; STORE SPACING IN STACK
                MOV     ES,AX
                MOV     DI,0                    ; DATA POINTER
                MOV     DX,003DH                ; POINT TO INPUT LSB PORT
                MOV     AL,5
                OUT     3CH, AL                 ; SET MOTOR IN FORWARD DIRECT.
                MOV     CX,4
DELAY0:         LOOP    DELAY0                  ; WAIT ~20 MICROSECS
                MOV     AL,7
                OUT     3CH, AL                 ; START THE MOTION FORWARD
PRESET:         MOV     AL,23                   ; PRESET THE A/D
                OUT     3CH,AL
                POP     CX                      ; LOAD CX WITH FRINGE SPACING
                PUSH    CX                      ; RESTORE SPACING IN STACK
CHECK:          IN      AL,3CH                  ; LOOK AT PIN #24
                CMP     AL,4                    ; CHECK IF DATA IS READY
                JNZ  SHORT CHECK                ; IF SO THEN CONTINUE
                DEC     CX                      ; COUNT DOWN SPACING
                JCXZ    ADTRIG                  ; IF ZERO TRIGGER THE A/D
                PUSH    CX
                MOV     CX,60
DELAY1:         LOOP    DELAY1                  ; WAIT ~300 MICROSECS
                POP     CX
                JMP     CHECK
```

```
ADTRIG:         MOV     AL,7
                OUT     3CH,AL          ;TRIGGER THE A/D
                MOV     CX,4            ; MUST WAIT ~20 MICROSECONDS
DELAY2:         LOOP    DELAY2          ; FOR A/D TO SEND READY SIG.
                IN      AX,DX           ; READ THE DATA BITS
                STOSW                   ; STORE THEM
                DEC     BX              ; COUNT DOWN THE POINT #
                MOV     CX,BX
                JCXZ SHORT RETURN       ; CHECK FOR LAST POINT
                MOV     CX,40
DELAY3:         LOOP    DELAY3          ; WAIT ~200 MICROSECS
                JMP     PRESET          ; CHECK FOR NEXT POINT
RETURN:         MOV     AL,2
                OUT     3CH,AL          ; REVERSE MOTOR DIRECTION
                NOP
                MOV     AL,10           ; START THE SCAN BACKWARDS
                OUT     3CH,AL          ; AND SEARCH FOR LOWER LIMIT.
                POP     CX              ; UNLOAD THE STACK IN
                POP     ES              ; REVERSE ORDER.
                POP     DS
                STI                     ; SET INTERUPT FLAG
                RET                     ; RETURN TO MAIN PROGRAM
START           ENDP
ADCODE          ENDS
                END     START
```

```
10 REM                 LOCKIN.BAS
20 REM
30 REM        WRITTEN          23-MAY-86
40 REM       REVISED          19-SEP-86
50 REM
60 REM ***************************************************************
70 REM
80 REM        PROGRAM FOR STEPPING THE INTERFEROMETER MIRROR,
90 REM        READING THE MODULATION WITH A LOCKIN AMPLIFIER,
100 REM       TAKING READINGS WITH THE A/D CONVERTER
110 REM       AND AVERAGING THE RESULTS.
120 REM
130 REM         PROGRAM EMPLOYS TWO ASSEMBLY ROUTINES:
140 REM
150 REM        1.  STEP1.ASM - STEPS THE INTERFEROMETER MIRROR IN MULTIPLES
160 REM                        OF 0.5 microns.
170 REM
180 REM         2.  ADREAD.ASM - READS N-DATA POINTS FROM THE A/D CONVERTER
190 REM                          AND AVERAGES THEIR SUM.
200 REM
210 REM                        PROGRAM STRUCTURE :
220 REM
230 REM        1.       SET THE DATA TAKING PARAMETERS
240 REM
250 REM                 A.      THE PROGRAM INVOLVING THE A/D:
260 REM
270 REM                         a.      MPOINTS - TOTAL NUMBER OF POINTS
280 REM                         b.      SPACE   - SET THE SPACE (MILLISECONDS)
290 REM                                           BETWEEN A/D READINGS TO BE
300 REM                                           AVERAGED.
310 REM                         c.      AVPNT   - # A/D READINGS TO BE AVERAGED
320 REM                                           PER DATA POINT.
330 REM
340 REM                 B.      THE ASSEMBLY ROUTINE INVOLVING THE STEPPING
350 REM
360 REM                         a.      ENABLE - SET THE MOTOR ENABLE TIME.
370 REM                         b.      DISABLE - SET THE MOTOR DISABLE TIME.
380 REM                         c.      JUMP - SET THE INITIAL MIRROR JUMP.
390 REM                         d.      FRINGE - SET THE FRINGE SPACING.
400 REM
410 REM                 C.      FOR COMPLETELY MANUAL OPERATION SET LOCKTIME=0
420 REM
430 REM                         FOR AUTOMATIC OPERATION THE LAG TIME BETWEEN
440 REM                         MOVING THE MIRROR AND TAKING DATA MUST BE
450 REM                         SPECIFIED. IT IS NORMALLY SOME MULTIPLE OF THE
460 REM                         LOCK-IN AMPLIFIER TIME CONSTANT.
470 REM
480 REM        2.       ONCE THE MOTION IS STARTED ANY DATA POINT CAN BE
490 REM                 DELETED AND RETAKEN. TO STOP THE PROGRAM WHEN IN THE
```

```
500 REM                AUTOMATIC MODE, PRESS <CNT C>. THIS WILL DISPLAY THE
510 REM                RUNNING  MENU AND WILL ALLOW FOR RESETTING ANY OF THE
520 REM                INITIAL PARAMETERS.
530 REM
540 REM        3.      WHEN ALL THE DESIRED DATA POINTS WERE TAKEN, THE PROGRAM
550 REM                WILL SHIFT TO THE DATA ANALYSIS SECTION, WHERE THE
560 REM
570 REM
580 REM ************************************************************************
590    CLS
600    CLEAR ,&HC000
610    DEFINT I,J,K,L
620    LOCKTIME=10!                        :REM    EXPANSION FACTOR
630    EX=0                                :REM    EXPANSION FACTOR
640    IAVG=0
650    DEF USR0=&H0
660    DEF USR1=&H0
670    DEF SEG=&H2000 : GOSUB 5810  : DEF SEG
680    DEF SEG=&H2000
690    I3=PEEK(59) : I4=PEEK(60)
700    SPACE=256*I4 + I3
710    I3=PEEK(21) : I4=PEEK(22)
720    AVPNT=256*I4 + I3
730    MPOINTS=140
740    REM
750    DEF SEG=&H1F00 : GOSUB 5930: DEF SEG
760    DEF SEG=&H1F00
770    I3=PEEK(5) : I4=PEEK(6)
780    ENABLE=256*I4 + I3
790    I3=PEEK(8) : I4=PEEK(9)
800    DISABLE=256*I4 + I3
810    I3=PEEK(23) : I4=PEEK(24)
820    JUMP=256*I4 + I3
830    I3=PEEK(15) : I4=PEEK(16)
840    FRINGE=256*I4 + I3
850    CLS
860    LOCATE 1,30,1:PRINT" MAIN PROGRAM MENU "
870    LOCATE 3,10,1:PRINT" 1. TOTAL NUMBER OF DATA POINTS   : ", MPOINTS
880    LOCATE 4,10,1:PRINT" 2. # A/D READINGS PER DATA POINT : ", AVPNT
890    LOCATE 5,10,1:PRINT" 3. TIME SPACING OF A/D READINGS  : ", SPACE
900    LOCATE 7,10,1:PRINT" 4. MOTOR ENABLE TIME  (100/msec) : ", ENABLE
910    LOCATE 8,10,1:PRINT" 5. MOTOR DISABLE TIME (100/msec) : ", DISABLE
920    LOCATE 9,10,1:PRINT" 6. INITIAL JUMP TIME  (100/msec) : ", JUMP
930    LOCATE 10,10,1:PRINT" 7. FRINGE STEPS                 : ", FRINGE
940    LOCATE 12,10,1:PRINT" 8. AUTOMATIC SCAN  [ NO=0 ]     : ", LOCKTIME
950    REM
960    MENU0=0
970    LOCATE 14,59,1 :PRINT"                    "
980    LOCATE 14,10,1
```

```
990    INPUT" ENTER : [CONTINUE=0]   SETUP : type 1-8 & <RET> ",MENU0
1000    LOCATE 14,10,1
1010    PRINT"                                                                "
1020    IF MENU0=0 THEN GOTO 1880
1030    IF MENU0 < 3 THEN GOTO 1060
1040           DEF SEG=&H1F00
1050           GOTO 1070
1060           DEF SEG=&H2000
1070    LOCATE 15,10,1
1080    ON MENU0 GOTO 1110, 1170, 1260, 1350, 1460, 1570, 1680, 1760
1090    GOTO 960
1100 REM ************************************************************************
1110    INPUT " ENTER NUMBER OF DESIRED DATA POINTS : ",MPOINTS
1120    LOCATE 15,1,1
1130    PRINT "                                                                "
1140    LOCATE 3,10,1:PRINT" 1. TOTAL NUMBER OF DATA POINTS   : ", MPOINTS
1150    GOTO 960
1160 REM ************************************************************************
1170    INPUT " ENTER # OF A/D READINGS PER DATA POINT: ",AVPNT
1180    I5=AVPNT
1190    I1=INT(I5/256) : I2=INT(I5-I1*256)
1200    POKE 21, I2 : POKE 22, I1
1210    LOCATE 15,1,1
1220    PRINT "                                                                "
1230    LOCATE 4,10,1:PRINT" 2. # A/D READINGS PER DATA POINT : ", AVPNT
1240    GOTO 960
1250 REM ************************************************************************
1260    INPUT " ENTER TIME SEPARATION OF A/D READINGS : ",  SPACE
1270    I5=SPACE
1280    I1=INT(I5/256) : I2=INT(I5-I1*256)
1290    POKE 59,I2 : POKE 60,I1
1300    LOCATE 15,1,1
1310    PRINT "                                                                "
1320    LOCATE 5,10,1:PRINT" 3. TIME SPACING OF A/D READINGS  : ", SPACE
1330    GOTO 960
1340 REM ************************************************************************
1350    INPUT " ENTER THE DESIRED ENABLE TIME : ",ENABLE
1360    LOCATE 15,10,1
1370    PRINT "                                                                "
1380    I5=ENABLE
1390    I1=INT(I5/256) : I2=INT(I5-I1*256)
1400    POKE 5, I2 : POKE 6, I1
1410    LOCATE 7,10,1:PRINT" 4. MOTOR ENABLE TIME  (100/msec) : ", ENABLE
1420    GOTO 960
1430 REM ************************************************************************
1440 REM               SET THE DISABLE TIME CYCLES
1450 REM ************************************************************************
1460   INPUT " ENTER THE DESIRED DISABLE TIME : ",DISABLE
1470   I5=DISABLE
```

```
1480   I1=INT(I5/256) : I2=INT(I5-I1*256)
1490   POKE 8 ,I2 : POKE  9 ,I1
1500   LOCATE 15,10,1
1510   PRINT "                                                                    "
1520   LOCATE 8,10,1:PRINT" 5. MOTOR DISABLE TIME (100/msec) : ", DISABLE
1530   GOTO 960
1540 REM ************************************************************************
1550 REM               SET THE SIZE OF THE INITIAL JUMP
1560 REM ************************************************************************
1570   INPUT " ENTER THE INITIAL JUMP SIZE    : ",JUMP
1580   LOCATE 15,10,1
1590   PRINT "                                                                    "
1600   I5=JUMP
1610   I1=INT(I5/256) : I2=INT(I5-I1*256)
1620   POKE 23,I2 : POKE  24,I1
1630   LOCATE 9,10,1:PRINT" 6. INITIAL JUMP TIME  (100/msec) : ", JUMP
1640   GOTO 960
1650 REM ************************************************************************
1660 REM               SET THE NUMBER OF MULTIPLE STEPS
1670 REM ************************************************************************
1680   INPUT " ENTER THE DESIRED FRINGE STEPS : ",FRINGE
1690   I5=FRINGE
1700   I1=INT(I5/256) : I2=INT(I5-I1*256)
1710   LOCATE 15,1 ,1
1720   PRINT"                                                                     "
1730   POKE 15,I2 : POKE 16, I1
1740   LOCATE 10,10,1:PRINT" 7. FRINGE STEPS                 : ", FRINGE
1750   GOTO 960
1760 REM ************************************************************************
1770 REM               SET THE AUTOMATIC SCAN CONDITIONS
1780 REM ************************************************************************
1790   LOCATE 15,1 ,1
1800   PRINT"                                                                     "
1810   LOCATE 15,10,1
1820   INPUT " ENTER THE LOCKIN SETTLING TIME (secs) : ",LOCKTIME
1830   LOCATE 15,10,1
1840   PRINT"                                                                     "
1850   LOCATE 12,10,1:PRINT" 8. AUTOMATIC SCAN  [ NO=0 ]    : ", LOCKTIME
1860   GOTO 960
1870 REM ************************************************************************
1880   IF IRESET=1 THEN GOTO 2710
1890   X1=65535!                        :REM   RESOLUTION OF 16-BIT A/D
1900   N0=0
1910   DIM Y(1105)                      :REM   SETS THE MAXIMUM # DATA POINTS
1920   I0=100
1930   TOTAL = INT(MPOINTS)
1940   F1=1                             :REM    BOTTOM LIMIT
1950   F2=MPOINTS                       :REM    TOP LIMIT
1960   INAME=0                          :REM    TITLE OF PLOT HAS BEEN STORED
```

```
1970   GOSUB 4120              :REM PLOT THE COORDINATES OF THE INTERFEROGRAM
1980 REM ************************************************************************
1990 REM
2000 REM       START THE MAIN LOOP THAT COLLECTS THE DATA
2010 REM
2020 REM       1.      MOVE THE MIRROR.  [ROUTINE USR0(0)]
2030 REM       2.      CHECK IF AUTOMATIC SCAN IS DESIRED.
2040 REM           A.  IF YES --- WAIT A SPECIFIED TIME THEN TAKE DATA
2050 REM           B.  IF  NO --- DECIDE WHEN TO TAKE DATA MANUALLY.
2060 REM       3.      DATA TAKING ROUTINE IS USR0(1)
2070 REM
2080 REM
2090 REM ************************************************************************
2100   FOR I=1 TO MPOINTS
2110          JJ=I
2120          LOCATE 25,1,1
2130          PRINT"                                                              "
2140          LOCATE 25,35,1
2150          PRINT " MOVING  "
2160          DEF SEG=&H1F00
2170          DUMMY=USR0(0)
2180          LOCATE 25,1,1
2190          PRINT"                                                              "
2200          IRESET=0                  : REM     FLAG TELLING THAT OPERATING
2210                                    : REM     CONDITIONS ARE BEING CHANGED
2220          IF LOCKTIME = 0 THEN GOTO 2300 : REM      MANUAL DELAY
2230          IDELAY=23*LOCKTIME
2240          M=0
2250          FOR J=1 TO IDELAY
2260                 M=0
2270                 FOR II=1 TO 100    : M=M+1 : NEXT II
2280          NEXT J
2290          GOTO 2320
2300          LOCATE 25,1,1
2310          INPUT"    TAKE DATA       ", NOTHING
2320          GOSUB   5660                    :REM   TAKE A/D DATA
2330         LOCATE 2,30,1 : PRINT"                                               "
2340          LOCATE 2,30,1 : PRINT I, Y(I), "  VOLTS"
2350         IF INKEY$=CHR$(3) THEN GOTO 2370       :REM   <CTL C> TO STOP RUN
2360          IF LOCKTIME <> 0 THEN GOTO  2780       :REM   MOVR TO NEXT POINT
2370          LOCATE 25,1,1
2380 REM ************************************************************************
2390 REM
2400 REM       RUN MENU
2410 REM
2420 REM       [NEXT = 0 ] --- DEFAULT OF MANUAL OPERATION, MOVE TO NEXT
2430 REM                       MIRROR POSITION.
2440 REM       CONT  = 1   --- STOP TAKING DATA, GO ON TO ANALYZE WHAT'S IN
2450 REM                       MEMORY.
```

```
2460 REM       DEL   - 2   --- DELETE THE CURRENT DATA POINT, WAIT THE
2470 REM                       SPECIFIED TIME, THEN RE-READ THE A/D.
2480 REM       RESET - 3   --- GO BACK TO THE TOP MENU TO CHANGE ANY OF THE
2490 REM                       INITIAL PARAMETERS.
2500 REM       REV   - 4   --- REVERSE THE MOTOR DIRECTION TO ENABLE A MANUAL
2510 REM                       RETURN OF THE MIRROR TO THE STARTING POINT.
2520 REM       FOR   - 5   --- CHANGE THE MOTOR DIRECTION TO ENABLE THE
2530 REM                       FORWARD MOTION OF THE MIRROR.
2540 REM       NEW   - 6   --- START A NEW DATA SCAN, ZERO ALL PREVIOUS DATA.
2550 REM
2560 REM
2570 REM ************************************************************************
2580          MENU1=0
2590          PRINT"                                                            "
2600         INPUT"[NEXT=0]  CONT=1  DEL=2 RESET=3 REV=4 FOR=5 NEW=6: ", MENU1
2610          IF MENU1=0 THEN GOTO 2780   :REM      NEXT POINT
2620         ON MENU1 GOTO 2800,  2660 ,2700 , 2640, 2650, 590
2630          GOTO 2370
2640         OUT &H3C,0  : GOTO 2370
2650         OUT &H3C,5  : GOTO 2370
2660         X=(I-1)*W
2670          YY=200 - 20*Y(I)
2680          PRESET(X,YY)            :REM    TAKE OFF PREVIOUS POINT
2690          GOTO 2180
2700          IRESET=1  : GOTO 850
2710          IRESET=0
2720          GOSUB 4120      :REM PLOT THE COORDINATES OF THE INTERFEROGRAM
2730          FOR J=1 TO JJ
2740                 X=(J-1)*W : YY=200 - 20*Y(J) : PSET(X,YY)
2750          NEXT J
2760          I=JJ
2770          GOTO 2370
2780   NEXT I
2790   I=I-1                                :REM    DECREMENT I TO MATCH MPOINTS
2800   REM
2810   MPOINTS=I                            :REM    TOP LIMIT
2820   EX=0                                 :REM    EXPANSION FACTOR
2830   F1=1                                 :REM    BOTTOM LIMIT
2840   F2=MPOINTS                           :REM    TOP LIMIT
2850   INAME=0                              :REM    TITLE OF PLOT HAS BEEN STORED
2860   TOTAL = INT(MPOINTS)
2870   EX=0                                 :REM    EXPANSION FACTOR
2880   F1=1                                 :REM    BOTTOM LIMIT
2890   F2=MPOINTS                           :REM    TOP LIMIT
2900   GOSUB 4120                 :REM PLOT THE COORDINATES OF THE INTERFEROGRAM
2910   FOR I=1 TO TOTAL
2920            X=I*W
2930            AA=200-20*Y(I)
2940            PSET(X,AA)        :REM PLOT THE DATA
```

```
2950   NEXT I
2960   GOSUB 3720                    :REM    PLOT THE Y-AXIS COORDINATES
2970 REM ************************************************************************
2980 REM
2990 REM        DATA ANALYSIS MENU
3000 REM
3010 REM        ZOOM - 1 --- ZOOM ON THE DESIRED SECTION OF X-AXIS.
3020 REM        EXP  - 2 --- EXPAND THE PLOT VERTICALLY.
3030 REM        CORR - 3 --- CORRECT THE DATA FOR THE OFFSET OF THE A/D.
3040 REM        ORG  - 4 --- ORIGINAL DATA READ FROM A DISK FILE "DATA".
3050 REM        DSK  - 5 --- STORE THE CURRENT DATA ON A DISK FILE "DATA".
3060 REM        NEW  - 7 --- TAKE A NEW SCAN.
3070 REM
3080 REM ************************************************************************
3090   IFLAG=0
3100   MENU=0
3110   LOCATE 25,1,1
3120 PRINT"                                                                    "
3130   INPUT"ZOOM=1  EXP=2  CORR=3  ORG=4  DUMP=5  DSK=6  NEW=7 ";MENU
3140   IF MENU=0 THEN GOTO 3060
3150   ON MENU GOTO 3320, 3340, 3250, 2820, 3170, 3220 ,590
3160   GOTO 3060
3170 REM ************************************************************************
3180   GOSUB 3520                :REM    DUMP THE SCREEN TO PRINTER
3190 INAME=1
3200 GOTO 3060
3210 REM ************************************************************************
3220 REM                                STORE IN DISK
3230 GOSUB 3390  : GOTO 3060
3240 REM ************************************************************************
3250 REM                                CORRECT THE DATA FOR A/D OFSET
3260 PRINT "                                                                   "
3270 INPUT" Y-INTERCEPT and SLOPE : ", YINT, SLOPE
3280 FOR I=1 TO MPOINTS
3290            Y(I)= Y(I)*SLOPE + YINT
3300 NEXT I
3310 GOTO 2870                      :REM    PLOT THE CORRECTED DATA
3320 REM ************************************************************************
3330 GOSUB 4840  : GOTO 3060     :REM    ZOOM ON THE INTERVAL
3340 REM ************************************************************************
3350 GOSUB 5220  : GOTO 3060     :REM     EXPAND THE PLOT
3360 REM ************************************************************************
3370 LOCATE 1,5,1: STOP : END
3380 REM
3390 REM ************************************************************************
3400 REM                OUTPUT THE DATA ONTO A DISK
3410 REM ************************************************************************
3420 POINTS=INT(F2-F1+1)
3430 OPEN "O",#1,"DATA"
```

```
3440 PRINT #1,POINTS
3450 PRINT #1,FRINGE
3460 FOR I=F1 TO F2
3470            PRINT #1, Y(I)
3480 NEXT I
3490 CLOSE #1
3500 DEF SEG
3510 RETURN
3520 REM ************************************************************************
3530 REM                                  DUMP SCREEN TO THE TERMINAL
3540 REM ************************************************************************
3550 IF INMAE=1 THEN GOTO 3590          :REM    SKIP IF NAME WAS ALREADY STORED
3560 LOCATE 25,1,1
3570 PRINT"                                                                                "
3580 INPUT " ENTER THE DATE & NAME [i.e. 15-AUG-85-name] : "; DAY$
3590 PRINT"                                                                                "
3600 LOCATE 25,30,1
3610 PRINT"DATA POINTS " , DAY$
3620 REM
3630 REM  Have the printer work during one direction only
3640 LPRINT CHR$(27)+"["
3650 IF INKEY$=CHR$(3) THEN GOTO 3680
3660 FOR I=1 TO 1000 : I=I+1 : NEXT I : BEEP
3670 GOTO 3650
3680 LPRINT CHR$(27)+"]"
3690 LOCATE 25,1,1
3700 LPRINT "         "
3710 RETURN
3720 REM ************************************************************************
3730 REM                          NUMBER THE Y-AXIS COORDINATES
3740 REM ************************************************************************
3750 IF EX <> 0 THEN GOTO 3900    :REM    IF EXP=0 PLOT THE ORIGINAL DATA
3760 YAX=1000.001/100
3770 L=1
3780 YAXT=INT(YAX*1000.1)
3790 YAX=YAXT/1000
3800 LOCATE L,2 : PRINT YAX
3810 L=L+4.2
3820 YAX=YAX-2.00001
3830 IF YAX<1.9999  THEN GOTO 3870
3840 IF YAX>4.00001 THEN GOTO 3780
3850 L=L+1
3860 GOTO 3780
3870 YAX=.001
3880 LOCATE 22,3 : PRINT YAX
3890 RETURN
3900 REM
3910 GOSUB 4540                         :REM    AVERAGE THE DATA
3920 VMAX=Y(IMAX) : VMIN=Y(IMIN)        :REM    MIN/MAX DATA POINTS
```

```
3930 RANGE=ABS((VMAX-VMIN)*100/EX)      :REM    OVERALL Y-AXIS RANGE
3940 YSTEP=RANGE/5                      :REM    Y-AXIS STEPS
3950 YAX=VMAX+(RANGE-(VMAX-VMIN))/2     :REM    TOP COORDINATE
3960 YMIN=YAX-RANGE                     :REM    TOP COORDINATE
3970 L=1
3980 YAXT=INT(YAX*1000.1)
3990 YAX=YAXT/1000
4000 LOCATE L,2 : PRINT YAX
4010 L=L+4.2
4020 YAX=YAX-YSTEP
4030 IF YAX<YMIN+.9*(YSTEP) THEN GOTO 4070
4040 IF YAX>YMIN+(YSTEP)*2   THEN GOTO 3980
4050 L=L+1
4060 GOTO 3980
4070 YAXT=INT(YMIN*1000)
4080 YAX=YAXT/1000
4090 LOCATE 22,2 : PRINT YAX
4100 RETURN
4110 REM ************************************************************************
4120 REM                        Plot the coordinates
4130 REM ************************************************************************
4140 CLS :PI=4*ATN(1)
4150 LINE (0,0)-(640,200),,B
4160 TOTAL = F2-F1+1
4170 FOR J=0 TO 60 : W=640/60
4180           LINE(J*W,200)-(J*W,198)
4190 NEXT J
4200 FOR J=1 TO 6 : W=640/6
4210           LINE(J*W,200)-(J*W,195): NEXT J
4220 FOR J=0 TO 200 STEP 20
4230           LINE (0,J)-(7,J)
4240 NEXT J
4250 FOR J=0 TO 200 STEP 5
4260           LINE (0,J)-(3,J)
4270 NEXT J
4280 FOR J=0 TO 200 STEP 20
4290           LINE (633,J)-(640,J)
4300 NEXT J
4310 FOR J=0 TO 200 STEP 5
4320           LINE (637,J)-(640,J)
4330 NEXT J
4340 W=640/TOTAL
4350 XLAB=TOTAL/6
4360 A0= 640/6
4370 L=23
4380 XAX=A0
4390 LOCATE 23,1,1:PRINT F1
4400 FOR I=1 TO 6
4410   XAX=A0* I
```

```
4420   N=XAX/8.600001
4430   XL% = F1+XLAB*I - .5
4440   IF I<3 THEN GOTO 4460
4450           N=N+1
4460   IF I<5 THEN GOTO 4480
4470           N=N+1
4480   IF I<5.9 THEN GOTO 4510
4490           XL% = F2
4500           N=N-1
4510   LOCATE L,N : PRINT XL%
4520 NEXT I
4530 RETURN
4540 REM ************************************************************************
4550 REM                          AVERAGE THE DATA
4560 REM ************************************************************************
4570 SUM=0!
4580 FOR I=F1 TO F2
4590          SUM=SUM+Y(I)
4600 NEXT I
4610 AVJ=SUM/(F2-F1+1)
4620 AMAX =AVJ
4630 AMIN =AVJ
4640 FOR I=F1 TO F2
4650          IF Y(I) < AMAX  THEN GOTO 4690
4660                  AMAX = Y(I)
4670                  IMAX=I
4680                   GOTO 4720
4690          IF Y(I) > AMIN THEN GOTO 4720
4700                  AMIN= Y(I)
4710                   IMIN=I
4720 NEXT I
4730 AMAX=200-20*AMAX
4740 AMIN=200-20*AMIN
4750 RETURN
4760 FOR I=IL1 TO IL2
4770           W=640/(F2-F1):J=W*(I-F1)
4780           YY=YYINT+SL*I
4790           YY=200-20*YY
4800           YY=BOT-CC*(AMIN-YY)
4810           PSET(J,YY)
4820 NEXT I
4830 RETURN
4840 REM ************************************************************************
4850 REM                          ZOOM IN ON DESIRED INTERVAL
4860 REM ************************************************************************
4870 LOCATE 25,1,1
4880 PRINT"                                                                      "
4890 PRINT "OLD LIMITS: ",F1,F2
4900 LOCATE 25,40:INPUT"F1 , F2 = ", F1,F2
```

```
4910 GOSUB 4120                          :REM    PLOT THE GRAPH
4920 GOSUB 3720                           :REM    PLOT THE Y-AXIS
4930 IF EX<>0 THEN GOTO 5000
4940 FOR I=F1 TO F2
4950          W=640/(F2-F1):J=W*(I-F1)
4960         AA=200-20*Y(I)
4970          PSET(J,AA)
4980 NEXT I
4990 RETURN
5000 GOSUB 4540                 : REM   AVERAGE THE DATA
5010 EXABS=ABS(EX)
5020 CC=2*EXABS/(AMIN-AMAX)
5030 BOT = 100+EXABS
5040 TOP = 100-EXABS
5050 IF EX > 0 THEN GOTO 5150
5060 FOR I=F1+1 TO F2
5070           W=640/(F2-F1):J=W*(I-F1)
5080           AA0=200-20*Y(I-1)
5090           AA0=BOT-CC*(AMIN-AA0)
5100           AA1=200-20*Y(I)
5110           AA1=BOT-CC*(AMIN-AA1)
5120           LINE(J-W ,AA0)-(J,AA1)
5130 NEXT I
5140 RETURN
5150 FOR I=F1 TO F2
5160           W=640/(F2-F1):J=W*(I-F1)
5170           AA=200-20*Y(I)
5180           AA=BOT-CC*(AMIN-AA)
5190           PSET(J,AA)
5200 NEXT I
5210 RETURN
5220 REM ************************************************************************
5230 REM                          EXPAND THE DATA VERTICALLY
5240 REM ************************************************************************
5250 LOCATE 25,1,1
5260 EX = 0
5270 PRINT"                                                                      "
5280 INPUT"% OF Y-AXIS EXPANSION : (100-0)%-PNT, -(1-100)%-LINE   ";EX
5290 GOSUB 4120                : REM    PLOT THE X-AXIS
5300 GOSUB 3720                 : REM    PLOT THE Y-AXIS
5310 GOSUB 4540                 : REM   AVERAGE THE DATA
5320 EXABS=ABS(EX)
5330 CC=2*EXABS/(AMIN-AMAX)
5340 BOT = 100+EXABS
5350 TOP = 100-EXABS
5360 IF EX > 0 THEN GOTO 5460
5370 FOR I=F1+1 TO F2
5380           W=640/(F2-F1):J=W*(I-F1)
5390           AA0=200-20*Y(I-1)
```

```
5400           AA0=BOT-CC*(AMIN-AA0)
5410           AA1=200-20*Y(I)
5420           AA1=BOT-CC*(AMIN-AA1)
5430           LINE(J-W ,AA0)-(J,AA1)
5440 NEXT I
5450 RETURN
5460 FOR I=F1 TO F2
5470           W=640/(F2-F1):J=W*(I-F1)
5480           AA=200-20*Y(I)
5490           AA=BOT-CC*(AMIN-AA)
5500           PSET(J,AA)
5510 NEXT I
5520 RETURN
5530 REM
5540 SUMY=0
5550 INPUT "INTERVAL = ", INT1, INT2
5560 FOR I=INT1 TO INT2
5570           SUMY=Y(I)+SUMY
5580 NEXT I
5590 YAV=SUMY/(INT2-INT1+1)
5600 REM               WRITE THE Y-LEVEL ON THE SCREEN
5610 L=22
5620 RETURN
5630 REM ************************************************************************
5640 REM                      DATA TAKING AND PLOTTING
5650 REM ************************************************************************
5660   DEF SEG=&H2000
5670   DUMMY=USR1(0)
5680   DEF SEG=&H2200
5690   A=PEEK(N0)
5700   B=PEEK(N0+1)
5710   C=A+256*B
5720   YY=-(C-X1)*10/X1
5730   Y(I)=YY
5740   X=(I-1)*W
5750   YY=200 - 20*YY
5760   PSET(X,YY)
5770   RETURN
5780 REM ************************************************************************
5790 REM       ASSEMBLY SUBROUTINE THAT MOVES THE MIRROR       [ STEP1.ASM ]
5800 REM ************************************************************************
5810 FOR X= 0 TO  92:READ Y:POKE X,Y:NEXT X
5820 DATA 250,252,30,6,187,1,0,83,184,0,34,142,192,191,0
5830 DATA 0,176,5,230,60,185,0,4,81,81,187,0,0,186,0
5840 DATA 0,176,21,230,60,144,176,5,230,60,185,4,0,226,254
5850 DATA 229,61,248,3,216,115,1,66,89,73,227,18,81,184,1
5860 DATA 0,139,200,227,222,72,185,3,1,226,254,144,144,235,242
5870 DATA 139,195,89,247,241,171,89,73,227,3,81,235,188,7,31
5880 DATA 251,203,0
```

```
5890 RETURN
5900 REM ************************************************************************
5910 REM       ASSEMBLY SUBROUTINE THAT TAKES THE DATA   [ ADREAD.ASM  ]
5920 REM ************************************************************************
5930 FOR X= 0 TO  95:READ Y:POKE X,Y:NEXT X
5940 DATA 250,252,30,6,187,60,0,186,94,1,176,5,230,60,185
5950 DATA 2,0,81,176,37,230,60,185,136,19,73,227,15,228,60
5960 DATA 60,4,117,247,176,5,230,60,89,73,227,49,81,176,5
5970 DATA 230,60,185,232,3,235,28,144,176,37,230,60,139,203,73
5980 DATA 227,12,228,60,60,4,117,247,176,5,230,60,235,220,176
5990 DATA 5,230,60,139,202,73,227,226,228,60,60,4,117,247,235
6000 DATA 203,7,31,251,203,0
6010 RETURN
```

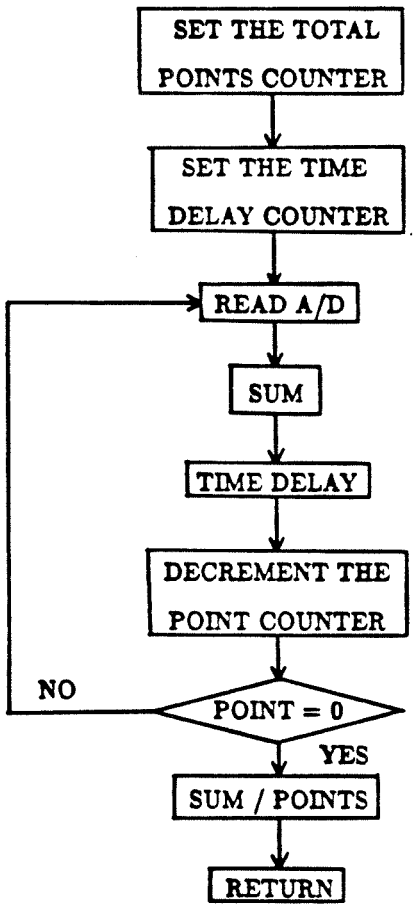

Figure 2. A flow chart of the assembly code ADREAD.ASM, which reads the A/D converter (used in program LOCKIN.BAS).

```
;                   ADREAD.ASM
;
;       written:    27-MAY-86   BY GIDI
;       revised:     7-NOV-86
;
;       PROGRAM IS FOR DATA TAKING WITH LOCKIN.BAS
;
;       PROGRAM READS THE A/D N-TIMES.
;       THE TIME BETWEEN A/D READINGS IS SET BY COUNTERS WHICH CAN
;       BE PEEKED AND POKED FROM SOFTWARE.
;       THE SUM OF ALL THE THE A/D READING IS DIVIDED BY THE TOTAL NUMBER
;       OF DATA POINTS TO YIELD THE AVERAGE OF THE DATA.
;       THIS IS DONE BY AN INTERNAL DIVISION ROUTINE (DIV) AND TAKES ABOUT
;       0.1-0.2 milliseconds.
;
ADCODE          SEGMENT
                ASSUME  CS:ADCODE
START           PROC    FAR
                CLI                             ; CLEAR INTERUPT FLAG
                CLD                             ; CLEAR DIRECTION FLAG
                PUSH    DS
                PUSH    ES
                MOV     BX,1                    ; GET NUMBER OF DATA POINTS
                PUSH    BX
                MOV     AX,2200H                ; LOAD A REG: AH=32, AL=0
                MOV     ES,AX
                MOV     DI,0
                MOV     AL,5                    ; STORE 0 IN AL
                OUT     3CH, AL                 ; PRESET BIT #5 TO 0
LOOP1:          MOV     CX, 0400H               ; TAKE 1024 A/D READINGS
                PUSH    CX                      ; LOAD POINTS INTO THE STACK
                PUSH    CX                      ; LOAD POINTS INTO THE STACK
                MOV     BX, 0000H               ; BX REGIS. COUNTS DOWN POINT No
                MOV     DX, 0000H               ; DX REGIS. COUNTS THE OVERFLOW
DATATAKE:       MOV     AL,21
                OUT     3CH, AL                 ; RAISE BIT# 5 HIGH
                NOP                             ; WAIT ~0.5 MICROSEC
                MOV     AL,5                    ; RESTORE 0 IN AL
                OUT     3CH, AL                 ; TRIGGER THE A/D TO CONVERT
                MOV     CX,4
DELAY1:         LOOP    DELAY1                  ; WAIT ~20 MICRO SECS
                IN      AX,003DH                ; GET A 2-BYTE WORD
                CLC                             ; CLEAR THE CARRY FLAG
                ADD     BX,AX                   ; ADD THE CURRENT DATA TO TOTAL
                JNB   SHORT NOCARRY             ; JUMP IF NO OVERFLOW OCCURED

                INC     DX                      ; KEEP TRACK OF OVERFLOW
NOCARRY:        POP     CX                      ; COUNT DOWN THE POINTS
                DEC     CX
                JCXZ    LOOP2                   ; JUMP OUT AFTER TAKING DATA
                PUSH    CX
                MOV     AX,0001H                ; # OF MULTIPLES OF 1 msec
CYCLE:          MOV     CX, AX
                JCXZ    DATATAKE                ; TAKE NEXT A/D READING
                DEC     AX
                MOV     CX,259                  ;\
```

```
DELAY2:     LOOP    DELAY2              ; \     DELAY CONVERTION
            NOP                         ; /     BY
            NOP                         ;/      1 MSEC
            JMP     CYCLE
LOOP2:      MOV     AX,BX               ; LOWER BYTE INTO (AX) REGISTER
            POP     CX                  ; DIVISOR INTO (CX) REGISTER
            DIV     CX                  ; 32-BIT DIV OF (FFFF*DX+AX)/CX
            STOSW                       ; STORE THE RESULT (AX)
            POP     CX
            DEC     CX                  ; CHECK TOTAL No OF DATA PTS.
            JCXZ    SHORT RETURN        ; JUMP OUT WHEN TOTAL No PTS.
            PUSH    CX                  ; SAVE CURRENT DATA POINT
            JMP     LOOP1               ; TAKE ANOTHER DATA POINT
RETURN:     POP     ES                  ; RESET THE REGISTERS
            POP     DS
            STI                         ; RESTORE THE INTERRUPTS
            RET                         ; RETURN TO BASIC
START       ENDP
ADCODE      ENDS
            END     START
```

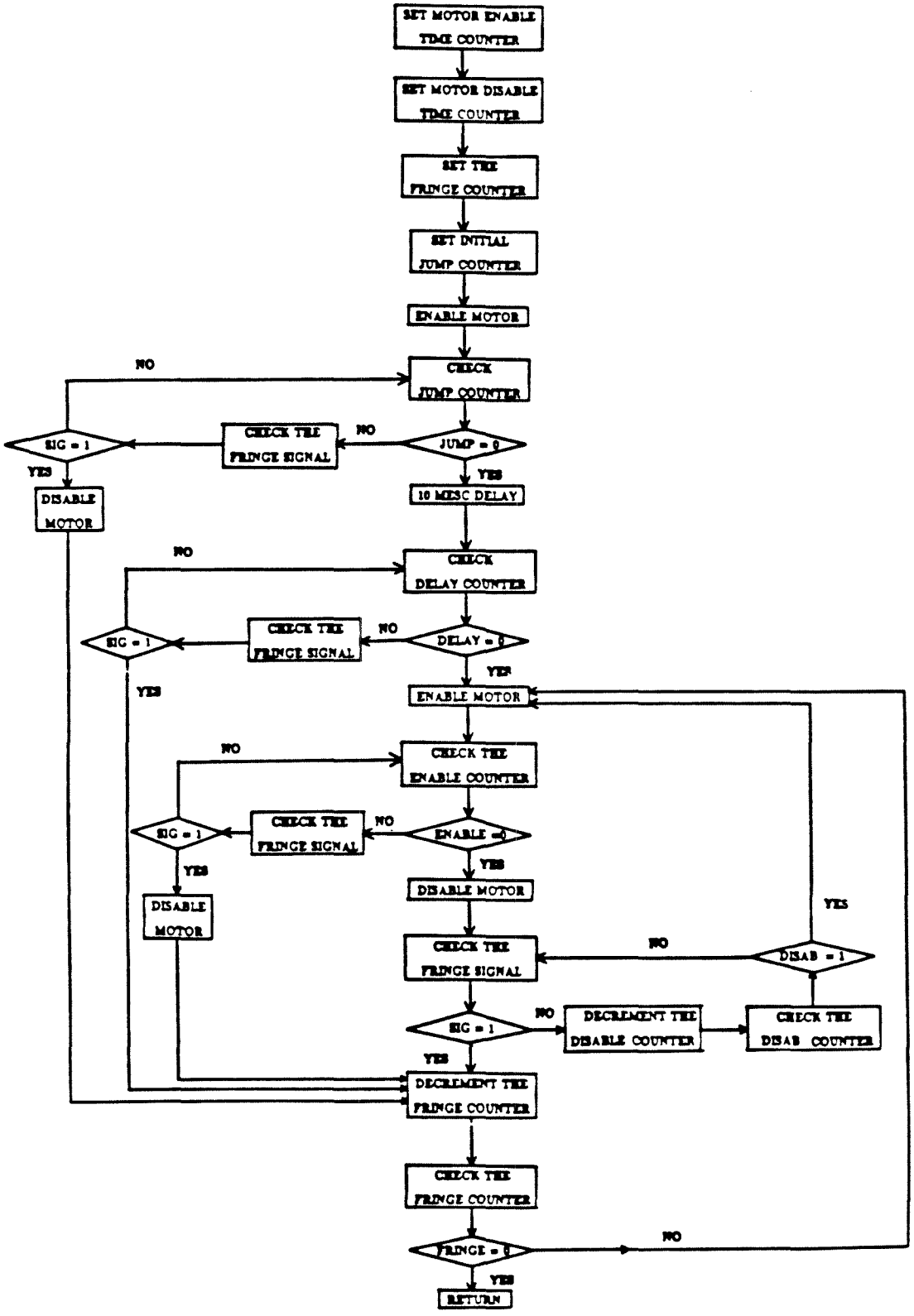

Figure 3. A flow chart of the assembly code STEP1.ASM, which steps the interferometer mirror.

```
;               STEP1.ASM                WRITTEN: 19-MAY-86
;                                        REVISED:  4-JUL-86
;
;               STEPPING THE MIRROR MOTOR  ASSEMBLY ROUTINE. WRITTEN FOR
;               LOCKIN.BAS
;
;               THIS ROUTINE STEPS THE MIRROR IN INTERVALS THAT ARE MULTIPLES
;               OF 0.5 microns AS GIVEN BY SIGNAL FROM THE MOIRE ENCODER
;               METROLOGY. THE ROUTINE THEN RETURNS TO THE MAIN PROGRAM.
;
;               THE MIRROR IS MOVED BY APPLYING A TRAIN OF SQUARE PULSES
;               TO THE D.C. MOTOR DRIVING THE MIRROR. THE TWO PARAMETERS
;               UNDER CONTROL ARE THE LENGHTH OF THE ENABLE PULSE AND THE TIME
;               TO BE WAITED FOR THE MIRROR TO COME TO REST AGAIN. WHEN THE
;               ENCODER SENDS OUT THE FRINGE SIGNAL, THE PULSES ARE IMMEDIATELY
;               DISABLED (EVEN IN THE MIDDLE OF A PULSE).
;               THE INITIAL PULSE IS EXTENDED TO REDUCE THE OVERALL STEPPING
;               TIME.
;
ADCODE          SEGMENT
                ASSUME  CS:ADCODE
START           PROC    FAR
                CLI
                CLD
                PUSH    DS
                PUSH    ES
                MOV     BX,60                   ; ENABLE  LOOP LENGTH
                MOV     DX,350                  ; DISABLE LOOP LENGTH
                MOV     AL, 5                   ; STORE 5 IN AL
                OUT     3CH, AL                 ; MOVE IN FORWARD DIRECTION
                MOV     CX, 2                   ; NUMBER OF REPEATED STEPS
                PUSH    CX                      ; STORE ON THE STACK
                MOV     AL, 37                  ; RAISE PIN #6 HIGH TO:::
                OUT     3CH, AL                 ; ENABLE MOTOR
                MOV     CX, 5000                ; INITIAL STEP JUMP
JUMP:           DEC     CX                      ; DECREMENT THE FRINGE COUNTER
                JCXZ    HALT                    ; STOP THE PULSE TRAIN
                IN      AL,3CH                  ; CHECK ENCODER SIGNAL
                CMP     AL,4                    ; STRIP FIRST TWO BITS
                JNZ  SHORT JUMP                 ; ENABLE MOTOR
                MOV     AL,5
                OUT     3CH, AL                 ; DISABLE MOTOR
FRINGE:         POP     CX
                DEC     CX                      ; DECREMENT COUNTER
                JCXZ    RETURN                  ; STOP AT CORRECT TOTAL TRAVEL
                PUSH    CX                      ; STORE VALUE
HALT:           MOV     AL,5
                OUT     3CH, AL                 ; DISABLE MOTOR
                MOV     CX, 1000                ; STOP MOTOR FOR ~10 msecs
                JMP     DELAY
MOVE:           MOV     AL, 37
                OUT     3CH, AL                 ; ENABLE MOTOR
                MOV     CX,BX
ENABLE:         DEC     CX
                JCXZ    DISABLE
```

```
                IN      AL,3CH                  ; CHECK ENCODER SIGNAL
                CMP     AL,4                    ; STRIP FIRST TWO BITS
                JNZ  SHORT ENABLE               ; ENABLE MOTOR
                MOV     AL,5
                OUT     3CH, AL                 ; DISABLE MOTOR
                JMP  SHORT FRINGE               ; CHECK FOR CORRECT FRINGE
DISABLE:        MOV     AL,5
                OUT     3CH, AL                 ; DISABLE MOTOR
                MOV     CX, DX
DELAY:          DEC     CX
                JCXZ    MOVE                    ; SEND ANOTHER PULSE
                IN      AL,3CH                  ; CHECK ENCODER SIGNAL
                CMP     AL,4                    ; STRIP FIRST TWO BITS
                JNZ  SHORT DELAY                ; CONT DELAY
                JMP  SHORT FRINGE               ; CHECK FOR CORRECT FRINGE
RETURN:         POP     ES
                POP     DS
                STI                             ; RESTORE THE INTERUPT FLAG
                RET                             ; RETURN
START           ENDP
ADCODE          ENDS
                END     START
```

```
10 REM                          SHOW.BAS
20 REM
30 REM         Written     20-JUL-1985  by GIDI
40 REM
50 REM         Revised      6-NOV-1986
60 REM
70 REM ************************************************************************
80 REM
90 REM         1.      First read the interferogram from a file called
100 REM                DATA where the first entry is the total number
110 REM                of points stored in the file.
120 REM
130 REM         2.     Analyze the interferogram :
140 REM
150 REM             a. Expand and center the data so that total points
160 REM                are a power of two .
170 REM             b. You can also select to invert only one side of
180 REM                the interferogram or its inverse if you so choose.
190 REM             c. Correct any of the data points for the lag time
200 REM                in the capacitor.
210 REM             d. Duplicate any portion of the spectrum onto its
220 REM                mirror point relative to the center of the data.
230 REM             e. Copy new data onto any portion of the curve.
240 REM             f. Reduce the baseline drift by normalizing all
250 REM                points to a common reference, by method of least
260 REM                squares.
270 REM
280 REM         3.     Invert the data in a subroutine called FFT, which
290 REM                returns the spectrum in a vector Q(I) (recall
300 REM                that there are only N/2 spectral points for N
310 REM                data points).
320 REM
330 REM         4.     Analyze the spectrum:
340 REM
350 REM             a. Expand it vertically.
360 REM             b. Zoom-in on region of interest.
370 REM             c. Add and average previous scans with the
380 REM                current one.
390 REM
400 REM          5.    Account for the Instrument Line Function.
410 REM
420 REM ************************************************************************
430 DIM X(1105), Y(1105)
440 DIM A(1105), B(1105), Q(1105), R(1105)
450 CLS
460 IAVG=0
470 DEFINT I,J,K,L
480 DEFSTR Z
490 OPEN "I",#1,"DATA"
```

```
500 INPUT #1, POINTS  : ORGPNT=POINTS
510 INPUT #1, FRINGE
520 IF IAVG=0 THEN GOTO 550
530            IF IFRINGE=FRINGE THEN GOTO 550
540                    PRINT"MISMATCH IN FRINGE STEPS" :STOP
550 INTER = 0          :REM   INTER=0 means that the current file name
560                    :REM   of the data set has not been entered.
570 POWER=0
580 TOTAL = INT(POINTS)
590 PT = INT(POINTS)
600 PT=PT/2 : IF PT<1 THEN GOTO 620
610 POWER=POWER+1 : GOTO 600
620 M=POWER : MPOINTS=2^M : ORGMP=MPOINTS
630 LOCATE 23,1,1
640 PRINT " TOTAL NUMBER OF POINTS : ", TOTAL
650 LOCATE 24,1,1
660 PRINT " POWER OF POINTS = ",M
670 LOCATE 25,1,1
680 PRINT " FRINGE SPACING  = ",FRINGE
690 FOR I=1 TO POINTS
700            INPUT #1, Y(I)
710           X(I)=Y(I)
720            IF EOF(1) THEN GOTO 740
730 NEXT I
740 CLOSE #1
750 TOTAL=INT(POINTS)
760 GOSUB 4910                 :REM    PLOT COORDINATES+DATA
770 REM ************************************************************************
780 REM
790 REM         MANIPULATE THE INTERFEROGRAM BEFORE TAKING THE FFT
800 REM
810 REM                          RAW DATA STORED IN  Y(I)
820 REM
830 REM        FFT = 0 --- [ DEFAULT ] COMPUTE THE FFT OF DATA IN A(I).
840 REM        EX  = 1 --- EXPAND THE PLOT VERTICALLY (% OF THE GRAPH).
850 REM        ZOM = 2 --- ZOOM ON A SECTION OF THE X-AXIS.
860 REM        CEN = 3 --- CENTER THE PEAK OF THE INTERFEROGRAM.
870 REM        INV = 4 --- INVERT THE INTERFEROGRAM.
880 REM        ORG = 5 --- GET THE ORIGINAL INTERFEROGRAM FROM THE DISK.
890 REM        DMP = 6 --- DUMP THE DISPLAYED DATA TO A PRINTER.
900 REM        SEL = 7 --- SELECT A STARTING POINT OF THE INTERFEROGRAM.
910 REM        FIX = 8 --- GO TO A SUB MENU FOR FIXING THE DATA.
920 REM
930 REM ************************************************************************
940 LOCATE 25,1,1
950 PRINT"                                                                      "
960 MENU = 0
970 INPUT"FFT=0 EX=1 ZOM=2 CEN=3 INV=4 ORG=5 DMP=6 SEL=7 FIX=8 ";MENU
980 IF MENU = 0 THEN GOTO 1400
```

```
990 IF MENU = 8 THEN GOTO 1210
1000 ON MENU GOSUB 8420,5660,6080,6530,8330,7270,8110
1010 GOTO 940
1020 REM ************************************************************************
1030 REM
1040 REM                        SECOND LEVEL MENU
1050 REM
1060 REM        RTN = 0 --- [ DEFAULT ] RETURN TO FIRST MENU LEVEL.
1070 REM        INS = 1 --- INSERT A NEW DATA FILE STORED IN "ADD".
1080 REM        DSK = 2 --- STORE THE DATA (IN Y(I)) IN FILE "DATA".
1090 REM        LST = 3 --- LIST THE VALUE OF SOME POINTS ON SCREEN.
1100 REM        COR = 4 --- CORRECT THE VALUE OF A SPECIFIC POINT.
1110 REM        INV = 5 --- INVERT THE INTERFEROGRAM.
1120 REM        DUP = 6 --- DUPLICATE A REGION OF THE DATA W.R.T. THE
1130 REM                    CENTER POINT, (THE EQUAL ARM POINT).
1140 REM        ORG = 7 --- GET THE ORIGINAL DATA FROM DISK FILE "DATA".
1150 REM        NOR = 8 --- NORMALIZE THE DATA BETWEEN TWO LIMITS (N1-N2)
1160 REM                    TO THE 5.0 VOLT LINE.
1170 REM        1/2 = 9 --- REDUCE THE NUMBER OF POINTS TO ONE HALF THE
1180 REM                    ORIGINAL VALUE.
1190 REM
1200 REM ************************************************************************
1210 MENU=0
1220 LOCATE 25,1,1
1230 PRINT"                                                                      "
1240 INPUT"RTN=0 INS=1 DSK=2 LST=3 COR=4 INV=5 DUP=6 ORG=7 NOR=8 1/2=9  ",MENU
1250 IF MENU = 0 THEN 760
1260 ON MENU GOSUB 6750, 8760, 8240, 6610,6530, 7540, 8330, 7830, 6420
1270 IF EX=0 THEN 1210
1280 IF MENU=3 THEN 1210
1290 ISUB=1 : GOSUB 8420
1300 GOTO 1210
1310 REM ************************************************************************
1320 REM                FFT    INVERSION OF THE DATA
1330 REM
1340 REM                SYMBOLS USED IN SUBSEQUENT PROGRAM:
1350 REM                1.      IBEG    -       STARTING PLOT POINT
1360 REM                2.      IEND    -       ENDING     "     "
1370 REM                3.      INOR    -       NORMALIZATION FLAG
1380 REM
1390 REM ************************************************************************
1400 N = MPOINTS :LOCATE 25,1,1
1410 PRINT "                                                                     "
1420 EX=0 : PI=4*ATN(1) :CLS :LOCATE 25,30,1 : PRINT"COMPUTING FFT"
1430 GOSUB 9880                         :REM    Take FFT of the data
1440 NSCANS=0
1450 IBEG=1000 : IEND=2250
1460 EX=80 :Y0=180: ISHIFT=0 : INOR=0
1470 GOSUB 10760
```

```
1480 REM ************************************************************************
1490 REM
1500 REM                        MANIPULATE THE SPECTRUM
1510 REM
1520 REM       ADD = 0 --- [ DEFAULT ] ADD A SPECTRUM IN MEMORY, STORED
1530 REM                   IN A FILE CALLED "PNT".
1540 REM       LIM = 1 --- CHOOSE THE LIMITS, (N1, N2, IN WAVENUMBERS) OF
1550 REM                   THE SPECTRUM.
1560 REM       EXP = 2 --- EXPAND THE SPECTRUM IN THE VERTICAL DIRECTION
1570 REM                   BY NORMALIZING TO THE LARGEST Y-VALUE.
1580 REM       ORG = 3 --- THE ORIGINAL SPECTRUM (NOT APPLICABLE AFTER
1590 REM                   AVERAGING A WITH ANOTHER SPECTRUM).
1600 REM       DMP = 4 --- DUMP THE SCREEN TO A TERMINAL PRINTER.
1610 REM       DSK = 5 --- STORE THE SPECTRUM ON A DISK, EITHER IN A "PNT"
1620 REM                   FILE FOR FURTHER AVERAGING, OR IN "PNT1" AS AN
1630 REM                   X-Y FILE FOR BETTER PLOTTING.
1640 REM       PEAK= 6 --- MOVE A CURSOR ON THE SPECTRUM TO LOCATE PEAKS
1650 REM                   AND LABEL THEM.
1660 REM       ILF = 7 --- CORRECT THE SPECTRUM FOR THE INSTRUMENT LINE
1670 REM                   FUNCTION.
1680 REM
1690 REM ************************************************************************
1700 MENU=0 : Y0=180 : ISHIFT=0 :LOCATE 25,1,1
1710 PRINT"                                                                    "
1720 INPUT"[ADD=0], LIM=1, EXP=2, ORG=3, DUMP=4, DSK=5, PEAK=6, ILF=7";MENU
1730 IF MENU=0 THEN GOTO 2110
1740 ON MENU GOTO 1910, 1990, 1790, 2070, 1890, 3440 ,3990
1750 GOTO 1700
1760 REM ************************************************************************
1770 REM                        RESTORE THE ORIGINAL SPECTRUM
1780 REM ************************************************************************
1790 IREAD=0
1800 LOCATE 25,1,1
1810 PRINT "                                                                   "
1820 INPUT"WANT TO RE-READ THE DISK ? ", IREAD
1830 IF IREAD=0 THEN GOTO 1850
1840 GOTO 460
1850 FOR I=1 TO MPOINTS
1860          Q(I)=Y(I)
1870 NEXT I : GOTO 1450
1880 REM ************************************************************************
1890 GOSUB 8980 :GOTO 1700     :REM    OUTPUT THE SPECTRUM TO A DISK
1900 REM ************************************************************************
1910 PRINT "                                                                   "
1920 PRINT "OLD LIMITS: ",IBEG,IEND
1930 LOCATE 25,40:PRINT"                                  "
1940 LOCATE 25,40:INPUT"NEW  LIM = ", IBEG,IEND
1950 GOSUB 10760 : GOTO 1700
1960 REM ************************************************************************
```

```
1970 REM                          EXPAND THE PLOT
1980 REM ************************************************************************
1990 LOCATE 25,1,1
2000 EX = 0
2010 PRINT "                                                                    "
2020 INPUT"% OF Y-AXIS EXPANSION : (-100-0)%-PNT, (1-100)%-LINE   ";EX
2030 GOSUB 10760 : GOTO 1700
2040 REM ************************************************************************
2050 REM                          DUMP THE SCREEN ONTO A PRINTER
2060 REM ************************************************************************
2070 GOSUB 10230  : GOTO 1700
2080 REM ************************************************************************
2090 REM                          DISPLAY THE SPECTRUM IN MEMORY
2100 REM ************************************************************************
2110 CLOSE #2
2120 OPEN "I",#2,"PNT"
2130 INPUT #2, IPOINTS
2140 INPUT #2, FRIN
2150 IF FRIN=FRINGE THEN GOTO 2170
2160 PRINT"STEPS IN SUB FILE DON'T MATCH CURRENT FILE" : GOTO 1700
2170 FOR I=1 TO IPOINTS
2180            INPUT #2, R(I)
2190            IF EOF(2) THEN GOTO 2210
2200 NEXT I
2210 RMAX = 0 : CLOSE #2
2220 IF IPOINTS=MPOINTS THEN 2420   :REM   IF RESOLUTION IS DIFFERENT
2230 FT1=INT(F1/2):FT2=INT(F2/2)    :REM   SET LIMITS OF NEW SPECTRUM SO
2240 IF F1>1 THEN 2250 : FT1=1      :REM   POINTS OVERLAP EACH OTHER.
2250 F1=FT1*2 : F2=FT2*2            :REM   RESET THE ORIGINAL POINTS.
2260 GOSUB 10760                     :REM   PLOT COORD. + ORIG. SPECTRUM
2270 FOR I=FT1 TO FT2
2280            IF R(I) < RMAX THEN GOTO 2300
2290            RMAX = R(I)
2300 NEXT I
2310 RNORM = RMAX
2320 FOR I=FT1+1 TO FT2
2330          J=W0*(RESOL*I-IBEG) : J0=W0*(RESOL*(I-1)-IBEG)
2340          Q1=Y0-INT(EX*1.8*R(I-1)/RNORM)
2350          R1=Y0-INT(EX*1.8*R(I)/RNORM)
2360           Y(I-1)=Q1
2370           PSET(J-W,Q1)
2380 NEXT I
2390 PSET(J,R1)
2400 Y(FT2)=R1
2410 GOTO 2560                          :REM    GO TO THE SUB MENU
2420 FOR I=F1 TO F2
2430            IF R(I) < RMAX THEN GOTO 2450
2440            RMAX = R(I)
2450 NEXT I
```

```
2460 RNORM = RMAX
2470 FOR I=F1+1 TO F2
2480           J=W0*(RESOL*I-IBEG) : J0=W0*(RESOL*(I-1)-IBEG)
2490           Q1=Y0-INT(EX*1.8*R(I-1)/RNORM)
2500            Y(I-1)=Q1
2510           R1=Y0-INT(EX*1.8*R(I)/RNORM)
2520            LINE(J0,Q1)-(J,R1)
2530 NEXT I
2540 CIRCLE(0,Y(F1)),2
2550 Y(F2)=R1
2560 F1T=F1
2570 F2T=F2
2580 ISHIFT = 0
2590 FIL=0
2600 REM ************************************************************************
2610 REM
2620 REM                          DISPLAY AND AVERAGE ANOTHER SPECTRUM
2630 REM
2640 REM       RTN = 0 --- [ DEFAULT ] RETURN TO MAIN MENU
2650 REM                     ONE RESOLUTION.
2660 REM       SHIF-R = 1 --- SHIFT THE ADDED SPECTRUM TO THE RIGHT BY
2670 REM                     ONE RESOLUTION.
2680 REM       SHIF-L = 1 --- SHIFT THE ADDED SPECTRUM TO THE LEFT BY
2690 REM                     ONE RESOLUTION.
2700 REM       AVG = 3 --- AVERAGE THE CURRENT SPECTRUM WITHE THE
2710 REM                   DISPLAYED ONE.
2720 REM       DMP = 4 --- DUMP THE DISPLAYED SPECTRUM TO A TERMINAL PRINTER.
2730 REM       DSK = 5 --- STORE THE SPECTRUM IN Q(I) ON A DISK FILE CALLED
2740 REM                   "PNT", FOR FURTHER AVERAGING.
2750 REM
2760 REM ************************************************************************
2770 LOCATE 25,1,1
2780 FIL=0
2790 PRINT"                                                                    "
2800 INPUT"[RTN=0]  SHIF-R=1  SHIF-L=2  AVG=3  DMP=4  DSK=5 "; FIL
2810 IF FIL=0 THEN 3230
2820 ON FIL GOTO  2840, 2910, 3000, 3190, 3310
2830 GOTO 2560
2840 IF FT1=1 THEN 2560
2850 RTEMP=R(IPOINTS)
2860 FOR I=1 TO IPOINTS-1
2870           K=IPOINTS-I
2880           R(K+1)=R(K)
2890 NEXT I
2900 R(1)=RTEMP : GOTO 2210
2910 IF FT1=IPOINTS THEN 2560
2920 RTEMP=R(1)
2930 FOR I=2 TO IPOINTS
2940           R(I-1)=R(I)
```

```
2950 NEXT I
2960 R(IPOINTS)=RTEMP : GOTO 2210
2970 REM ************************************************************************
2980 REM                          AVERAGE THE NEW DATA
2990 REM ************************************************************************
3000 LOCATE 25,1,1 : PRINT"                                                      "
3010 NSCANS=1
3020 INPUT" NUMBER OF PREVIOUS SCANS AVERAGED : ", NSCANS
3030 IF MPOINTS <> IPOINTS THEN 3080
3040 FOR I=1 TO MPOINTS
3050           Q(I)= (Q(I)/NORM + R(I)/RNORM*NSCANS)/(NSCANS+1)
3060 NEXT I
3070 GOSUB 10760 : GOTO 1700
3080 IF MPOINTS < IPOINTS THEN 3070
3090 IMULT=MPOINTS/IPOINTS
3100 FOR I=1 TO IPOINTS/2
3110           J=IMULT*I : K=J+1 : RAVG=(R(I)+R(I+1))/2
3120           Q(J)= (Q(J)/NORM + R(I)/RNORM*NSCANS)/(NSCANS+1)
3130           Q(K)= (Q(K)/NORM + RAVG/RNORM*NSCANS)/(NSCANS+1)
3140 NEXT I
3150 GOSUB 10760 : GOTO 1700
3160 REM ************************************************************************
3170 REM                          DUMP THE SCREEN ONTO A PRINTER
3180 REM ************************************************************************
3190 GOSUB 10200  : GOTO 2590
3200 REM ************************************************************************
3210 REM                          RETURN TO MAIN SPECTRUM MENU
3220 REM ************************************************************************
3230 F1=F1T                              :REM  Set the old limits F1, F2
3240 F2=F2T
3250 IF EX<> 0 THEN 3270
3260 EX=60
3270 GOSUB 10760 : GOTO 1700
3280 REM ************************************************************************
3290 REM                          OUTPUT THE AVERAGED RESULT TO A DISK
3300 REM ************************************************************************
3310 GOSUB 8980  : GOTO 2590
3320 REM ************************************************************************
3330 REM
3340 REM                          LOCATE AND PRINT PEAK POSITION:
3350 REM
3360 REM       RTN = 0 ---- [ DEFAULT ] RETURN TO MAIN SPECTRUM MENU.
3370 REM       R(FST) = 1 - MOVE THE CURSOR FAST TO THE RIGHT
3380 REM       R(SLO) = 2 - MOVE THE CURSOR BY ONE DATA POINT TO RIGHT
3390 REM       L(FST) = 3 - MOVE THE CURSOR FAST TO THE LEFT.
3400 REM       L(SLO) = 4 - MOVE THE CURSOR BY ONE DATA POINT TO LEFT.
3410 REM       LAB = 5 --- LABEL THE PEAK WAVENUMBER AND Y-VALUE.
3420 REM
3430 REM ************************************************************************
```

```
3440 IPOINT=F1+2 : IPOINTOLD=F1+2
3450 MENU = 0
3460 LOCATE 25,1,1
3470 PRINT "                                                                    "
3480 INPUT"[RTN=0] R(FST)-1  R(SLO)-2  L(FST)-3  L(SLO)-4  LAB-5 :  "; MENU
3490 PRINT "                                                                    "
3500 IF MENU=0 THEN GOTO 2560
3510 REM ************************************************************************
3520 REM               INCREMENT THE POINTER FOR LABELING PURPOSES.
3530 REM ************************************************************************
3540 ON MENU GOTO 3560, 3600, 3640, 3680, 3720
3550 GOTO 3450
3560 IF IPOINT+10 > F2 THEN GOTO 3450
3570 IPOINTOLD=IPOINT
3580 IPOINT=IPOINT+10 : GOSUB 10520
3590 GOTO 3450
3600 IF IPOINT+1 > F2 THEN GOTO 3450
3610 IPOINTOLD=IPOINT
3620 IPOINT=IPOINT+1 :GOSUB 10520
3630 GOTO 3450
3640 IF IPOINT-10 < F1 THEN GOTO 3450
3650 IPOINTOLD=IPOINT
3660 IPOINT=IPOINT-10 : GOSUB 10520
3670 GOTO 3450
3680 IF IPOINT-1  < F1 THEN GOTO 3450
3690 IPOINTOLD=IPOINT
3700 IPOINT=IPOINT-1  : GOSUB 10520
3710 GOTO 3450
3720 IPEAK=80*(IPOINT-F1+1)/(F2-F1+1)
3730 LOCATE 2,40,1   : PRINT"                                  "
3740 LOCATE 3,40,1   : PRINT"                              "
3750 N=INT(18*(1-YPEAK/180))
3760 LOCATE N,IPEAK,1 : PRINT XVAL
3770 I=IPOINT+1                          :REM  REFILL THE BACKGROUND
3780          J=W0*(RESOL*I-IBEG) : J0=W0*(RESOL*(I-1)-IBEG)
3790          Q1=Y0-INT(EX*1.8*Q(I-1)/NORM)
3800          R1=Y0-INT(EX*1.8*Q(I)/NORM)
3810           LINE(J0,Q1)-(J,R1)
3820 GOTO 3450
3830 REM ************************************************************************
3840 REM
3850 REM        COMPUTES THE INSTRUMENT LINE FUNCTION BASED ON THE
3860 REM        RADIATION AT A GIVEN TEMPEARURE, AND ON THE MEASURED
3870 REM        TRANSMISSION FUNCTION OF THE VARIOUS OPTICAL COMPONENTS
3880 REM        IN THE INTERFEROMETER.
3890 REM
3900 REM          DATA IS CONTAINED IN   :    TRANS.DAT
3910 REM
3920 REM          X(I) -- WAVENUMBERS CORRESPONDING TO TRANSMISSION
```

```
3930 REM          B(I) -- INSTRUMENT TRANSMISSION FUNCTION
3940 REM          F(I) -- BLACK BODY RELATIVE SPECTRUM
3950 REM          Z(I) -- B(I)*F(I)
3960 REM          A(I) -- Z(I) NORMALIZED TO 2500 WAVENUMBERS
3970 REM
3980 REM ************************************************************************
3990 INOR=1 : OPEN "I",#1,"TRANS.DAT"
4000 REM                        ZERO THE VECTORS
4010 FOR I=1 TO MPOINTS
4020           X(I)=0!: A(I)=0! :B(I)=0!
4030 NEXT I
4040 I=0
4050           I=I+1
4060           INPUT #1, X(I)
4070           INPUT #1, B(I)
4080           IF EOF(1) THEN GOTO 4100
4090           GOTO 4050
4100 CLOSE #1 : ISPEC=I
4110 GOSUB 10960                          :REM  COMPUTE THE I.L.F.
4120 FOR I=1 TO ISPEC
4130           X(I)=X(I)/1000
4140           A(I)=A(I)/100
4150 NEXT I
4160 FOR J=F1 TO F2
4170           XVAL=RESOL*J/1000
4180           FOR I=1 TO ISPEC -1
4190                  IF XVAL >=  X(I)  THEN  GOTO 4220
4200           NEXT I
4210           PRINT "DESIRED WAVENUMBER BELOW  RANGE" : STOP
4220           I2=I
4230           IF XVAL<>X(I2) THEN 4250
4240           YVAL=A(I2) : GOTO  4390
4250           IF I2>1 THEN GOTO 4270
4260           PRINT "DESIRED WAVENUMBER ABOVE  RANGE" : STOP
4270           I1=I2-1 : I3=I2+1
4280           REM
4290           REM  COMPUTE THE CONSTANTS FOR  :  YY = A*X**2 + B*X + C
4300           REM
4310           AZ1 =   A(I3)*(X(I2)^2 - X(I1)^2)
4320           AZ2 =   A(I2)*(X(I1)^2 - X(I3)^2)
4330           AZ3 =   A(I1)*(X(I3)^2 - X(I2)^2)
4340           BB=AZ1*AZ2*AZ3/(X(I3)-X(I2))/(X(I1)-X(I3))/(X(I2)-X(I1))
4350           AZ4 = A(I3) - A(I1) - BB*(X(I3)-X(I1))
4360           AA = AZ4/( X(I3)^2 - X(I1)^2 )
4370           CC = A(I2) - AA*X(I2)^2 - BB*X(I2)
4380           YVAL=AA*XVAL^2+BB*XVAL+CC
4390           YVAL= YVAL*100
4400           Q(J)=Q(J)*YVAL
4410 NEXT J
```

```
4420 REM                RENORMALIZE W.R.T. LAST YVAL
4430 FOR I=F1 TO F2
4440           Q(I)=Q(I)/YVAL
4450 NEXT I
4460 GOTO 1460
4470 STOP : END
4480 REM
4490 REM
4500 REM                          NUMBER THE Y-AXIS COORDINATES
4510 REM
4520 IF EX <> 0 THEN GOTO 4670    :REM    IF EXP=0 PLOT THE ORIGINAL DATA
4530 YAX=1000.001/100
4540 L=1
4550 YAXT=INT(YAX*1000.1)
4560 YAX=YAXT/1000
4570 LOCATE L,2 : PRINT YAX
4580 L=L+4.2
4590 YAX=YAX-2.00001
4600 IF YAX<1.9999  THEN GOTO 4640
4610 IF YAX>4.00001 THEN GOTO 4550
4620 L=L+1
4630 GOTO 4550
4640 YAX=.001
4650 LOCATE 22,3 : PRINT YAX
4660 RETURN
4670 REM
4680 GOSUB 5430                           :REM    AVERAGE THE DATA
4690 VMAX=Y(IMAX) : VMIN=Y(IMIN)          :REM    MIN/MAX DATA POINTS
4700 RANGE=ABS((VMAX-VMIN)*100/EX)        :REM    OVERALL Y-AXIS RANGE
4710 YSTEP=RANGE/5                        :REM    Y-AXIS STEPS
4720 YAX=VMAX+(RANGE-(VMAX-VMIN))/2       :REM    TOP COORDINATE
4730 YMIN=YAX-RANGE                       :REM    TOP COORDINATE
4740 L=1
4750 YAXT=INT(YAX*1000.1)
4760 YAX=YAXT/1000
4770 LOCATE L,2 : PRINT YAX
4780 L=L+4.2
4790 YAX=YAX-YSTEP
4800 IF YAX<YMIN+.9*(YSTEP) THEN GOTO 4840
4810 IF YAX>YMIN+(YSTEP)*2   THEN GOTO 4750
4820 L=L+1
4830 GOTO 4750
4840 YAXT=INT(YMIN*1000)
4850 YAX=YAXT/1000
4860 LOCATE 22,2 : PRINT YAX
4870 RETURN
4880 REM ************************************************************************
4890 REM            REDRAW THE COORDINATES AND PLOT THE DATA IN Y(I)
4900 REM ************************************************************************
```

```
4910 F1=1 : F2=TOTAL : FF1=1 : FF2=TOTAL
4920 GOSUB 5030                :REM PLOT THE COORDINATES OF THE DATA
4930 GOSUB 5460                :REM AVERAGE THE DATA
4940 GOSUB 4520                :REM PLOT THE Y-COORDINATES
4950 FOR I=1 TO TOTAL
4960          YY=200 - 20*Y(I) :X=I*W : PSET(X,YY) : A(I)=YY
4970 NEXT I
4980 RETURN
4990 REM ************************************************************************
5000 REM                Subroutine that draws the coordinates
5010 REM                              OF THE INTERFEROGRAM
5020 REM ************************************************************************
5030 CLS :PI=4*ATN(1)
5040 LINE (0,0)-(640,200),,B
5050 TOTAL = F2-F1+1
5060 FOR J=0 TO 60 : W=640/60
5070          LINE(J*W,200)-(J*W,198)
5080 NEXT J
5090 FOR J=1 TO 6 : W=640/6
5100          LINE(J*W,200)-(J*W,195): NEXT J
5110 FOR J=0 TO 200 STEP 20
5120          LINE (0,J)-(7,J)
5130 NEXT J
5140 FOR J=0 TO 200 STEP 5
5150          LINE (0,J)-(3,J)
5160 NEXT J
5170 FOR J=0 TO 200 STEP 20
5180          LINE (633,J)-(640,J)
5190 NEXT J
5200 FOR J=0 TO 200 STEP 5
5210          LINE (637,J)-(640,J)
5220 NEXT J
5230 W=640/TOTAL
5240 XLAB=TOTAL/6
5250 A0= 640/6
5260 L=23
5270 XAX=A0
5280 LOCATE 23,1,1:PRINT F1
5290 FOR I=1 TO 6
5300   XAX=A0* I
5310   N=XAX/8.600001
5320   XL% = F1+XLAB*I - .5
5330   IF I<3 THEN GOTO 5350
5340          N=N+1
5350   IF I<5 THEN GOTO 5370
5360          N=N+1
5370   IF I<5.9 THEN GOTO 5400
5380          XL% = F2
5390          N=N-1
```

```
5400   LOCATE L,N : PRINT XL%
5410 NEXT I
5420 RETURN
5430 REM ************************************************************************
5440 REM                FIND THE MAXIMUM AND AVERAGE OF THE DATA
5450 REM ************************************************************************
5460 SUM=0!
5470 FOR I=F1 TO F2
5480          SUM=SUM+Y(I)
5490 NEXT I
5500 AVJ=SUM/(F2-F1+1) : YAVG=AVJ
5510 AMAX =AVJ
5520 AMIN =AVJ
5530 FOR I=F1 TO F2
5540          IF Y(I) < AMAX  THEN GOTO 5580
5550                  AMAX = Y(I)
5560                  IMAX=I
5570                   GOTO 5610
5580          IF Y(I) > AMIN THEN GOTO 5610
5590                  AMIN= Y(I)
5600                   IMIN=I
5610 NEXT I
5620 YMAX=AMAX : YMIN=AMIN
5630 AMAX=200-20*AMAX
5640 AMIN=200-20*AMIN
5650 RETURN
5660 REM ************************************************************************
5670 REM                        ZOOM IN ON DESIRED INTERVAL
5680 REM ************************************************************************
5690 LOCATE 25,1,1
5700 PRINT"                                                                      "
5710 PRINT "OLD LIMITS: ",F1,F2
5720 LOCATE 25,40:INPUT"F1 , F2 = ", F1,F2
5730 FF1=F1 : FF2=F2
5740 GOSUB 5010                         :REM    PLOT THE GRAPH
5750 GOSUB 4490                          :REM    PLOT THE Y-AXIS
5760 IF EX<>0 THEN GOTO 5830
5770 FOR I=F1 TO F2
5780          W=640/(F2-F1):J=W*(I-F1)
5790         AA=200-20*Y(I)
5800          PSET(J,AA)
5810 NEXT I
5820 RETURN
5830 GOSUB 5430               : REM   AVERAGE THE DATA
5840 EXABS=ABS(EX)
5850 CC=2*EXABS/(AMIN-AMAX)
5860 BOT = 100+EXABS
5870 TOP = 100-EXABS
5880 IF EX < 0 THEN GOTO 5980
```

```
5890 FOR I=F1+1 TO F2
5900          W=640/(F2-F1):J=W*(I-F1)
5910          AA0=200-20*Y(I-1)
5920          AA0=BOT-CC*(AMIN-AA0)
5930          AA1=200-20*Y(I)
5940          AA1=BOT-CC*(AMIN-AA1)
5950          LINE(J-W ,AA0)-(J,AA1)
5960 NEXT I
5970 RETURN
5980 FOR I=F1 TO F2
5990          W=640/(F2-F1):J=W*(I-F1)
6000          AA=200-20*Y(I)
6010          AA=BOT-CC*(AMIN-AA)
6020          PSET(J,AA)
6030 NEXT I
6040 RETURN
6050 REM ************************************************************************
6060 REM                          CENTER THE INTERFEROGRAM
6070 REM ************************************************************************
6080 LOCATE 25,1,1
6090 PRINT"                                                                      "
6100 ICENTER = 1
6110 GOSUB 5460                  :REM   AVERAGE THE DATA + MIN/MAX
6120 FF1=IMAX-(MPOINTS/2)+1  : F1=1
6130 FF2=IMAX+(MPOINTS/2)    : F2=MPOINTS
6140 TOTAL = MPOINTS
6150 GOSUB 5010                 :REM    PLOT THE COORDINATES
6160 GOSUB 4520                 :REM    WRITE THE Y-AXIS
6170 IF EX <> 0 THEN GOTO 6280
6180 FOR I=1 TO TOTAL
6190          K=FF1 + I -1
6200          YY=100 - 10*(Y(K)-YAVG)
6210          A(I)=YY
6220          Y(I)=Y(K)
6230          X=I*W
6240          PSET(X,YY)
6250 NEXT I
6260 FF1=1:FF2=TOTAL
6270 RETURN
6280 FOR I=2 TO TOTAL
6290          K=FF1 + I -1
6300          YY1=100 - EX*(Y(K-1)-YAVG)/YNORM
6310          Y(I-1)=Y(K-1)
6320          A(I-1)=YY1
6330          YY2=100 - EX*(Y(K)-YAVG)/YNORM
6340          X=I*W
6350          LINE(X-W,YY1)-(X,YY2)
6360 NEXT I
6370 A(TOTAL)=YY2:Y(TOTAL)=Y(K):FF1=1:FF2=TOTAL
```

```
6380 RETURN
6390 REM ************************************************************************
6400 REM                          HALF THE INTERFEROGRAM
6410 REM ************************************************************************
6420 GOSUB 5460                  :REM AVERAGE THE DATA
6430 OGRMP = MPOINTS : MPOINTS=MPOINTS/2 : TOTAL=MPOINTS
6440 I1=IMAX - MPOINTS/2 + 1  : I2=IMAX+MPOINTS/2
6450 FOR I=1 TO MPOINTS
6460           Y(I)= Y(I+I1-1)
6470 NEXT I
6480 GOSUB 4910                  :REM    PLOT COORDINATES+DATA
6490 RETURN
6500 REM ************************************************************************
6510 REM                          INVERT THE INTERFEROGRAM
6520 REM ************************************************************************
6530 FOR I=1 TO TOTAL
6540          Y(I) = 10! - Y(I)
6550 NEXT I
6560 GOSUB 4910                  :REM    PLOT COORDINATES+DATA
6570 RETURN
6580 REM ************************************************************************
6590 REM                           FIX A DATA POINT
6600 REM ************************************************************************
6610 LOCATE 25,1,1
6620 PRINT"                                                                      "
6630 INPUT "POINT No. FIXED : ", IFIX
6640 PRINT"                                                                      "
6650 PRINT"OLD VALUE : ", Y(IFIX)
6660 LOCATE 25,40,1 : INPUT"NEW VALUE : ", YFIX
6670 X=IFIX*W
6680 YY=200 - 20*Y(IFIX) : PRESET(X,YY)
6690 Y(IFIX)=YFIX
6700 YY=200 - 20*Y(IFIX) : PSET(X,YY)
6710 RETURN
6720 REM ************************************************************************
6730 REM               READ AND INSERT A MODIFICATION DATA FILE
6740 REM ************************************************************************
6750 OPEN "I",#1,"ADD"
6760 INPUT #1, POINTS1
6770 INPUT #1, FRINGE1
6780 IF FRINGE1= FRINGE THEN 6820
6790 LOCATE 2,10,1
6800 PRINT" FRINGES OF CORRECTION FILE DON'T MATCH MAIN FILE "
6810 RETURN
6820 LOCATE 2,20,1
6830 PRINT " TOTAL NUMBER OF POINTS : ", POINTS1
6840 FOR I=1 TO POINTS1
6850           INPUT #1, B(I)
6860           IF EOF(1) THEN GOTO 6880
```

```
6870 NEXT I
6880 CLOSE #1
6890 LOCATE 25,1,1
6900 PRINT"                                                                    "
6910 GOSUB 5460                :REM AVERAGE THE DATA
6920 INPUT "OFFSET OF THE DATA (INITIAL POINT #): ",OFFSET
6930 IF OFFSET+POINTS1-1 < POINTS THEN 7010
6940 TOTAL=OFFSET+POINTS1-1
6950 F1=1 : F2=TOTAL : FF1=1 : FF2=TOTAL
6960 GOSUB 5030                :REM PLOT THE COORDINATES OF THE DATA
6970 GOSUB 4520                :REM PLOT THE Y-COORDINATES
6980 FOR I=1 TO POINTS
6990          YY=200 - 20*Y(I) :X=I*W : PSET(X,YY) : A(I)=YY
7000 NEXT I
7010 FOR I=1 TO POINTS1
7020          YY=200 - 20*B(I)
7030          X=(I+OFFSET-1)*W
7040          PSET(X,YY)
7050 NEXT I
7060 LOCATE 25,1,1
7070 PRINT"                                                                    "
7080 INPUT "MERGE? [Y=1=N1], START/END [ N2,N3 ]  ",N1,N2,N3
7090 IF N1=0 THEN 7220
7100 IF N2=1 THEN 7150
7110 FOR I=1  TO N2
7120          II=I+OFFSET-1  : X=II*W
7130          YY=200 - 20*B(I) : PRESET(X,YY)
7140 NEXT I
7150 FOR I=N2 TO N3
7160          II=I+OFFSET-1  : X=II*W
7170          IF II>ORGPNT THEN 7190
7180          YY=200 - 20*Y(II) : PRESET(X,YY)
7190          Y(II)=B(I) : YY=200 - 20*Y(II) : PSET(X,YY)
7200 NEXT I
7210 RETURN
7220 GOSUB 4910                :REM    PLOT COORDINATES+DATA
7230 RETURN
7240 REM ************************************************************************
7250 REM                              DUMP SCREEN TO THE TERMINAL
7260 REM ************************************************************************
7270 COPY = 1
7280 LOCATE 25,1,1
7290 PRINT"                                                                    "
7300 LOCATE 25,1,1
7310 PRINT"                                                                    "
7320 INPUT"START ROW/COL [N1,N2] [N1=0--NO LABEL] : ", N1,N2
7330 IF N1=0 THEN 7400         :REM    NO LABELS
7340 IF INTER=1 THEN 7370
7350 PRINT"                                                                    "
```

```
7360 INPUT " ENTER THE DATE & NAME [i.e. 15-AUG-85-A] : "; DAY$
7370 LOCATE N1  ,N2,1 : PRINT " DATA SET : "; DAY$
7380 LOCATE N1+2,N2,2 : PRINT " TOTAL DATA POINTS = "; POINTS
7390 LOCATE 25,1,1 :INTER=1
7400 PRINT"                                                                    "
7410 LOCATE 25,30
7420 PRINT"DATA POINTS "
7430 REM  Have the printer work during one direction only
7440 LPRINT CHR$(27)+"["
7450 IF INKEY$=CHR$(3) THEN GOTO 7480
7460 FOR I=1 TO 1000 : I=I+1 : NEXT I : BEEP
7470 GOTO 7450
7480 LPRINT CHR$(27)+"]"
7490 LOCATE 25,1,1
7500 RETURN
7510 REM ************************************************************************
7520 REM                    DUPLICATE A PART OF THE INTERFEROGRAM
7530 REM ************************************************************************
7540 LOCATE 25,1,1
7550 GOSUB 5460                :REM AVERAGE THE DATA
7560 PRINT"                                                                    "
7570 INPUT" [N1,N1] OF DUPLICATED REGION  ",N1,N2
7580 I1=2*IMAX-N2
7590 IF I1>0 THEN 7730
7600 OLDTOT=TOTAL : TOTAL=TOTAL-I1+1 : IMAX=IMAX-I1+1
7610 F1=1 : F2=TOTAL : FF1=1 : FF2=TOTAL : EX=0
7620 PT = INT(TOTAL) : POWER=0
7630 PT=PT/2 : IF PT<1 THEN GOTO 7650
7640 POWER=POWER+1 : GOTO 7630
7650 M=POWER : MPOINTS=2^M
7660 GOSUB 5030                :REM PLOT THE COORDINATES OF THE DATA
7670 GOSUB 4520                :REM PLOT THE Y-COORDINATES
7680 FOR I=1 TO OLDTOT
7690           I2=TOTAL-I+1 : I3=OLDTOT-I+1: Y(I2)=Y(I3)
7700           YY=200 - 20*Y(I2) :X=I2*W : PSET(X,YY) : A(I2)=YY
7710 NEXT I
7720 N1=N1-I1+1 : N2=N2-I1+1
7730 FOR I=N1 TO N2
7740           I2=2*IMAX-I       : X=I2*W
7750           YY=200 - 20*Y(I2) : PRESET(X,YY)
7760           Y(I2)=Y(I) : YY=200 - 20*Y(I2) : PSET(X,YY)
7770 NEXT I
7780 RETURN
7790 REM ************************************************************************
7800 REM              NORMALIZE THE PLOT BY A LINEAR SQUARES FIT.
7810 REM              ENTER ONE INTERVAL AT A TIME THEN CONTINUE.
7820 REM ************************************************************************
7830 N1=0 : N2=0
7840 LOCATE 25,1,1
```

```
7850 PRINT"                                                                    "
7860 LOCATE 25,1,1  : PRINT"OLD INTERVAL ",N1,N2
7870 LOCATE 25,40,1 : INPUT"NEW [N1,N2]  ",N1,N2
7880 IF N1=0 THEN 7960
7890 GOSUB 8000                 :REM    LIN SQUARE FIT
7900 FOR I=N1 TO N2
7910           DIFF=SLOPE*I+YINTER-Y(I)
7920           X=I*W : YY=200 - 20*Y(I) : PRESET(X,YY)
7930           Y(I)=5!-DIFF : YY=200 - 20*Y(I) : PSET(X,YY)
7940 NEXT I
7950 GOTO 7840
7960 RETURN
7970 REM ************************************************************************
7980 REM                          LEAST SQUARES FIT
7990 REM ************************************************************************
8000 YSQ=0! : XSQ=0! : YS=0! : XS=0! : XYP=0! : POI=N2-N1+1
8010 FOR I=1 TO POI
8020           XSQ=XSQ+I*I : XS=XS+I
8030           YS=YS+Y(I+N1-1) : XYP=XYP+I*Y(I+N1-1)
8040 NEXT I
8050 SLOPE=(XS*YS/POI-XYP)/(XS*XS/POI-XSQ)
8060 YINTER=(YS-SLOPE*XS)/POI : YINTER=YINTER-SLOPE*(N1-1)
8070 RETURN
8080 REM ************************************************************************
8090 REM                          SELECT THE STARTING POINT
8100 REM ************************************************************************
8110 LOCATE 25,1,1
8120 PRINT"                                                                    "
8130 INPUT" SELECT STARTING POINT   : ", ISEL
8140 IF ISEL+MPOINTS-1 > POINTS THEN GOTO 8110
8150 FOR I=1 TO MPOINTS
8160            II=I+ISEL-1 : Y(I) = Y(II)
8170 NEXT I
8180 TOTAL=MPOINTS
8190 GOSUB 4910                 :REM    PLOT COORDINATES AND DATA
8200 RETURN
8210 REM ************************************************************************
8220 REM                          LIST SOME DATA POINTS
8230 REM ************************************************************************
8240 LOCATE 25,1,1
8250 PRINT"                                                                    "
8260 INPUT" ENTER  [N1,N2]  RANGE : ", IN1,IN2
8270 LOCATE 2,3,1
8280 FOR I=IN1 TO IN2 : PRINT"POINT # ",I, "=", Y(I) : NEXT I
8290 RETURN
8300 REM ************************************************************************
8310 REM               ORIGINAL  INTERFEROGRAM
8320 REM ************************************************************************
8330 TOTAL=ORGPNT : POINTS=TOTAL :MPOINTS=ORGMP: EX=0
```

```
8340 FOR I=1 TO TOTAL
8350          Y(I)=X(I)
8360 NEXT I
8370 GOSUB 4910                  :REM    PLOT COORDINATES AND DATA
8380 RETURN
8390 REM ************************************************************************
8400 REM                          EXPAND THE PLOT
8410 REM ************************************************************************
8420 LOCATE 25,1,1
8430 IF ISUB=1 THEN 8470         :REM    COMING  OUT OF  THE SUB MENU
8440 EX = 0
8450 PRINT "                                                                    "
8460 INPUT"% OF Y-AXIS EXPANSION : (-100-0)%=PNT, (1-100)%=LINE   ";EX
8470 ISUB=0                      :REM    RESET THE SUB MENU FLAG
8480 GOSUB 5010                  :REM PLOT THE COORDINATES
8490 GOSUB 5460                  :REM AVERAGE THE DATA
8500 GOSUB 4520                  :REM PLOT THE Y-AXIS
8510 YNORM1=YAVG-YMIN: YNORM2=YMAX-YAVG
8520 YNORM=YNORM1
8530 IF YNORM1 > YNORM2 THEN GOTO 8550
8540 YNORM=YNORM2
8550 IF EX > 0 THEN GOTO 8630
8560 FOR I=1 TO TOTAL
8570             K=FF1 + I -1
8580             W=640/TOTAL :J=W*K
8590             Q1 = 100- INT(EX*(Y(K)-YAVG)/YNORM)
8600             A(I)=Q1: PSET(J,Q1)
8610  NEXT I
8620 RETURN
8630 FOR I=2 TO TOTAL
8640          K=FF1 + I -1
8650          YY1=100 - EX*(Y(K-1)-YAVG)/YNORM
8660          A(I-1)=YY1
8670          YY2=100 - EX*(Y(K)-YAVG)/YNORM
8680          X=I*W
8690          LINE(X-W,YY1)-(X,YY2)
8700 NEXT I
8710 A(TOTAL)=YY2
8720 RETURN
8730 REM ************************************************************************
8740 REM               OUTPUT THE INTERFEROGRAM TO A DISK
8750 REM ************************************************************************
8760 IBM=0  : LOCATE 25,1,1
8770 PRINT"                                                                     "
8780 INPUT" WANT AN Y(I) FILE  [YES=1]  ",IBM
8790 IF IBM=1 THEN 8880
8800 OPEN "O",#3,"DATA"
8810 PRINT #3, POINTS
8820 PRINT #3, FRINGE
```

```
8830 FOR I=1 TO POINTS
8840          PRINT #3, Y(I)
8850 NEXT I
8860 CLOSE #3
8870 RETURN
8880 OPEN "O",#3,"DATA1"
8890 FOR I=1 TO MPOINTS
8900          YY=Y(I)*1!
8910          PRINT #3, YY
8920 NEXT I
8930 CLOSE #3
8940 RETURN
8950 REM ************************************************************************
8960 REM               OUTPUT THE SPECTRUM TO A DISK
8970 REM ************************************************************************
8980 IBM=0  : LOCATE 25,1,1
8990 PRINT"                                                                      "
9000 INPUT" WANT AN X(I)-Y(I) FILE  [YES=1]  ",IBM
9010 IF IBM=1 THEN 9100
9020 OPEN "O",#3,"PNT"
9030 PRINT #3, MPOINTS
9040 PRINT #3, FRINGE
9050 FOR I=1 TO MPOINTS
9060          PRINT #3, Q(I)
9070 NEXT I
9080 CLOSE #3
9090 RETURN
9100 IF INOR=1 THEN 9120
9110 OPEN "O",#3,"PNT1" :GOTO 9130
9120 OPEN "O",#3,"PNT2"
9130 FOR I=F1 TO F2
9140          XJ=RESOL*I
9150          PRINT #3, XJ
9160          QQ=Q(I)
9170          PRINT #3, QQ
9180 NEXT I
9190 CLOSE #3
9200 RETURN
9210 REM ************************************************************************
9220 REM               Subroutine that draws the coordinates
9230 REM                        OF THE SPECTRUM
9240 REM ************************************************************************
9250 CLS
9260 LINE(0,0)-(640,190),,B
9270 ISM = 640/40
9280 FOR J=0 TO 40                          :REM     ISM = Small tic marks
9290 LINE(J*ISM,190)-(J*ISM,187)
9300 NEXT J
9310 ILG = 640/5
```

```
9320 FOR J=0 TO 5
9330 LINE(J*ILG,190)-(J*ILG,184)          :REM     ILG = Large tic marks
9340 NEXT J
9350 IY1=INT(Y0/10)
9360 IY2=INT(Y0/20)
9370 FOR J=IY1 TO Y0 STEP IY1
9380           LINE(0,J)-(6,J)
9390 NEXT J
9400 FOR J=IY2 TO Y0 STEP IY2
9410           LINE (0,J)-(3,J)
9420 NEXT J
9430 LINE (0,Y0)-(640,Y0)               :REM   Place the zero baseline
9440 YAX=100
9450 L=1
9460 IF ISHIFT=0 THEN GOTO 9540
9470 TOTN= Y0*25/235
9480 SPACEN= TOTN/5
9490 LOCATE L,2 : PRINT YAX
9500 YAX=YAX-20
9510 IF YAX<0 THEN GOTO 9640
9520 L=L+SPACEN
9530 GOTO 9490
9540 TOTN= Y0*25/220
9550 SPACEN= TOTN/5
9560 LOCATE L,2 : PRINT YAX
9570 YAX=YAX-20
9580 IF YAX<0 THEN GOTO 9640
9590 L=L+SPACEN
9600 GOTO 9560
9610 REM ************************************************************************
9620 REM                                DRAW THE X-AXIS COORDINATES
9630 REM ************************************************************************
9640 MAXWAVE = 9145!/2!/FRINGE           :REM   Maximum wave number
9650 RESOL = MAXWAVE*2/MPOINTS          :REM   Resolution in (1/cm)
9660 XAX=IBEG : XAXMAX=IEND
9670 RANGE= IEND-IBEG  : SPACE=RANGE/5 : W=80/5.34 : N0=1
9680 FOR J=1 TO 6
9690           LOCATE 23,N0 : PRINT XAX
9700           XAX = INT(XAX+SPACE)
9710           IF J<=2 THEN GOTO 9730
9720                  N0=N0+1
9730           N0=INT(N0+W)
9740 NEXT J
9750           N0=INT(N0+W)
9760 F1=0                               :REM    FIND THE LOWER/UPPER LIMITS
9770 IF F1*RESOL>IBEG THEN 9790
9780 F1=F1+1 : GOTO 9770
9790 F2=F1
9800 IF F2*RESOL> IEND THEN 9820
```

```
9810 F2=F2+1 : GOTO 9800
9820 F2=F2-1
9830 RETURN
9840 REM
9850 REM ***************************************************************************
9860 REM                          FFT SUBROUTINE
9870 REM ***************************************************************************
9880 BB=(N/2) + 1
9890 FOR I=1 TO N
9900 A(I)=A(I) *COS(PI*(I-BB)/N) :B(I)=0     :REM   Apodize the signal
9910                                             REM    cosine function
9920 NEXT I
9930 J=1:L=1
9940 IF L>= J THEN 9960 ELSE 9950
9950 SWAP A(L),A(J)
9960 K=N/2
9970 IF K>=J THEN 10010 ELSE 9980
9980 J=J-K
9990 K=K/2
10000 GOTO 9970
10010 J=J+K:L=L+1
10020 IF L=N-1 THEN 10030 ELSE GOTO 9940
10030 P=1
10040 U=1:V=0:J=1:K=2^(P-1):C=COS(PI/K):S=-SIN(PI/K)
10050 L=J
10060 TR=A(L+K)*U-B(K+L)*V :TI=A(L+K)*V+B(L+K)*U
10070 A(K+L)=A(L)-TR  : A(L)=A(L)+TR
10080 B(K+L)=B(L)-TI  : B(L)=B(L)+TI
10090 L=L+2^P
10100 IF L>N THEN 10110 ELSE 10060
10110 U1=U*C+V*S : V1=V*C-U*S :U=U1:V=V1 :J=J+1
10120 IF J>K THEN 10130 ELSE 10050
10130 P=P+1
10140 IF P>M THEN 10150 ELSE  10040
10150 FOR I=1 TO N
10160           Q(I) = SQR(A(I)*A(I) + B(I)*B(I))*2/N
10170           Y(I)=Q(I)
10180 NEXT I
10190 RETURN
10200 REM ***************************************************************************
10210 REM                              PREPARE GRAPH TO BE PLOTTED
10220 REM ***************************************************************************
10230 LOCATE 25,1,1
10240 PRINT"                                                                        "
10250 INPUT" START ROW/COL.  [N1,N2] [N1=0--NO TITLE :  ", N1,N2
10260 IF N1=0  THEN 10380
10270 IF INTER=1 THEN GOTO 10310
10280 PRINT"                                                                        "
10290 LOCATE 25,1,1
```

```
10300 INPUT " ENTER THE DATE & NAME : "; DAY$
10310 LOCATE N1  ,N2,1 : PRINT DAY$
10320 LOCATE N1+2,N2,1 : PRINT " SPECTRAL POINTS       : "; MPOINTS/2
10330 LOCATE N1+3,N2,1 : PRINT " LOWER LIMIT           : ";F1
10340 LOCATE N1+4,N2,1 : PRINT " UPPER LIMIT           : ";F2
10350 LOCATE N1+5,N2,1 : PRINT " RESOLUTION (1/cm)     : ";FIX(RESOL)
10360 LOCATE N1+6,N2,1 : PRINT " FRINGE STEP           : ";FRINGE
10370 LOCATE N1+7,N2,1 : PRINT " No  SCANS AVERAGE     : ";NSCANS+1
10380 LOCATE 25,1,1
10390 PRINT"                                                                    "
10400 LOCATE 25,30
10410 PRINT"WAVENUMBER  (1/cm)"
10420 REM  Have the printer work during one direction only
10430 LPRINT CHR$(27)+"["
10440 IF INKEY$=CHR$(3) THEN GOTO 10470
10450 FOR I=1 TO 1000 : I=I+1 : NEXT I: BEEP
10460 GOTO 10440
10470 LPRINT CHR$(27)+"]"
10480 RETURN
10490 REM ************************************************************************
10500 REM    RETURN THE Y-VALUE OF A POINT ON X-AXIS , PASSED IN POINTER
10510 REM ************************************************************************
10520 IF EX <> 0 THEN GOTO 10560
10530 LOCATE 2,40,1 : PRINT"                                    "
10540 LOCATE 2,40,1 : PRINT" EXPAND PLOT FIRST "
10550 RETURN
10560 YPEAK=EX*1.8*Q(IPOINT)/NORM
10570 I=IPOINTOLD+1
10580           J=W0*(RESOL*I-IBEG) : J0=W0*(RESOL*(I-1)-IBEG)
10590           Q1=Y0-INT(EX*1.8*Q(I-1)/NORM)
10600           R1=Y0-INT(EX*1.8*Q(I)/NORM)
10610            LINE(J0,Q1)-(J,R1)
10620 I=IPOINT+1
10630           J=W0*(RESOL*I-IBEG) : J0=W0*(RESOL*(I-1)-IBEG)
10640           Q1=Y0-INT(EX*1.8*Q(I-1)/NORM)
10650           R1=Y0-INT(EX*1.8*Q(I)/NORM)
10660            LINE(J0,Q1)-(J,R1),0
10670 XVAL= INT(RESOL*IPOINT)                  :REM   The starting point
10680 LOCATE 2,40,1 : PRINT"                                    "
10690 LOCATE 2,40,1 : PRINT XVAL ," 1/CM "
10700 LOCATE 3,40,1 : PRINT"                          "
10710 LOCATE 3,40,1 : PRINT YPEAK
10720 RETURN
10730 REM ************************************************************************
10740 REM                        EXPAND THE DATA AND REPLOT IT
10750 REM ************************************************************************
10760 GOSUB 9250
10770 QMAX = 0
10780 FOR I=F1 TO F2
```

```
10790            IF Q(I) < QMAX THEN GOTO 10810
10800            QMAX = Q(I)
10810 NEXT I
10820 NORM = QMAX
10830 W0=640/(IEND-IBEG)
10840 FOR I=F1+1 TO F2
10850           J=W0*(RESOL*I-IBEG) : J0=W0*(RESOL*(I-1)-IBEG)
10860           Q1=Y0-INT(EX*1.8*Q(I-1)/NORM)
10870            X(I-1)=Q1
10880           R1=Y0-INT(EX*1.8*Q(I)/NORM)
10890            LINE(J0,Q1)-(J,R1)
10900 NEXT I
10910 X(F2)=R1
10920 RETURN
10930 REM ************************************************************************
10940 REM                COMPUTE THE INSTRUMENT LINE FUNCTION
10950 REM ************************************************************************
10960 LOCATE 25,1,1
10970 PRINT "                                                                      "
10980 INPUT"ENTER TEMPERATURE [K]  : ",TEMP
10990 A0=2500
11000 C1=14388!/TEMP
11010 B0= EXP(C1/4) - 1
11020 XX = (4^5)*B0
11030 J=0
11040 FOR I=1 TO 27
11050           J=J+1 : A=A0 - 50*(I-1) : W=10000/A
11060           B1=EXP(C1/W)-1 : B2= XX/(W^5)/B1 : A(J)=B2
11070 NEXT I
11080 A0=1175
11090 FOR I=1 TO  7
11100           J=J+1 : A=A0 - 25*(I-1) : W=10000/A
11110           B1=EXP(C1/W)-1 : B2= XX/(W^5)/B1 : A(J)=B2
11120 NEXT I
11130 A0=1000
11140 FOR I=1 TO 11
11150           J=J+1 : A=A0 - 20*(I-1) : W=10000/A
11160           B1=EXP(C1/W)-1 : B2= XX/(W^5)/B1 : A(J)=B2
11170 NEXT I
11180 C3=A(1)*B(1)
11190 FOR I=1 TO ISPEC
11200           A(I)= A(I)*B(I) : A(I)=C3/A(I)
11210 NEXT I
11220 RETURN
```

```
C ***************************************************************************
C
C       RADA.FOR
C
C       RADIUS  FOR AN    (NH4)2SO4    PARTICLE
C       Radius based terminal velocity
C
C       Written  26-MAR-85
C       Revised   7-NOV-86
C
C       Subroutines used:     PRESS --  For pure water pressure.
C                             CORR  --  For Cunningham correction (CUNN.FOR).
C                             FITT  --  For spline fit of the data files,
C                                       (SPLINE.FOR).
C
C       Data files used are: RH.DAT -- For water activity
C                            DEN.DAT - For particle density
C
C       In all cases the fit to the data is done by a spline routine.
C
C ***************************************************************************
        PROGRAM RADIUS
        DIMENSION DIA(20)
        DIMENSION VMASS(20)
        CHARACTER*64 FNAME
        PI  = 3.14159265
 15     FORMAT(I2)
 20     FORMAT(F10.3)
 22     FORMAT(E10.2)
C
 30     I = 0
        ERRMIN=0.0005
        TICS=10.0
C
C ***************************************************************************
C       Main loop
C ***************************************************************************
 45     WRITE(*,50)
 50     FORMAT('        ',/)
        WRITE(*,60) TM, PR, WM, DM, VOFSET, TIME, TICS, ERRMIN
 60     FORMAT(' 1. TEMPERATURE ',4X,    ' = ',1X,F7.1,' deg C'/
     1          ' 2. PRESSURE ',7X       ' = ',1X,F8.2,' mm    '/
     2          ' 3. WET MASS ',7X       ' = ',F10.3  ,' VOLTS'/
     3          ' 4. DRY MASS ',7X       ' = ',F10.3  ,' VOLTS'/
     4          ' 5. OFFSET VOLTAGE ',1X,' = ',F10.3  ,' VOLTS'/
     5          ' 6. FALL TIME ',6X      ' = ',1X,F8.2,' SECS '/
     6          ' 7. DISTANCE ',7X       ' = ',1X,F8.2,' Tics '/
     7          ' 8. ERROR TOLERANCE =  ',F12.5, ' '/
     8          ' 9. AVERAGE THE DIAMETERS '    )
C
        WRITE(*,50)
        MENU=0
 70     WRITE(*,80)
 80     FORMAT(' MENU: [DIAM=0], Press 1 - 8 then <RTN> : '\)
        READ(*, 15) MENU
```

```
C
      IF (MENU.EQ.0) GOTO 110
      GOTO (82, 84, 88, 92, 96, 100, 104, 108, 400 ) MENU
      GOTO 45
C
 82   WRITE(*,83)
 83   FORMAT(' ENTER TEMERATURE IN Deg C : '\)
      READ (*,20) TM
      GOTO 45
C
 84   WRITE(*,86)
 86   FORMAT(' ENTER PRESSURE IN MM : '\)
      READ(*,20) PR
      GOTO 45
 88   WRITE(*,90)
 90   FORMAT(' ENTER WET WEIGHT IN VOLTS : '\)
      READ(*,20) WM
      GOTO 45
C
 92   WRITE(*,94)
 94   FORMAT(' ENTER DRY WEIGHT IN VOLTS : '\)
      READ(*,20) DM
      GOTO 45
C
 96   WRITE(*,98)
 98   FORMAT(' ENTER OFFSET VOLTAGE : '\)
      READ(*,20) VOFSET
      GOTO 45
C
100   WRITE(*,102)
102   FORMAT(' ENTER TIME [Seconds] : '\)
      READ(*,20) TIME
      GOTO 45
C
104   WRITE(*,106)
106   FORMAT(' FALL DISTANCE [Tics] : '\)
      READ(*,20) TICS
      GOTO 45
C
108   WRITE(*,109)
109   FORMAT(' ERROR TOLERANCE      : '\)
      READ(*,20) ERRMIN
      GOTO 45
C
110   I=I+1
      VMASS(I)=WM
C
C     Calculate the water mole fraction
C
      SM = 132.12
      AM = 28.0
      WF = (WM - DM)/WM
      SF = 1.0 - WF
      XW = (WF/18.0)/(WF/18.0 + SF/SM)
```

```
C
C       The average properties
C
        TEMP = 273.15 + TM
        RGAS = 82.05
C ***************************************************************************
C               THE VISCOSITY OF THE GASES INVOLVED :
C       The water viscosity is based on data in the range : 20-26 C.
C       The nitrogen viscosity is based on data from Hirshfelder.
C ***************************************************************************
        VISH2O = 3.944E-4*TM**2 - .04003*TM + 1.6478
        VISH2O = VISH2O*1.0E-4
        VISN2 = 1.02712E-5*TEMP**0.5
C
C ***************************************************************************
C       Compute the water pressure (based on the pure water pressure),
C       the chamber temperature, and the Relative Humidity (based on the
C       relative balancing voltages).
C       Recall that YVAL=INPUT
C                   XVAL=OUTPUT
C ***************************************************************************
        CALL PRESS(TM,PO)
        ICALL=0
        YVAL=WM/DM
        FNAME='RH.DAT'
        CALL FITT(FNAME,ICALL,XVAL,YVAL)
        PWATER = XVAL*PO/100.0
C
        PN2   = PR - PWATER
        IF(PN2 .LT. 0.0 .OR. PWATER .GT. PO) STOP 'PRESSURE ERROR'
C
        AVM = 18.0*PWATER/PR + AM*PN2/PR
        DEN = (PR/760.0/TEMP/RGAS)*AVM
        VIS = VISH2O*PWATER/PR + VISN2*PN2/PR
        SFPER = SF*100.0
C
        ICALL=0
        YVAL=DM/WM*100.0
        FNAME='DEN.DAT'
        CALL FITT(FNAME,ICALL,XVAL,YVAL)
        SPEGR=XVAL
C
C       particle diameter based on falling rates
C
        DIST=TICS*0.0065974
        VEL = DIST/TIME
        RAD    = (4.5*VIS*VEL*WM/(WM - VOFSET)/980.0/SPEGR)**(0.5)
        DP0 = 2.0*RAD
C
C       Get the Cunningham correction   (Output:DPA )
C
        CALL CORR(DP0,DPA,PR,TEMP,VIS,AVM,ERRMIN)
C
        DPUM = DPA*1E+4
        WRITE(*,170) DPUM
```

```
170     FORMAT(1X,' DIAMETER = ',F8.3,' microns')
        DIA(I) = DPUM
        GOTO 45
C
400     CONTINUE
C
C       Find the average diameter
C
        WRITE(*,405)
405     FORMAT(1X,'The initial diameters')
        IMAX = I
        SUMDIA=0.0
C
        DO 420 I=1,IMAX
                SUMDIA = SUMDIA + DIA(I)
                WRITE(*,   410) I, DIA(I)
410             FORMAT(1X,' DIAMETER ',I2,' = ',F8.3,' microns')
420     CONTINUE
        WRITE(*,425)
425     FORMAT(1X,//)
C
        AVDIA = SUMDIA/FLOAT(IMAX)
        WRITE(*,425)
        WRITE(*,435) AVDIA
435     FORMAT(1X,' AVERAGE DIAMETER = ',F8.3,' microns')
        GOTO 30
C
500     STOP
        END
C
C       Pure water vapor pressure (mm)
C
        SUBROUTINE PRESS(TM,PO)
        A = 18.73 - 4066.16/(TM + 236.28)
        PO = EXP(A)
        RETURN
        END
```

```
C ***************************************************************************
C                       SPLINE.FOR
C
C       Compute the average value of a curve by fitting a parabola
C       between intermediate points
C
C               ICALL -- Tells the program that data file was already read
C               XVAL  -- Output data point
C               YVAL  -- Input data point
C               FNAME -- Data file name
C
C               Written    28-SEP-85
C               Updated    19-AUG-86
C
C ***************************************************************************

        SUBROUTINE FITT(FNAME, ICALL, XVAL, YVAL)
        CHARACTER*64 FNAME
        DIMENSION XX(20) , YY(20)
        PI  = 3.14159265
 15     FORMAT(I2)
 20     FORMAT(F12.5)
 21     FORMAT(A)
        IF(ICALL .EQ. 1) GOTO 30
        I = 0
C
C       Main loop
C
        OPEN (2, FILE=FNAME)
        I=0
 25     READ (2,20,END=30) PTX
        READ (2,20,END=28) PTY
                I=I+1
                IMAX=I
                XX(I)=PTX
                YY(I)=PTY
        GOTO 25
C
 28     CONTINUE
        STOP ' UNEQUAL ( X,Y ) PAIRS IN THE FITTING DATA '
C
 30     CLOSE(2)
C
C       Locate the bracket of BETA from the data and fit a parabola
C       to the curve. After that find the value of the corresponding
C       ALPHA.
C       If the desired point is out of the range of the data (in the
C       density routine especially), set the XVAL output to either
C       the maximum or minimum value.
C
        DO 120 I=1, IMAX-1
                IF (YVAL .LE. YY(I) ) GOTO 140
120     CONTINUE
        XVAL=XX(IMAX)
        GOTO    250
```

```
C
140     I2=I
        IF(I2 .NE. 1) GOTO 200
        XVAL=XX(1)
        GOTO 250
C
200     IUP = 0
        IF(I2 .EQ. IMAX) THEN
                IUP=1
                I3=I2
                I1=I2-2
                I2=I2-1
                IF(I1 .LT. 1) STOP ' Y-DATA-POINT IS TOO LOW '
        ELSE
                I1=I2-1
                I3=I2+1
                IF(I1 .LT. 1) STOP ' Y-DATA-POINT IS TOO LOW '
        ENDIF
C
C               COMPUTE THE CONSTANTS FOR  :  YY = A*X**2 + B*X + C
C
        BB = ( YY(I3)*(XX(I2)**2 - XX(I1)**2) +
     1         YY(I2)*(XX(I1)**2 - XX(I3)**2) +
     1         YY(I1)*(XX(I3)**2 - XX(I2)**2) ) /
     1        (XX(I3) - XX(I2)) / (XX(I1)-XX(I3)) / (XX(I2)-XX(I1))
C
        AA = ( YY(I3) - YY(I1) - BB*(XX(I3)-XX(I1)) ) /
     1       ( XX(I3)**2 - XX(I1)**2 )
C
        CC = YY(I1) - AA*XX(I1)**2 - BB*XX(I1)
C
        C1 = BB**2 + 4.0*AA*(YVAL - CC)
        IF(C1 .LE. 0.0) STOP ' CANT TAKE ROOT OF A NEG. NUMBER '
        XVAL1 = ( - BB + C1**0.5)/2.0/AA
        XVAL2 = ( - BB - C1**0.5)/2.0/AA
        IF(IUP .EQ. 1) THEN
                IF(XVAL1 .GE. XX(I2) .AND. XVAL1 .LT. XX(I3)) THEN
                        XVAL = XVAL1
                        GOTO 250
                ELSEIF(XVAL2 .GE. XX(I2) .AND. XVAL2 .LT. XX(I3)) THEN
                        XVAL=XVAL2
                        GOTO 250
                ELSE
                        STOP ' DID NOT BRACKET THE UPPER X-POINT DATA '
                ENDIF
        ELSE
                IF(XVAL1 .GT. XX(I1) .AND. XVAL1 .LE. XX(I2)) THEN
                        XVAL = XVAL1
                        GOTO 250
                ELSEIF(XVAL2 .GT. XX(I1) .AND. XVAL2 .LE. XX(I2)) THEN
                        XVAL=XVAL2
                        GOTO 250
                ELSE
                        STOP ' DID NOT BRACKET THE LOWER X-POINT DATA '
                ENDIF
```

```
      ENDIF
250   CONTINUE
      RETURN
      END
```

```
C
C                       CUNN.FOR
C
C       Cunningham correction to particle size
C       Written   11-SEP-85
C       Revised   19-AUG-86
C
        SUBROUTINE CORR(DP0,DPA,PR,TEMP,VIS,AVM,ERRMIN)

        FP=36.456*VIS*TEMP**0.5/PR/AVM
        RATE=0.95
        CC=1.0
        DPTRY=DP0
        DPMAX=DP0
        CONA=DP0**2
        IFLAG=0
C
450     FKN = 2.0*FP/DPTRY
        CUNN=1.0 + FKN*(1.257 + 0.4*EXP(-1.1/FKN))
        CONB=CUNN*DPTRY**2
        ERR=(CONB-CONA)/CONA
        ABSERR= ABS(ERR)
        IF (ABSERR .LT. ERRMIN) GOTO 500
                IF (ERR .GT. 0.0 .AND. IFLAG .EQ. 0 ) GOTO 480
                        IFLAG=1
                        IF(ERR .LT. 0.0) GOTO 460
C
                        DPMAX = DPTRY
                        DPTRY = (DPMIN+DPMAX)/2.0
                        GOTO 450
C
460                     DPMIN = DPTRY
                        DPTRY = (DPMIN+DPMAX)/2.0
                        GOTO 450
C
480             DPMAX = DPTRY
                DPTRY = DPMAX*RATE
                GOTO 450
C
500     CONTINUE

        DPA = DPTRY
        RETURN
        END
```

DEN.DAT

THE SPECIFIC GRAVITY OF AMMONIUM SULFATE SOLUTION
AS A FUNCTION OF THE SALT WEIGHT PERCENT.

TO BE USED IN SIZING ROUTINE "RADA.FOR" WITH A SPLINE
INTERPOLATION BETWEEN THE GIVEN DATA POINTS.

S.G.	% SALT(wt)
1.1059	18.0
1.1174	20.0
1.1289	22.0
1.1403	24.0
1.1516	26.0
1.1629	28.0
1.1742	30.0
1.1854	32.0
1.1966	34.0
1.2077	36.0
1.2188	38.0
1.2298	40.0

RH.DAT

THE RELATIVE HUMIDITY AROUND AN AMMONIUM SULFATE SOLUTION
AS A FUNCTION OF THE RATIO OF THE WET-TO-DRY MASS IN A
SOLUTION DROPLET.

TO BE USED IN "RADA.FOR" TO OBTAIN THE SIZE OF DROPLETS
BY THE SEDIMENTATION METHOD.

R.H.	1 / Salt Fraction
80.7	2.34
82.0	2.43
83.0	2.51
84.0	2.60
85.0	2.69
86.0	2.80
87.0	2.93
88.0	3.08
89.0	3.25
90.0	3.46
91.0	3.73
92.0	4.07
93.0	4.45

APPENDIX B

ELECTRICAL CIRCUITS

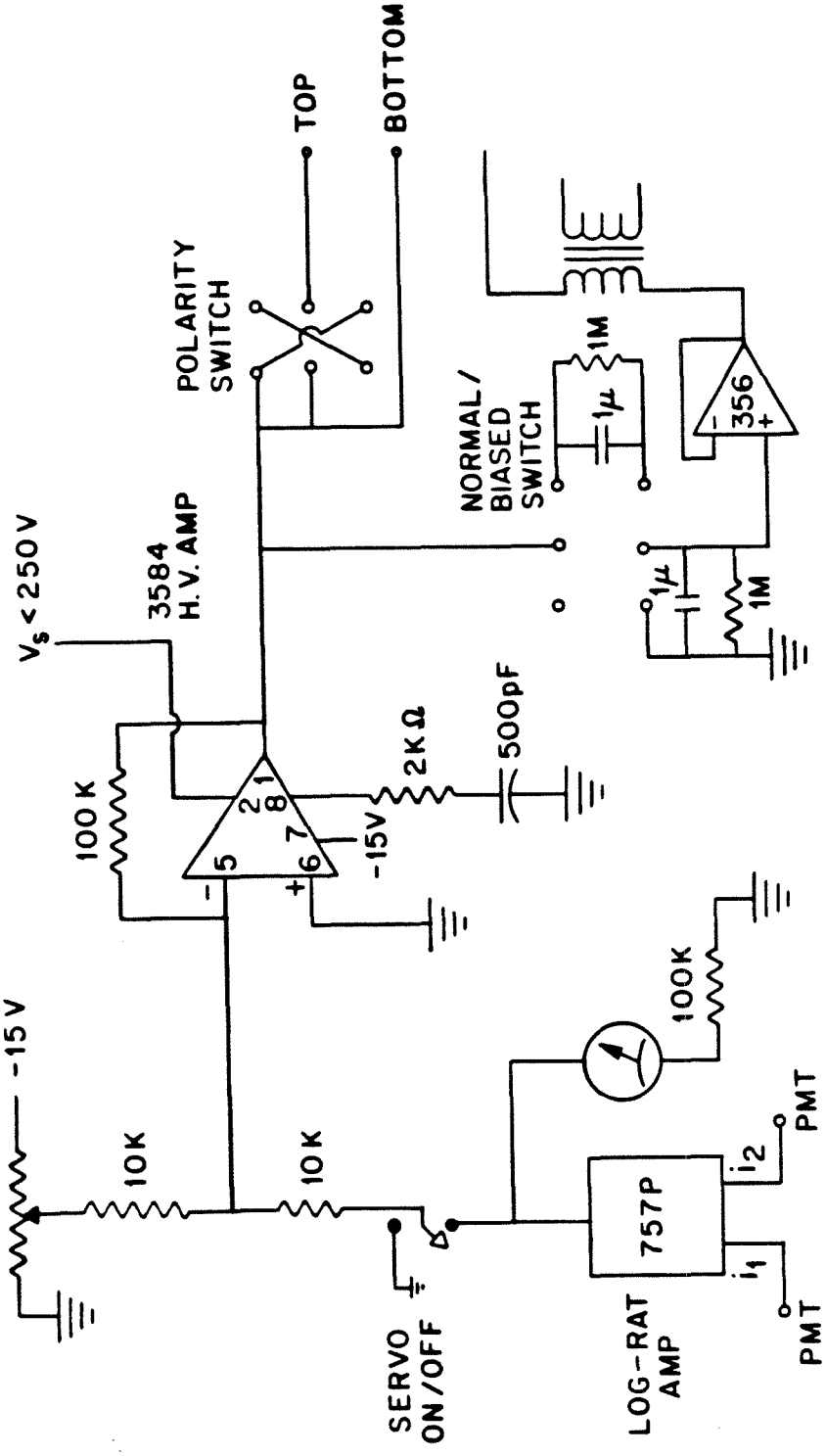

Figure 1. The balancing electronics and automatic servo system for levitating a single particle in the electrodynamic balance.

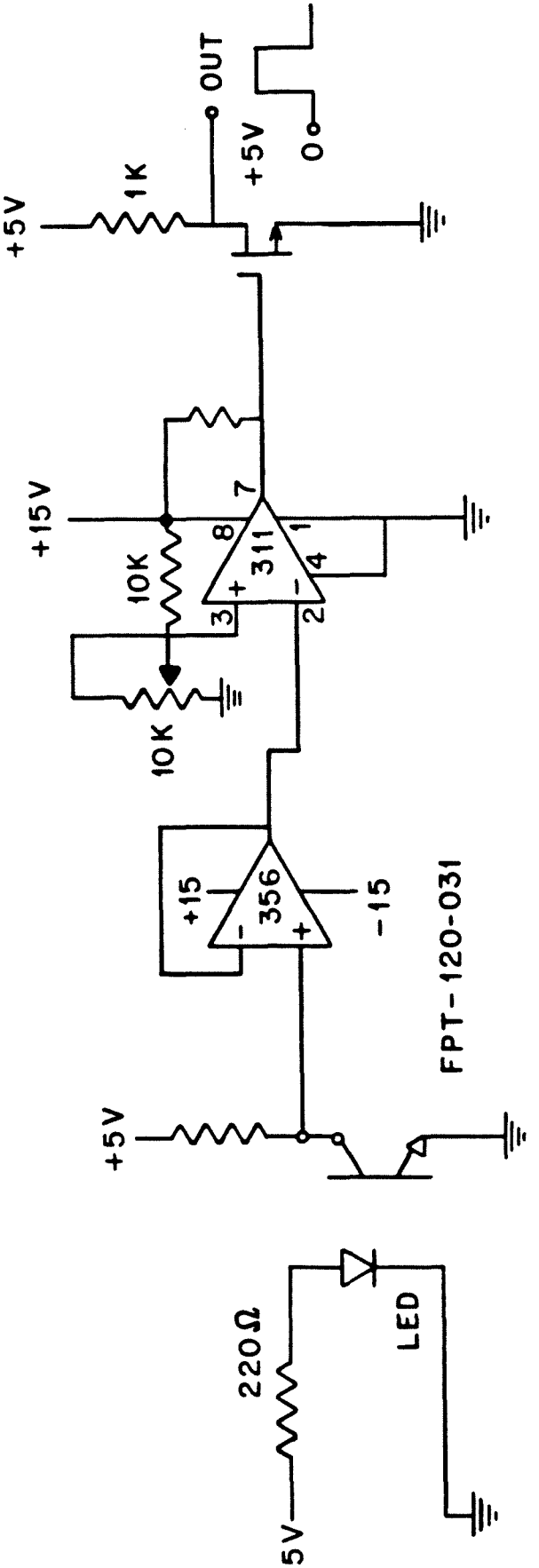

Figure 2. A circuit for obtaining a 5 volt TTL pulse from the chopper to drive the lock-in amplifier.

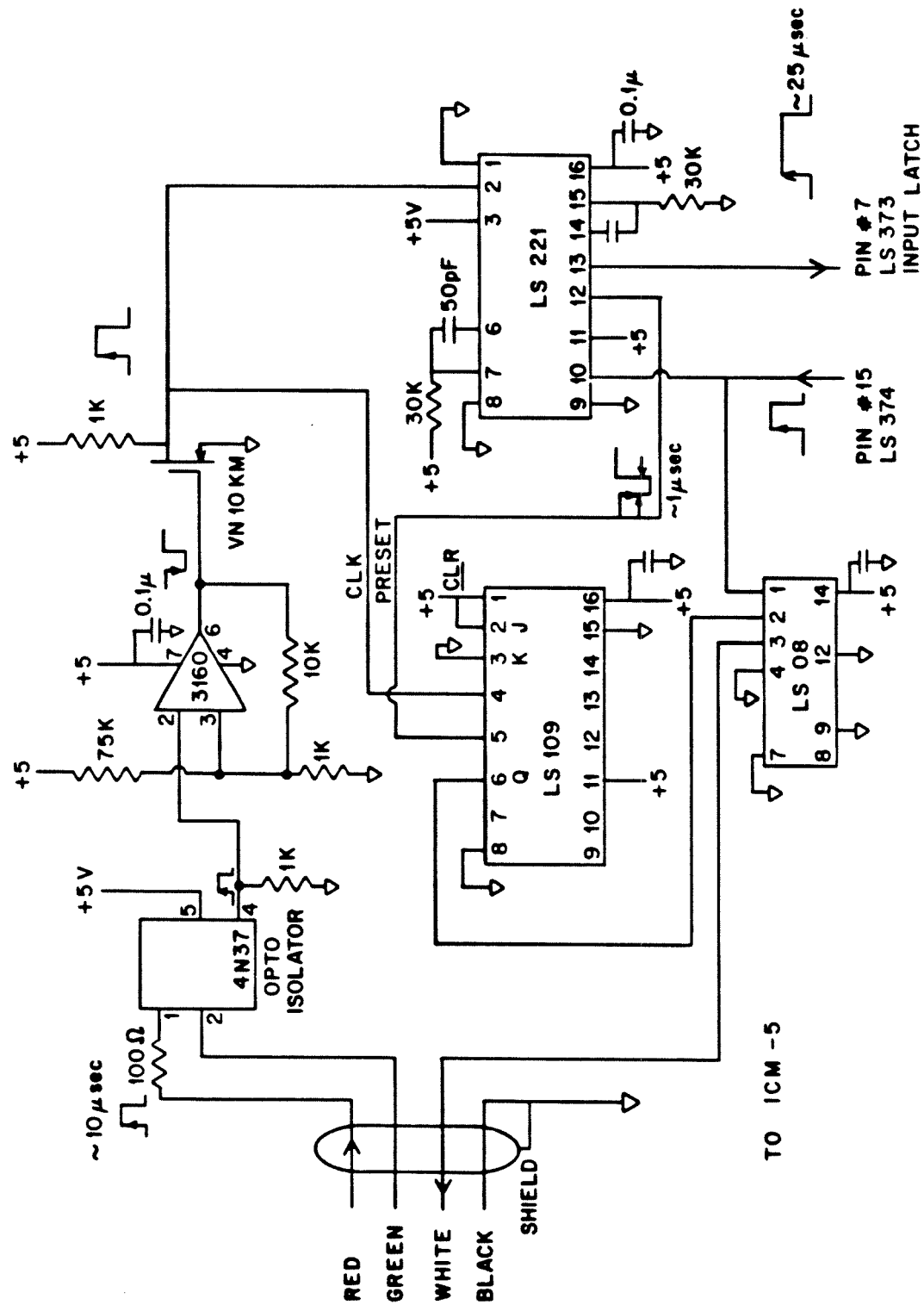

Figure 3. The electronic interface to step the interferometer mirror.

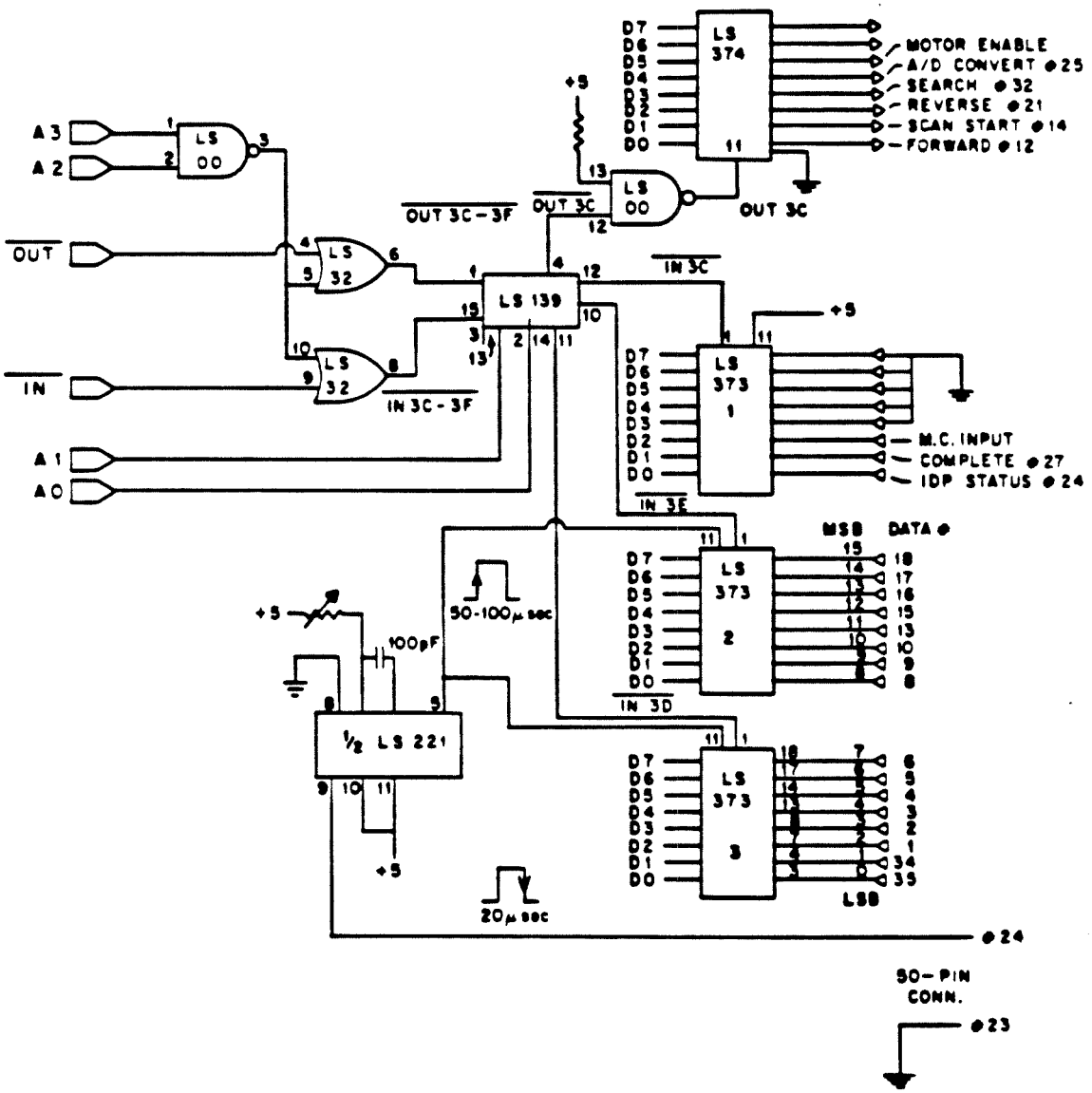

Figure 4. A circuit to latch the 16-bit A/D converter data in parallel to enable the direct memory access to the computer.

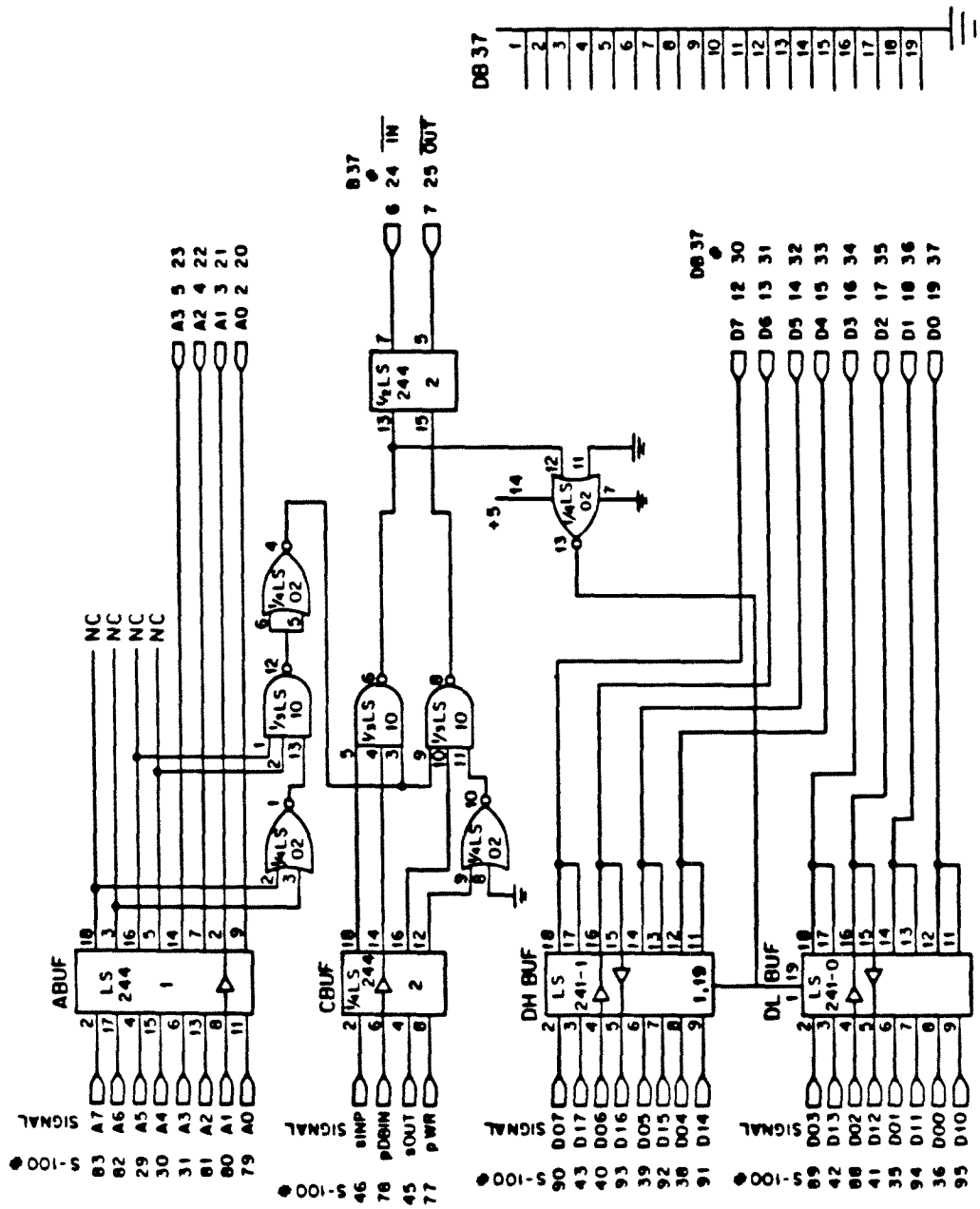

Figure 5. The S-100 interface circuit for reading the A/D data (adapted from John Lee).